

Investigations on Wind Resource Assessment and Wind Farm Layout Using Hybrid Algorithms and Simulation Tools

THESIS

Submitted in partial fulfilment
of the requirements for the degree of
DOCTOR OF PHILOSOPHY

by

BALAKRISHNA MOORTHY C

Under the Supervision of

Prof. M. K. Deshmukh



BITS Pilani
Pilani|Dubai|Goa|Hyderabad

BIRLA INSTITUTE OF TECHNOLOGY AND SCIENCE, PILANI

2015

BIRLA INSTITUTE OF TECHNOLOGY AND SCIENCE, PILANI

CERTIFICATE

This is to certify that the thesis entitled **“Investigations on Wind Resource Assessment and Wind Farm Layout Using Hybrid Algorithms and Simulation Tools”** which is submitted by **Balakrishna Moorthy C**, ID No. **2007PHXF409G** for award of Ph.D. degree of the Institute, embodies original work done by him under my supervision.

Signature of the Supervisor:



Name in capital block letters: **Prof. M. K. DESHMUKH**

Designation: Professor & Head of Department

Department of EEE and E&I

Date: 17/12/2015

DECLARATION

I, **Balakrishna Moorthy C**, hereby declare that this thesis entitled “**Investigations on Wind Resource Assessment and Wind Farm Layout Using Hybrid Algorithms and Simulation Tools**” submitted by me under the guidance and supervision of **Prof. M. K. Deshmukh** is a bonafide research work. I also declare that it has not been submitted previously in part or in full to this University or any other University or Institution for the award of any degree.

Signature of the Student: 

Name: **Balakrishna Moorthy C**

Reg. No.: 2007PHXF409G

Date: 17/12/2015

*Dedicated to
My Parents
Teachers
and
Friends*

Abstract

In recent years, globally wind power development has been strongly supported by advent of newer computer based techniques for prediction, assessment, optimization and forecasting. Although in recent years, accelerated wind power development has been witnessed, much larger on-shore as well as off-shore wind power potential still remains to be utilized. Wind power developers often rely on computer based models for speedy generation of accurate and reliable estimates of wind resource and wind power generation at a wind farm site. Researchers have reported several efforts to develop applications of modern artificial intelligence based algorithms and software tools for simulation of wind farms. In the present work, the focus is on applying artificial intelligence techniques to predicting rate of growth of wind power generation capacity, estimating characteristics of wind resource at a wind farm site, optimizing of position of wind turbine in a wind farm and forecasting wind power generated over short duration ranging from few hours to few days. The developed techniques and results obtained provide useful insight to wind power developers for re-assessment of wind resource at a site and for re-powering of existing wind farms.

The thesis is presented in eight chapters. The introduction, survey of recent relevant literature on wind resource assessment and wind farm layout, is followed by investigation of application of genetic algorithm in predicting increase in cumulative installed wind power generation capacity on annual basis. The accuracy of the technique is established with respect to actually recorded growth in installed capacity, in terms of root mean square error (RMSE) of prediction. It is confirmed that accuracy of prediction depends on volume of recorded data input. Next, use of genetic algorithm in obtaining optimum values of shape (k) and scale parameters (c), required for defining characteristic Weibull probabilistic distribution function at an existing wind farm site in Tamil Nadu, a southern state of India, is demonstrated. Using the Weibull Distribution function for the site, the options for re-powering of the wind farm are explored by obtaining estimates of variation of wind power potential with height above ground level and by identifying new positions of wind turbine corresponding to maximum power generation. It is shown that use of genetic algorithm for obtaining refined values of the shape parameter and scale parameter, improves accuracy of estimates of wind resource potential and capacity factor significantly. The accuracy of results is measured in terms of RMSE, computed with respect to actually recorded data. It is shown that genetic algorithm based approach leads to estimation of wind resource with reduction in error

by about 12.24 %. Also, the estimated annual capacity factor for the wind farm is very close to actually recorded capacity factor of 38.3 %. On the hand, it is shown that use of WindSim, Methodyn and WindFarmer, the industry-scale software tools for determining capacity factors of the existing wind farm, tend to over-estimate the capacity factor. Next, genetic algorithm based approach to determining optimum position of wind turbine in a wind farm is developed. The approach allows designer to search optimum positions of wind turbine corresponding to maximum power potential and minimum wake effect. Also, using the WindFarmer software tool, new positions in the existing wind farm for placing wind turbines in future are identified. An application of genetic algorithm in conjunction with feed forward neural network is developed for predicting power generation over short duration, ranging from few hours to few days. It is confirmed that accuracy of prediction depends on both volume of past recorded data as input and time scale for prediction. The thesis concludes with summary of results obtained and future scope of work.

Keywords:

Wind Resource Assessment, Wind Farm Layout, Prediction and Forecasting of Wind Power Generation, Genetic Algorithm, Artificial Neural Network, Back Propagation Algorithm, Windographer, WindSim, Meteodyn, WindFarmer.

Acknowledgement

I express my profound gratitude towards my Supervisor and mentor Prof. M.K. Deshmukh, Professor and Head of the Department, for his continuous encouragement and his outstanding guidance in conducting this research. He has always been a source of inspiration, motivation and scholarly guidance. I shall always remember the lively and rewarding moments that I had with him while doing discussions during my research work. He had whole-heartedly helped me in this endeavor at all stages of this work. From bottom of my heart, I extend my sincere thanks to him for all his efforts and help at various levels without which this work not have been completed. He was instrumental in conceptualizing and developing the theme and supported me in all stages of work.

I thank Prof. V.S Rao, Acting Vice-Chancellor, Prof. Ashoke Kumar Sarkar, Director, BITS Pilani - Pilani Campus, Prof. K. E. Raman, Former Director, Prof. G. Raghurama, Former Director, BITS Pilani - Pilani Campus, Prof. S. K. Verma, Dean, ARD, BITS Pilani - Pilani Campus, Prof. Sasikumar Punnekkat, Director, Prof. Prasanta Kumar Das, Associate Dean, ARD, Prof. Sunil Bhand, Dean, SRCD, Prof. S. D. Manjare and Prof. D. M. Kulkarni, Dean, Administration, BITS, Pilani - K. K. Birla Goa Campus, for giving me an opportunity to carry out research studies at the institute and also by providing necessary infrastructure and facilities to carry out my work.

I acknowledge with deep gratitude and respect to Late Prof. T.C. Goel, Former Director, BITS-Pilani, K.K. Birla Goa Campus for his encouragement that resulted in the inception of this thesis and inspiring me to strive towards obtaining a Ph.D. degree.

I am grateful to members of my Doctoral Advisory Committee for thesis mentorship and guidance, Dr. N.S. Manjarekar and Dr. K.Chandram for sparing their valuable time in reviewing my thesis and giving constructive suggestions to improve it. Their valuable suggestions have helped in greatly enhancing the quality of the thesis.

I also wish to thank Dr. Shashidhara Mecha Kotian for agreeing to review my thesis and giving constructive suggestions at all stages for refinement.

I would extend my sincere thanks to Prof. K.R. Anupama and Prof. V.K. Deshpande, former-Head, Dept.of EEE for their constant support at various levels. I also extend my sincere thanks to Dr. C.K. Ramesha, DRC Convener, for support and motivation.

I would extend my sincere thanks to Dr. P. V. Pathak, member secretary and Mr. Gouresh, Goa Energy Development Agency (GEDA), Goa, for their constant support, encouragement and providing me opportunity for attending training programme on Wind Resource Assessment on their behalf at NIWE, Chennai, India.

I sincerely thank Mr. A. K. Patil, Maintenance officer and Mr. Jayaram Gayatri, Electrical Engineer, Mr. Pai, Civil Engineer for providing necessary support in erection and commissioning of wind climate data monitoring facility in campus.

I thank Shri. Sudip Jain, I.A.S, Chairman & Managing Director, TamilNadu Energy Development Agency, Government of TamilNadu, Shri. Madusudhan Khema, Chairman & Managing Director, ReGen Wind Power Tech Pvt. Ltd., Mr. T.S. Saravanan and Mr. Arul, ReGen Wind Power Tech Pvt. Ltd. for providing necessary data for wind farm at Periyapatti, Coimbatore, Tamilnadu, India.

I thank Mr. T.F. Jaysurya, Country Manger, India, WindSim software for providing technical support in using software. I would extend my sincere thanks to Mr. Sachin Bhandare, Wind Energy Engineer, Head India operations, Meteodyn software and providing possible help in addressing various queries in using software.

I acknowledge with due gratitude to Mr. Pravin Mane for sparing his valuable time in helping me in writing my thesis in Latex format and giving constructive suggestions to improve it.

I also thank Dr. Arun Karthik, Dr. Nitin Sharma, Mr. G. Surendran, Ms. Chayadevi, Mr. Meghanand Bhambare, Mr. Shailenda Dhakad, Mr. Abhilash, Mr. Srejith and Ms. Metilda, for their constant support, motivation and suggestions.

I acknowledge with due gratitude to Mr. A. Bharatbhushan, Mr. Prince Mathew, Ms. Darshana Mukherejee, Mr. Hemanth Kumar, Mr. Ankur Agarwal, Mr. Karthik Singhivi and Ms. Rajalekshmi for their constant support and motivation.

I would extend my sincere thanks to Mr. Pusharaj and Mr. Shivaraj Rathod, lab technicians for their constant help during my research work carried out in the lab.

I acknowledge all my colleagues for their continuous support, encouragement and motivation.

I would like to express my sincere gratitude to my loving parents Mr. P. Chellan and Mrs. K. Thankam, for always believing in me, for their continuous support, encouragement, motivation and prayers. Without them I could not have made it here.

I thank my beloved daughter, Akshara R Moorthy and my brothers, Mr. C. Balasubramanian and Mr. C. Balakrishan, my nephew, Mr. B. Bhagavath Shankar, my niece, Ms. B. Harshini Devi and all my family members for their pertinence and patience during this research. They deserve special thanks for their continuous encouragement and motivation.

I am thankful to all my friends and relatives who directly or indirectly helped me in completing my Thesis.

Above all, my gratitude towards the power that controls everything, without his blessings and mercy I can not accomplish anything in this world. Thank you God.

Balakrishna Moorthy C

Contents

Certificate	i
Declaration	i
Abstract	ii
Acknowledgement	iv
Table of Contents	vii
List of Figures	xii
List of Tables	xv
List of Acronyms	xviii
List of Symbols	xx
1 Introduction	1
1.1 Application of Heuristic Techniques in Wind Power Development	2
1.2 Challenges in Wind Power Generation	3
1.3 Scope and Objectives of Research Work	5
1.4 Organization of Thesis	6
2 Literature Survey	8
2.1 Forecasting Growth in Installed Wind Power Generation Capacity	8
2.2 Methods of Wind Resource Assessment	9
2.2.1 Weibull Probability Density Distribution Method for Determining Distribution of Wind Speed	10
2.2.1.1 Graphical Method for Determining Parameters of Weibull Probability Density Distribution Function	11
2.2.1.2 Standard Deviation Method for Determining Parameters of Weibull Probability Density Distribution Function	12

2.2.1.3	Energy Pattern Factor Method for for Determining Parameters of Weibull Probability Density Distribution Function	12
2.2.1.4	Maximum Likelihood Method for Determining Parameters of Weibull Probability Density Distribution Function	13
2.2.2	Method for Estimation of Capacity Factor of Wind Farm	14
2.2.3	Methods for Estimation of Wind Power Density at Different Heights Above Ground	15
2.3	Methods for Optimizing Wind Farm Layout	16
2.4	Methods for Prediction of Wind Power Generation	18
2.4.1	Method for Prediction using Physical Approach	18
2.4.2	Statistical Approach for Prediction of Wind Power Generation	19
2.4.3	Artificial Intelligence-based Approach for Prediction	20
2.4.4	Hybrid Approach for Prediction	22
2.5	Conclusion	23
3	Forecasting Wind Power Generation Capacity	24
3.1	Introduction	24
3.2	Growth in Wind Power Generation Capacity	25
3.2.1	Growth of Wind Power Generation in India	26
3.2.2	Growth of Wind Power Generation in China	26
3.3	Logistic Function Method for Forecasting Installed Wind Power Generation Capacity	28
3.3.1	Genetic Algorithm	29
3.4	Application of GA for Forecasting Growth in Installed Wind Power Generation Capacity	30
3.5	Simulation Results	32
3.5.1	Comparison of Proposed Method with Reported Results using Logistic Function Method	32
3.5.2	Forecasting of Growth in Wind Power Generation Installed Capacity in India	34
3.5.3	Forecasting of Growth in Installed Wind Power Generation Capacity in China	37
3.6	Conclusion	39
4	Assessment of Wind Power Potential	41
4.1	Introduction	41
4.2	Standard Procedure for Determining Characteristics of Wind Resource	43
4.2.1	Average Wind Speed	45
4.2.2	Standard Deviation of Wind Speed	45
4.2.3	Air Density	45
4.2.4	Wind Power Density	46
4.2.5	Turbulence Intensity	47
4.2.6	Energy Pattern Factor	47

4.3	Weibull Probability Distribution Function	48
4.3.1	Graphical Method for Determination of Shape and Scale Parameters	49
4.3.2	Standard Deviation Method for Determination of Shape and Scale parameters	49
4.3.3	Energy Pattern Factor Method for Determination of Shape and Scale Parameters	50
4.3.4	Maximum Likelihood Estimation Method for Determination of Shape and Scale Parameters	51
4.3.5	Determination of Probabilistic Characteristics using Shape and Scale of Weibull Distribution	52
4.3.6	Estimation of Wind Speed Distribution	53
4.4	Rayleigh Probability Distribution Function	54
4.4.1	Determination of Probabilistic Characteristics of Rayleigh Distribution	54
4.5	Proposed Approach to Improve the Accuracy in Estimation of Distribution of Wind Speed	55
4.6	Variation of Wind Power Density with Height	57
4.7	Estimation of Capacity Factor	58
4.8	Campaign for WRA-Measurement of Wind Climatological Data	60
4.8.1	Description of Site-I: Wind Climatological Data Recording Station	61
4.8.2	Description of Site-II: Model Wind Farm	66
4.8.2.1	Weibull Probability Distribution Analysis using Graphical Method	70
4.8.2.2	Comparison of Weibull and Rayleigh Distribution Methods	72
4.8.2.3	Use of Proposed Approach to Improve the Accuracy in Estimation of PDF	73
4.8.2.4	Variation of Wind Power Density with Heights	74
4.8.2.5	Wind Turbine Characteristics and Capacity Factor	75
4.9	Conclusion	75
5	Effect of Terrain on Wind Resource Assessment	78
5.1	Introduction	79
5.2	WindSim Simulation Software Tool	79
5.2.1	Steps in Simulation using WindSim Software	79
5.2.2	Simulation of Site-II: Model Wind Farm using WindSim	81
5.2.2.1	Wind Climate Condition at Site-II	84
5.2.2.2	Simulation using WindSim at Site-II	87
5.3	Meteodyn Simulation Software Tool	92
5.3.1	Steps in Simulation using Meteodyn Software Tool	92
5.3.2	Simulation of Site-II: Model Wind Farm using Meteodyn	93
5.3.2.1	Description of Wind Farm Layout at Site- II	95

5.3.2.2	Simulation of Model Wind Farm using Meteodyn (Site-II)	96
5.3.2.3	Simulation Results Obtained using Meteodyn Software (Site-II)	97
5.4	WindFarmer Simulation Software Tool	101
5.4.1	Steps Involved in Simulation using WindFarmer	101
5.4.2	Simulation of Site II: Model Wind Farm using WindFarmer	102
5.5	Comparison of Softwares for Simulation of Wind Farm	106
5.6	Conclusion	107
6	Effectiveness of Positioning of Wind Turbine in a Wind Farm	109
6.1	Introduction	109
6.2	Wind Wake Models	110
6.3	Application of Genetic Algorithm to Optimize Positioning of Wind Turbines	114
6.3.1	Survey of Reported Results for Optimal Positioning of Wind Turbines	115
6.4	Genetic Algorithm Based Proposed Approach of Positioning of Wind Turbines	118
6.5	Optimization of Positioning of Wind Turbines using WindFarmer Software Simulation Tool	121
6.5.1	Optimizing Layout of Model Wind Farm	121
6.6	Conclusion	127
7	Prediction of Power Generation in Wind farm	128
7.1	Introduction	128
7.2	Prediction of Wind Power Generation	129
7.2.1	Artificial Neural Networks	129
7.2.1.1	Feed Forward Neural Network	129
7.2.2	Learning Algorithms in Artificial Neural Network	131
7.2.2.1	Back Propagation Algorithm	132
7.3	Data from Model Wind Farm for Prediction of Wind Power Generation	134
7.3.1	Results and Discussion of Prediction of Wind Power Generation	139
7.4	Conclusion	141
8	Summary and Future Scope of Work	143
8.1	Summary	143
8.2	Future Scope of Work	146
A	Introduction to Genetic Algorithm	148
A.1	Evolutionary Algorithms - Genetic Algorithm	148
A.1.1	Phases of GA	149
B	Wind Resource Assessment at Model Wind Farm	152
B.1	Site-II: Model Wind Farm	152

B.1.1	Standard Deviation Method-based Analysis	152
B.1.2	Energy Pattern Factor Method-based Analysis	154
B.1.3	Maximum Likelihood Method-based Analysis	155
B.1.4	Rayleigh Distribution Method-based Analysis	157
B.1.5	Comparison of Weibull Distribution Method to Rayleigh Dis- tribution Method	158
B.1.6	Variation of Wind Power Density with Height	158
C	Optimizing Position of Wind Turbine using PSO	161
C.1	Simulation of Wind Farm using Particle Swarm Optimization	161
D	Architecture of Artificial Neural Network using BPA and GA	164
D.1	Artificial Neural Network	164
D.2	Details of Parametric Variation of Back Propagation Algorithm in De- ciding the ANN Architecture	166
D.3	Details of Parametric Variation of Genetic Algorithm in Deciding the ANN Architecture	167
	Bibliography	176
	Publications Based on Present Work	194
	Brief Biography of the Candidate	196
	Brief Biography of the Supervisor	197

List of Figures

3.1	Historic development of installed wind power generation capacity in World (2000-2014).	26
3.2	Growth of installed cumulative wind power generation capacity in India.	27
3.3	Growth of installed cumulative wind power generation capacity in China.	27
3.4	Logistic growth curve.	28
3.5	Flowchart for the proposed method to forecast installed WPG capacity	31
3.6	Comparison of installed wind power generation capacity of reported results with the results from proposed method (1991-2014).	34
3.7	Comparison of installed WPG capacity predicted by using conventional method and proposed method with actual data in India.	36
3.8	Variation of cumulative WPG capacity upto 2050 in India.	36
3.9	Variation of annual rate of increase of WPG capacity upto 2050 in India.	36
3.10	Comparison of installed WPG capacity predicted by using logistic method and proposed method with actual data in China.	38
3.11	Variation of cumulative WPG capacity upto 2050 in China.	38
3.12	Variation of annual rate of increase of WPG capacity upto 2050 in China.	39
4.1	Wind power density map at 50 m height (India)	44
4.2	Flowchart of proposed method for determining wind speed distribution	56
4.3	Flowchart for extrapolation of wind power density	58
4.4	Flowchart for estimation of capacity factor	60
4.5	Wind climate data measurement at 20 m (AGL) at site-I	62
4.6	Month wise variation of daily average wind speed at site-I (20 m)	63
4.7	Month wise variation of daily average temperature at site-I	63
4.8	Month wise variation of daily average relative humidity at site-I	64
4.9	Wind rose diagram at site-I (20 m)	64
4.10	Met mast installed at a height of 85 m AGL at site-II	67
4.11	Month wise variation of daily average wind speed at site-II (85 m)	68
4.12	Wind rose diagram at site-II (83 m)	69
4.13	Wind rose diagram showing distribution of wind speed in the prevalent direction at site-II	69
4.14	Month wise variation of daily average temperature at site-II	70
4.15	Comparison of proposed approach with other methods in estimation of pdf (site-II)	74
5.1	Overview of WindSim software simulation tool.	80

5.2	Flowchart for simulating wind farm using WindSim simulation software tool	82
5.3	Google map of site-II (vertical view).	84
5.4	Google map of site-II (horizontal view).	85
5.5	View of terrain and wind farm layout using WindSim simulation.	85
5.6	Power curve and thrust coefficient curve of wind turbine used for simulation.	86
5.7	Wind rose and frequency distribution with Weibull fitting for all sectors	87
5.8	Terrain elevation and roughness at site-II	88
5.9	schematic view of horizontal grid resolution and vertical grid resolution of site-II	89
5.10	Wind resource map with average wind speed at 85 m, site-II	90
5.11	Flowchart for simulating wind farm using Meteodyn simulation software tool.	94
5.12	Terrain data in-terms of orography and roughness at site-II	95
5.13	Wind rose and histogram of wind speed distribution at site-II.	96
5.14	Simulated average wind speed at hub height at site-II as obtained by using Meteodyn.	99
5.15	Simulated wind power density at hub height at site-II as obtained by using Meteodyn.	99
5.16	Flowchart for simulating wind farm using WindFarmer software.	103
5.17	Terrain and wind farm layout of site-II.	104
5.18	Wind speed and wind power density map at site II.	104
6.1	Schematic of Jensen wake model	112
6.2	Flow chart describing genetic algorithm for placement of wind turbines	116
6.3	Reported wind farm layout of 26 & 30 turbines	117
6.4	Reported wind farm layout of 32 & 30 turbines	117
6.5	Proposed wind farm layout of wind turbines consisting of 10 turbines. .	119
6.6	Proposed wind farm layout of wind turbines consisting of 20 turbines. .	119
6.7	Proposed wind farm layout of wind turbines consisting of 26 turbines. .	120
6.8	Proposed wind farm layout of wind turbines consisting of 30 turbines. .	120
6.9	Proposed wind farm layout of wind turbines consisting of 32 turbines. .	120
6.10	Flowchart for optimization of locations of wind turbine using WindFarmer software.	122
6.11	The optimization curve for wind turbine positioning at model wind farm	125
6.12	Wind speed and wind energy map at site-II	125
7.1	General schematic architecture of multi layer feed forward neural network	130
7.2	Different learning algorithms of ANN	131
7.3	Flow diagram of Back propagation of error	132
7.4	Monthly variation of average wind speed at site-II	134
7.5	Proposed neural network architecture for prediction of wind power generation	136

7.6	Flowchart describing BPA algorithm used for predictions of wind power generation	137
7.7	Flowchart describing FFNN-GA algorithm used for predictions of wind power generation	138
7.8	Comparison of actual and predicted data using GA for 10 % testing data	141
7.9	Comparison of actual data and predicted data using GA for 5 % testing data	141
A.1	Basic schematic of genetic algorithm cycle	149
C.1	Proposed wind farm layout of wind turbines consisting of 10 & 20 turbines using PSO	162
C.2	Proposed wind farm layout of wind turbines consisting of 26 & 30 turbines using PSO	162
C.3	Proposed wind farm layout of wind turbines consisting of 32 turbines using PSO	163
D.1	Basic structure of a artificial neuron	165

List of Tables

1.1	Installed capacity of wind power generation in leading countries as on December 2014	3
3.1	Cumulative installed generation capacity in India (1991-2014).	32
3.2	Assumed parameters of GA used in simulation of proposed method	33
3.3	Results obtained using reported values using logistic method.	33
3.4	Results obtained using proposed method for forecasting growth in installed WPG capacity.	33
3.5	Comparison of forecasted data with proposed method with actual data (1991-2014).	35
3.6	Comparison of logistic method with proposed method (1991-2014).	35
3.7	Cumulative installed wind power generation capacity in China.	37
3.8	Comparison of proposed method with conventional logistic method for forecasting growth in WPG in China.	37
4.1	The parameters and their assumed value for finding optimum values of k and c	57
4.2	Technical specifications of sensors used at site-I	62
4.3	Month-wise variation of statistical characteristics at site-I	65
4.4	Wind power classification on the basis of wind speed and wind power density at 50 m AGL	66
4.5	Month-wise variation of statistical parameters at Site-II	71
4.6	Month-wise variation of Weibull parameters and their associated statistical parameters using graphical method at site-II	72
4.7	Comparison of Weibull distribution methods to Rayleigh distribution method at site-II	73
4.8	Improvement in RMSE using proposed approach for site-II.	73
4.9	Variation of wind power density with height (AGL) at site-II	74
4.10	The wind turbine characteristics for wind turbine models for site-II	75
4.11	Estimation of capacity factor for wind turbine models at site-II	75
5.1	Location of wind turbine positions specified in terms of UTM coordinates at site-II	83
5.2	Specifications of wind turbine used at site-II	84
5.3	Average wind speed, frequency of distribution and Weibull parameters (shape, k and scale c) versus sectors	86
5.4	Coordinates, extensions and resolution of the DTM (site-II)	87

5.5	Grid spacing and number of cells used for simulation using WindSim (site-II)	87
5.6	Setting used for simulation using WindSim (site-II)	88
5.7	Simulation time, number of iterations and convergence status using WindSim (site-II)	89
5.8	Comparison of AEP and capacity factor with and without wake effect at site-II generated by WindSim simulation tool.	91
5.9	The wind farm production characteristics using WindSim at site-II.	92
5.10	Description of wind farm (site-II) for simulation using Meteodyn.	95
5.11	Wind speed distribution for 12 directional sectors at site-II	96
5.12	CFD directional calculations properties (site-II).	97
5.13	Variation of average wind speed, Weibull parameters and wind power density at site-II using Meteodyn	98
5.14	Comparison of AEP and capacity factor with and without wake effect at site-II generated by Meteodyn	100
5.15	The wind-farm production characteristics using Meteodyn for site-II	100
5.16	Comparison of AEP and capacity factor with and without wake effect at site-II generated by WindFarmer simulation tool.	105
5.17	The wind-farm production characteristics using WindFarmer at site-II.	106
5.18	Comparison of simulation softwares used for WRA	107
6.1	Wind turbine data assumed for simulation for position of turbines	115
6.2	Comparison of results obtained by researchers using GA and fixed position of wind turbines at centre of cell	117
6.3	Comparison of results obtained by the proposed approach using GA with variation of wind turbines.	118
6.4	Comparison of increase in efficiency with reported results.	119
6.5	Location of wind turbine positions specified in terms of UTM coordinates at site-II, before optimization.	123
6.6	Position of wind turbine in-terms of UTM coordinates after optimization.	124
6.7	Average wind speed, AEP without and with wake, wake losses, capacity factor after optimization using WindFarmer	126
6.8	Comparison of AEP and capacity factor (before and after) optimization at site-II using WindFarmer	126
7.1	Best results for BPA with variation of training data sets	140
7.2	Best results for GA with variation of training data sets	140
B.1	Month-wise variation of Weibull parameters and their associated statistical parameters using SD method at site-II	153
B.2	Month-wise variation of Weibull parameters and their associated statistical parameters using EPF method at site-II	154
B.3	Month-wise variation of Weibull parameters and their associated statistical parameters using MLE method at site-II	156
B.4	Month-wise variation scale parameter and its associated statistical parameters using Rayleigh distribution method at site-II	157

B.5	Best values of RMSE and R^2 from different distribution methods for site-II	159
B.6	Variation of wind power density with height (AGL) at site-II	160
C.1	Comparison of results obtained by the proposed approach using PSO with variation of wind turbines.	161
C.2	Increase in efficiency using PSO	162
D.1	Types of activation function in ANN	166
D.2	Variation of parameters of BPA for 80 % of input data for Training . . .	168
D.3	Variation of parameters of BPA for 80 % of input data for Training (contd.)	169
D.4	Variation of parameters of BPA for 90 % of input data for Training . . .	170
D.5	Variation of parameters of BPA for 90 % of input data for Training (contd.)	171
D.6	Variation of parameters of GA for 80 % of input data for Training . . .	172
D.7	Variation of parameters of GA for 80 % of input data for Training (contd.)	173
D.8	Variation of parameters of GA for 90 % of input data for Training . . .	174
D.9	Variation of parameters of GA for 90 % of input data for Training (contd.)	175

List of Acronyms

AGL	Above Ground Level
AEP	Annual Energy Production
AI	Artificial Intelligence
ANN	Artificial Neural Network
AR	Auto Regressive
ARIMA	Auto Regressive Integrated Moving Average
BPA	Back Propagation Algorithm
CWET	Center for Wind Energy Technology
CEA	Central Electricity Authority
CFD	Computational Fluid Dynamics
CDF	Cumulative Distribution Function
DTM	Digital Terrain Model
EPF	Energy Pattern Factor
EA	Evolutionary Algorithm
FFNN	Feed Forward Neural Network
GA	Genetic Algorithm
GP	Graphical Method
GWh/y	Giga Watt hours per year
GWEC	Global Wind Energy Council
GIS	Geographic Information System
IITM-FRU	Indian Institute Tropical Meteorology
IWTMA	Indian Wind Turbine Manufacturers Association
IEC	International Electrotechnical Commission

MLE	Maximum Likelihood Estimator Method
MAE	Mean Absolute Error
MSL	Mean Sea Level
MSE	Mean Square Error
MWh/y	Mega Watt hours per year
MNRE	Minstry of New and Renewable Energy
NIWE	National Institute of Wind Energy
NWP	Numerical Weather Prediction
PDF	Probalility Distribution Function
RDD	Rayleigh Density Distribution
RANS	Reynolds Averaged Navier Strokes Equation
RMSE	Root Mean Square Error
SRTM	Shuttle Radar Topography Mission
SD	Standard Deviation Method
TI	Turbulence Intensity
UTM	Universal Transverse Mercator
WDD	Weibull Density Distribution
WECS	Wind Energy Conversion System
WPD	Wind Power Density
WPG	Wind Power Generation
WRA	Wind Resource Assesement

List of Symbols

Symbol	Name	Unit
A	Swept area	m^2
a	Regression coefficient, location coefficient	
b	Regression coefficient, shape coefficient	
c	Weibull scale parameter	m/s
D	Diameter of rotor	m
f	Neuron activation function	
h	Desired height	m
k	Weibull shape parameter	
L	Upper limit of installed capacity	
N	Number of samples or observations	
P	Atmospheric pressure	mb
r	Down stream rotor radius	m
R	Universal gas constant	J/kgK
t	Air temperature	$^{\circ}\text{C}$
T	Air temperature	K
v	Desired wind speed	m/s
x	Down stream distance	m
Y	Limiting value of the output	
z	Hub height	m
e_1	axial induction factor	
c_R	Rayleigh scale parameter	m/s

C_f	Capacity factor	%
C_T	Thrust coefficient	
M_d	Molar mass of dry air	kg/mol
$f(V)$	Weibull probability density distribution function	
$F(V)$	Weibull cumulative density distribution function	
$f_R(V)$	Rayleigh probability density distribution function	
$F_R(V)$	Rayleigh cumulative density distribution function	
h_o	Known hub height of turbine	m
P_x	Wind power density at desired height	W/m ²
P_r	Wind power density at measured height	W/m ²
P_W	Power density at desired height	W/m ²
P_o	Power density at measured height	W/m ²
P_v	Vapour pressure	mb
P_d	Dry pressure	Pa
P_{sat}	Saturated pressure	Pa
P_{out}	Mean output power	W
P_{eR}	Rated electrical power	W
r_o	Radius of rotor	m
R^2	Correlation coefficient	
v_m	Average wind speed	m/s
v_i	Instantaneous wind speed	m/s
v_c	Cut in wind speed	m/s
v_r	Rated wind speed	m/s
v_f	Cut out wind speed	m/s
V_{mp}	Most probable wind speed	m/s
$V_{max,E}$	Wind speed carrying maximum energy	m/s
V_{mpR}	Most probable wind speed- Rayleigh	m/s
$V_{max,ER}$	Wind speed carrying maximum energy - Rayleigh	m/s
V_{mW}	Weibull average wind speed	m/s
V_{mR}	Rayleigh average wind speed	m/s
V_x	Wind speed at desired height	m/s

WPD_M	Measured wind power density	W/m^2
WPD_R	Rayleigh wind power density	W/m^2
x_i	Estimated data	
x_{norm}	Normalized data	
x_{min}	Minimum value of data	
x_{max}	Maximum value of data	
$X_{O,i}$	Observed values	
$X_{m,i}$	Predicted values	
y_i	Measured data	
z_i	Mean value	
z_o	Surface Roughness	
ρ	Air density	kg/m^3
ρ_h	Activation function	
ρ_{RH}	Air density with relative humidity	kg/m^3
ϕ	Relative humidity	
σ	Standard deviation	m/s
Γ	Gamma function	
α	power law index exponent	
β	Entrainment constant	
δ_k	Error at output neuron	
η	Rotor efficiency	%
η_T	Total efficiency	%
η_L	Learning rate	
τ	Epoch	
Δ	Gradient	

Chapter 1

Introduction

Wind energy is the one of the most commercialized renewable energy sources. However, the increasing of renewable energy source, in particular, wind energy conversion systems (WECS) in the conventional power system has posed tremendous challenges to the power system operators and planners, responsible for reliable and secured operation of the power grid. As power generation using WECS continues to increase manifolds in future, several researchers have investigated effects of grid-integrated wind power generating systems on overall stability of the power system.

It is noted in the literature [1] that wind speed, wind direction and wind wake have significant effect on energy production in an operational wind farm at a given location. The effect of terrain at the site and the wind farm layout are required to be known at the design stage. These requirements necessitate use of computer models for predicting or forecasting the performance of wind farms. It is important to know the effect of these factors on overall performance of wind farms in terms of power production for appropriate operation of grid-connected wind farms. The effect of these factors on available wind resource in a given time interval can be investigated through statistical analysis. The results of such analysis can often be useful in forecasting overall performance of wind farm.

Thus, there is emerging need to develop heuristic techniques using statistical approaches for investigating the effects of these parameters on the available wind resource in a region of interest. Several researches have used heuristic techniques for developing science and engineering applications including wind energy development. The present-work focuses on using artificial intelligence techniques for improving accuracy and efficiency of conventional methods.

1.1 Application of Heuristic Techniques in Wind Power Development

The conventional energy sources, including coal, fossil fuels and nuclear fuels, produce deleterious emissions and byproducts, which are unfriendly to the environment. It is well known that use of these fuels for energy produces emissions such as airborne particulate, carbon monoxide, hydrocarbons, hydrochloric acid, solid ash and waste, ionizing radiation and trace elements that affect environment.

Renewable energy sources are known to provide solution to the aforementioned problems. Among the renewable energy sources, wind energy source has rapidly matured as source for power generation. Wind energy has emerged as clean, affordable, inexhaustible and environment friendly source of energy.

Wind power is harnessed by converting the kinetic energy in the wind to mechanical energy and then to electrical energy. The blade of wind machines derives its rotational energy from the kinetic energy of the wind and moves a prime mover involving gear system thus converting the wind energy to mechanical energy. The shaft torque drives a generator to produce electric power. It has been claimed that efficiency of conversion of kinetic energy of wind to mechanical energy is reported as 59.3 % [2, 3].

As the wind power is proportional to the cube of wind speed, a detailed knowledge of the site-specific wind characteristics becomes critically important. The actual power production by grid-connected wind farm depends on wind speed and production hours. In

a grid-connected wind farms, the power produced as well as quality of power must comply with series of International Electro-technical Commission (IEC) standards [4].

As the penetration level of wind power in power systems increases, it becomes important to predict the behavior of wind farms [5, 6]. The overall performance of the grid-connected wind farm is required to be predicted in view of wide variation of different factors such as wind speed, wind direction, wind wake etc. For this purpose heuristic techniques such as artificial neural networks, genetic algorithm, particle swarm optimization, are proposed to be used.

1.2 Challenges in Wind Power Generation

Globally installed capacity of wind power generation (WPG) has crossed 369553 MW [7]. In India, total installed capacity of 254 GW of electricity generation is recorded as on 31 December 2014, consisted of about 31791 MW [8] from all renewable energy sources and about 22465 MW from wind energy [9]. India ranks fifth in wind power installed capacity, with China leading with installed wind power generation capacity of 114763 MW. Table 1.1 shows installed wind power generation capacity in five leading countries [7]. The wind-power programme in India was started at the end of the

Table 1.1. Installed capacity of wind power generation in leading countries as on December 2014 [7]

S.No.	Country	Installed generation capacity (MW)
1	China	114763
2	USA	65879
3	Germany	39165
4	Spain	22987
5	India	22465

sixth five year plan, in 1983-84 by the Government of India. A market-oriented strategy was adopted from inception, which has led to the successful commercial development of the wind-power programme in India [10]. The programme includes wind resource assessment, implementation of demonstration projects to create awareness, opening up

of new sites, involvement of utilities and industry, development of infrastructure capability, installation, operation and maintenance of wind turbine generators and policy support. In early years, the wind resource assessment campaign was implemented through the state nodal agencies by the field research unit of Indian Institute of Tropical Meteorology (IITM-FRU), Bengaluru, India. Since 1998, Centre of Wind Energy Technology, CWET, Chennai, India has been conducting assessment of wind resources at 50 m height above ground level (AGL). CWET has also been conducting campaign for WRA at 80 m height (AGL). Recently, CWET has been renamed as National Institute of Wind Energy (NIWE).

In India, the installed capacity of wind power generation has reached 22465 MW at the end of the year 2014, against the estimated wind power potential of 49130 MW at 50 m (AGL) [11]. The corresponding re-assessed wind power potential at 80 m (AGL) is 102788 MW [11]. It is important to continue to re-assess available wind resource at wind farms for various reasons including concurrent advancement in wind power generation technology.

Several researchers have investigated a wide ranging concerns related to grid-integrated WECS [12–15]. It is noted in literature that the knowledge of variation in dynamic characteristics of wind resource at the site will be essential pre-requisite for developing strategies to overcome and/ or prevent grid-failures. The grid-connected wind farm is required to be monitored for its possible dependence on variable wind resource with respect to variations in wind farm output, variations in real and reactive power flow from / to grid, variations in output frequency and voltage.

Several researchers have attempted investigating effect of variation of wind speed at a location. The effect of wind speed on active and reactive power in a grid-connected WECS is investigated by Panda *et al.* [13]. Three different types such as constant, linear and random changes of wind speeds are considered for this study. It is concluded that active power generated by the wind turbine induction generators (WTIGs) depends on wind speed and the reactive power consumption varies with the variation in active power generation. Linh *et al.* and Melico *et al.* [14, 15] have investigated effect of variation of wind speed on quality of wind power generated in terms of harmonics, flicker and

voltage variations. Their results show that sudden variation in speed leads to increase in the flicker emission and power variation, which in turn lead to grid instability.

Since wind power production is dependent on the wind speed, the output of a turbine and wind farm varies over time under the influence of meteorological fluctuations. These variations occur on all time scales: by seconds, minutes, hours, days, months, seasons and years. Understanding and predicting these variations at a site is critically important for successful integration of wind power into the power system. Thus researchers should make efforts to develop improvised heuristic approaches using computer simulation models to predict, forecast and validate effect of variability of wind resource at a site on short-term as well as long-term performance of grid-integrated wind farms. The techniques developed will be useful for simulation as well as evaluation of prospective sites for installing future wind farms.

1.3 Scope and Objectives of Research Work

In view of above, the objectives of the present work are as follows:

1. To develop improvised heuristic technique for forecasting installed wind power generation capacity in a region.
2. To develop improvised heuristic technique for estimation of wind resource potential in a region for wind power development.
3. To investigate effect of terrain on performance of existing wind farm using industry scale computer simulation tools.
4. To develop improvised heuristic technique for optimizing the position of wind turbine in the wind farm.
5. To develop improvised heuristic approach for prediction of power generated in a wind farm over short term as well as long term.

1.4 Organization of Thesis

The thesis is organized as follows:

Chapter 2: In this chapter, a detailed literature survey is presented on prediction of growth in wind power generation capacity, wind resource assessment, application of heuristic techniques for wind power development and conclusions are presented.

Chapter 3: In this chapter, improvised heuristic approach using genetic algorithm and logistic function is developed for forecasting the increase in installed wind power generation capacity in the context of two leading nations in wind power development, namely, China and India. The results obtained using the new method are compared with those obtained using conventional logistic function method to demonstrate superiority of the new method over conventional method.

Chapter 4: In this chapter, most widely used statistical methods namely, Weibull probability distribution function and Rayleigh probability distribution function for determining of wind power distribution at a given site are described. These methods are functions of two parameters, namely, shape parameter and scale parameter. These parameters are determined by using four different statistical methods, namely, graphical method, standard deviation method, energy pattern factor method and maximum likelihood method. The methods are used for determining the parameters for the two sites, namely, Goa campus (site-I) and model grid integrated wind farm, Periyapatti, Tamilnadu (site-II), where data is measured at two or more different heights. The accuracy of wind speed distribution determined by Weibull distribution function and Rayleigh distribution function, is measured in-terms of root mean square error with respect to observed wind speed distribution. Further, in an effort to improve the accuracy of determining distribution of wind speed using these methods, an improvised method for determining optimum values of shape parameter and scale parameter, using genetic algorithm is developed. The effect of air density on wind power density of the site is also investigated.

Chapter 5: In this chapter, accuracy of estimating annual energy production and capacity factor is compared for three different software tools, namely, WindSim, Meteodyn

and WindFarmer. The effect of terrain is also taken into account for estimation of annual energy production and capacity factor at a site representing complex terrain.

Chapter 6: In this chapter, an improvised technique is developed for recommending optimum location of wind turbine in a wind farm corresponding to maximum power output and minimum wake effect. The technique allows designer to search optimum location of wind turbine corresponding to maximum power generation and minimum wake effect. The results obtained using improvised technique are compared with the results reported by researchers. Further, in this chapter, “WindFarmer” software is used for searching optimum positions of wind turbine in an existing grid-connected wind farm. The results show that the optimum positions determined by “WindFarmer” software are different than the actual positions of the wind turbines in the existing wind farm.

Chapter 7: In this chapter, an improvised technique for predicting wind power production in a wind farm is presented. The researchers in the past have used feed forward artificial neural network to predict wind power generation and used back propagation algorithm as learning algorithm in ANN by prefixing parameters of algorithms. Genetic algorithm is proposed in conjunction with artificial neural network for prediction of wind power generation. The parameters prefixed for back propagation algorithm are learning rate and momentum coefficient. The parameters affect the performance in genetic algorithm are elite count, crossover fraction and number of generations. In the present work, results are obtained by varying values of these parameters for both the algorithms. The effect of variation of values of these parameters in practical ranges on prediction of wind power generation is investigated. The effect of number of neurons in the hidden layer on predicted power generation is also investigated. The chapter concludes with results of investigation of prediction of wind power generation.

Chapter 8: The chapter presents conclusions of the research work in the thesis and scope for future work.

Chapter 2

Literature Survey

In this chapter, an account of survey of relevant literature reported by the researchers in recent years, is presented. The insights gained through literature survey, have been used to identify scope for improvising methods of statistical analysis and modeling for forecasting, estimation and prediction of wind resource potential and power generated at a given site.

2.1 Forecasting Growth in Installed Wind Power Generation Capacity

Carolin *et al.* [16] developed a method to forecast growth of installed capacity of wind power generation. They have used logistic function-based method to forecast cumulative installed wind power generation (WPG) capacity in a year. They have used data available on installed WPG over past 15 years (i.e.,1991 to 2006) for five different states in India and India as a whole. They have forecasted that the WPG capacity would reach 34,524 MW, 46520 MW and 50353 MW by the end of year 2015, 2020 and 2025, respectively. Further, it is forecasted by authors that about 99 % of available wind potential in India will be exploited by the year 2030 when the WPG capacity would reach 51249 MW. It is noted that whereas authors had forecasted that WPG capacity

in India would reach 30875 MW by 2014, actually installed WPG capacity in India is 22465 MW. This indicates that, the method over estimates the installed WPG capacity.

Ishan *et al.* [17] also used logistic function based method to project WPG capacity for six states in India and for India as a whole. They have used data on wind power generation installed capacity over 18 years (i.e., 1991 to 2009). They have forecasted that the WPG capacity would reach approximately 11531 MW by the end of the year 2020, whereas the installed WPG capacity is already 22465 MW in the year 2014. This indicates that, the method under estimates the installed WPG capacity.

However, the actual installed capacity in India as on Dec 2014 is about 22465 MW, indicating that there is scope for improvising conventional logistic function-based methods, used in [16] and [17] for improving accuracy of forecasting installed WPG capacity.

2.2 Methods of Wind Resource Assessment

Wind resource assessment (WRA) at a prospective wind farm site is the first step in developing a wind farm project at a site of potential for power generation. The economic viability of wind farm project is largely determined by accurate estimates by potential for wind power generation. The economic viability of wind power project determines bankability of the project. In recent times researchers have reported the need to improvise the methods for improved accuracy in estimation. Panda *et al.* [13] have investigated the effect of wind speed on active and reactive power penetration to the distribution network. It is shown that active power generated by the wind turbine generators depends upon wind speed and the reactive power consumption varies with the variation in active power generation. Nguyen *et al.* [14] have shown that the power quality problems are due to the variations in wind speed. The increase in turbulence leads to increase in the flicker emission and power variability, which in turn lead to severe impact on wind turbines and grid integration. Vanitha *et al.* [18] investigated the effect of wind speed on power quality issues. They have reported that, the real power and reactive power generated fed and into grid and power factor, which largely determine

quality of the power and stability of power system are all functions of wind speed at the site.

In this section, results of survey of work reported by researchers on different statistical methods for determining distribution of wind speed probability over wind speed namely, Weibull probability density distribution [19–34, 34–46], Rayleigh probability density distribution [47–50] and log normal distribution [51] are presented.

2.2.1 Weibull Probability Density Distribution Method for Determining Distribution of Wind Speed

Weibull probability density distribution method is the widely used method by researchers for determining wind potential at a site. In this method, the analytical expression requires user to define two empirical parameters, namely, shape parameter (k) and scale parameter (c). The accuracy of estimation is largely determined by accuracy of determining k and c . It has been shown that normally empirical values of k ranges from 1.5 to 3.5 and empirical values of c is about 1.2 times the annual average wind speed at the site. Thus depending on the values of k and c , chosen in a case, the wind speed probability distribution characteristics for the site is determined. When the values of k the shape parameter is chosen to be equal to 2 the original Weibull distribution function is called as Rayleigh wind speed probability distribution function. Thus, the Rayleigh wind speed probability distribution function is considered as a special case of Weibull wind speed probability distribution function. In order to determine the parameters of Weibull probability density distribution function, different methods namely, graphical method [19–27], standard deviation method [28–39], energy pattern factor method [40–42], maximum likelihood method [43–46] and modified maximum likelihood method [52–58] have been used by researchers.

2.2.1.1 Graphical Method for Determining Parameters of Weibull Probability Density Distribution Function

Researchers [19–27] have used graphical method (GP) to determine Weibull parameters. Ulgen *et al.* [19] used wind speed data obtained at height of 15 m AGL over a period of five-years (i.e.,1995 to 1999) to determine Weibull parameters for Izmir, a region in Turkey. They reported that Weibull distribution function is found to give accurate better fitment with the actual data than the Rayleigh distribution function. Results obtained by authors [20–22] also concludes the same observations. Youm *et al.* [20] analyzed two year wind data (1998 to 1999) at five different locations for the region of the northern coast of Senegal along the Atlantic Ocean. Akpinar *et al.* [21] have used hourly data recorded at a height of 10 m (AGL) over a period of 6 years in four different regions in Turkey for estimation of Weibull parameters using graphical method. They reported that method is found to be more accurate method in distribution of wind speed. Odo *et al.* [22] analyzed the wind data collected at 10 m AGL to estimate energy potential at Enugu, Nigeria employing 13 years (1995 to 2007). They reported that the graphical method is accurate in estimation of wind speed distribution.

Ganeshan *et al.* [23] have used the hourly data obtained at two different heights of 50 m and 70 m measured over a period of one year from 2004 to 2005 to estimate Weibull parameters for a region in Bhopal, India. Issac *et al.* [24] used hourly wind speed data consisting of thirty years from 1968 to 1997 to determine Weibull parameters for three different locations, namely, a city area, an extremely exposed area and an open sea area, in Hong Kong. Jing *et al.* [25] also used a long-term data measured over 15 years data from 1986-2000 to determine Weibull parameters for two different regions in Fujian province, China. They reported that WDD function using GP method fitted the measured data more accurately. Similar observations are reported in [26, 27]. Fadare [26] used ten years data from 1995-2004 to estimate Weibull parameters for analyzing wind energy potential of a region in Nigeria. Jamdade *et al.* [27] have used five years data i.e.,2007 to 2011, measured at a height of 50 m AGL to analyze the wind potential in four different regions in Ireland, namely, Malin head, Dublin airport, Belmullet and

Mullingar. They reported that the method employing graphical method estimates the wind speed distribution function accurately.

2.2.1.2 Standard Deviation Method for Determining Parameters of Weibull Probability Density Distribution Function

In order to determine the Weibull parameters, standard deviation (SD) method has been used in [28–39]. Celik used one year data measured at a height of 5 m AGL during 1996 to determine Weibull parameters for the region Cardiff, UK [28]. Similarly, one year data-based analysis is reported in [29–33]. Their work concluded that SD-based WDD function leads to accurate fitment of the measured data. Researchers have carried out WRA in Grenda (West Indies), four different locations in Indonesia and Algeria, respectively [29–31]. Kumaraswamy *et al.* have used Standard deviation method to estimate Weibull parameters for Chitradurga, Karnataka, employing the wind speed data obtained at a height of 50 m AGL and 40 m AGL, respectively [32] and [33]. Celik has used one year data for finding Weibull parameters to estimate the wind energy potential in the region of Iskenderun, Turkey. The results obtained using standard deviation method are compared with those obtained using Rayleigh distribution. They reported that Weibull distribution is accurate method compared to Rayleigh distribution method [34]. The same analysis is carried out by researchers in [35–39] and reported that Weibull distribution is accurate method compared to Rayleigh distribution method.

2.2.1.3 Energy Pattern Factor Method for Determining Parameters of Weibull Probability Density Distribution Function

Energy pattern factor (EPF) method, to determine the Weibull parameters is reported by researchers in [40–42]. Seyit *et al.* [40] introduced EPF method also known as power density method to determine Weibull parameters for four different regions, namely, Maden, Gokceada, Canakkale and Bozcaada in Turkey [40]. Ugur *et al.* [41] and Yuyu *et al.* [42] also used the same method and they have reported that method is found to be accurate in estimating the wind power density (WPD).

2.2.1.4 Maximum Likelihood Method for Determining Parameters of Weibull Probability Density Distribution Function

Maximum likelihood (MLE) method [43–46] uses an iterative procedure to determine Weibull parameters unlike aforementioned three methods. Kaoga *et al.* [43] have used MLE method on a six year data measured over 2007 to 2012 of north region of Cameroon to determine Weibull parameters. The MLE method is reported to provide accurate results as reported in [44, 45]. A comparative study for determining Weibull parameters is carried out and they have reported that the results obtained using the MLE method are in good agreement with the measured data when compared to Rayleigh distribution method [46].

Comparison of Methods for Determining Parameters of Weibull Distribution:

Seguro *et al.* have used three methods for Weibull parameters, namely, graphical, maximum likelihood and modified maximum likelihood methods are used to study WRA and the results are compared [52]. They have reported that the MLE method is accurate method when the wind speed data is available in time-series format. On the other hand, when the data is available in the frequency distribution format, the modified MLE method is recommended.

Genec *et al.* and Bagiorgas *et al.* compared the three different methods, namely, graphical, standard deviation and maximum likelihood method. They have reported that all the methods yields results in close agreement with the measured data [59, 60]. Mukut *et al.* [61] have used Weibull methods namely, graphical, standard deviation and energy pattern factor are compared with Rayleigh distribution methods. They reported that all the Weibull methods are in close agreement with the measured data than the Rayleigh distribution method.

Odo *et al.* [62] used graphical, standard deviation and energy pattern factor methods to determine Weibull parameters and it is reported that the standard deviation method is more accurate method. Similar observations are reported in [53, 63]. Seyit *et al.* [40] analyzed wind power potential in a region of Turkey. They reported that energy pattern

factor method is more efficient when compared to graphical, standard deviation and maximum likelihood method. Similar observations are reported in [54–56].

Tian *et al.* [57] have used different methods such as moment, empirical, graphical, maximum likelihood, modified maximum likelihood and energy pattern factor to estimate Weibull parameters. They reported that maximum likelihood method provides more accurate estimation of Weibull parameters. Paulo *et al.* [58] have used numerical methods, namely, graphical, empirical, moment, energy pattern factor, maximum likelihood, modified maximum likelihood and equivalent energy method for determining Weibull parameters. They have reported that the maximum likelihood method is an accurate method for determining Weibull distribution. From the above, it is observed that there are different methods for determining Weibull parameters, however these methods varies from data and site.

Rayleigh distribution function method:

The another widely used distribution function which is extensively used in modeling of the site wind speed is the Rayleigh distribution function. Rayleigh distribution function is a special case of Weibull distribution where the scale parameter, k , has a fixed value of $k = 2$. This function is found to typically model the wind speed at some sites where the Weibull function could not accurately model. This method also used to find wind speed distribution to fit the measured data accurately for some of the sites as reported in [47–49, 64, 65].

2.2.2 Method for Estimation of Capacity Factor of Wind Farm

Wind energy conversion system can operate at maximum efficiency depends on wind characteristics at the site such as the rated power, cut-in and cut-out wind speeds [66]. The capacity factor is defined as the ratio of the mean power output to the rated electrical power of the wind turbine [66, 67]. The performance of a wind turbine installed in a given site can be examined by the amount of mean power output over a period of time and the conversion efficiency or capacity factor of the turbine.

Dursun *et al.* [68] used hourly data recorded for a period of two years, 2006 to 2008 to determine the wind energy characteristics of four different regions, namely, Gonen, Bandirma, Dursunbey and Ayvalik in Turkey. The highest capacity factor is obtained as 42 % for Bandirma region with Vestas V90-1.8 MW wind turbine. The lowest capacity factor is obtained as 14 % for the Dursunbey region. Similar study has been carried out by Akpinar [69] for the four regions namely, Elazig, Maden, Agin and Keban in Turkey. Maden is found to be best site for the wind generation as the capacity factor is maximum for this site [69].

Muyiwa *et al.* [70] examined the wind energy potential and the economic viability of using wind turbine for electricity generation in six selected sites along the coastal region of Ghana. Four different turbines are considered in this study. The capacity factors are calculated and it is shown that the coastal region is suitable only for small scale application. A similar study has been carried out by Oyedepo *et al.* [71] for three selected locations (Enugu, Owerri and Onitshain) of Nigeria and they reported that the highest capacity factor is found to be Enugu site.

Ohunakin *et al.* [72] carried out wind turbine performance assessment and economic analysis of selected commercial WECS are examined across all geopolitical zones in Nigeria. It is found that the capacity factor has the least value in Uyo, 0.22 %, with GEV-HP turbine at 70 m hub height and the highest value in Kano, 89.8 %, with G3120 model at 42.7 m hub height. Himri *et al.* [73] analyzed the wind power potential for three locations Adrar, Timimoun and Tindouf in Algeria and reported that capacity factors are found to be 38 %, 30 % and 21 %, respectively.

2.2.3 Methods for Estimation of Wind Power Density at Different Heights Above Ground

The wind speed is usually measured at meteorological heights typically 10 m or even less. But the wind turbines are installed at greater heights, typically at or above 50 m. It is of the interest to know the wind speed and wind power density at different heights as technology for installing wind turbine heights above 50 m has become available. Two

analytical methods namely, log law and power law are used to estimate wind speeds at higher heights [74–77]. Power law method is preferred as it is proved to be more accurate than log law [47, 50, 69, 78].

Various software, namely WindSim, Meteodyn and WindFarmer have become available for wind resource assessment. Leroy [79] tested the WindSim program with the experimental data of Askervein Hill in 1999 and pointed out that results would change significantly with the grid spacing and grid refinement. Wallbank [80] investigated the difference between linear modeling and non-linear modeling using WindSim program in 2007. In order to validate results, the measurements collected from erected masts in complex terrain are utilized. Gravidahl *et al.* [81] presented the validation study of Bolund experiment with WindSim program in 2011. Terrain and roughness data are taken into account in the analysis. Gravidahl studied the parameter sensitivity on numerical field modeling and the AEP in 2007 [82]. To avoid this conflict, CFD gets accurate results. Smooth and complex terrains are selected in that study. Besides, Gravidahl [83] carried out the test validations for optimized micro siting. Several wind farm sites in Europe are investigated according to different grid resolutions. Gravidahl *et al.* [84] considered wake modeling to determine the wind turbines to be erected properly. Improvement in AEP was observed remarkably. Simisiroglou and Fallo used WindSim program to determine AEP estimation and wake effects, in a wind farm installed in complex terrain in Greece and Central Italy, respectively [85, 86].

From the above survey of literature, it is observed that the most widely used methods for charactering the site are Weibull and Rayleigh distribution method.

2.3 Methods for Optimizing Wind Farm Layout

The design of wind farm layout is of critical importance for ensuring the profitability of a wind farm project in long term. A poorly layout of wind farm would lead to lower wind power capture and increased maintenance cost. The design of wind farm depends on several factors such as maximum desired installed capacity of the wind farm, site constraints, noise assessment, visual impact and the total cost. The objectives of a wind

farm design are to maximize the power production and reduce the total cost associated with the wind farm.

The technique used for designing of the layout of a wind farm often called as “micro-siting”. When a wind turbine extracts power from the wind, it generates a “wake” of turbulence that propagates downwind, so that the wind speed and the power extracted by the turbines are reduced. In large wind farms, wake effects lead to considerable power loss and thus it is desirable to minimize them in order to maximize the expected power output.

The primary concern is to develop an efficient algorithm which can generate the optimal layout of the turbines in the wind farm that corresponds to maximum power output at least cost. Wind turbine wakes have been studied for many years and various models have been developed by researchers. These models can be divided into two main categories, namely, analytical wake models and computational wake models. An analytical wake model characterizes the wind velocity in wake, by a set of analytical expressions, whereas, in computational wake models, fluid flow equations, are solved to obtain the wake velocity field.

Jensen presented model, based on global momentum conservation in the wake downstream of the wind turbine. The author has explained basic principle regarding wake effect, mathematical equations describing the effect in a wind farms and between turbines [87].

Mosetti *et al.* [88] and Grady *et al.* [89] have used GA approach obtaining optimum positions of wind turbines in a wind farm. Jensen wake model has been used for the analysis.

Emami *et al.* [90] also used GA approach for optimal positions of wind turbines in wind farm. Marmidis *et al.* [91] proposed Monte Carlo simulation method for the optimal placement of wind turbines. Evolutive algorithm has been used in [92] to optimize the wind farm layout. Carlos *et al.* [93] proposed a new viral based optimization algorithm for optimizing the placement of wind turbines in wind farms.

Peng-Yeng *et al.* proposed a Greedy randomised adaptive search procedure-variable neighborhood search algorithm for the optimal placement of wind turbines [94]. A binary particle swarm optimization with time-varying acceleration coefficients has been used in for optimal placement of wind turbines within a wind farm [95].

2.4 Methods for Prediction of Wind Power Generation

The unpredictability of wind and the possible sudden loss of wind generation is a serious concern among grid integrated wind farm operation as this increases the cost of integrating wind energy into the existing power system. The wind power predictions help the power system operators to schedule the spinning reserve capacity and to manage the grid operations. In addition, wind power prediction plays an important role in the allocation of balancing power. Besides, wind power prediction is used for the day-ahead scheduling of conventional power plants and trading of electricity on the spot market. Various method such as physical, statistical, artificial intelligence (AI) and hybrid methods [96–99] are used for wind power prediction.

2.4.1 Method for Prediction using Physical Approach

The physical method aims at estimating the wind data by numerical weather prediction (NWP) methods, therefore the input variables will be the physical or meteorology information. The physical method needs a detailed physical consideration of terrain to give a good prediction precision. It is usually used for long term prediction.

Several physical models have been developed for wind speed forecasting and wind power predictions. In addition to the weather data, these models take into account effect of several factors such as obstacles, local surface roughness, effects of orography, speed up or down, scaling of the local wind speed within wind farms, wind farm layouts etc. On wind speed, collecting the information such as terrain conditions is one of the major difficulties in the implementation of physical models [100]. Since NWP models

are complex mathematical models, they are usually run on super computers, which limits the usefulness of NWP methods for on-line or very-short-term operation of power system. In other words, meteorological models with high resolution are often more accurate but require high computation time. An unstable atmospheric situation can lead to very poor numerical weather predictions and thus leads to inaccurate predictions [101].

2.4.2 Statistical Approach for Prediction of Wind Power Generation

The statistical methods include the Auto Regressive (AR), Auto Regressive Moving Average (ARMA), Auto Regressive Integrated Moving Average (ARIMA) and Bayesian approach [98]. Statistical methods can be used to solve the problems in engineering, economics and natural sciences, when large volume of data on interdependent variables is available.

The ARIMA model comprises three components, i.e., autoregressive, integrated and moving average. ARIMA model is data independent. Milligian *et al.* have been employed several statistical ARMA models to predict both wind speed and wind power output in hour-ahead markets [102]. The authors in [103] predicted the hourly average wind speed up to 1-10 hours in advance by using ARMA models. Wang *et al.* employed ARMA for short term wind speed forecast based on historical wind speed data [104]. Miranda *et al.* developed a statistical method that use Bayesian framework to model the wind speed time series as an AR process, where the Markov Chain Monte Carlo simulation is used to estimate the model parameters [105]. Erdem *et al.* have used four different versions of ARMA method for forecasting wind speed and direction. The authors concluded that the component model is better for predicting the wind direction than the traditional-linked ARMA model, whereas for the prediction of wind speed the ARMA model is accurate than the component model [106].

Kavasseri *et al.* [107] used fractional-ARIMA models to forecast wind speeds on the day-ahead (24 hours) and two-day-ahead (48 hours) horizons. The models are applied to wind speed records obtained from four potential wind generation sites in North

Dakota. The forecasted wind speeds are used in conjunction with the power curve of an operational turbine to obtain corresponding forecasts of wind power production. The forecast errors in wind speed/power are analyzed and compared with the persistence model. Results indicate that significant improvements in forecasting accuracy are obtained with the proposed models compared to the persistence method. Ramirez-Rosado *et al.* used fractional-ARIMA models to model and forecast hourly average wind speeds [108]. The forecasted meteorological variable values obtained from a numerical weather prediction model and electric power-generation registers from the SCADA system of the wind farm are used for the analysis.

2.4.3 Artificial Intelligence-based Approach for Prediction

Recently, with the development of artificial intelligence (AI), various new AI methods for wind speed and power prediction have been developed. The new developed methods include artificial neural network (ANN), adaptive neuro-fuzzy inference system, fuzzy logic, support vector machine, neuro-fuzzy network and evolutionary optimization algorithms [99].

Artificial neural network basically involves learning the relationship between inputs and outputs by a non-statistical approach. It does not require any predefined mathematical models. The different ANN models are multilayer feed forward neural network (FFNN) and recurrent neural network (RNN) [97, 98]. ANN based methods also include back propagation neural networks, recurrent neural networks, radial basis function (RBF) neural networks, ridgelet neural network and adaptive linear element neural network.

Anurag *et al.* [109] two wind forecasting methodologies namely, FFNN (employing back propagation algorithm) and RNN are employed to forecast daily and monthly wind speed time series in India. It is shown that both FFNN and RNN perform better than the traditional statistical (ARIMA) model [109]. Rohrig *et al.* [110] have used ANN to predict day-ahead wind power in Germany. For training, measured wind power data is used to learn physical coherence of wind speed and wind power output. The advantage of ANN application is that it can easily use additional meteorological data, such as air

pressure or temperature, and power curves of individual plants to improve the accuracy of the forecasts [110].

The authors [111, 112] have used a method based on FFNN to predict the average hourly wind speed and wind power respectively. Fernandez *et al.* [113] also predicted wind power in some regions of TamilNadu using ANN Techniques. The model accuracy is evaluated by comparing the simulated results with the measured values at the wind farms and is found to be in good agreement.

Wang *et al.* [114] used ANN-based predictor to predict wind speed, which can be mathematically modeled as a highly nonlinear random process [114]. The whole process of analysis is divided into two parts ANN for predicting short-term value and the results are obtained according to the long term pattern. The authors compared the results with those obtained from linear regression approaches. From the experimental results, the authors concluded that the prediction-modification process improves short-term as well as long-term predictions.

Carolin *et al.* [115] have reported results of FFNN model based on back propagation algorithm to predict the wind energy at a site in Tamil Nadu for a period from April 2002 to March 2005. The input variables for the developed ANN have been selected as monthly average wind speed, monthly average relative humidity and monthly generation hours. The output variable is the wind energy output of wind farms. They have implemented FFNN with back propagation algorithm using MATLAB toolbox to develop the energy yield prediction model. The architecture with one hidden layer with four neurons is used in the analysis. The logarithmic sigmoid function is used in the hidden layer and linear activation function is used at the output layer. 3–4–1 architecture, 3 neurons in input layer, 4 neurons in hidden layer and 1 neuron in output layer was chosen. From the results, the authors concluded that the predicted wind energy output using ANN model shows a good agreement with the actual values. Damousis *et al.* [116] have presented a fuzzy expert system that forecasts the wind speed and generated electrical power.

2.4.4 Hybrid Approach for Prediction

Lei *et al.* [96] reviewed various models for wind speed and wind power prediction. The authors concluded that the new methods using artificial intelligence and mathematical technique when combined give more accurate results than the conventional methods.

Kani *et al.* [117] carried out short term wind speed forecasting employing ANN in conjunction with Markov Chain approach. In [118], the application of hybrid intelligent systems for short term wind power forecasting has been discussed. A hybrid model based on the combination of Wavelet transform and ANN is used in [119, 120]. Potter *et al.* [121] used an adaptive neuro-fuzzy inference system for very short-term wind power prediction.

Sideratos *et al.* [122] studied a combination of neural networks and fuzzy logic techniques for accurate estimation of wind farm output. Jursa *et al.* [123] used two optimization algorithms, namely particle swarm optimization and genetic algorithm for short-term prediction of wind power.

Shi *et al.* [124] proposed two hybrid models, such as, ARIMA-ANN and ARIMA-SVM, for wind speed and power forecasting. These hybrid approaches are shown to be viable options for forecasting both wind speed and wind power generation time series, but they do not always produce superior forecasting performance for all the forecasting time horizons investigated.

Shiet al. [125] also used a hybrid forecasting model which is a combination of least squares support vector machine and Radial basis function neural networks (RBFNN) is used to predict wind speed and wind power. From the above, it is observed that most efficient and accurate technique used for prediction of wind power is the artificial neural network. However, the accuracy can be improved by variation of parameters of learning algorithms.

2.5 Conclusion

The survey of literature as presented in above sections clearly shows that

1. There is scope for improving accuracy of conventional logistic function method when used for predicting growth in installed wind power generation capacity.
2. The Weibull and Rayleigh distribution functions are widely used for characterizing the wind power potential at a prospective site. The accuracy of characterizing a site can be further enhanced by variations of relative humidity at a site.
3. Genetic algorithm is widely used technique to determine optimum layout of a wind farm. Researchers in the past have tried optimization of layout of wind farm by considering the land for wind farm to be consisting of square cells. Further in their work, they have assumed that the turbines are always placed at the center of the square cell. However, under actual site conditions it may not be possible to place the turbines at the center of the square cell. In such cases, it becomes necessary to find out the effect of placing wind turbines at any other point in the square cell of the land. For this purpose, appropriate heuristic technique should be developed.
4. Researchers have used artificial intelligence techniques employing different learning algorithms for prediction of wind power in a grid-connected WECS. The use of hybrid approaches are also proposed for this purpose. However, it is noted that the parameters in the learning algorithms are taken as default values or fixed values on a trial and error basis. Thus, there is scope for developing method of choosing optimized values of these parameters of learning algorithms for prediction of wind power thereby improving accuracy of prediction.

In the following chapters, heuristic methods are proposed for addressing above requirement.

Chapter 3

Forecasting Wind Power Generation Capacity

3.1 Introduction

In the previous chapter, literature survey is presented to identify techniques for forecasting the growth in installed wind power generation capacity in a region. There it is noted that results forecasted by earlier researchers are not in agreement with actual recorded increase in the cumulative installed wind power generation capacity. Thus, there is scope for improving methods for forecasting cumulative wind power generation capacity on an annual basis in future. In this chapter, it is demonstrated that application of genetic algorithm in currently used logistic function method leads to improvement in accuracy of forecasting.

It is of interest to wind farm developers and promoters to know in advance that the wind power generation capacity likely to be installed in future in the region of interest. The logistic function method can be used to forecast future scenario for various purposes such as to forecast population growth, bacteria growth in food and wind power generation capacity in a region [126]. The logistic function method uses two regression coefficients, which are calculated based on the input data supplied. The accuracy of prediction largely depends on the values of regression coefficients which is determined

by using curve fitting technique (Verhulst model) [126]. Using conventional logistic function method, Carolin *et al.* [16] forecasted that the wind power generation capacity in India by the year 2020 as 46570 MW. Similarly, Ishan *et al.* [17] also used conventional logistic function method to forecast the WPG capacity in India by the year 2020 as 11,531 MW. However, the actual installed capacity in India was 22,465 MW by the year 2014, which clearly shows that the conventional logistic function-based method used need to be updated for improving the accuracy of forecasting.

In the present work, a method has been proposed in which genetic algorithm is used in conjunction with the logistic function method to revise the regression coefficients of conventional logistic function method. Using the proposed method, growth of installed wind power generation capacity is forecasted for two leading countries in wind power development namely, China and India.

3.2 Growth in Wind Power Generation Capacity

Over past decades, continuous growth of wind power generation capacity has been reported. The recorded rate of growth in wind power generation capacity is shown in Fig. 3.1. There is rapid increase in installed generation capacity since the year 2000. From the figure, it is noted that the cumulative installed wind power generation capacity reached 17,400 MW at the end of 2000, which grew to 1,94,152 MW by the end of 2010. Next, the cumulative installed wind power generation capacity has increased to 3,69,553 MW by 2014. This indicates that in the last four years, the world wide installed wind power generation capacity has increased by 47.46 % [7]. The major contributors to wind power generation in the world, as on 31 December 2014 are China, USA, Germany, Spain and India [7]. The installed generation capacity of the top five producers are listed in Table 1.1.

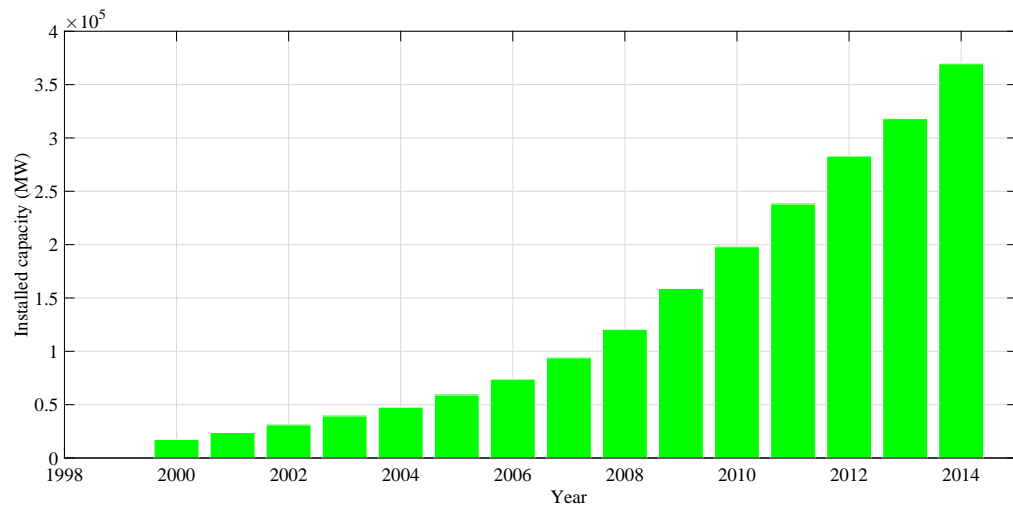


Fig. 3.1. Historic development of installed wind power generation capacity in World (2000-2014).

3.2.1 Growth of Wind Power Generation in India

In this section, the growth of installed wind power generation in India is discussed. By the end of 2014, the installed wind power generation capacity has reached 22,465 MW [7]. As per NIWE assessment the wind power potential at 50 m height is reported to be 49,130 MW [11]. Thus, India has installed only 45.72 % of the total estimated wind power potential so far. By the end of 2010, the cumulative installed capacity of India was 13065 MW (see Fig. 3.2). The growth in the installed capacity is 41.84 % in the last four years.

3.2.2 Growth of Wind Power Generation in China

In this section, the growth of wind power generation in China is discussed. At the end of 2014, the cumulative installed capacity has reached 1,14,763 MW [127]. The installed WPG capacity was 41,800 MW at the end of the year 2010, recorded growth of 63.57 % in the last four years. According to China academy of meteorological sciences, the country possesses a total of 235000 MW wind power potential [7]. Thus, currently only 48.83 % of wind power potential is utilized and about 51.16 % of estimated wind

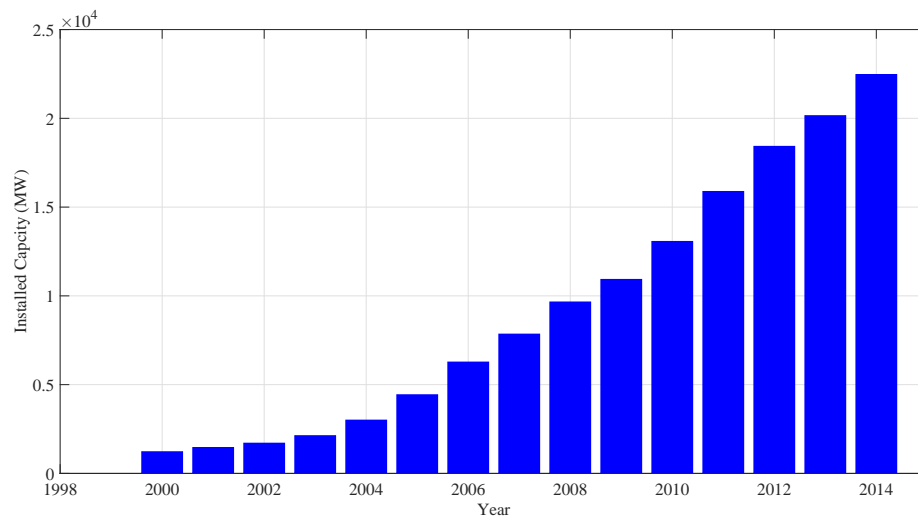


Fig. 3.2. Growth of installed cumulative wind power generation capacity in India.

power potential remained to be tapped. The growth of wind power generation installed capacity of China from the year 2000 to 2014 is shown in Fig. 3.3. Thus, it is clear that

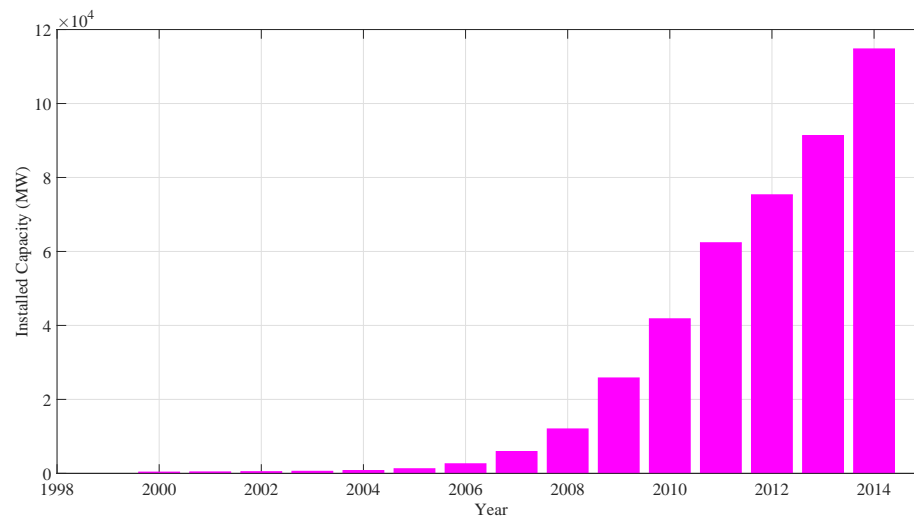


Fig. 3.3. Growth of installed cumulative wind power generation capacity in China.

wind power generation capacity is set to increase globally as well as in leading countries such as, China and India. Therefore, it is in the interest of wind farm developers to know in advance the wind power generation capacity, likely to be installed in future. Thus, there is a need to develop accurate technique for forecasting wind power generation capacity likely to be installed in future.

3.3 Logistic Function Method for Forecasting Installed Wind Power Generation Capacity

In this section, the conventional logistic function method, used for forecasting growth in wind power generation capacity, to be installed in future, is described. The logistic function, described as Verhulst model or logistic growth curve is a S-shaped sigmoid curve, that is used to forecast population growth [128]. It is also used in various fields such as demographics, biology, economics, engineering, etc [126].

Logistic curve is classified as symmetric (or simple) and non symmetric (complex) type curves, which are consequently classified as simple logistic functions or complex ones. Non-symmetric logistic curves have limited application due to their complexity and low efficiency for technology forecasts [129].

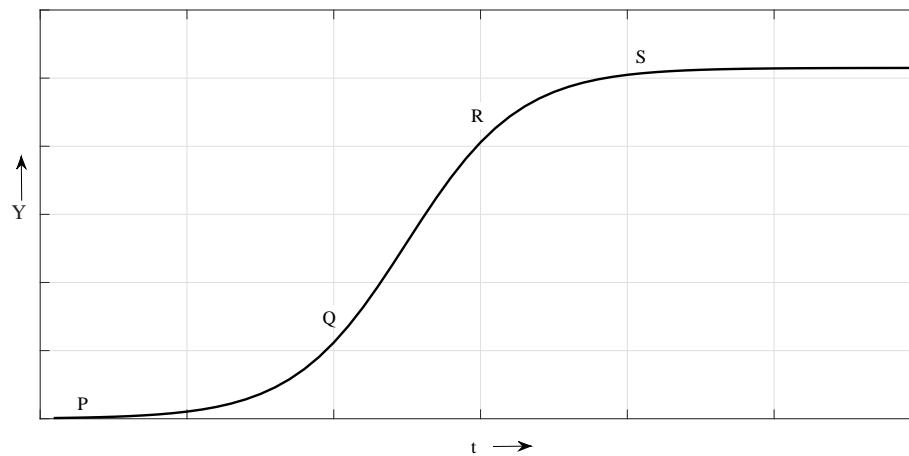


Fig. 3.4. Logistic growth curve.

The S-shape characteristic of the symmetric logistic curve is shown in Fig. 3.4. During first phase, from region P to Q, the growth is very slow. Beyond point Q, the growth increases exponentially from Q to R and then again the growth slows down while approaching the maximum upper limit S. The logistic function is represented by the following equation as follows:

$$Y = \frac{L}{(1 + ae^{-bt})} \quad (3.1)$$

where L is the upper limit to the maximum value of Y , while a and b are the regression coefficients. In the present work, Y represents cumulative wind power generation capacity to be installed until end of year in future and L represents maximum cumulative wind power generation capacity that can be expected to be installed in a region. Thus maximum value of L is taken to be equal to maximum estimated wind power potential in a region. For example, L is taken to be equal to 49,130 MW at 50 m height above ground in the case of India and 2,35,000 MW in the case of China [7]. The regression coefficients must be positive, so that the logistic function value must be positive. The function $Y(t)$ represents the projected cumulative wind capacity at time (t), denoting end of particular year. The accuracy of forecast depends on the value of a and b . The regression coefficients are determined as follows:

$$a = \frac{L(Y(t_1) - 1)}{e^{-bt_1}}, \quad (3.2)$$

$$b = \frac{1}{t_2 - t_1} \left(\frac{\ln\left(\frac{L}{Y(t_1)-1}\right)}{\ln\left(\frac{L}{Y(t_2)-1}\right)} \right). \quad (3.3)$$

In conventional logistic function method, a and b are calculated using (3.2) and (3.3). These a and b can be further refined by using genetic algorithm to get more accurate forecasting results.

3.3.1 Genetic Algorithm

Authors have reported that the most popular evolutionary algorithms (EA) are genetic algorithm (GA), evolutionary programming, differential evolution, evolution strategies, genetic programming, population-based incremental learning, particle swarm optimization and ant colony optimization [130–134]. The basic concept of all the above listed evolutionary algorithms is to simulate the evolution of individual structures via, processes of selection, reproduction and mutation.

Genetic algorithm is the most popular type of evolutionary algorithms [135]. This type of evolutionary algorithm is often used in optimization problems since genetic algorithm

can find a good near-optimal feasible solutions in a reduced computational time [135]. More detailed information on Genetic Algorithm is provided in Appendix A.

3.4 Application of GA for Forecasting Growth in Installed Wind Power Generation Capacity

A conventional method as described above, has been modified for improving the accuracy of prediction of growth in installed wind power generation capacity. In the proposed method, genetic algorithm has been used to evolve or update the regression coefficients of conventional logistic function through genetic operations of the evolutionary algorithms.

In conventional logistic function method, a and b are calculated using (3.2) and (3.3), and are directly used for forecasting future growth in installed wind power generation capacity. In the present work, GA is used to refine the regression coefficients (a and b) to obtain better accuracy in forecasting the growth in installed wind power generation capacity.

The RMSE represents the error in forecasting the output of logistic function and the actual installed wind power generation capacity. The RMSE is frequently used to measure difference between values predicted by a model and the values actually observed from the environment that is being modeled. The RMSE is given by

$$\text{RMSE} = \sqrt{\frac{\sum_{t=1}^n (x_{1t} - x_{2t})^2}{n}} \quad (3.4)$$

where x_{1t} is the actual cumulative installed capacity data, x_{2t} is forecasted using logistic function and by using new approach, n is the total number of data sets (years). The root mean square error (RMSE) is chosen as the objective function for GA [136].

Objective function = Minimize RMSE

Subjected to

$0 < a < 1500$;

$0 < b < 1$;

Fig. 3.5, explains the steps involved in the proposed method as flowchart. In the follow-

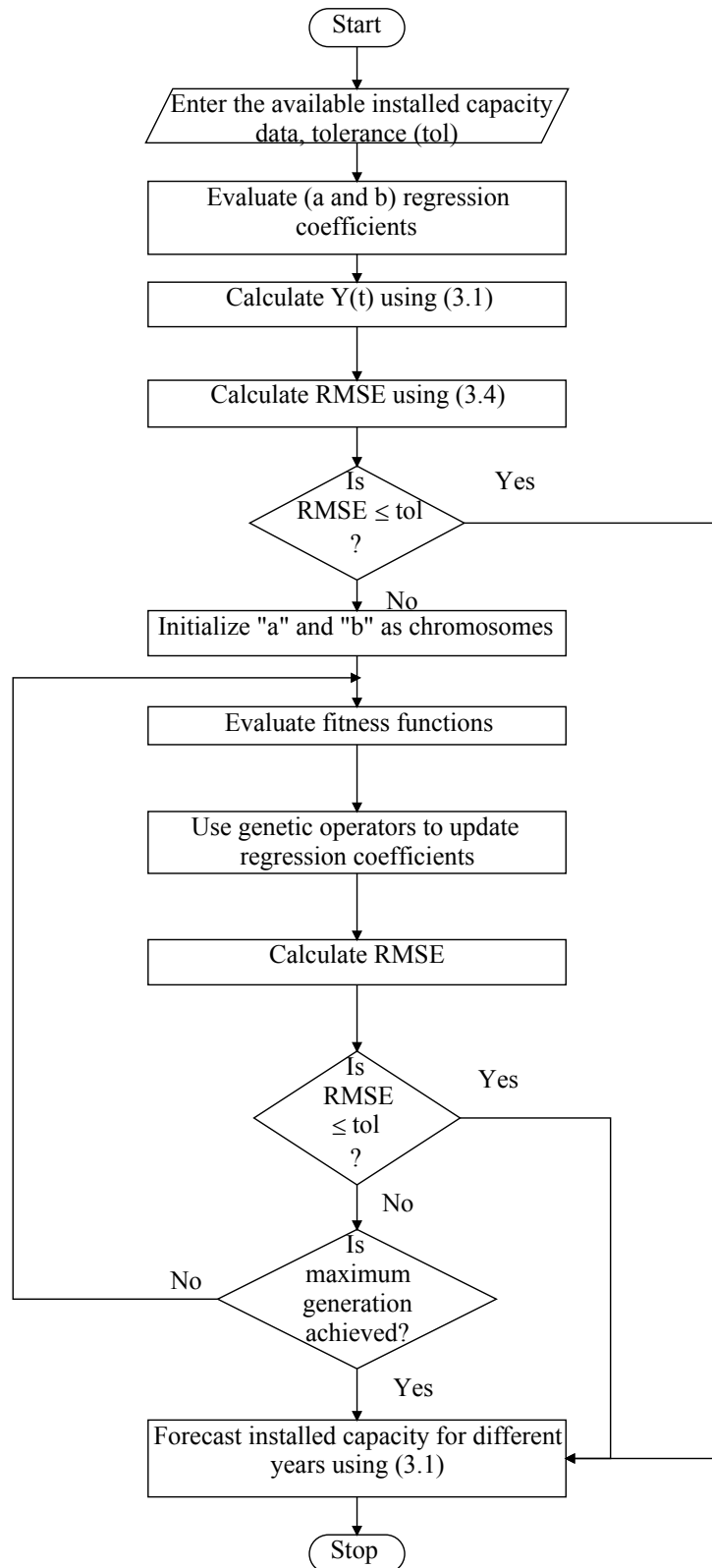


Fig. 3.5. Flowchart for the proposed method to forecast installed WPG capacity

ing section, results obtained using conventional logistic function method (i.e., without

application of GA) and results obtained using proposed method (logistic function with application of GA), in two cases, India and China are presented. In each case, the results obtained by the two methods are compared with actual recorded cumulative installed wind power capacity by the end of year in the recent past. The accuracy of forecast is measured in terms of RMSE.

3.5 Simulation Results

In this section, the growth of installed wind generation capacity is forecasted using logistic function method and proposed method are described.

3.5.1 Comparison of Proposed Method with Reported Results using Logistic Function Method

The purpose of this section is to examine the effectiveness of the proposed method. For this purpose, the cumulative installed generation capacity of the data of India from 1991-2006 is considered as in Carolin *et al.* [16]. The cumulative installed capacities of India during the period of 1991-2014 are listed in Table 3.1 [127].

Table 3.1. Cumulative installed generation capacity in India (1991-2014) [127].

S.no	Year	Cumulative installed capacity (MW)	S.no	Year	Cumulative installed capacity (MW)
1	1991	39	13	2003	2125
2	1992	39	14	2004	3000
3	1993	79	15	2005	4430
4	1994	185	16	2006	6270
5	1995	576	17	2007	7845
6	1996	820	18	2008	9655
7	1997	940	19	2009	10926
8	1998	1015	20	2010	13065
9	1999	1077	21	2011	9655
10	2000	1220	22	2012	10926
11	2001	1456	23	2013	13065
12	2002	1702	24	2014	22465

The GA parameters assumed to be used for the simulation are listed in Table 3.2. Here, the results of Carolin *et al.* [16] reproduced (-see Table 3.3). It is to be noted that the values of L , a and b chosen as 51500, 782.2 and 0.3072, respectively. The same L is chosen for the analysis by both the methods for the purpose of comparison. The regression coefficients are further revised using the proposed method and are listed in Table 3.4.

Table 3.2. Assumed parameters of GA used in simulation of proposed method

S.No	Parameters	Typical value
1	Number of chromosomes	30
2	Number of generations	500
3	Cross over probability	0.8
4	Elitism probability	0.1

Table 3.3. Results obtained using reported values using logistic method.

Regression coefficients		Maximum of absolute error		RMSE	
a	b	1991-2006	1991-2014	1991-2006	1991-2014
782.2	0.3072	527	8410	304.546	2591.114

Table 3.4. Results obtained using proposed method for forecasting growth in installed WPG capacity.

Regression coefficients		Maximum of absolute error		RMSE	
a	b	1991-2006	1991-2014	1991-2006	1991-2014
407.85	0.252	490	1879	267.489	831.584

From Table 3.3, it is observed that work reported by Carolin *et al.* [16], RMSE determined for the data set for the year 1991 to 2006. The maximum of absolute error is found to be 527 and the corresponding RMSE is found to be 304.546. Using the proposed method, RMSE is found to be 267.489 and the maximum of absolute error is found to be 490. Similarly, RMSE is also determined for the data set from the year 1991 to 2014. The maximum of absolute error and RMSE are found to be 8410, 2591.113, respectively. From the proposed method, these corresponding values are found to be 1879 and 831.5, respectively. The comparison of logistic function method with the proposed method is shown in Fig. 3.6.

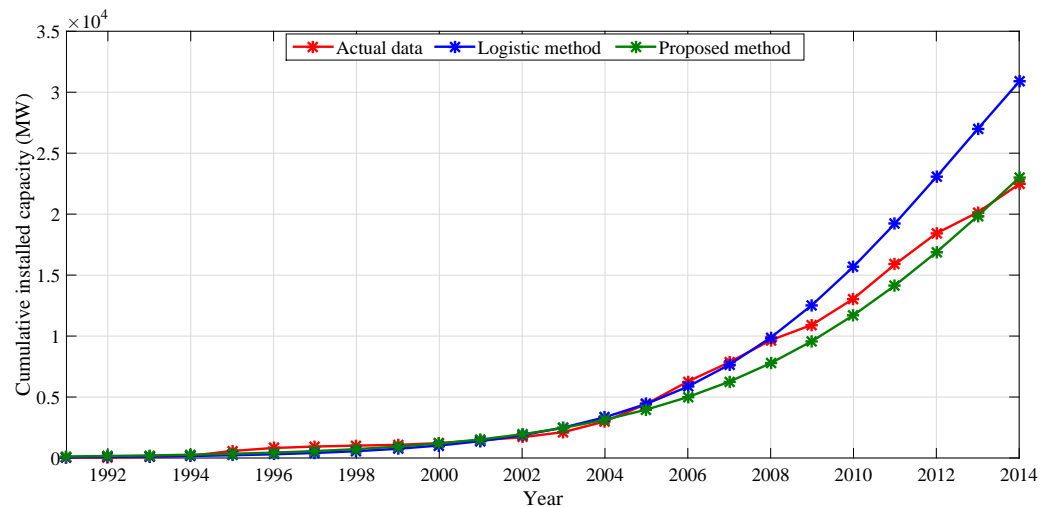


Fig. 3.6. Comparison of installed wind power generation capacity of reported results with the results from proposed method (1991-2014).

From Fig. 3.6, it is observed that the logistic function over estimates the installed wind power generation capacity for the year 2014. However, the proposed method provides the estimates which are close to the actual values. This comparative study provide the justification for the use of proposed method for forecasting installed wind power generation capacity in future.

3.5.2 Forecasting of Growth in Wind Power Generation Installed Capacity in India

In this section, results are presented for both conventional and modified logistic function method (proposed method), taking into account a complete data set (i.e., period of 1991-2014). The upper limit (L) value is taken as 49130 MW [11]. The cumulative installed capacities of India during the period of 1991-2014 are given in Table 3.1 [127].

From the complete data set available, using the conventional logistic function method, different combination are tried to arrive at best values of a and b . These results are listed in Table 3.5. From the table, it is observed that the RMSE is minimum for the combination of years 2000 and 2006. The corresponding regression coefficients a and

b are 742.698 and 0.2914, respectively. These coefficients are further refined by using GA and are listed in Table 3.6.

Table 3.5. Comparison of forecasted data with proposed method with actual data (1991-2014).

S.No.	Year	Year	a	b	maximum of absolute error	RMSE
1	1992	1999	3357.20	0.4771	24808	12329.654
2	1991	1996	2385.10	0.6124	36363	22048.515
3	1994	2010	835.44	0.2852	3248	1552.123
4	2010	2013	290.37	0.2173	6224	2890.187
5	2004	2008	1690.00	0.3312	4367	1560.221
6	1996	2004	164.27	0.1679	11437	4741.184
7	2004	2012	799.76	0.2777	3887	1987.102
8	2001	2006	1059.80	0.3133	5035	1474.100
9	2000	2006	742.69	0.2914	3228	1047.144
10	2002	2008	1341.70	0.3199	4012	1416.297
11	2002	2005	1680.10	0.3386	6489	1913.152

Table 3.6. Comparison of logistic method with proposed method (1991-2014).

Logistic method				Proposed method (LF +GA)			
a	b	maximum of absolute error	RMSE	a	b	maximum of absolute error	RMSE
742.698	0.2914	3228	1047.145	440.338	0.2621	1618	727.538

From the table it is observed that RMSE is further reduced when proposed method is used. The forecasted values of wind power generation capacities obtained using both the methods are shown in Fig. 3.7. The cumulative installed capacities forecasted up to year 2050 using the proposed method are shown in Fig. 3.8. It is observed that India will reach 99 % of its wind potential installed capacity by the year 2032. From the figure, the forecasted wind power generation capacity to be added during a future year can be obtained and is shown in Fig. 3.9. It is observed from the figure, the inflection point is the year 2017.

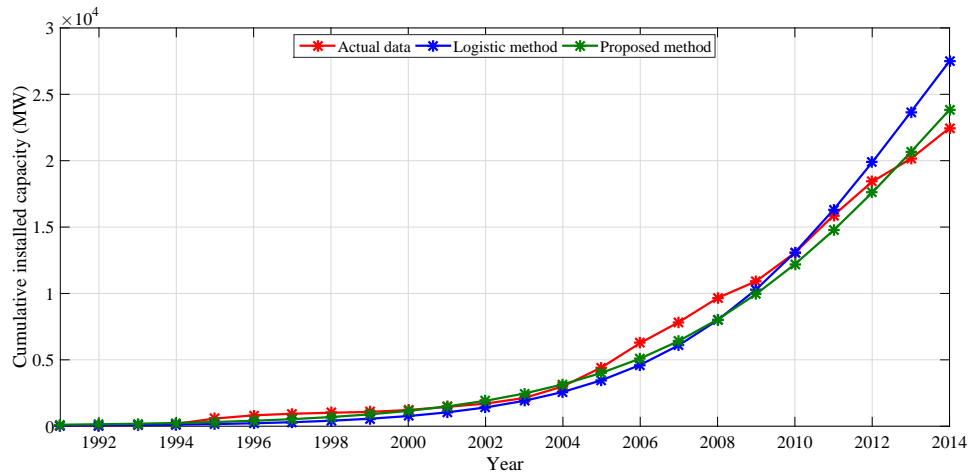


Fig. 3.7. Comparison of installed WPG capacity predicted by using conventional method and proposed method with actual data in India.

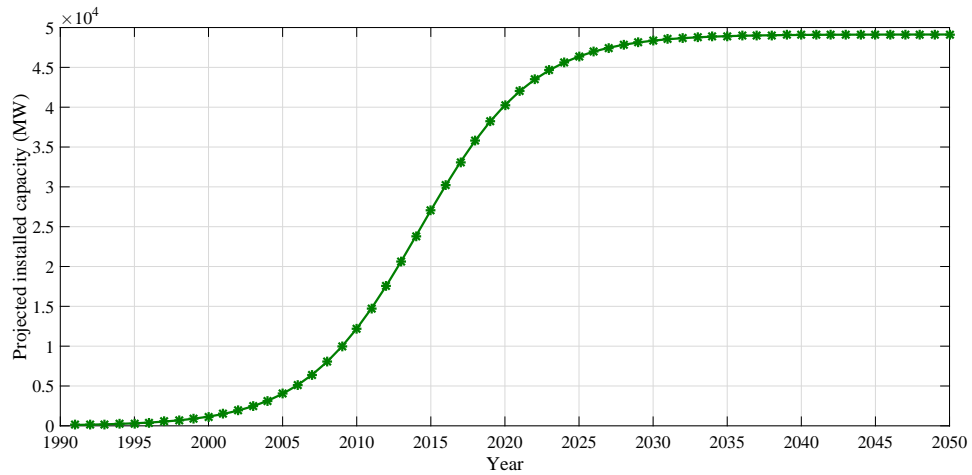


Fig. 3.8. Variation of cumulative WPG capacity upto 2050 in India.

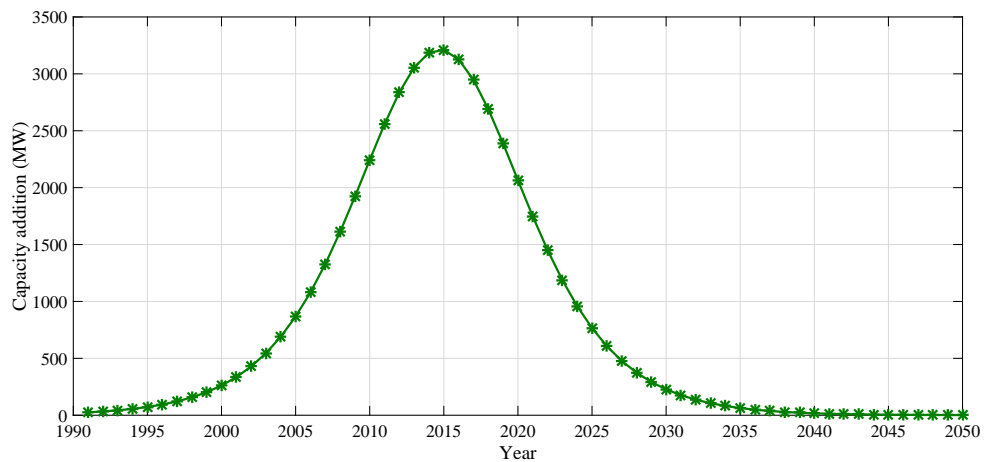


Fig. 3.9. Variation of annual rate of increase of WPG capacity upto 2050 in India.

3.5.3 Forecasting of Growth in Installed Wind Power Generation Capacity in China

The case studies carried out in the previous section which corresponds to forecasting of growth in installed wind power generation capacity in India are extended to China. Table 3.7 lists the cumulative installed capacity of China for the year 1995-2014 [127].

Table 3.7. Cumulative installed wind power generation capacity in China [127].

S.no	Year	Cumulative installed capacity (MW)	S.no	Year	Cumulative installed capacity (MW)
1	1995	38	11	2005	1260
2	1996	79	12	2006	2599
3	1997	170	13	2007	5910
4	1998	224	14	2008	12020
5	1999	268	15	2009	25805
6	2000	346	16	2010	41800
7	2001	402	17	2011	62364
8	2002	469	18	2012	75564
9	2003	567	19	2013	91412
10	2004	764	20	2014	114763

The upper limit (L) value for China is taken as 235 GW[127]. The final results are given in Table 3.8 and is shown in Fig. 3.10.

Table 3.8. Comparison of proposed method with conventional logistic method for forecasting growth in WPG in China.

Logistic method			Proposed method		
Regression coefficients		RMSE	Regression coefficients		RMSE
a	b		a	b	
10894.86	0.429	13469.31	10587.686	0.475	5471.31

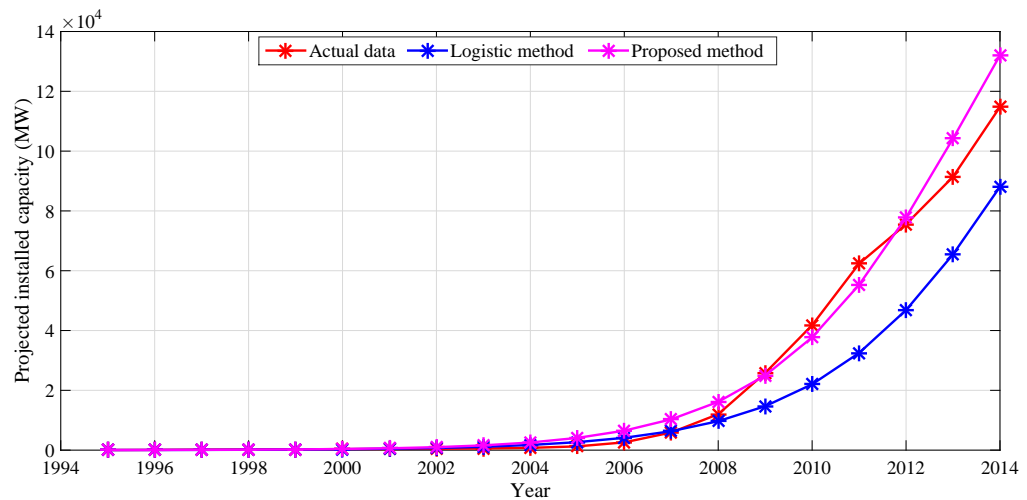


Fig. 3.10. Comparison of installed WPG capacity predicted by using logistic method and proposed method with actual data in China.

The cumulative installed capacities are forecasted up to year 2050 using the proposed method are shown in Fig. 3.11. It is observed from the figure that China will reach 99 % of its onshore wind potential installed capacity by the year 2024.

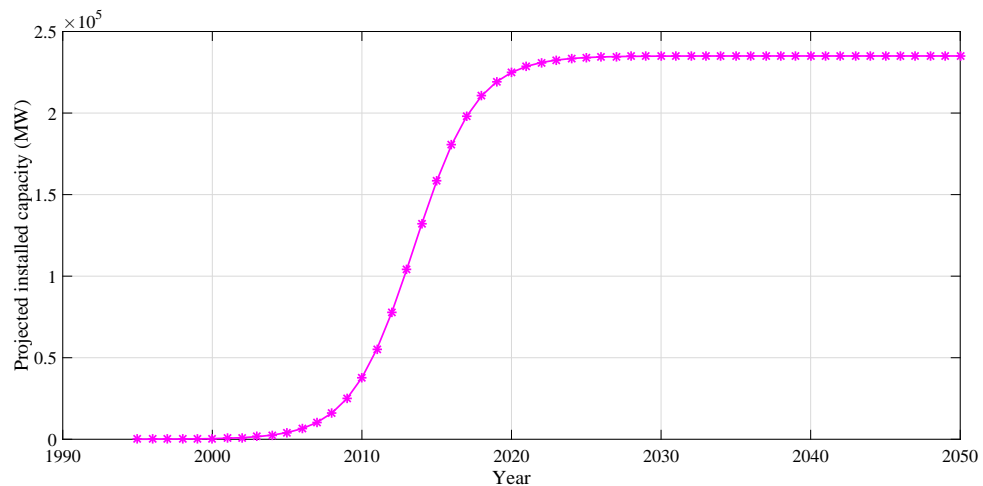


Fig. 3.11. Variation of cumulative WPG capacity upto 2050 in China.

Fig. 3.12 shows capacity additions per year forecasted in China. It is seen, the rate of increase in cumulative wind power generation capacity is rapid during short span of 2010 to 2020. Beyond 2020, the rate of increase is steady until 2050. It shows that the inflection point, the point after which the yearly capacity addition starts to decrease, is the year 2016.

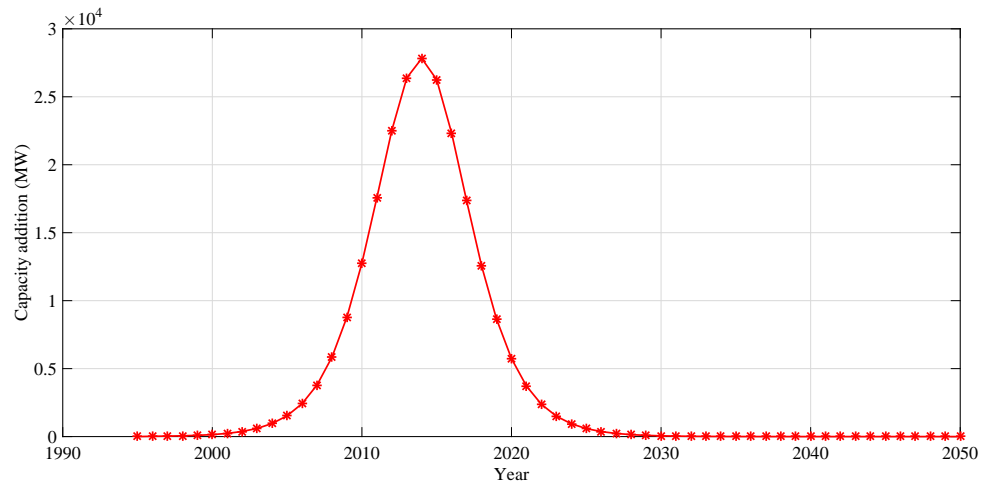


Fig. 3.12. Variation of annual rate of increase of WPG capacity upto 2050 in China.

3.6 Conclusion

In this chapter, a method is proposed to refine the values of regression coefficients using genetic algorithm is described. The proposed method has been employed for forecasting growth of wind power generation capacity in the leading countries, China and India. The simulation results obtained are compared with the actual cumulative installed generation capacity by the end of the year 2014. The following conclusions are drawn from the study:

1. The results are obtained on the basis of assumptions that exploitable wind power generation capacity in India is 49,130 MW and for China as 2,35,000 MW. The forecasted year in which the exploitable wind power generation capacity to reach 99 % is determined. The results obtained using the proposed method shows that the installed wind power generation capacity will become 49,688.7 MW by year 2032 in India and 2,32,650 MW in China by the year 2024.

In both the cases, the forecasted year depends on the estimated wind power potential, rate of growth of wind power generation in the past and the regression coefficients, which in turn depends on the data set available.

2. In the case of India, by the end of year 2014, the modified GA based logistic function method (proposed method) forecast cumulative wind power generation capacity to reach 23,838 MW compared to the cumulative wind power generation capacity of 27500 MW by using conventional logistic function method. However, by the end of year 2014, installed wind power generation capacity is recorded as 22,465 MW. Similarly, in the case of China, by the end of year 2014, the modified GA based logistic function method forecast cumulative wind power generation capacity to reach 1,22,027.78 MW. By using conventional logistic method it is found to be 88,057.77 MW. However, by the end of year 2014, it is recorded as 1,14,763 MW. Thus it is observed that, the forecast based on modified logistic function method is much closer to actually recorded value. Thus it is observed that, the forecast based on modified logistic function method is much closer to actually recorded value.
3. Alternatively, in the case of India, the RMSE in forecast obtained by using modified logistic function method is found to be 727.538, whereas the RMSE in forecast obtained by using conventional logistic function method is found to be 1047.145. Likewise, in the case of China, the RMSE in forecast obtained by using modified logistic function method is found to be 5471.31. Whereas, the RMSE in forecast obtained by using conventional logistic function method is found to be 13469.31. Thus it is seen that RMSE is very much reduced in the case of modified logistic function method.
4. Above results show that the proposed logistic function method improves accuracy of forecasting wind power generation capacity significantly.

Chapter 4

Assessment of Wind Power Potential

4.1 Introduction

In the previous chapter, the improvised method for forecasting of cumulative wind power generation capacity installed for any year in future is described. There it was noted that in India the estimated wind power potential is 49,130 MW at 50 m height. By the end of the year 2014, the recorded wind power installed generation capacity was 22,465 MW. Thus the installed generation capacity accounts for about 45.72 % of estimated wind power potential, and 54.27 % of estimated wind power potential still remains to be utilized [11]. Also, in India the estimated wind power potential at 80 m height is 1,02,000 MW which suggests that there is large scope for adding wind power generation capacity in foreseeable future. It should be noted that in actual utilization of wind power potential, due to site constraints it may not be possible to install all wind turbines at uniform hub height either 50 m or 80 m. This fact underlines importance of accurate assessment of wind power potential at different given hub heights at a given prospective wind farm sites. Also there is need to continue reassessing wind power potential at certain wind farm sites [2, 64].

Wind resource assessment (WRA) helps wind farm developers to determine the technical and economic feasibility of wind farm deployment at pre-investment stage. WRA involves measuring and analyzing the wind speed and other meteorological data, namely,

temperature, pressure and relative humidity at a site. Other characteristics of the site can also be determined are distribution of wind speed, wind direction, wind power density, wind shear and turbulence intensity. The annual energy production and capacity factor, the two important descriptors of economic viability of the wind farm project can also be estimated [137, 138].

In this chapter, most widely used Weibull probability distribution method and Rayleigh distribution function method for determination of wind speed probability density function at prospective sites, are described. Weibull probability density distribution function consists of two parameters, namely, shape parameter (k) and scale parameter (c). The shape parameter and scale parameter are determined by using each of four different statistical methods, namely, graphical method, standard deviation method, energy pattern factor method and maximum likelihood method. Rayleigh distribution function is special case of Weibull distribution function that corresponds to value of shape parameter, ($k= 2$) and the value of scale parameter, (c) equals to 1.2 times of annual average wind speed at the site. In practice, both Weibull and Rayleigh methods are used for characterizing available wind resource at a given site, so that complete understanding characteristic of available wind resource is developed. Once the characteristics are determined, the site can be evaluated for its suitability for wind power generation.

In the present work, two sites namely, BITS Pilani K. K. Goa campus, Goa (Lat. $15^{\circ}23' N$, Long. $73^{\circ}49' E$), (referred to as site-I) and Periyapatti, TamilNadu (Lat. $10^{\circ}45'18.5'' N$, Long. $77^{\circ}15'11.0'' E$), (referred to as site-II) are considered for assessment of available wind resource at these sites. The site-I typifies wind climate data measurement site and site-II typifies model grid connected wind power plant, state of Tamilnadu, India. For these two sites, detailed time series wind climate data is recorded for a period of minimum one year. The data been analyzed by using standard methods for determining characteristics of wind resource available at these sites. The results presented here serve the purpose of reassessment of wind power potential at these sites. Wind resource potential at a site is characterized in terms of average speed, wind speed distribution, wind power density, air density, energy pattern factor and turbulence intensity. Out of these characteristics, wind speed distribution can be determined by either Weibull distribution function or Rayleigh distribution function. The other characteristics are determined

once speed distribution of the site is determined. Thus, accuracy of determination of wind speed distribution becomes critically important. The accuracy of determining distribution of wind speed either by Weibull or Rayleigh, can be further improved if optimization algorithm such as genetic algorithm can be used for determining refined values of k and c . In this chapter, application of genetic algorithm is developed so as to obtain refined values of the parameters k and c . The effectiveness of refined values of k and c in obtaining accurate Weibull distribution function for the site is measured with respect to Weibull distribution defined by conventional statistically determined k and c . Using improved Weibull function other site characteristics such as wind power density and capacity factor are obtained. The wind speed distributions and wind power density are recalculated by using refined values of k and c in Weibull distribution at the site. The accuracy in estimation of wind speed distribution is quantified in terms of root mean square error. The RMSE obtained for wind speed distribution and wind power density are compared with the corresponding values of measured data. It is concluded that use of genetic algorithm to obtain refined values of k and c improves estimates significantly.

4.2 Standard Procedure for Determining Characteristics of Wind Resource

The characteristics of wind resource can be determined on the basis of detailed wind climate data at the site. The detailed time series wind climate data can be measured at the site for a minimum period of one year as per the standard procedure [139, 140]. Alternatively, such data can also be obtained from NIWE Chennai for certain sites. Under National wind resource assessment programme, Ministry through National Institute of Wind Energy, Chennai and state nodal agencies had installed and monitored 794 dedicated wind monitoring stations of height ranging from 20 m to 120 m throughout the country. Fig. 4.1 shows the wind energy density map of India. It is observed that high wind concentration is mainly in the states of Tamilnadu, Maharashtra, Karnataka, Gujarat and Andhra Pradesh.

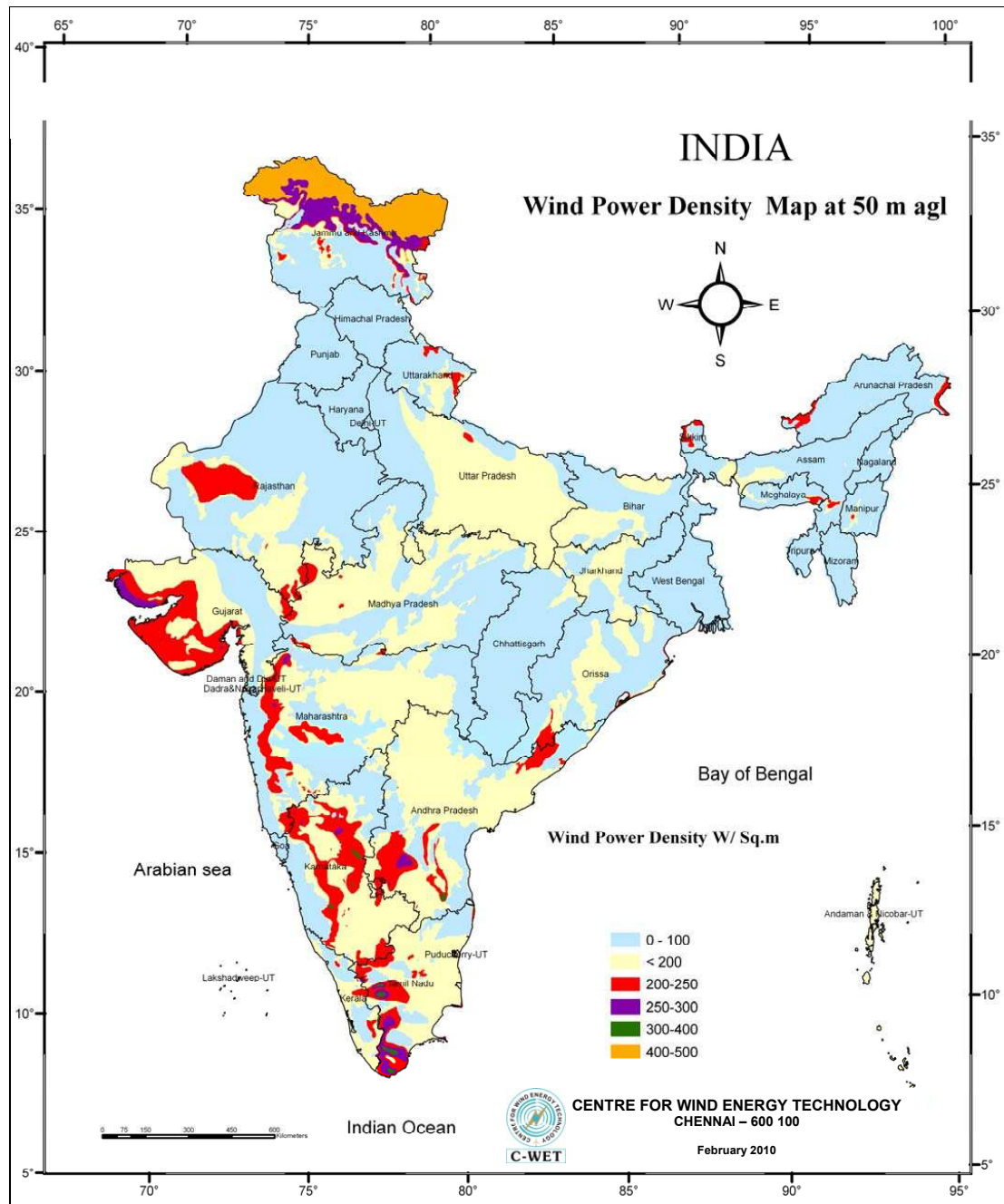


Fig. 4.1. Wind power density map at 50 m height (India) [11].

Wind climate data includes time series data on wind speed, direction, temperature, pressure and relative humidity measured at a standard height. When the detailed climate data is available, the characteristic of the site such as average wind speed, wind power density, standard deviation, air density, turbulence intensity, energy pattern factor, probability density function (PDF) and cumulative distribution function (CDF). The characteristics at a given site are determined as described below:

4.2.1 Average Wind Speed

The average value of wind speed is calculated using instantaneous values recorded as time series data over a measurement interval of five minutes or ten minutes. The average value of wind speed is taken to be representing value of instantaneous wind speed at the end of the corresponding measurement interval. The average value is calculated using equation below: [34]:

$$V_m = \frac{1}{N} \sum_{i=1}^N V_i \quad (4.1)$$

where, V_i , is instantaneous value of wind speed, V_m is the average value of wind speed and N is the total number of observations during ten minutes interval. The above equation can also be used to calculate hourly/ monthly/ annual average wind speed etc.

4.2.2 Standard Deviation of Wind Speed

The standard deviation of wind speed distribution, σ , is determined over measurement interval by using following equation [34]:

$$\sigma = \sqrt{\frac{1}{N-1} \sum_{i=1}^N (V_i - V_m)^2} \quad (4.2)$$

The value of standard deviation is required for estimation of turbulence intensity at the site. The standard deviation is a measure of closeness of the set of data to the actual average value.

4.2.3 Air Density

The instantaneous value of air density is required for determining wind power density. The average value of air density is determined using instantaneous values recorded as time series data over a measurement interval of five minutes or ten minutes. This average value of air density is taken as representative value of instantaneous air density at the end of the corresponding measurement interval. The air density is usually assumed to

be constant (1.225 kg/m³). Alternatively, using the recorded hourly average values of air temperature (t in °C), and atmospheric pressure (p , in Pa), the air density (in kg/m³) is calculated using the following equation [44, 141]:

$$\rho = \frac{p}{RT} \quad (4.3)$$

where ($T = t + 273.3$, in K), R is the universal gas constant (287 J/kg K). In the present work, instead of assuming air density as constant, it is calculated using the expression (4.4) [142, 143], which takes into account the relative humidity (in addition to temperature and pressure) on the air density.

$$\rho_H = \frac{p_d M_d + p_v M_v}{RT} \quad (4.4)$$

where,

$$p_v = \phi \cdot p_{sat} \quad (4.5)$$

$$p_{sat} = 6.1078 * 10^{\left(\frac{7.5t}{t+273.3}\right)} \quad (4.6)$$

$$p_d = p - p_v \quad (4.7)$$

where t is the temperature in °C, M_d is the molar mass of dry air = 0.028964 kg/mol, M_v is the molar mass of water vapour = 0.018016 kg/mol, p is the pressure in Pa, ϕ is the relative humidity, p_v is the vapour pressure in Pa and p_d is the dry pressure in Pa, ρ_H is the air density with relative humidity into account.

4.2.4 Wind Power Density

The measured wind speed data has been used to estimate power in the wind (in watts), as follows [34]:

$$P_W = \frac{1}{2} \rho_i A V_i^3 \quad (4.8)$$

The measured values of wind speed and air density are averaged over measurement interval of 5 minutes or 10 minutes. The average values of wind speed and air density are taken to be representative values of corresponding variable at the end of respective

measurement intervals. The instantaneous values of wind speed (V_i) and air density (ρ_i) are used to determine wind power density using following equation [34].

$$WPD_M = \frac{1}{2}\rho_i V_i^3 \quad (4.9)$$

where WPD_M is the measured wind power density in W/m^2 , A is the swept area and ρ_i is the instantaneous air density.

4.2.5 Turbulence Intensity

Wind turbulence is the rapid disturbance or irregularity in the wind speed. The turbulence intensity (TI) is defined as the ratio of standard deviation of wind speed to the average wind speed over a time interval of measurement, as follows [144]:

$$TI = \left(\frac{\sigma}{V_m} \right) \quad (4.10)$$

Wind turbulence is an important site characteristic, because high turbulence levels may decrease power output and cause extreme loading on wind turbine components, particularly in the complex terrain. The most common indicator of turbulence for siting purposes is the standard deviation of wind speed. The turbulence intensity (TI) less than or equal to 0.10 indicates low level of turbulence. The turbulence intensity value of 0.25 indicates moderate turbulence. Turbulence intensity greater than 0.25, indicates high level of turbulence at the site.

4.2.6 Energy Pattern Factor

Energy pattern factor (EPF) is a useful parameter that indicates fluctuation of energy available in the wind with respect to average value of energy available in wind. At a given site, EPF is determined on monthly as well as annual basis. The EPF is a ratio of the sum of the cube of the instantaneous wind speed during the period of observation to

the cube of the mean wind speed during the period of observation and is given by [40]:

$$\text{EPF} = \left(\frac{\sum_{i=1}^N V_i^3}{N(V_m)^3} \right) \quad (4.11)$$

4.3 Weibull Probability Distribution Function

The Weibull probability distribution function for a site gives probability of finding wind speed at a site. In Weibull distribution, the variations in wind speed are characterized by the two functions namely, PDF and CDF [145].

Weibull distribution function is the widely used distribution function because of its flexibility and simplicity of estimation of its two parameters (k and c) which can be determined by various methods as discussed in the following sections. The various methods used in this chapter for determining the Weibull parameters are graphical method (least square method), standard deviation method (empirical method), energy pattern factor method (power density method) and maximum likelihood method (MLE).

The Weibull PDF, $f(V)$, and CDF, $F(V)$, are determined at the site [2, 3, 64, 146]. The PDF indicates the fraction of time for which the wind speed probably prevails at the location of measurement.

$$f(V) = \left(\frac{k}{c} \right) \left(\frac{V}{c} \right)^{k-1} \exp \left(- \frac{V}{c} \right)^k \quad (4.12)$$

The CDF indicates the fraction of time that the wind speed is below a particular speed.

$$F(V) = 1 - \exp \left(- \frac{V}{c} \right)^k \quad (4.13)$$

The scale parameter c (in m/s) indicates how ‘windy’ a wind location under consideration is, whereas, the shape parameter, k (a dimensionless quantity), defines the shape of the curve. The typical values of k range from 1.5 to 4.0 for most wind conditions and the typical value of c is 1.2 times the average wind speed [147].

4.3.1 Graphical Method for Determination of Shape and Scale Parameters

The application of the graphical method (GP) requires the wind speed data in cumulative frequency distribution format. Time-series data must therefore be sorted into bins (wind speed data is segregated into wind speed intervals [52]. Alternatively, the Weibull cumulative distribution function is transformed into a linear equation by taking double natural logarithm on both sides. The best fit line is found from the given data, as follows [27]:

$$\ln[\ln(1/[1 - F(V)])] = k \ln(V_i) - k \ln c \quad (4.14)$$

Let, $X_i = \ln V_i$ and $Y_i = \ln[\ln(1/[1 - F(V)])]$ The linear approximation of this data is obtained using the method, in the form of straight line equation $Y_1 = a_1 X + b_1$, where k gives the slope of this line (a_1) and $(-k \ln c)$ represents the intercept (b_1). Thus Weibull parameters are obtained as follows [27]:

$$k = a_1 \quad (4.15)$$

$$c = e^{\left(\frac{-b_1}{a_1}\right)} \quad (4.16)$$

The parameters k and c are used to construct Weibull distribution function using 4.12.

4.3.2 Standard Deviation Method for Determination of Shape and Scale parameters

The standard deviation (SD) method is also one of the methods for determining shape and scale parameters. The parameters k and c are determined using the average value of wind speed V_m and standard deviation of wind speed σ , as follows [70]:

$$k = \left(\frac{\sigma}{V_m}\right)^{-1.086} \quad (4.17)$$

$$c = \frac{V_m}{\Gamma(1 + 1/k)} \quad (4.18)$$

where $\Gamma(y)$ is the gamma function given by

$$\Gamma(y) = \int_0^{\infty} x^{y-1} e^{-x} dx$$

The value of gamma function is obtained from using standard Tables. The values of k and c when substituted in 4.12 gives Weibull probability distribution function.

4.3.3 Energy Pattern Factor Method for Determination of Shape and Scale Parameters

This is a new method proposed by Akdag and Ali in 2009 for estimation of shape and scale parameters. Energy pattern factor (EPF) is the ratio of the total power available in the wind to the power corresponding to the cube of the mean wind speed. The advantages of this method is that: (i) it has a simple formulation, (ii) it does not require binning and solving linear least square problem or iterative procedure, (iii) also it is more suitable to estimate power density for wind energy applications. The main advantage of this method is that, if the wind power density and mean wind speed at a site are known, then Weibull parameters can be estimated by using (4.23) and (4.24) [40].

The average wind speed can be calculated as follows

$$V_m = c\Gamma(1 + 1/k) \quad (4.19)$$

The mean cubic wind speed (using the population moment equation) is,

$$(V^3)_m = c^3\Gamma(1 + 3/k) \quad (4.20)$$

$$E_{pf} = \frac{P_{total}}{P_{(V_m)^3}} = \frac{(V^3)_m}{(V_m)^3} \quad (4.21)$$

Equation (4.21) can be rewritten as follows [40],

$$E_{pf} = \frac{\Gamma(1 + 3/k)}{\Gamma^3(1 + 1/k)} \quad (4.22)$$

Once the energy pattern factor, E_{pf} is calculated by using the above equation, the shape factor and scale factor can be estimated from the following equations:

$$k = 1 + \frac{3.69}{(E_{pf})^2} \quad (4.23)$$

$$c = \frac{V_m}{\Gamma(1 + 1/k)} \quad (4.24)$$

4.3.4 Maximum Likelihood Estimation Method for Determination of Shape and Scale Parameters

Maximum likelihood estimation (MLE) develops a likelihood function based on the available data and finds the values of the parameter that maximize the likelihood function. The MLE method has many large sample properties that makes it attractive for use. Let V_1, V_2, V_3, \dots be a random sample size N drawn from a PDF $f(V, \theta)$ where θ is an unknown parameter.

The MLE method entails of finding the values of the parameters which maximize the likelihood function. This method provides estimators which are asymptotically centered, have normal asymptotic distribution, and are efficient [148].

$$L = \prod_{i=1}^N f_{V_i}(V_i, \theta) \quad (4.25)$$

Now, the maximum likelihood method to estimate the Weibull parameters k and c [59, 63] is as follows:

$$L(V_1, V_2, \dots, V_N, k, c) = \prod_{i=1}^N (k/c)(V_i/c)^{k-1} e^{-(V_i/c)^k} \quad (4.26)$$

on taking logarithms of this equation and partially differentiating with respect to k and c to maximize the likelihood estimators,

$$\frac{\partial \ln L}{\partial k} = \frac{N}{k} + \sum_{i=1}^N \ln V_i - \frac{1}{c} \sum_{i=1}^N V_i^k \ln V_i = 0 \quad (4.27)$$

$$\frac{\partial \ln L}{\partial c} = \frac{-N}{k} + \frac{1}{c^2} \sum_{i=1}^N V_i^k = 0 \quad (4.28)$$

on simplifying (4.27) and (4.28),

$$\frac{\sum_{i=1}^N V_i^k \ln V_i}{\sum_{i=1}^N V_i^k} = \frac{1}{k} - \frac{1}{N} \sum_{i=1}^N \ln V_i \quad (4.29)$$

on simplifying (4.29), the value of k can be obtained and expressed as follows:

$$k = \left[\frac{\sum_{i=1}^N V_i^k \ln V_i}{\sum_{i=1}^N V_i^k} - \frac{1}{N} \sum_{i=1}^N \ln V_i \right]^{-1} \quad (4.30)$$

Now, after obtaining k , substituting this value in the (4.27),

$$c = \left[\frac{1}{N} \sum_{i=1}^N V_i^k \right]^{1/k} \quad (4.31)$$

The values of k and c when substituted in 4.12 gives Weibull distribution function. Thus, parameters, shape, k and scale, c can be determined by any of the four methods for a given site. However, for finding out most accurate method the RMSE between analytical Weibull probability distribution and actual distribution is required to be determined.

The method corresponding to minimum RMSE should be chosen for determining (k and c) for a site. The values of k and c so determined can be further used to determine probabilistic characteristic such as average wind speed, most probable wind speed, wind speed carrying maximum energy and wind power density.

4.3.5 Determination of Probabilistic Characteristics using Shape and Scale of Weibull Distribution

Using parameters k and c , the probabilistic characteristics such as average wind speed, most probable wind speed, wind speed carrying maximum energy and wind power density are determined as follows:

Average wind speed (V_{mW}): The average wind speed can be computed using Weibull

parameters as follows [149]:

$$V_{mW} = c\Gamma\left(1 + \frac{1}{k}\right) \quad (4.32)$$

Most probable wind speed (V_{mp}): The most probable wind speed denotes the most frequent wind speed for a given wind probability distribution and is determined as follows [149]:

$$V_{mp} = c\left(1 - \frac{1}{k}\right)^{1/k} \quad (4.33)$$

Wind speed carrying maximum energy ($V_{max,E}$): The wind speed corresponding to maximum energy at the site, is determined as follows [149]:

$$V_{max,E} = c\left(1 + \frac{2}{k}\right)^{1/k} \quad (4.34)$$

Wind power density (WPD_W): The wind power density at a given site is determined as follows [149]:

$$WPD_W = \frac{1}{2}\rho c^3\Gamma\left(1 + \frac{3}{k}\right) \quad (4.35)$$

Estimation of error in wind power density: The estimated wind power density using (4.35), at a given site differs from the wind power density obtained by (4.9). The error in estimation, is calculated as follows [34]:

$$Error (\%) = \frac{WPD_W - WPD_M}{WPD_M} \cdot 100 \quad (4.36)$$

4.3.6 Estimation of Wind Speed Distribution

The accuracy of wind speed distribution obtained is determined in terms of RMSE and correlation coefficient (R^2). The expression for RMSE is given by (3.4) and R^2 is determined as follows [21]:

$$R^2 = \frac{\sum_{i=1}^N (y_i - z_i)^2 - \sum_{i=1}^N (x_i - y_i)^2}{\sum_{i=1}^N (y_i - z_i)^2} \quad (4.37)$$

where y_i is the measured data, x_i is the estimated data and z_i is the mean value. The unity value of R^2 indicates complete agreement between measured data and the estimated data.

4.4 Rayleigh Probability Distribution Function

The most commonly used wind speed distribution functions for fitting a measured wind speed probability distribution in a given location over a certain period of time are the Weibull and Rayleigh distributions. In the previous section, Weibull distribution is described. The Rayleigh distribution function is derived from Weibull distribution function which is a special case of the Pierson Class III distribution, where the value of k is 2. The Rayleigh probability density distribution function, $f_R(V)$, is expressed as follows [64]:

$$f_R(V) = \left(\frac{2V}{c_R^2} \right) e^{-\left(\frac{V}{c_R} \right)^2} \quad (4.38)$$

where, c_R is Rayleigh scale parameter, which is determined as follows [48, 150]

$$c_R = 2 \frac{V_m}{\sqrt{\pi}} \quad (4.39)$$

The Rayleigh cumulative density function, $F_R(V)$, is determined as

$$F_R(V) = 1 - e^{-\left(\frac{V}{c_R} \right)^2} \quad (4.40)$$

4.4.1 Determination of Probabilistic Characteristics of Rayleigh Distribution

In this section, by using Rayleigh parameters, the average wind speed, most probable wind speed, wind speed corresponding to maximum energy and wind power density are determined.

Average wind speed (V_{mR}): The average wind speed can be computed using (4.41)

$$V_{mR} = c_R \sqrt{\frac{\pi}{4}} \quad (4.41)$$

Most probable wind speed (V_{mpR}): The most probable wind speed denotes the most frequent wind speed for a given wind probability distribution and is determined for the site, as follows [151]:

$$V_{mpR} = \frac{c_R}{\sqrt{2}} \quad (4.42)$$

Wind speed carrying maximum energy ($V_{max,ER}$): The wind speed corresponding to maximum energy at the site, is determined as follows [151]:

$$V_{max,ER} = c_R \sqrt{2} \quad (4.43)$$

Wind power density (WPD_R): The wind power density is determined using Rayleigh parameters as follows [151]:

$$WPD_R = \frac{3}{\pi} \rho V_{mR}^3 \quad (4.44)$$

where, V_{mR} is calculated from (4.41)

Estimation of error in wind power density: The error in wind power density is determined as follows [34]

$$Error (\%) = \frac{WPD_R - WPD_M}{WPD_M} \cdot 100 \quad (4.45)$$

4.5 Proposed Approach to Improve the Accuracy in Estimation of Distribution of Wind Speed

After finding the wind speed probability density distribution function at a site using the aforementioned five methods. Out of the five methods, the method corresponding to minimum RMSE (close to zero) and maximum R^2 (close to one) is chosen as the best method. In order to further improve the accuracy of the selected best method, in

this work, use of genetic algorithm is proposed to refine the values of ' k ' and ' c '. The RMSE is chosen as objective function for genetic algorithm. The steps involved in the proposed approach are shown in Fig. 4.2. The assumed values of parameters of genetic algorithm are listed in Table 4.1.

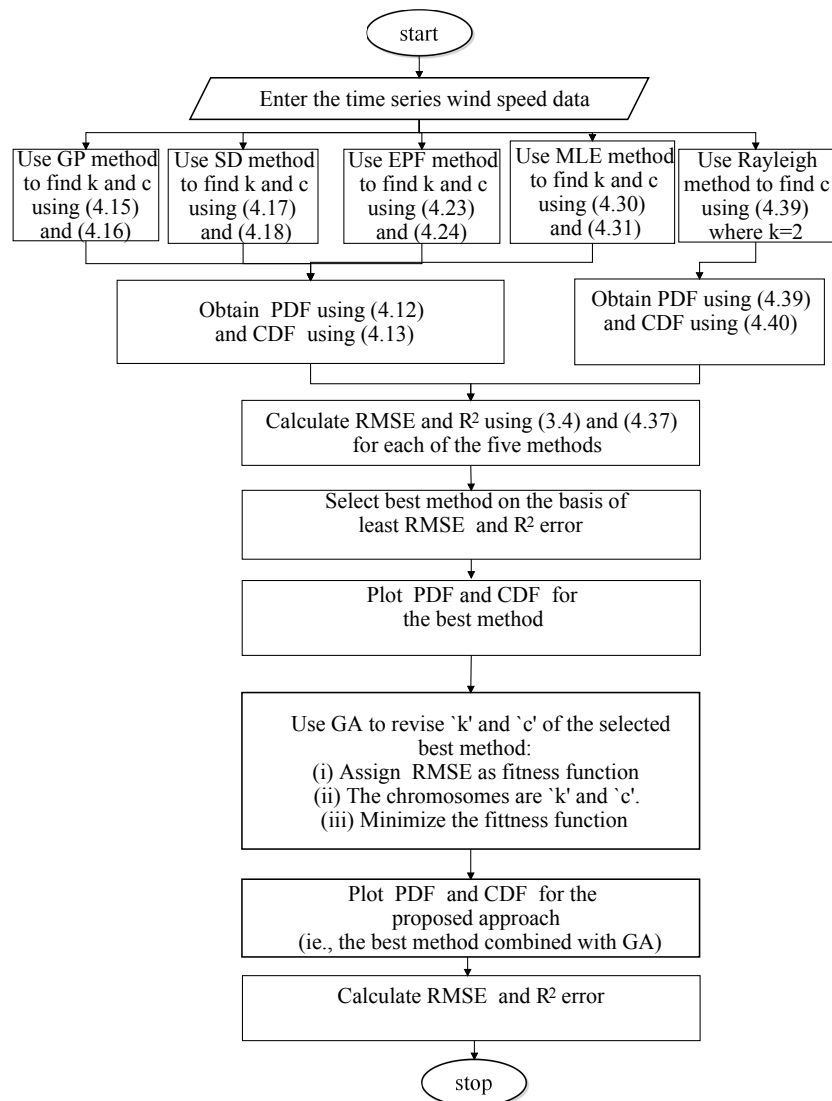


Fig. 4.2. Flowchart of proposed method for determining wind speed distribution

Table 4.1. The parameters and their assumed value for finding optimum values of k and c

S.No	Parameters	Typical value
1	Number of chromosomes	20
2	Number of generations	1500
3	Cross over probability	0.8
4	Elitism probability	0.1

4.6 Variation of Wind Power Density with Height

Using the measured wind data, wind speed and wind power density at different height can be estimated by using power law method [77, 152]. The wind speed V_x at desired heights (h_x) above ground is estimated using following equation [153] :

$$V_x = V_r \left[\frac{h_x}{h_r} \right]^\alpha \quad (4.46)$$

where V_r is the measured wind speed at a known height (h_r) and α is the power law index (exponent). The value of α is chosen as 0.14 [75].

If wind speeds (V_{r1} and V_{r2}) measured at two different heights (h_{r1} and h_{r2}) are known then, α can be determined as

$$\alpha = \left[\frac{\ln(V_{r2}) - \ln(V_{r1})}{\ln(h_{r2}) - \ln(h_{r1})} \right] \quad (4.47)$$

Then the wind speed (V_x) at desired height (h_x) is calculated using (4.46). Finally, the wind power density P_x is calculated as follows [154]:

$$P_x = P_r \left[\frac{h_x}{h_r} \right]^{3\alpha} \quad (4.48)$$

where P_r is the wind power density at measured height h_r . The detailed steps involved in the estimation of wind power density are shown in Fig. 4.3.

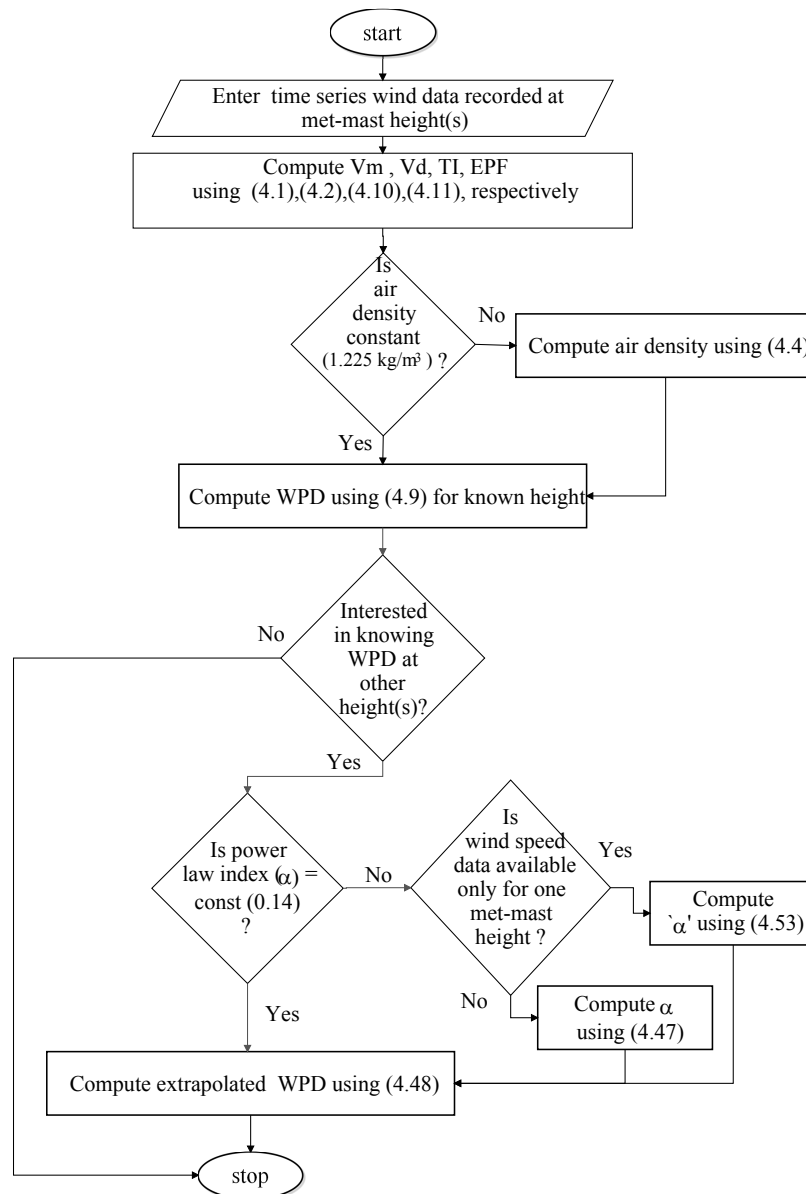


Fig. 4.3. Flowchart for extrapolation of wind power density

4.7 Estimation of Capacity Factor

With the knowledge of available wind resource at a site, the next step is to estimate probable capacity factor of the wind power project which will ultimately determine economic viability of the project. For wind farms, the range of values of capacity factor is generally from 20 % to 40 %. A low capacity factor may indicate that the wind resource is not adequate, or that the turbine is over-sized [155].

The performance of a wind machine installed at a given site can be evaluated on the

basis of the average output power over a given period of time and also its capacity factor [71]. At a site, the wind turbine characteristics such as rated power, cut in speed, rated speed and cut out speed parameters should be properly selected in order to get maximum capacity factor [66].

The mean output (P_{out}) can be calculated using the following expression based on distribution function [39, 72].

$$P_{out} = P_{eR} \left[\frac{e^{-(\frac{v_c}{c})^k} - e^{-(\frac{v_r}{c})^k}}{(\frac{v_r}{c})^k - (\frac{v_c}{c})^k} - e^{-(\frac{v_f}{c})^k} \right] \quad (4.49)$$

The capacity factor (C_f) is defined as the ratio of the mean output power to the rated electrical power (P_{eR}) of the wind turbine [70].

$$C_f = \frac{P_{out}}{P_{eR}} \quad (4.50)$$

where v_c , v_r and v_f are the cut in speed, the rated speed and the cut out wind speed of the wind turbine, respectively. The wind speed at which the wind turbine first starts to rotate and generate power is called cut-in speed. The wind speed at which the wind turbine reaches its rated power output is called rated speed. The wind speed at which the turbine is shut down and no power is generated above this speed is called cut-out speed. The hub height is the distance from the ground level to the rotor of an installed wind turbine.

It is commonly observed that in a wind farm, the hub height and meteorological mast height is different. It is necessary to estimate wind speeds at hub height. The probability density function can be used to obtain wind speeds at different heights (say the hub height) as follows [39, 70, 71]. The boundary layer development and the effect of the ground are non linear with respect to the wind speed, shape factor k and the scale factor c , of the distribution will change as a function of height by the following equations [71].

$$c(h) = c_0 \left(\frac{h}{h_0} \right)^\alpha \quad (4.51)$$

$$k(h) = k_0 \left[\frac{1 - 0.088 \ln \left(\frac{h_0}{10} \right)}{1 - 0.088 \ln \left(\frac{h}{10} \right)} \right] \quad (4.52)$$

where c_0 and k_0 are the scale factor and shape parameter obtained using the proposed approach, respectively at the measured height h_0 , and h is the hub height. The exponent (α) is defined as [71]:

$$\alpha = \left[\frac{0.37 - 0.088 \ln c_0}{1 - 0.088 \ln \left(\frac{h}{10} \right)} \right] \quad (4.53)$$

The above steps are shown in Fig. 4.4 in the form of flowchart.

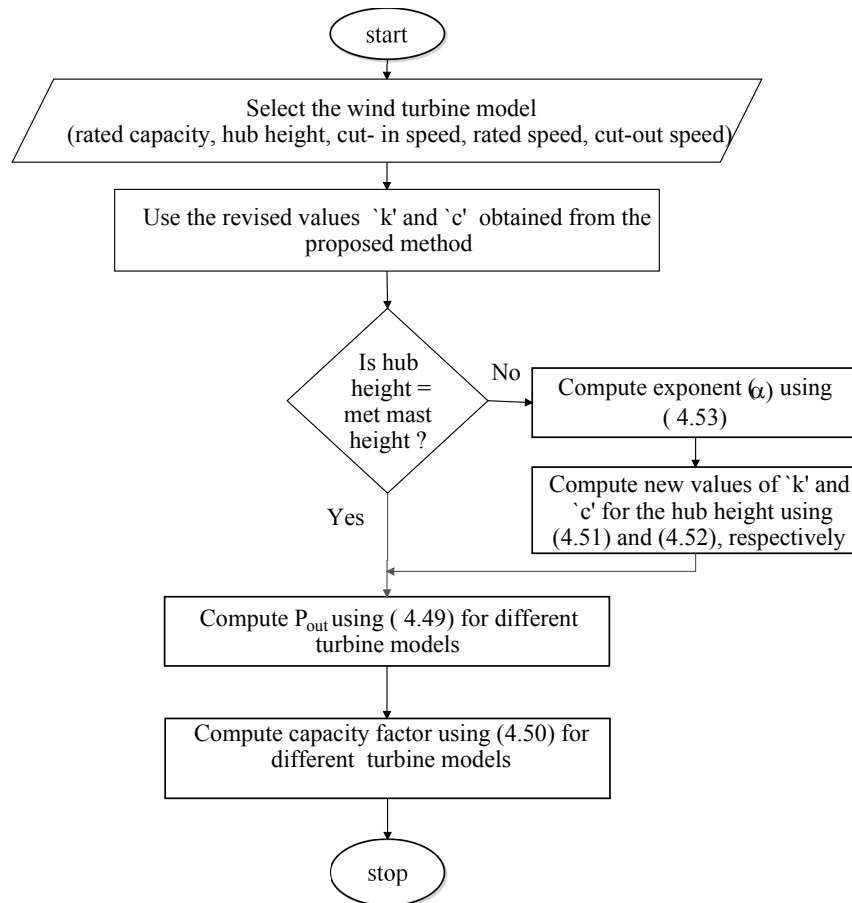


Fig. 4.4. Flowchart for estimation of capacity factor

4.8 Campaign for WRA-Measurement of Wind Climatological Data

Wind Resource assessment is time-wise extensive and expensive process. The campaign is, therefore, is supported by Government in several countries. The availability

of detailed data at several sites has generated confidence among wind power development. The basic steps in WRA at a site involve setting up meteorological mast for anemometer, wind vane and measuring instruments for measuring ambient temperature, pressure and humidity, with programmable data logger facility. Usually, detailed time-series data on wind speed, direction at 20 m, 50 m or 80 m height above ground and data on ambient air temperature, pressure and humidity at about 3 m above ground at a prospective wind farm site. The data recorded over a period of minimum one year is considered for characterizing the wind resource at the site.

In this section, first standard procedure for determining characteristic of wind resource using measured wind climatological data at experimental site at BITS Pilani K.K. Birla Goa campus is demonstrated. Next, following the standard procedure, the characteristics are determined using actual recorded data in a wind farm in Tamilnadu, a southern state in India.

The experimental WRA site at BITS Pilani K.K. Birla Goa campus, Goa is referred as site-I and existing commercial grid-connected wind farm is referred to as site-II in the following.

4.8.1 Description of Site-I: Wind Climatological Data Recording Station

The wind climatological data recording station at BITS-Pilani, K.K. Birla Goa campus, Goa, India was commissioned on 1 May 2014. Thus, data measured for one year full year upto 30 April 2015, is used for wind resource assessment at the site. The geographical location of the site is (Lat. $15^{\circ}23'N$, Long. $73^{\circ}49'E$), altitude 75 m mean sea level (MSL). The met mast installed at a height of 20 m AGL is shown in Fig. 4.5. The annual meteorological data recorded at five minutes interval includes, wind speed, wind direction, measured at a height of 10 m and 20 m AGL. In addition to the wind speed and direction data, air temperature, atmospheric pressure and relative humidity recorded at 3 m AGL, are listed in Table 4.2.

Table 4.2. Technical specifications of sensors used at site-I

S.No.	Parameter	Sensor	Measuring height	Range
1	Wind speed	3 cup anemometer	10 m and 20 m	0-65 m/s
2	Wind direction	Wind vane	10 m and 20 m	0-357 °
3	Air temperature	Platinum resistance	3 m	-40 °C to +60 °C
4	Relative humidity	Solid state capacitive type	3 m	0 to 99 %
5	Atmospheric pressure	Bellows connected to strain gauge	3 m	600 to 1100 hPa

**Fig. 4.5.** Wind climate data measurement at 20 m (AGL) at site-I

The recorded data is processed by using Windographer software [156]. The wind data is represented as graphical time-series data and wind direction data is represented as wind-rose diagram for the site. The five minutes data is used to obtain hourly average data for the analysis. Here, only the wind data measured at 20 m height is used for the analysis.

Fig. 4.6 shows month wise daily variation of average wind speed measured at 20 m (AGL). It is observed that the daily average wind speed varies between minimum of 1.38 m/s and maximum of 6.8 m/s occurring on 1 November and 22 July, respectively in 2014.

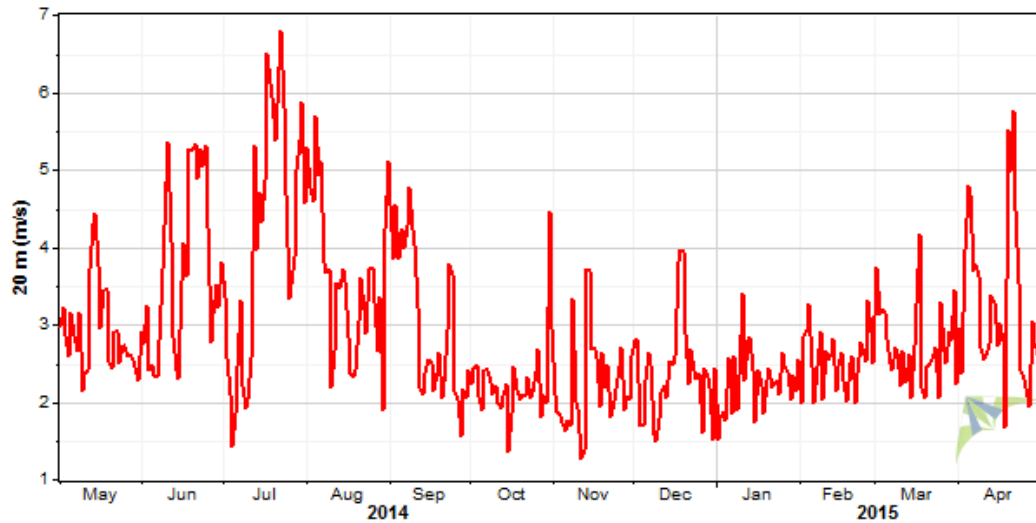


Fig. 4.6. Month wise variation of daily average wind speed at site-I (20 m)

Fig. 4.7 shows month wise daily variation of average temperature at the site. It is observed that the daily average temperature varies between minimum of 23.8 °C (11 July 2014) and maximum of 33.7 °C (6 June 2014).



Fig. 4.7. Month wise variation of daily average temperature at site-I

Fig. 4.8 shows month wise daily variation of average relative humidity at the site. It is observed that the daily average relative humidity varies between minimum of 43.2 % in 13 January 2015 and maximum of 97.2 % in 28 August 2014.

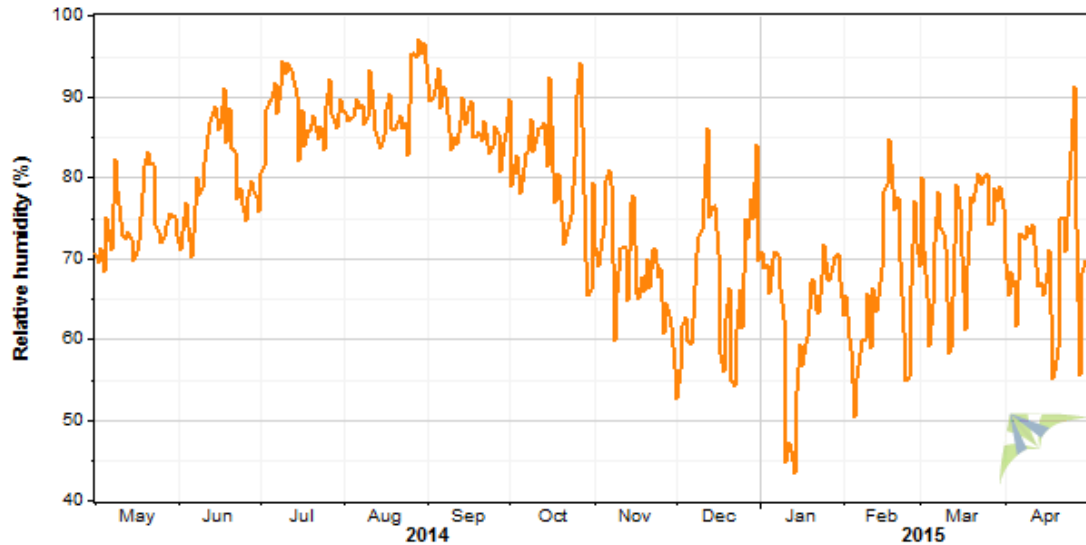


Fig. 4.8. Month wise variation of daily average relative humidity at site-I

Fig. 4.9 shows the wind rose diagram for the site. It is observed that prevalent direction of wind during the year is from west to east for most part of the year. It is observed that the predominant wind direction varies from month to month and the site mostly experiences wind from West (49.24 %) and North-West (33.4 %) directions.

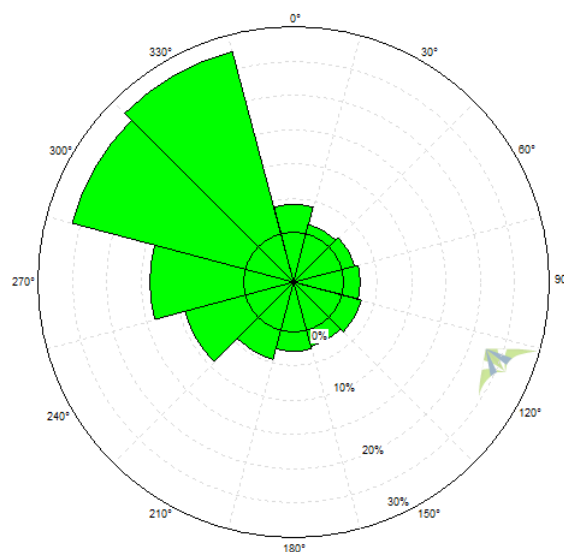


Fig. 4.9. Wind rose diagram at site-I (20 m)

Using the hourly wind data, the statistical parameters are obtained using MATLAB, for each month and year of measurement. These are monthly average wind speed (V_m), standard deviation (σ), air density (ρ), wind power density (WPD), turbulence intensity (TI) and energy pattern factor (EPF) are determined using (4.1), (4.2), (4.3), (4.4), (4.9), (4.10) and (4.11), respectively, and are listed in Table 4.3.

Table 4.3. Month-wise variation of statistical characteristics at site-I

Month Year	V_m (m/s)	V_d (m/s)	TI	EPF	ρ_C (kg/m ³)	ρ_H (kg/m ³)	WPD _C (W/m ²)	WPD _H (W/m ²)
May 2014	2.923	1.542	0.528	1.921	1.225	1.113	29.375	26.698
Jun 2014	3.740	1.639	0.438	1.584	1.225	1.114	50.767	46.176
Jul 2014	4.119	1.981	0.481	1.684	1.225	1.116	72.088	65.694
Aug 2014	3.595	1.618	0.450	1.612	1.225	1.102	45.870	41.271
Sep 2014	3.051	1.426	0.467	1.710	1.225	1.103	29.755	26.789
Oct 2014	2.248	0.959	0.426	1.630	1.225	0.952	11.349	8.824
Nov 2014	2.231	1.103	0.494	1.862	1.225	0.894	12.660	9.244
Dec 2014	2.400	1.206	0.502	1.881	1.225	0.892	15.922	11.597
Jan 2015	2.267	1.132	0.499	1.861	1.225	0.897	13.284	9.723
Feb 2015	2.545	1.496	0.588	2.195	1.225	0.893	22.169	16.161
Mar 2015	2.734	1.565	0.572	2.129	1.225	0.886	26.663	19.281
Apr 2015	3.296	1.809	0.549	2.001	1.225	0.885	43.890	31.714
Whole data	2.931	1.607	0.548	2.023	1.225	0.988	31.188	25.152

It is seen from the table that the monthly average wind speed, V_m varies between minimum of 2.231 m/s occurring in month of November 2014 to maximum of 4.119 m/s occurring in July 2014, in the year. The annual average wind speed is 2.93 m/s.

From Table 4.3, it is also noted that the minimum value of σ is 0.959 m/s which occurs in October and the maximum value of 1.981 m/s in July. The TI varies from minimum of 0.426 in October to maximum of 0.588 in February 2015. The EPF varies from minimum of 1.584 to a maximum of 2.195.

The air density (ρ_H), which takes into account of relative humidity in the calculation, varies from minimum of 0.886 kg/m³ in March 2015 to maximum of 1.116 kg/m³ in July

2014. The wind power density calculated using constant air density ($\rho_C = 1.225 \text{ kg/m}^3$), WPD_C , varies from a minimum of 11.349 W/m^2 to a maximum of 72.088 W/m^2 . Also the wind power density, WPD_H , corresponding to ρ_H varies from a minimum of 8.824 W/m^2 to a maximum of 65.694 W/m^2 . Table 4.4 lists the wind power classification on the ba-

Table 4.4. Wind power classification on the basis of wind speed and wind power density at 50 m AGL [139]

Wind power class		wind speed (m/s)	wind power density (W/m^2)
1	Poor	0-5.6	0-200
2	Marginal	5.6-6.4	200-300
3	Fair	6.4-7	300-400
4	Good	7.0-7.5	400-500
5	Excellent	7.5-8	500-600
6	Outstanding	8.0-8.8	600-800
7	Superb	> 8.8	>800

sis of wind speed and wind power density measured at 50 m AGL [139]. In the case of site-I, the wind power density at 20 m, 50 m, 100 m is found to be 25.15 W/m^2 , 84.38 W/m^2 and 210.82 W/m^2 , respectively. On the basis of wind power density, the measurement site falls under class 1 category and thus the site-I is considered to be small wind regime with low wind power density.

4.8.2 Description of Site-II: Model Wind Farm

The site-II represents grid integrated wind farm in India situated at Periyapatti, TamilNadu (hereafter named as “site-II”) (Lat. $10^\circ 45' 18.5'' N$, Long. $77^\circ 15' 11.0'' E$), altitude 327 m mean sea level. The site is located approximately 22 km from Udumalpet, Coimbatore, TamilNadu. The main source of wind is expected through Palghat pass. The site provided detailed wind climatological data measured for a period of two years from 1 October 2010 to 30 September 2012 at four different heights, viz., 35 m, 50 m, 70 m and 85 m at an interval of 10 minutes, wind direction measured at two different heights at 63 m and 83 m AGL. In addition, the data includes air temperature measured at 6 m AGL are used for the analysis. Fig. 4.10 shows the met mast installed at the site. The data recorded includes, time series data on wind speed measured Here, only the time-series

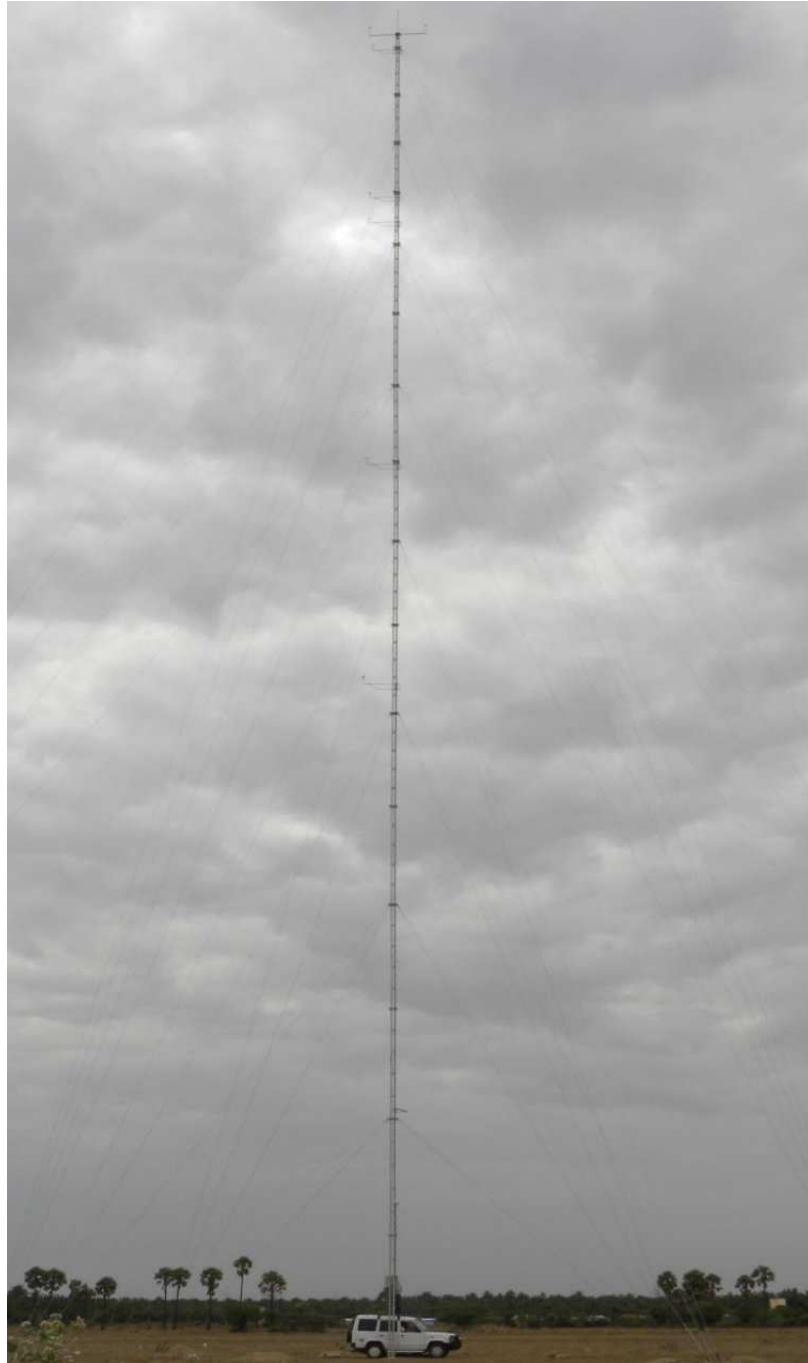


Fig. 4.10. Met mast installed at a height of 85 m AGL at site-II

wind data of 10 minutes interval recorded at 85 m height is used for the analysis. The raw time series measured data is processed using Windographer, Ver 3.3, the computational software obtained from WindoGrapher, Canada'[156]. The measured data is represented as graphical time-series data and measured wind direction data is represented as wind-rose diagram for the site.

Fig. 4.11 shows month wise daily variation of mean wind speed measured at 85 m (AGL). It is observed that, the daily mean wind speed varies between minimum of 1.38 m/s occurring on 3 December 2011 and maximum of 12.8 m/s occurring on 24 May 2012.

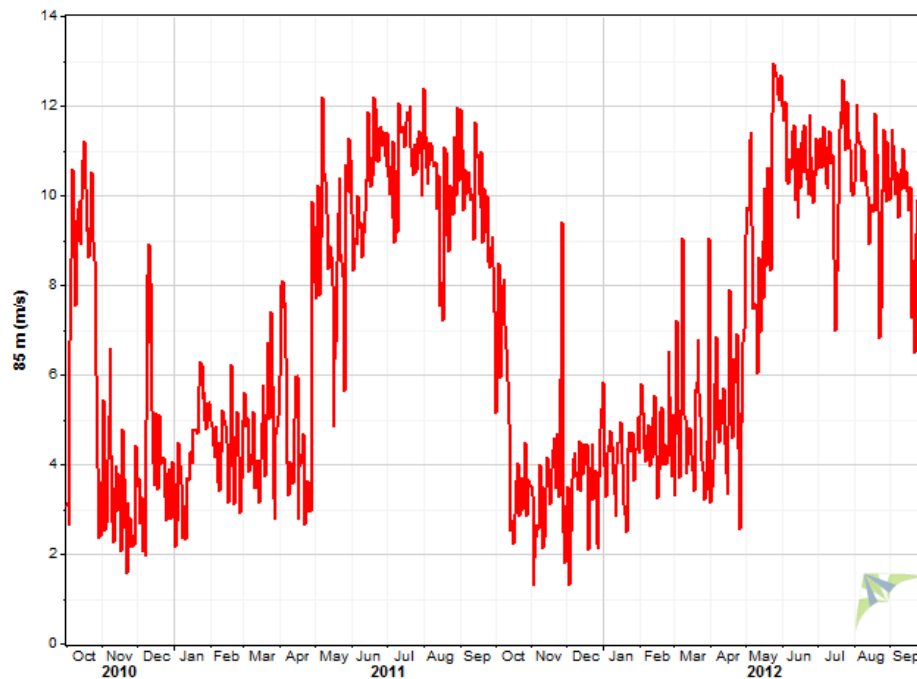


Fig. 4.11. Month wise variation of daily average wind speed at site-II (85 m)

Fig. 4.12 shows the wind rose diagram for the site which is measured at 83 m height. It is seen that predominant direction of the site mostly receives about 62 % from westerly winds for most part of the year. Fig. 4.13 shows the predominant direction with the wind speed distribution. It is observed that 35 % of the time the wind speed lies in the range of 8 m/s to 12 m/s in the western part of the site.

Fig. 4.14 shows month wise daily variation of mean temperature at the site. It is observed that, the daily mean temperature varies between minimum of 20.5 °C occur in the month of 27 December 2011 and maximum of 30.7 °C occur in 19 April 2012.

Using the hourly wind data, the statistical parameters are obtained using MATLAB, for the year of measurement. The average wind speed (V_m), standard deviation (σ), air density (ρ), wind power density (WPD), turbulence intensity (TI) and energy pattern factor (EPF) are determined using (4.1), (4.2), (4.3), (4.4), (4.9), (4.10) and (4.11), respectively, are listed in Table 4.5.

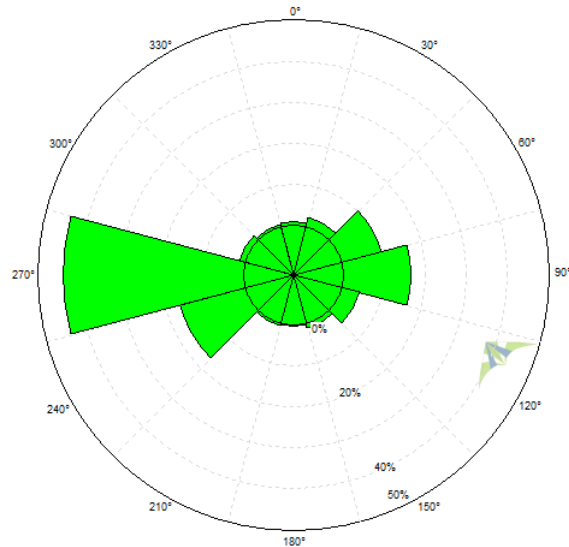


Fig. 4.12. Wind rose diagram at site-II (83 m)

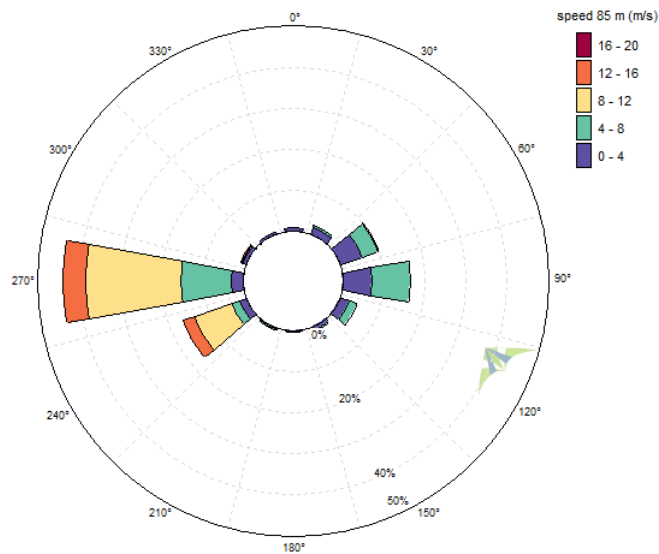


Fig. 4.13. Wind rose diagram showing distribution of wind speed in the prevalent direction at site-II

It is seen from the table that the monthly V_m varies between minimum of 3.344 m/s occurring on November 2010 to maximum of 10.904 m/s occurring on July 2011.

From Table 4.5, it is also noted that the minimum value of standard deviation (σ) is 1.251 m/s which occurs in January 2012 and maximum value of 3.307 m/s in October 2010. The TI varies from minimum of 0.171 in July 2011 to maximum of 0.607 in November 2010. The EPF varies from minimum of 1.088 in July 2011 to maximum of 2.212 in November 2010.

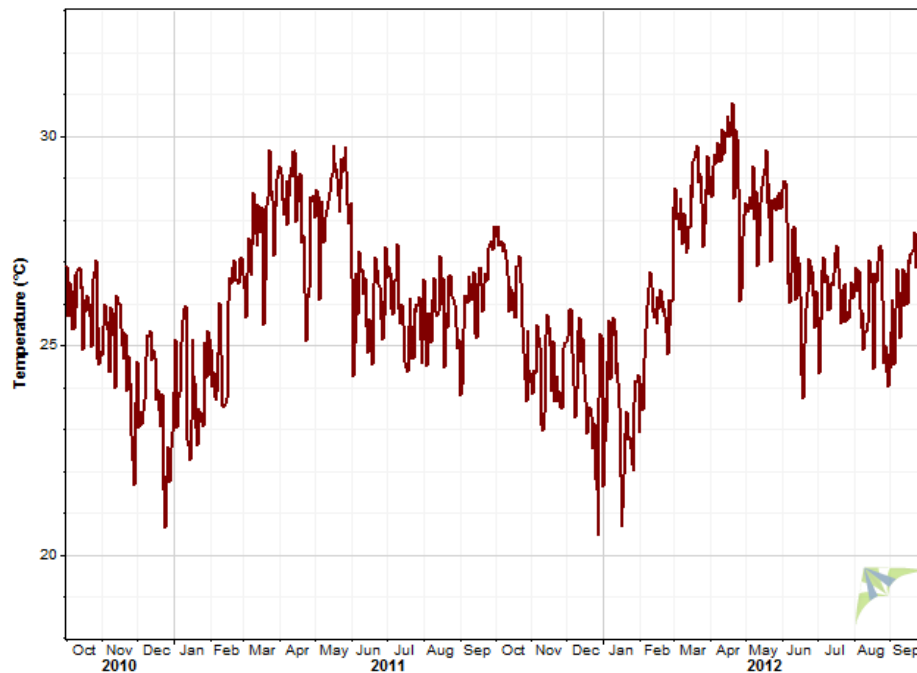


Fig. 4.14. Month wise variation of daily average temperature at site-II

The air density (ρ_H), which takes into account relative humidity in the calculation, varies from minimum of 1.167 kg/m^3 in April 2012 to maximum of 1.189 kg/m^3 in December 2010. The wind power density calculated by using for constant air density ($\rho_C = 1.225 \text{ kg/m}^3$), WPD_C , varies from a minimum of 50.681 W/m^2 to a maximum of 863.808 W/m^2 . Also the wind power density, WPD_H , corresponding to ρ_H varies from a minimum of 49.000 W/m^2 to a maximum of 832.306 W/m^2 .

4.8.2.1 Weibull Probability Distribution Analysis using Graphical Method

In this section, the shape and scale parameters determined by graphical method is discussed in this Section 4.3.1.

It is observed from Table 4.6 that V_{mW} varies from minimum of 3.424 m/s in November 2010 to maximum of 10.904 m/s in July 2011. Similarly, k varies from minimum of 1.394 occurring on November 2010 to maximum of 7.133 occurring on July 2011. Also, c varies from minimum of 3.754 m/s occurring on November 2010 to maximum of 11.666 m/s occurring on July 2011. The values of k and c over a period of two years are estimated as 1.749 and 7.578 m/s , respectively, as listed in Table 4.6.

Table 4.5. Month-wise variation of statistical parameters at Site-II

Data	V_m (m/s)	V_d (m/s)	TI	EPF	ρ_C (kg/m ³)	ρ_H (kg/m ³)	WPD _C (W/m ²)	WPD _H (W/m ²)
Oct 2010	7.543	3.307	0.438	1.527	1.225	1.180	401.369	386.493
Nov 2010	3.344	2.031	0.607	2.212	1.225	1.184	50.681	49.000
Dec 2010	4.240	2.108	0.497	1.827	1.225	1.189	85.307	82.820
Jan 2011	4.290	1.784	0.416	1.504	1.225	1.187	72.772	70.520
Feb 2011	4.300	1.841	0.428	1.558	1.225	1.182	75.870	73.209
Mar 2011	4.709	2.269	0.482	1.731	1.225	1.173	110.718	105.978
Apr 2011	5.000	2.921	0.584	2.107	1.225	1.171	161.322	154.208
May 2011	8.947	2.427	0.271	1.205	1.225	1.169	528.568	504.524
Jun 2011	10.315	2.160	0.209	1.132	1.225	1.179	761.185	732.594
Jul 2011	10.904	1.866	0.171	1.088	1.225	1.180	863.808	832.306
Aug 2011	10.209	2.134	0.209	1.128	1.225	1.180	734.918	707.908
Sep 2011	9.919	1.969	0.199	1.118	1.225	1.178	667.939	642.467
Oct 2011	4.683	2.540	0.542	1.958	1.225	1.178	123.219	118.541
Nov 2011	3.459	1.948	0.563	2.143	1.225	1.186	54.333	52.593
Dec 2011	3.722	1.651	0.444	1.615	1.225	1.188	51.007	49.460
Jan 2012	4.052	1.251	0.309	1.290	1.225	1.189	52.542	51.019
Feb 2012	4.567	1.754	0.384	1.446	1.225	1.181	84.364	81.316
Mar 2012	4.871	2.615	0.537	1.943	1.225	1.170	137.492	131.328
Apr 2012	5.284	2.747	0.520	1.849	1.225	1.167	167.021	159.117
May 2012	9.931	2.587	0.260	1.194	1.225	1.170	716.034	683.849
Jun 2012	10.831	1.923	0.178	1.095	1.225	1.177	852.127	818.667
Jul 2012	10.673	2.053	0.192	1.110	1.225	1.178	826.850	795.359
Aug 2012	10.166	2.135	0.210	1.131	1.225	1.180	727.674	700.717
Sep 2012	9.632	2.098	0.218	1.138	1.225	1.177	623.038	598.596
Whole data	6.913	3.630	0.525	1.846	1.225	1.179	373.599	359.544

It is observed from the table, that the V_{mp} varies from minimum of 1.516 m/s to maximum of 11.421 m/s and V_{maxE} varies from 5.242 m/s in January 2012 to 15.252 m/s in October 2010. The annual values of V_{mW} , V_{mp} and V_{maxE} are estimated as 6.749 m/s, 4.66 m/s and 11.719 m/s, respectively.

From the table, it is observed that WPD_{WC} corresponding to ρ_C varies from a minimum of 64.623 W/m² in the month of November 2011 to a maximum of 861.906 W/m² in the month of July 2011 and WPD_{WH} corresponding to ρ_H varies from 59.651 W/m² to a maximum of 830.473 W/m².

The percentage change in WPD_{WC} (416.811 W/m²) to WPD_{WH} (401.130 W/m²) is -3.59%. Also the percentage change in the annual variation of wind power density calculated using the actual value (359.544 W/m²) to that of the wind power density estimated using Weibull parameters (401.130 W/m²) is found to be 11.566 %. Also,

Table 4.6. Month-wise variation of Weibull parameters and their associated statistical parameters using graphical method at site-II

Month	V_{mW} (m/s)	k (m/s)	c	V_{mp}	V_{maxE} (kg/m ³)	WPD_C (kg/m ³)	WPD_V (W/m ²)	WPD_E (W/m ²)	RMSE	R^2
Oct-10	8.075	1.559	8.984	4.654	15.252	829.001	798.275	106.543	0.023	0.131
Nov-10	3.424	1.394	3.754	1.516	7.108	74.908	72.423	47.803	0.018	0.737
Dec-10	4.297	1.995	4.848	3.420	6.867	93.047	90.335	9.074	0.018	0.778
Jan-11	4.391	1.992	4.954	3.491	7.023	99.414	96.337	36.610	0.017	0.800
Feb-11	4.354	2.114	4.916	3.630	6.736	91.540	88.329	20.654	0.011	0.920
Mar-11	4.753	1.943	5.360	3.694	7.716	129.392	123.852	16.866	0.007	0.943
Apr-11	5.054	1.584	5.632	2.999	9.431	198.891	190.119	23.288	0.007	0.888
May-11	9.036	3.329	10.069	9.045	11.598	601.683	574.313	13.833	0.016	0.754
Jun-11	10.331	5.808	11.156	10.799	11.739	754.238	725.908	-0.913	0.008	0.931
Jul-11	10.923	7.133	11.666	11.421	12.077	861.906	830.473	-0.220	0.009	0.942
Aug-11	10.225	5.213	11.109	10.664	11.823	748.222	720.723	1.810	0.006	0.967
Sep-11	9.928	6.005	10.701	10.382	11.226	665.181	639.815	-0.413	0.006	0.972
Oct-11	4.727	1.756	5.309	3.285	8.185	142.502	137.093	15.650	0.007	0.940
Nov-11	3.521	1.692	3.945	2.326	6.255	61.623	59.651	13.418	0.020	0.791
Dec-11	3.805	1.931	4.290	2.941	6.199	66.789	64.764	30.942	0.022	0.770
Jan-12	4.080	3.317	4.547	4.081	5.242	55.478	53.870	5.588	0.013	0.949
Feb-12	4.637	2.374	5.232	4.155	6.768	100.172	96.554	18.738	0.012	0.911
Mar-12	4.907	1.799	5.518	3.515	8.359	154.905	147.960	12.665	0.005	0.960
Apr-12	5.302	1.878	5.973	3.985	8.786	186.166	177.356	11.463	0.007	0.914
May-12	9.984	3.738	11.057	10.173	12.400	771.621	736.937	7.763	0.008	0.909
Jun-12	10.850	6.977	11.601	11.347	12.028	847.348	814.076	-0.561	0.010	0.915
Jul-12	10.682	6.241	11.489	11.172	12.013	822.849	791.510	-0.484	0.006	0.971
Aug-12	10.172	5.584	11.009	10.627	11.629	725.663	698.781	-0.276	0.007	0.952
Sep-12	9.649	4.914	10.520	10.044	11.276	637.961	612.934	2.395	0.008	0.951
Whole data	6.749	1.749	7.578	4.666	11.719	416.811	401.130	11.566	0.010	0.703

from the table, the RMSE and R^2 for the whole data is found to be 0.0098 and 0.703, respectively.

Similar results obtained for monthly variation of parameters by using other methods such as standard deviation, energy pattern factor method, maximum likelihood method and Rayleigh distribution method are presented in Appendix B.

4.8.2.2 Comparison of Weibull and Rayleigh Distribution Methods

In this section, the results of the comparative study of Weibull distribution methods and Rayleigh distribution method are presented. From Table 4.7, it is observed that for the complete data the graphical method is the best method for site-II in terms of accuracy in fitting the PDF as indicated by RMSE and R^2 values. From Table 4.7, it is observed that the best values of k and c are 1.749 and 7.578 m/s. These values are revised using genetic algorithm method to improve the accuracy of estimation in terms of R^2 error in PDF.

Table 4.7. Comparison of Weibull distribution methods to Rayleigh distribution method at site-II

Method(s)	V_{mW} (m/s)	k	c (m/s)	V_{mp} (m/s)	V_{maxE} (m/s)	WPD_C (W/m ²)	WPD_V (W/m ²)	WPD_E (%)	RMSE	R^2
Graphical	6.749	1.749	7.578	4.666	11.719	416.811	401.130	11.566	0.0098	0.703
Standard deviation	6.913	2.013	7.802	5.546	10.991	384.041	369.593	2.795	0.0107	0.650
Energy pattern factor	6.913	2.083	7.805	5.701	10.783	371.572	357.593	-0.543	0.0112	0.615
Maximum likelihood	6.888	1.948	7.768	5.366	11.165	392.767	377.991	5.131	0.0103	0.674
Rayleigh distribution	6.913	2.000	7.801	5.516	11.032	386.682	372.135	3.502	0.0105	0.656

4.8.2.3 Use of Proposed Approach to Improve the Accuracy in Estimation of PDF

The proposed approach has been discussed in section 4.5. Using proposed approach, the annual values of k and c of the best method, i.e., GP method in this case are revised and corresponding RMSE is listed in Table 4.8. It is observed from the table, that the annual value of RMSE is improved by 12.24 % while using the proposed approach. This is evident in Fig. 4.15, where it is seen that the proposed approach (i.e., GP + GA) fits the whole data accurately. The actual wind power density is found to be 359.544 W/m², whereas the WPD calculated using the best method (i.e., graphical method) is found to be 401.137 W/m². Using the proposed method, the WPD obtains as 360.82 W/m². From this it is clear that the proposed method estimates the WPD very close to the actual calculated WPD than the best method (graphical method).

Table 4.8. Improvement in RMSE using proposed approach for site-II.

Parameters	Graphical method	Proposed approach (GP + GA)
k	1.749	2.082
c (m/s)	7.578	7.827
RMSE	0.0098	0.0086

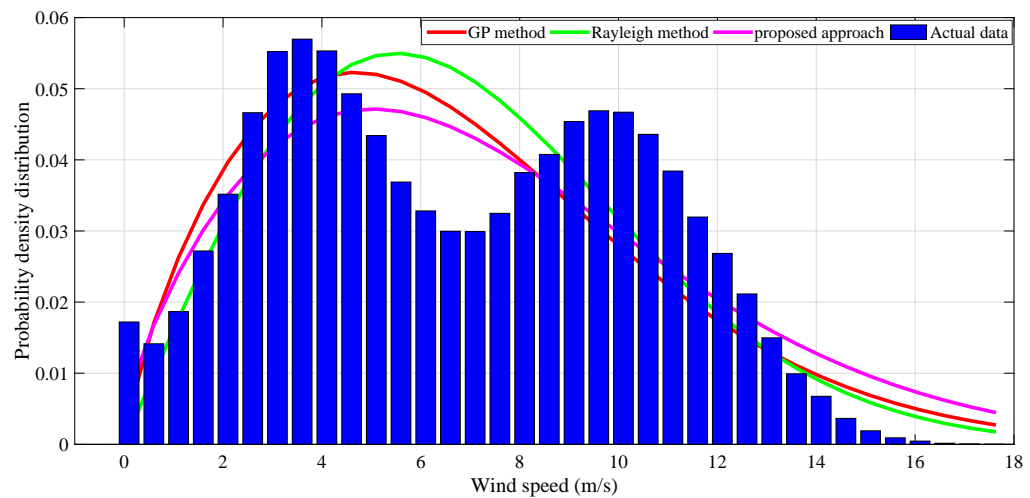


Fig. 4.15. Comparison of proposed approach with other methods in estimation of pdf (site-II)

4.8.2.4 Variation of Wind Power Density with Heights

The value of wind power density obtained at 85 m height AGL is estimated as 359.544 W/m^2 . Further the wind power density at different heights, viz., 100 m, 120 m and 150 m AGL, are estimated using the power law equation (4.46) and (4.48), respectively. The procedure is detailed in the form of flowchart shown in Fig. 4.3. As the wind speed data recorded at two different heights (70 m and 85 m) are 6.695 m/s and 6.913 m/s, respectively. The power law index, α is calculated using (4.47). The wind power density at different heights are listed in Table 4.9.

Table 4.9. Variation of wind power density with height (AGL) at site-II

Data	WPD_{m70} (W/m^2)	WPD_{m85} (W/m^2)	α	WPD_{100} (W/m^2)	WPD_{120} (W/m^2)	WPD_{150} (W/m^2)
whole data	332.249	359.544	0.165	389.643	426.419	476.185

The wind power density is estimated at higher heights, 100 m and 150 m AGL are found to be 389.64 W/m^2 and 476.18 W/m^2 , respectively.

4.8.2.5 Wind Turbine Characteristics and Capacity Factor

In this section, parameters (k and c) obtained from the proposed approach is used to find the capacity factor of the site for the selected wind turbine models. The procedure is detailed in the form of flowchart as shown in Fig. 4.4. The various wind turbine models with their specifications are shown in Table 4.10.

Table 4.10. The wind turbine characteristics for wind turbine models for site-II [157, 158]

S.No.	Manufactures	Cut-in speed (m/s)	Rated speed (m/s)	Cut-out speed (m/s)	Hub height (m)	Rated power P_{eR} (kW)
1	Vensys_77	3	13	22	85	1500
2	Vensys_82	3	12.5	22	85	1500
3	Vensys_87	3	12	22	85	1500
4	Suzlon_S_95	3.5	11	25	95	2100
5	Suzlon_S_97	3.5	11	20	97	2100

The capacity factors for site-II for different turbine models are listed in Table 4.11. From the table, it is observed that the capacity factor estimated for the actual wind turbine installed at the site (Vensys 82) is 38.3 %. Further the highest capacity factor of 44.6 % is estimated when wind turbine, Suzlon _S_95 is installed.

Table 4.11. Estimation of capacity factor for wind turbine models at site-II

S.No.	Turbine	α	k	c (m/s)	P_{out} (kW)	C_f (%)
1	Vensys_77	0.183	1.749	8.405	546.903	36.5
2	Vensys_82	0.183	1.749	8.405	575.144	38.3
3	Vensys_87	0.183	1.749	8.405	604.766	40.3
4	Suzlon_S_95	0.184	1.770	8.579	937.098	44.6
5	Suzlon_S_97	0.185	1.774	8.613	920.123	43.8

4.9 Conclusion

In this chapter, genetic algorithm is used for obtaining refined values of parameters k and c is developed. The values of these parameters are critically important in determining Weibull and Rayleigh distribution at the site. Using the standard procedure Weibull

distribution and Rayleigh distribution are obtained for two different sites. Site-I typifies wind climate measurement sites and site-II typifies existing grid connected wind farm. Next, genetic algorithm is used to obtain refined values of k and c for each of these sites. The two distributions, namely, Weibull distribution and Rayleigh distribution are obtained using refined values of k and c . The effectiveness of refined values of k and c in obtaining Weibull and Rayleigh distribution is determined in terms of root mean square error. Results show that analytically obtained distributions are closely agree with actual distributions obtained by using standard procedures. The distribution determined by refined values of k and c have been further used to determine wind power density with height above the ground. The values of probabilistic characteristic is in close agreement in terms of RMSE with the empirically obtained values. The following conclusions are drawn from the study:

1. In the case of site-I, the annual average wind speed measured at 20 m height is found to be 2.931 m/s.
2. The wind power density is estimated at 20 m, 50 m, 100 m height above ground is found to be 25.15 W/m², 84.38 W/m² and 210.82 W/m², respectively.
3. On the basis of wind power density, the site-I is classified as class-1 wind power classification and thus the site is considered to be small wind regime with low wind power density.
4. In the case of site-II, the average wind speed measured at met mast height of 85 m is found to be 6.931 m/s.
5. The wind power density is estimated at met mast height of 85 m is found to be 359.544 W/m² and it is further estimated at higher heights, 100 m and 150 m AGL are found to be 389.64 W/m² and 476.18 W/m², respectively.
6. On the basis of wind power density, the site-II falls under a class-3 wind power classification.
7. Graphical method is found to be best method in determining shape and scale parameters of wind speed probability density distribution.

8. The root mean square value in determining of shape and scale parameters of wind speed probability density distribution is found to be 0.0098, which is further improved to 0.0086 by using genetic algorithm. Thus the percentage change in error obtained is 12.24 %, leading to improvement in accuracy.
9. Further, capacity factor is determined for existing wind turbine installed at site-II is found to be 38.3 %.
10. Site-II is found to be suitable for commercial wind power generation.

However, the methods of assessment used in the chapter do not take into account on types of terrain (complex terrain or flat terrain). Also, the methods used in this chapter are valid for determining wind resource at the site of measurement. These methods cannot be used to estimate wind resource potential at any other location in the vicinity of met mast. In real wind farm, it is often the case that wind climate data is measured at one place and it is required to estimate wind resource potential at any other point in the vicinity. In such cases, the methods presented in this chapter cannot be used and use of powerful computer simulation tools becomes necessary. Using these tools, the complete performance of actual wind farm can be simulated, to be able to estimate annual energy production and capacity factor at the wind farm and effect of terrain can also be investigated. This is covered in the next chapter.

Chapter 5

Effect of Terrain on Wind Resource Assessment

In the previous chapter, procedure for wind resource assessment is demonstrated for estimates of wind power density at the point of measurement. However, the effect of terrain at the site is not taken into account. Also, the methods used are valid for determining wind resource at the point of measurement (met mast). These methods cannot be used to estimate wind resource potential at any other location in the vicinity of met mast. In this chapter, industry scale commercial softwares are used for estimating wind resource potential on area of land for wind farm when data measured at one point is available. The software tools used take into account on details of terrain such as orography (height variation of terrain) and roughness (obstacles due to tall buildings, vegetation) at the site. In the present chapter, use of software simulation tools taking into account the effect of terrain in wind resource assessment is presented. The software tools used are WindSim, Meteodyn and WindFarmer. The results are obtained for wind farm in the state of Tamilnadu (site-II).

5.1 Introduction

Wind resource assessment is the first step in development of wind-farm for electric power generation. Wind farm modeling software can be used to identify optimum locations of a given region. Further, the software tools facilitate improvements in cost efficiency and annual energy production (AEP). The software tools for complex terrain use Computational Fluid Dynamics (CFD) based mathematical models, whereas those for flat terrain use linear tools [159].

5.2 WindSim Simulation Software Tool

WindSim [160] is a industry scale commercial software developed by WindSim AS Tonsberg, Norway. WindSim simulation software is suitable for wind resource assessment in complex terrain. This software uses CFD based mathematical model using Reynolds Averaged Navier Stokes (RANS) equations using the finite volume method. This software can be used in wind power industry for estimation of annual energy production and capacity factor in complex terrain for evaluation of site in pre-investment stage.

5.2.1 Steps in Simulation using WindSim Software

WindSim Version.7, consists of six modules named as terrain, wind fields, objects, results, wind resources and energy [161]. The flowchart describing the different processes involved in WindSim simulation is shown in Fig. 5.1. The steps are described are as follows:

1. Using WindSim Express, the terrain data for a site from the Shuttle Radar Topography Mission (SRTM) data source. This includes, orography file, roughness and elevation of the site. The online map for the site is downloaded from Google earth using Global mapper. The Global mapper is a geographic information system (GIS) software package, which uses both vector, elevation data and provides viewing, conversion, and other general GIS features.

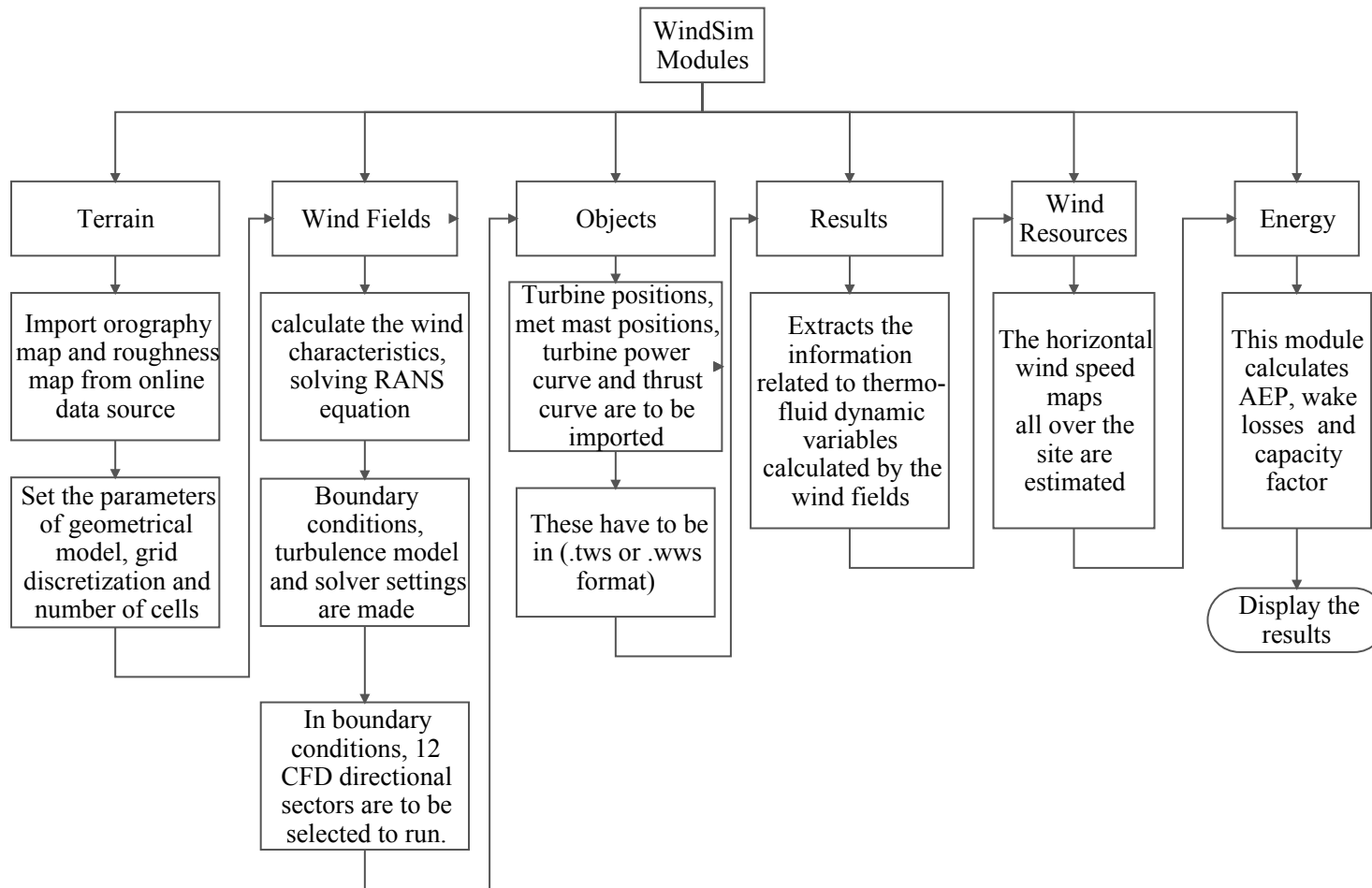


Fig. 5.1. Overview of WindSim software simulation tool.

2. The position of wind turbines in-terms of geographical coordinates, i.e., latitude and longitude of the site along with meteorological mast location in terms of latitude and longitude has to be imported to the software. Also the wind turbine specifications are to be supplied, viz., manufacturer name, turbine height and rotor diameter are required to be supplied.
3. The climatological data for the site namely, wind speed and direction is required as input to the software. The file generated by Windographer software as (.twc or .wvs format) is required to be input to estimate the wind flow pattern of the site. Thus, estimation for 12 different direction sectors of 30 degree each are estimated for the site.
4. The power curve and thrust coefficient values of wind turbines are also required to be input to the software for the wind flow simulation.
5. For estimation of wake effect, Jensen wake model is used by the WindSim software.
6. The software is capable of generating contour map of site, which gives information on wind speed and wind direction.
7. The capacity factor and annual energy production of the individual turbine as well as the that aggregated for entire site under consideration can be obtained.

The flowchart describing the steps in simulation to be followed are shown in Fig. 5.2.

5.2.2 Simulation of Site-II: Model Wind Farm using WindSim

The geographical coordinates of model wind farm is (Lat. $10^{\circ}45'18.5''N$, Long. $77^{\circ}15'11.0''E$), altitude 327 m MSL. The detailed description of model wind farm is given in section B.1.

The wind farm consists of 33 wind turbines that are located at widely separated locations on the site. Table 5.1 provides information of the turbine locations (turbine ID),

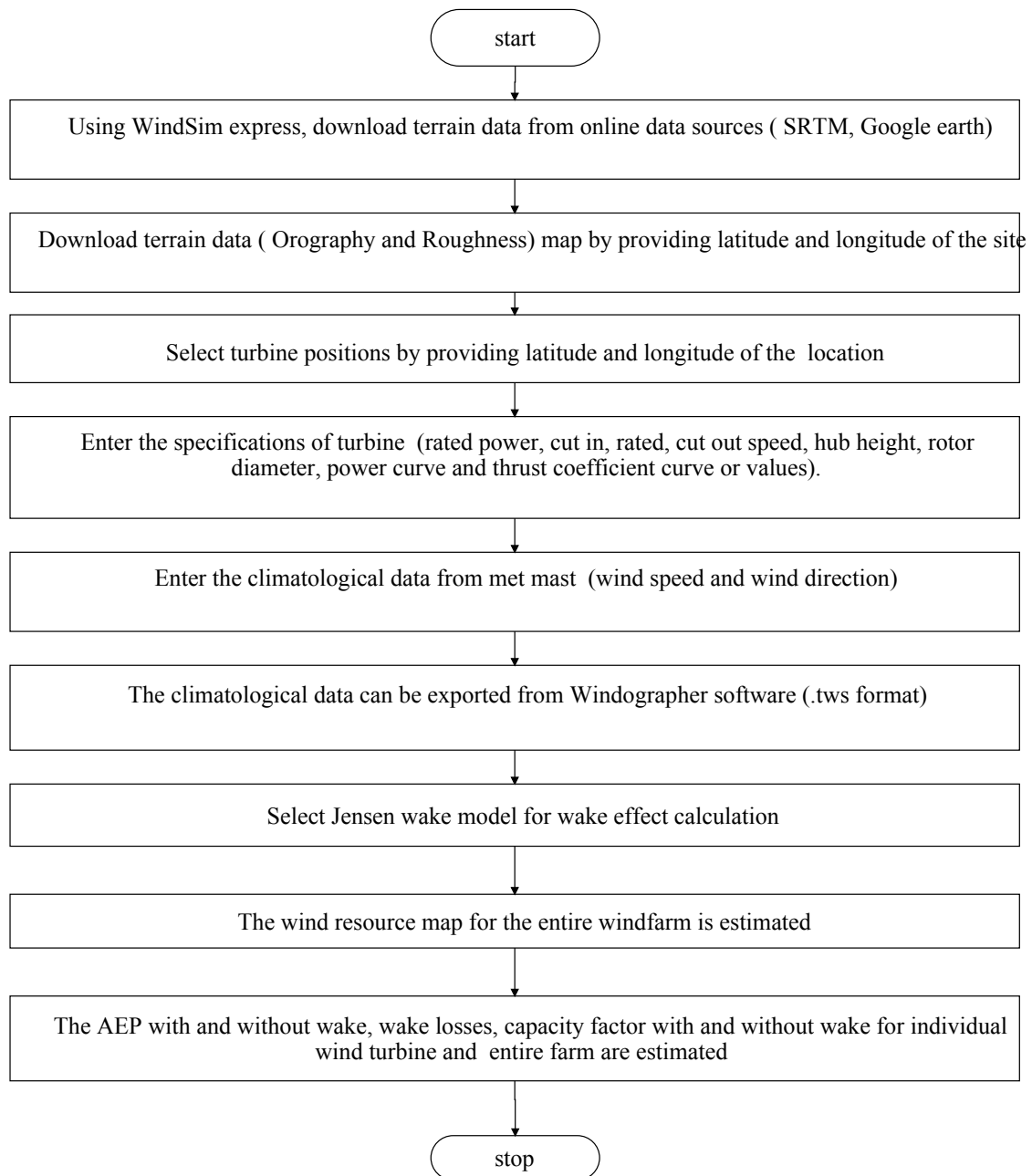


Fig. 5.2. Flowchart for simulating wind farm using WindSim simulation software tool

height of the hub above mean sea level, nearest turbine and the distance from the nearest turbine. These wind turbines and met mast are installed at a height of 85 m AGL.

The coordinate system used is Universal Transverse Mercator (UTM) coordinate system. The terms Eastings and Northings are geographic Cartesian coordinates for a point. Easting refers to the eastward-measured distance (or the x-coordinate), while northing refers to the northward-measured distance (or the y-coordinate) UTM-zones. The actual positions (vertical view and horizontal view) of the wind turbines in the wind-farm

Table 5.1. Location of wind turbine positions specified in terms of UTM coordinates at site-II

Turbine ID	Eastings (m)	Northings (m)	Height (m)	Nearest turbine ID	Distance to nearest turbine (m)
1	744820	1184171	333	15	499.2
2	741636	1183743	361	3	2145.7
3	743752	1184099	345	15	899.5
4	736383	1186434	356	6	948.9
5	737708	1184902	358	7	590.9
6	736932	1185660	353	7	720.8
7	737632	1185488	353	5	590.9
8	747458	1179314	340	12	1397.5
9	734493	1185390	364	10	580.7
10	735059	1185520	360	9	580.7
11	739179	1184331	360	5	1577.9
12	747541	1180709	335	13	1251.2
13	746338	1180365	339	12	1251.2
14	744693	1179009	350	13	2131.8
15	744575	1183736	334	1	499.2
16	743936	1182983	338	15	987.6
17	744176	1175324	357	27	1082.9
18	746895	1195407	331	24	577.0
19	746290	1195750	331	18	695.5
20	745026	1195822	335	23	645.3
21	743944	1195863	342	30	605.9
22	747898	1196242	334	28	905.8
23	745613	1195554	333	20	645.3
24	746861	1194831	329	31	518.4
25	745392	1197556	345	29	623.0
26	743285	1176472	363	27	936.3
27	744219	1176406	358	26	936.3
28	747026	1195997	338	18	604.4
29	745914	1197896	347	25	623.0
30	743798	1195275	345	21	605.9
31	747015	1194336	327	24	518.4
32	745103	1198371	354	25	864.7
33	744680	1190579	336	31	4423.5

obtained from Google earth are shown in Fig. 5.3 and Fig. 5.4, respectively. The terrain map and actual layout of wind turbines in the wind farm obtained by using WindSim are shown in Fig. 5.5.

The wind turbines used in the wind farm are of manufactured by ReGenTech, Ven-sys82 [157]. The wind turbine properties are listed in Table 5.2. Also the power curve and thrust coefficient curve of the wind turbine used are shown in Fig. 5.6.

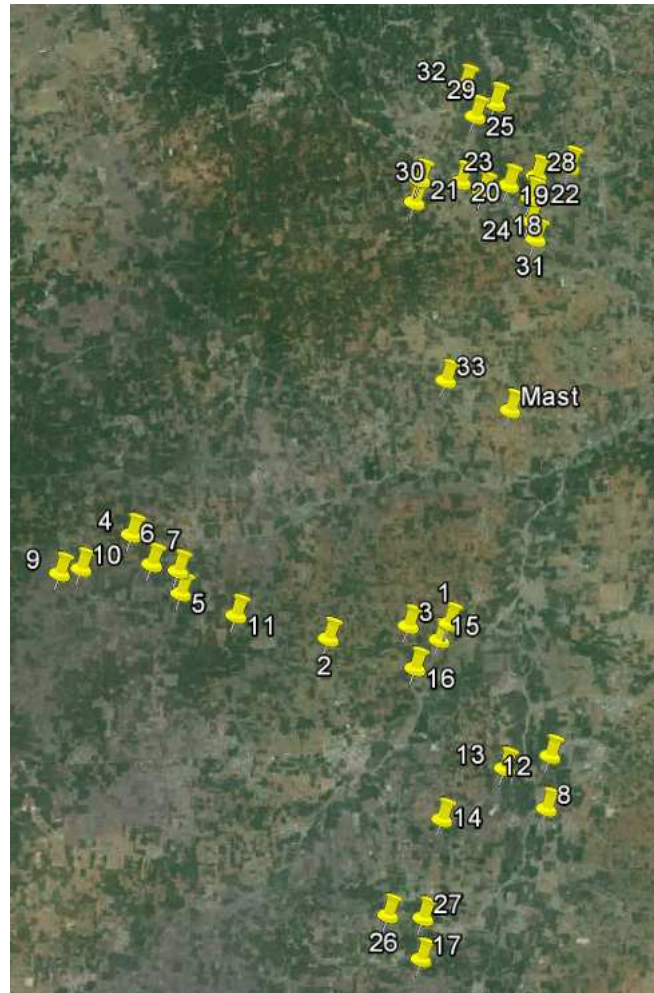


Fig. 5.3. Google map of site-II (vertical view).

Table 5.2. Specifications of wind turbine used at site-II

Name	Vensys82
Manufacturer	ReGen Tech
Rotor diameter	82 m
Hub height	85 m
Rated power	1500 kW
Air density	1.225 kg/m ³
Cut-in wind speed	3 m/s
Rated wind speed	12.5 m/s
Cut-out wind speed	22 m/s
Frequency	50 Hz

5.2.2.1 Wind Climate Condition at Site-II

The average wind condition at the site is used in the calibration of the wind resources and in the annual energy production estimation. A wind climatology is presented as a

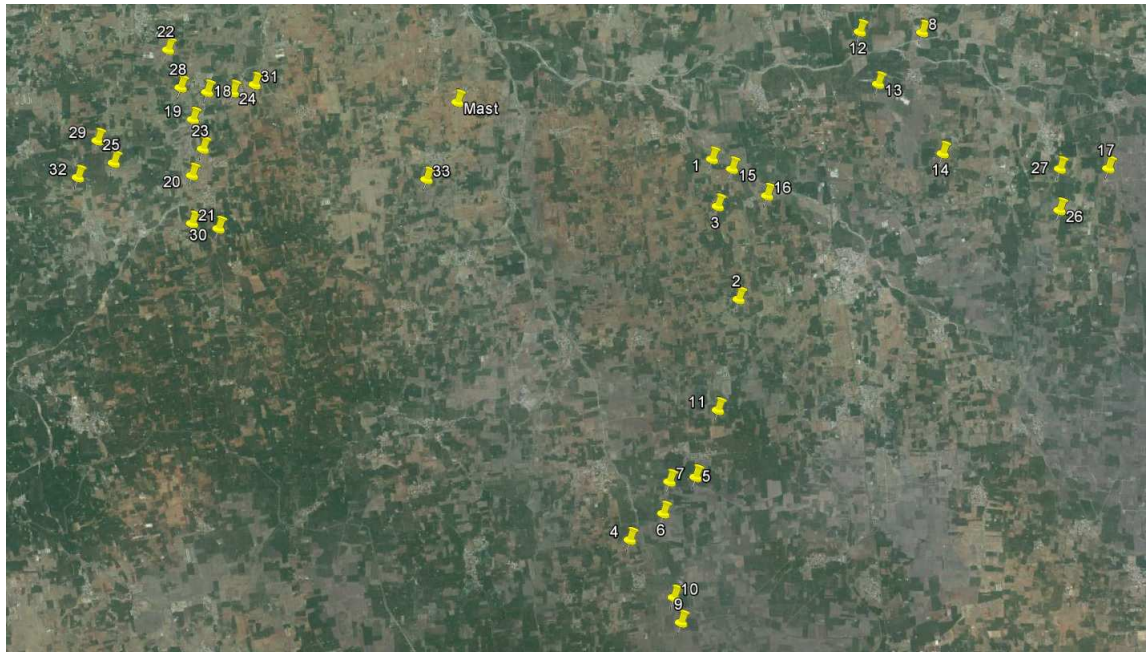
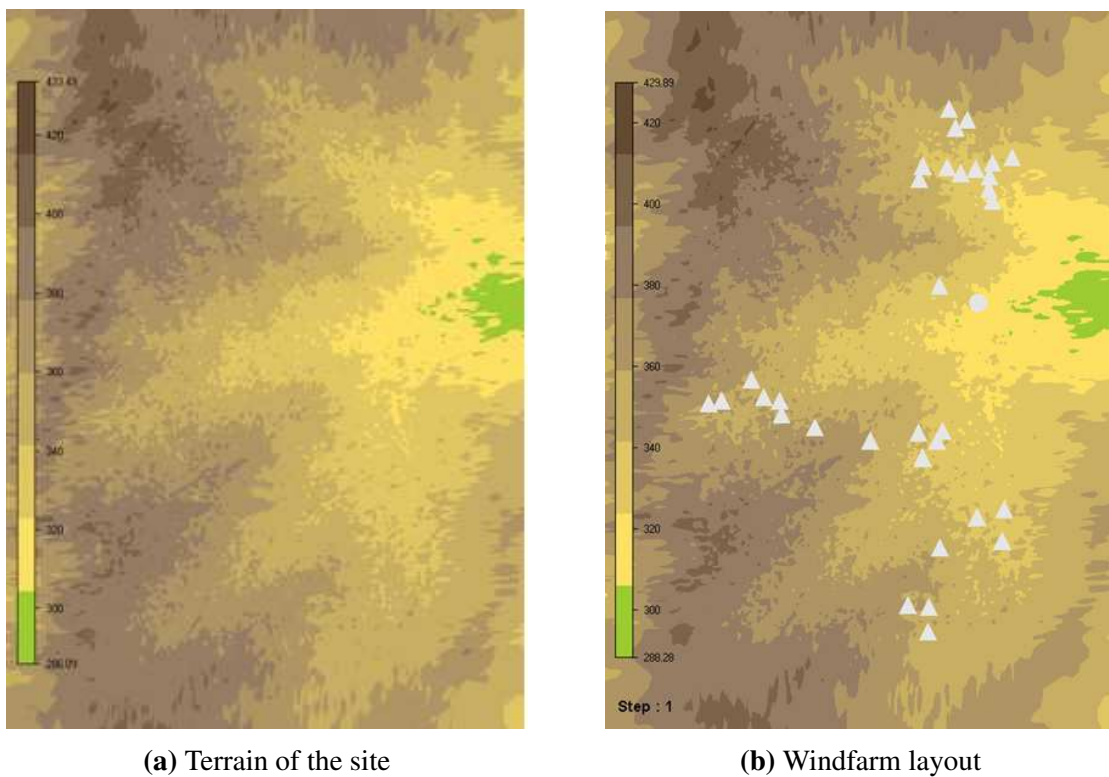


Fig. 5.4. Google map of site-II (horizontal view).



(a) Terrain of the site

(b) Windfarm layout

Fig. 5.5. View of terrain and wind farm layout using WindSim simulation.

wind rose, giving the average wind speed distribution divided in velocity intervals (bins) and wind directions (sectors). The wind directions are divided in 12 sectors of 30 degree each, where the first sector is centered around north.

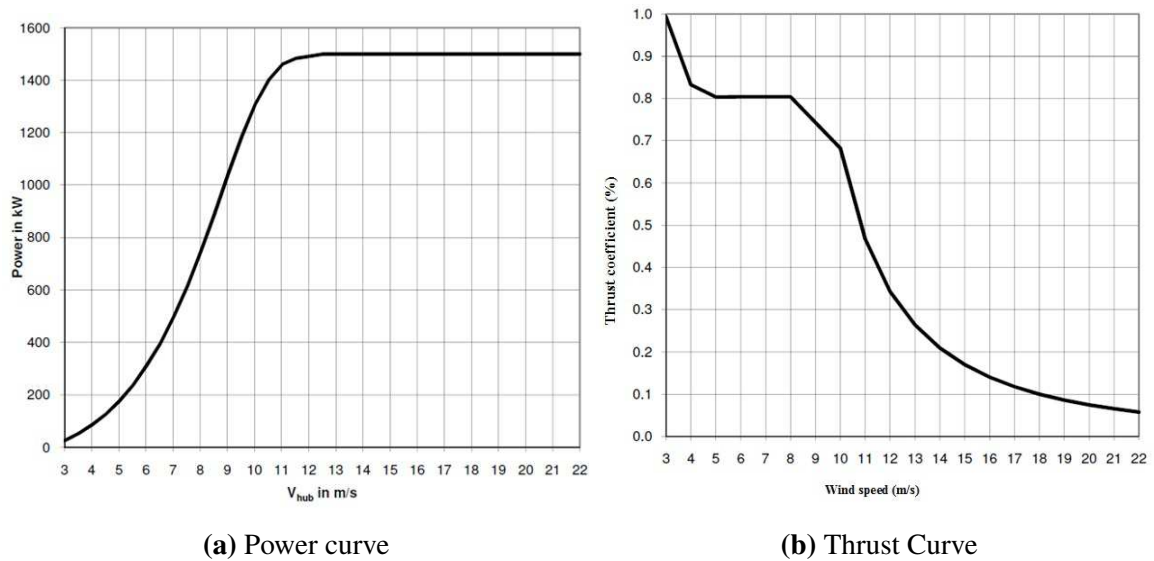


Fig. 5.6. Power curve and thrust coefficient curve of wind turbine used for simulation.

The average wind speed, frequency of distributions, Weibull parameters (i.e., shape, k , and scale, c) on 12 sectors are listed in Table 5.3. From the table, it is observed that the average wind speed is maximum (9.3 m/s) at the 9th sector and minimum (2.20 m/s) at the 7th sector. The wind rose diagram and Weibull distribution diagram are shown in Fig. 5.7. From the figures, it is observed that the site is having maximum % of frequency wind speed distribution (i.e., 44.21 %) obtained at 10th sector. The maximum value of Weibull shape (k) parameter recorded is 5.26 at 9th sector and minimum value recorded is 1.18 at 1st sector. Further, the maximum value of Weibull scale (c) parameter recorded is 10.66 m/s at 9th sector and minimum of 2.46 m/s is recorded at 7th sector.

Table 5.3. Average wind speed, frequency of distribution and Weibull parameters (shape, k and scale c) versus sectors

Sectors	1	2	3	4	5	6	7	8	9	10	11	12
Average wind speed (m/s)	2.35	2.93	3.81	4.28	3.66	2.62	2.20	2.26	9.31	8.83	2.77	2.27
Frequency (%)	1.09	2.41	10.00	16.57	4.56	1.22	0.56	0.62	16.56	44.21	1.46	0.74
Weibull shape, k	1.18	2.25	2.41	2.95	2.65	2.27	1.23	1.44	5.26	4.09	1.56	1.35
Weibull scale, c	2.58	3.44	4.30	4.82	4.24	3.15	2.46	2.58	10.66	9.95	3.11	2.50

Simulation and 3D Model Setup at Site-II:

A numerical wind database is established by CFD simulations and is used to transfer the wind conditions from the measurement point to the wind turbine hub positions. A digital terrain model (DTM) containing elevation and roughness data for the site are listed in

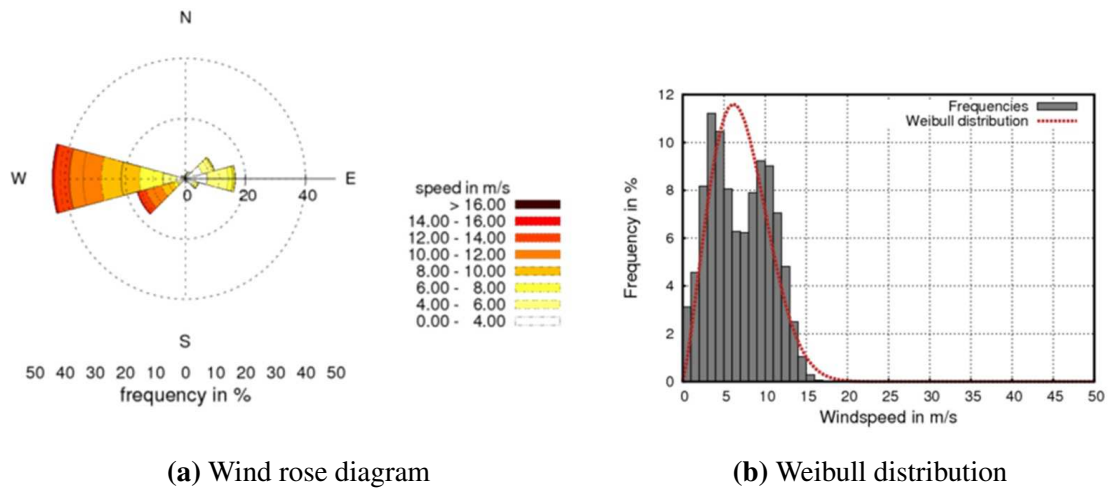


Fig. 5.7. Wind rose and frequency distribution with Weibull fitting for all sectors

Table 5.4 and corresponding maps are shown in Fig. 5.8. The complexity of the site

Table 5.4. Coordinates, extensions and resolution of the DTM (site-II)

	Min	Max	Extension	Resolution Terrain Data
Easting (m)	729452.6	752938.3	23485.7	38.0
Northing (m)	1170330.2	1203370.5	33040.2	38.0

determined by the variation in elevation and roughness. The elevation and roughness data are divided in cells with a variable, horizontal and vertical resolution. The grid is generated and optimized from the digital terrain model, are shown in Fig. 5.9. The grid spacing and number of cells used for the simulation are listed in Table 5.5.

Table 5.5. Grid spacing and number of cells used for simulation using WindSim (site-II)

	Easting	Northing	z	Total
Grid spacing (m)	63.2-551.0	63.3-545.9	Variable	-
Number of cells	248	400	18	1785600

5.2.2.2 Simulation using WindSim at Site-II

The digital model represents the computational domain where the Reynolds averaged Navier–Stokes equations have been numerically solved. Total 12 simulations have been performed in order to have a 3D wind field for every 30 degree sector. The solver setting

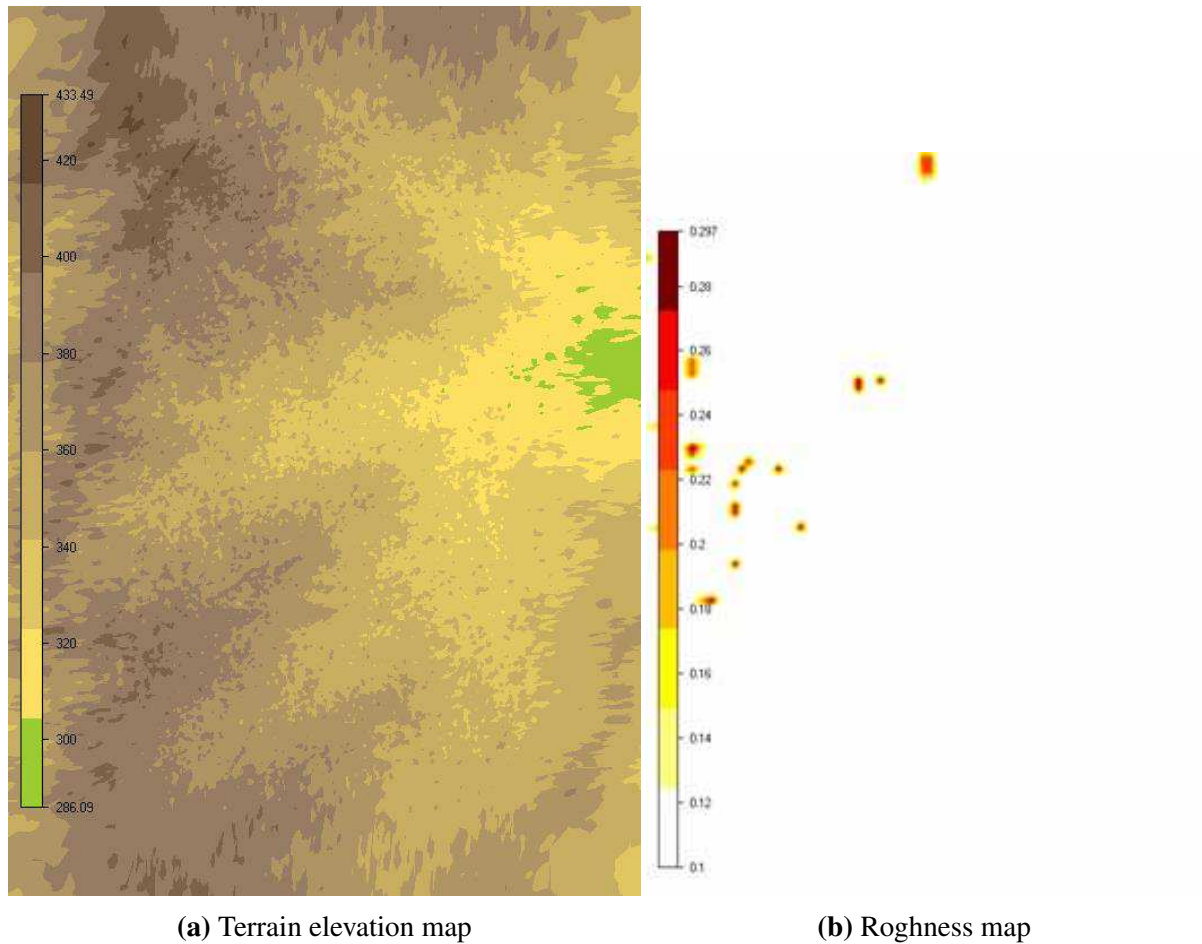


Fig. 5.8. Terrain elevation and roughness at site-II

used by WindSim is presented in Table 5.6. From the table it is observed that the maximum iterations assumed to be used for the simulation is 500. The simulation time and the number of iteration to reach a converged solution for each sector are presented listed in Table 5.7. The column “Status” should display as “C” indicating that the numerical procedure has converged, which means that the found solution actually is a solution of our specified problem.

Table 5.6. Setting used for simulation using WindSim (site-II)

Height of boundary layer (m)	500.0
Speed above boundary layer (m/s)	10.0
Boundary condition at the top	fix pres.
Potential temperature	No
Turbulence model	Standard
Solver	GCV
Maximum iterations	500

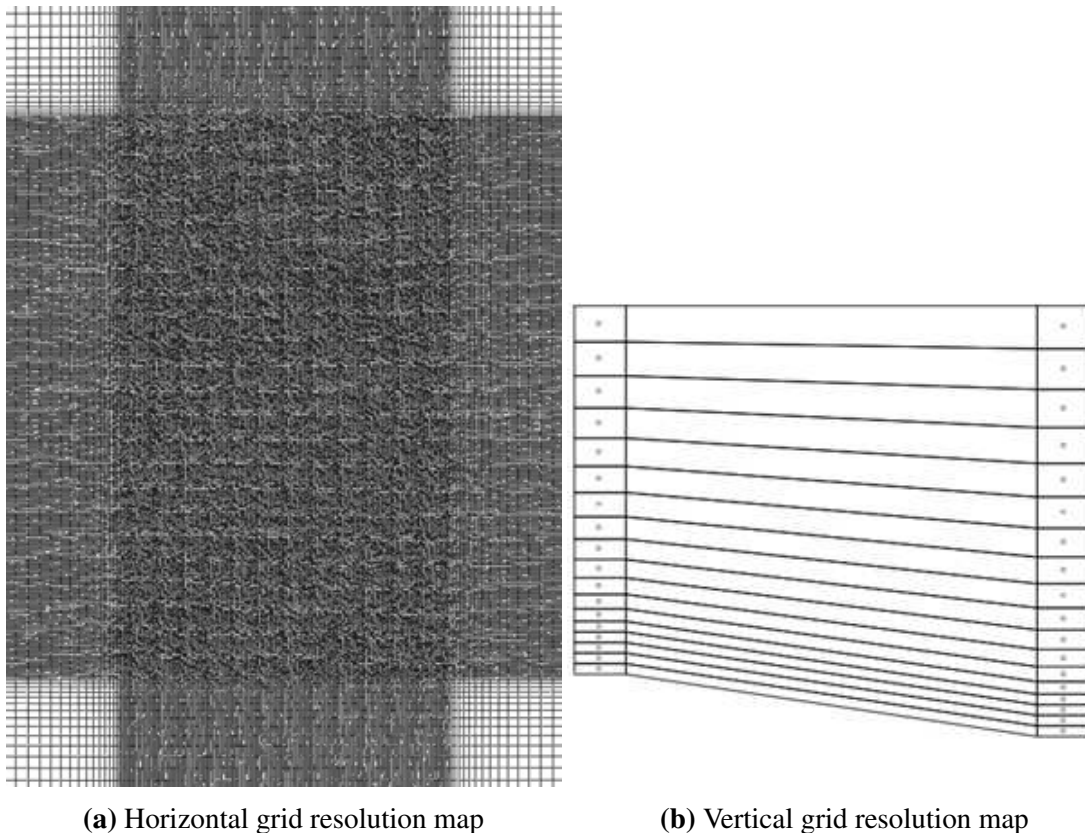


Fig. 5.9. schematic view of horizontal grid resolution and vertical grid resolution of site-II

Table 5.7. Simulation time, number of iterations and convergence status using Wind-Sim (site-II)

Sectors	Simulation time	Iterations	Status	Sectors	Simulation time	Iterations	Status
000	00:53:23	206	C	180	00:45:48	178	C
030	00:55:26	224	C	210	00:47:51	189	C
060	00:47:44	191	C	240	00:44:17	174	C
090	00:44:58	177	C	270	00:44:20	173	C
120	00:55:22	221	C	300	00:56:52	227	C
150	01:05:22	265	C	330	01:08:47	278	C

Wind Resource Map at Site-II using WindSim:

The wind resource map is used to identify the high wind speed area based on the average wind speed. The wind resource map is established by weighting the CFD results against the expected average conditions given as input. The corresponding wind resource map for the site-II after simulations is shown in Fig. 5.10.

Estimation of Energy Production and Capacity Factor:

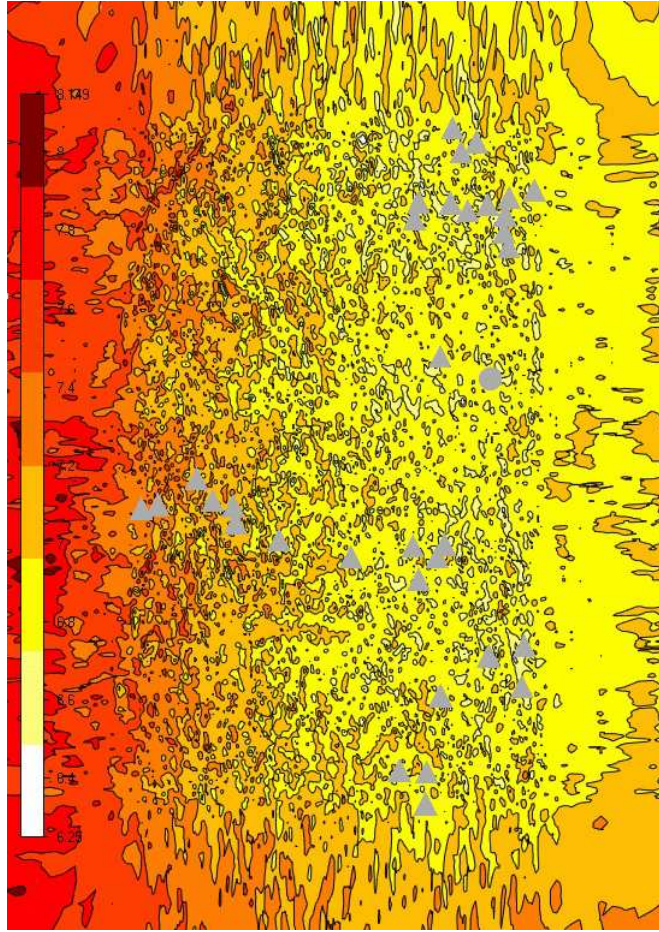


Fig. 5.10. Wind resource map with average wind speed at 85 m, site-II

The gross energy production is the energy production of the wind farm calculated by predicted free stream wind speed distribution at the hub height of each turbine location and the turbine's power curve provided by manufacturers. The wake effects is considered in the analysis is calculated by the WindSim wake model (Jensen wake model). Then the annual energy production is obtained by taking into account the wake losses. The average wind speed, AEP without wake effect, capacity factor with out considering the wake effects, wake losses, AEP with wake losses and capacity factor with wake effect for 33 wind turbines are presented in Table 5.8. From the table, it is noted that average wind speed (maximum of 7.27 m/s occurs at turbine ID-9 and minimum of 6.57 m/s occurs at turbine ID-31), AEP without wake (max: 6023 MWh/y (Mega Watt hours per year) for turbine ID-9 and min: 5186 MWh/y for turbine ID-19), capacity factor (max: 45.84 % for turbine ID-9 and min: 39.47 % for turbine ID-31). The maximum wake losses is 4.337 % obtained for turbine ID-19. The AEP with wake (max:

5982 MWh/y for turbine ID-9 and min: 5150 MWh/y for turbine ID-19), capacity factor (max: 45.53 % for turbine ID-9 and min: 39.19 % for turbine ID-19).

Table 5.8. Comparison of AEP and capacity factor with and without wake effect at site-II generated by WindSim simulation tool.

Turbine ID	Average wind speed (m/s)	Without wake		Wake Losses (%)	With wake losses	
		AEP (MWh/year)	capacity factor (%)		AEP (MWh/year)	capacity factor (%)
1	6.73	5403	41.12	2.56	5265	40.07
2	6.75	5455	41.51	0.44	5431	41.33
3	6.85	5556	42.28	1.20	5489	41.77
4	7.08	5860	44.60	0.38	5837	44.42
5	7.10	5883	44.77	0.37	5860	44.60
6	7.04	5825	44.33	1.32	5748	43.74
7	6.99	5761	43.84	2.42	5622	42.79
8	6.61	5248	39.94	0.54	5219	39.72
9	7.27	6023	45.84	0.67	5982	45.53
10	7.09	5877	44.73	4.16	5633	42.87
11	7.01	5776	43.96	0.06	5773	43.93
12	6.64	5288	40.24	1.30	5219	39.72
13	6.71	5366	40.84	0.45	5341	40.65
14	6.83	5535	42.12	0.11	5528	42.07
15	6.71	5391	41.03	0.62	5357	40.77
16	6.67	5337	40.62	0.20	5325	40.53
17	6.80	5483	41.73	0.01	5483	41.73
18	6.78	5447	41.45	2.11	5332	40.58
19	6.71	5383	40.97	4.33	5150	39.19
20	6.81	5501	41.86	3.25	5322	40.50
21	6.66	5321	40.49	0.44	5297	40.31
22	6.69	5328	40.55	2.47	5197	39.55
23	6.82	5512	41.95	1.98	5403	41.12
24	6.69	5339	40.63	0.39	5317	40.46
25	6.80	5486	41.75	0.43	5462	41.57
26	6.92	5645	42.96	0.44	5620	42.77
27	6.79	5480	41.70	2.58	5339	40.63
28	6.80	5480	41.70	2.63	5336	40.61
29	6.69	5353	40.74	2.07	5242	39.89
30	6.85	5555	42.28	0.35	5535	42.12
31	6.57	5186	39.47	0.15	5178	39.41
32	6.85	5537	42.14	0.10	5531	42.09
33	6.77	5463	41.58	0	5463	41.58

The wind farm production characteristics using WindSim software for the entire site-II are listed in Table 5.9. For the site, the installed capacity is 49.5 MW (33 turbines with 1500 kW each). The gross AEP (without wake) is estimated as 182.082 GWh/year. Therefore, the capacity factor estimated without considering the wake effect is estimated as

41.99 %. The total wake losses are estimated as 2.246 GWh/year. Thus, the net AEP estimated for the site after wake losses, is found to be 179.837 GWh/year (i.e., 1.23 % losses). Finally, the capacity factor of the site-II is 41.47 %.

Table 5.9. The wind farm production characteristics using WindSim at site-II.

No. of turbines	Capacity (MW)	Gross AEP (GWh/year)	Capacity factor (%)	Wake losses (GWh/year)	AEP with wake losses (GWh/year)	Capacity factor (%)
33	49.5	182.083	41.99	2.246	179.837	41.47

5.3 Meteodyn Simulation Software Tool

In this section, WRA is carried out using Meteodyn WT software. This software also uses CFD computations in complex terrains as WindSim software. Meteodyn WT [162] was developed in 2003 by Didier Delaunay. Meteodyn WT is also a CFD software including a Navier stokes equation solver as well as automatically boundary fitted mesher. Meteodyn WT has calculation ability over very large domains and unequaled speed of calculation because of the MIGAL solver.

The CFD code in Meteodyn WT is fully developed by Meteodyn, which removes all the limitations of Phoenics, used by WindSim, especially regarding the mesh. Mesh automatically aligned with the flow, it avoids numerical dispersion (better convergence with Meteodyn). Meteodyn WT generates a different mesh for each sector independently: Iteration number to reach convergence is lower than 25. WindSim generates an unique mesh that will run in all sectors, although sectors can be run independently, this system requires higher number of iterations to reach convergence.

5.3.1 Steps in Simulation using Meteodyn Software Tool

The steps involved in wind resource assessment using Meteodyn software are as follows:

1. The center point of the site in terms of UTM coordinates and the radius of the site in terms of meters are required to be supplied.

2. The South West and North East points in terms of UTM coordinates are required to be input as the boundary of the site.
3. Select the met mast point in UTM coordinates.
4. For the site considered, download orography and roughness data (terrain specifications) using SRTM corrected by Meteodyn, by selecting UTM coordinates, Northern hemisphere and selecting datum WGS84. The online map for the site is generated from Google earth using Global Mapper.
5. Using data management options, the mapping of the site for different heights can be obtained.
6. The wind turbine positions at the site (by specifying UTM coordinates and height of turbine) are required to be given as input to the software in .xyh format.
7. The wind turbine power curve (values) and thrust coefficient curve (values) obtained from the wind turbine manufacturer have to be imported to the software.
8. The climatological data for the site namely, wind speed and direction is required as input to the software. The file generated by Windographer software as (.tim format or .tab format) is required to be input to the software.
9. The simulation is carried out by selecting synthesis options, where the wind farm details namely turbine height, diameter of rotor, power curve values, thrust coefficient curve values are required to be input to the software.
10. The capacity factor and annual energy production of the individual turbine as well as the that aggregated for entire site under consideration can be obtained.

The flowchart describing the steps in simulation to be followed are shown in Fig. 5.11.

5.3.2 Simulation of Site-II: Model Wind Farm using Meteodyn

The description of the site is already presented in section 5.2.2. Table 5.10 gives detailed information of the site in-terms of site centre, radius, mapping, orography, roughness and met mast details.

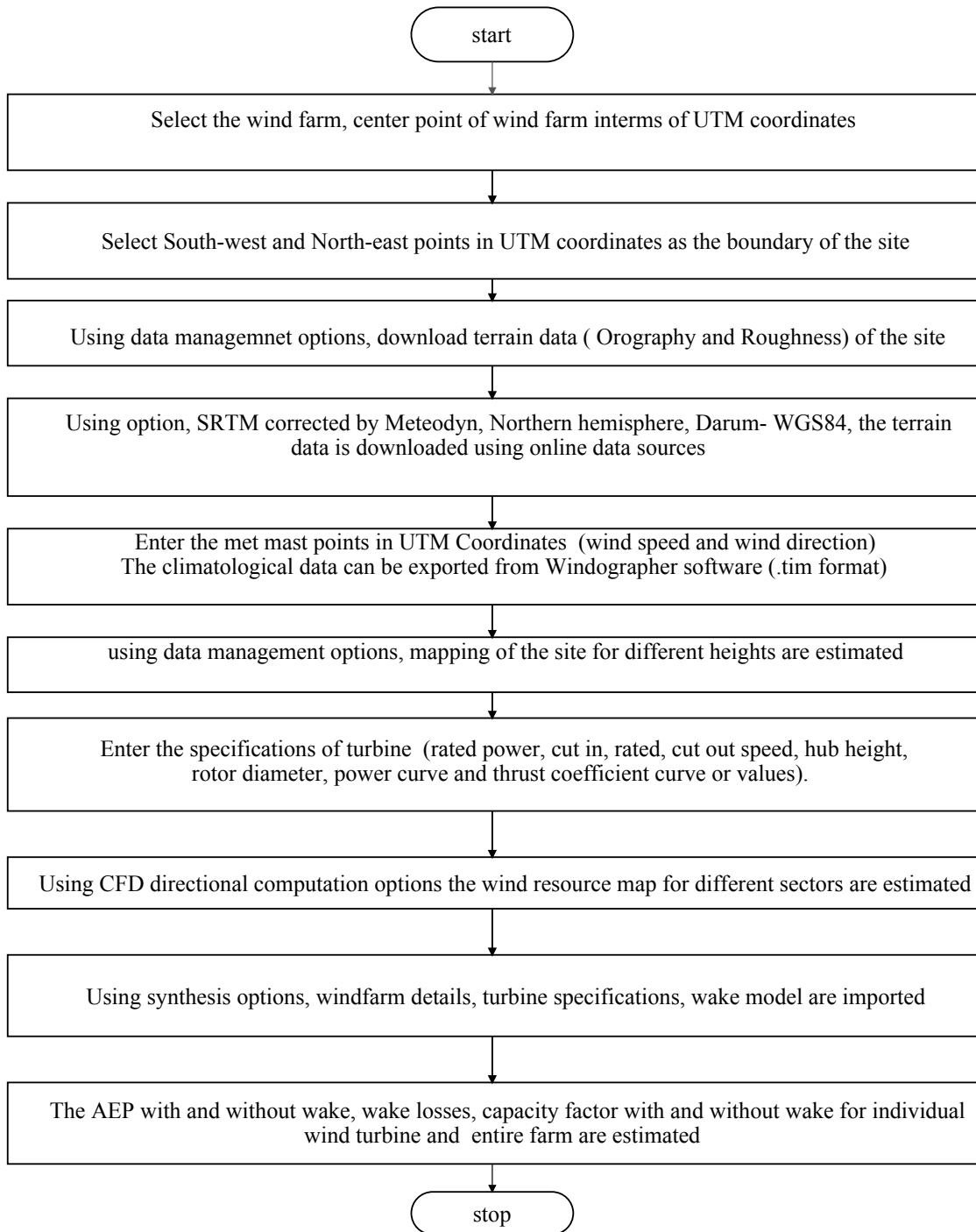
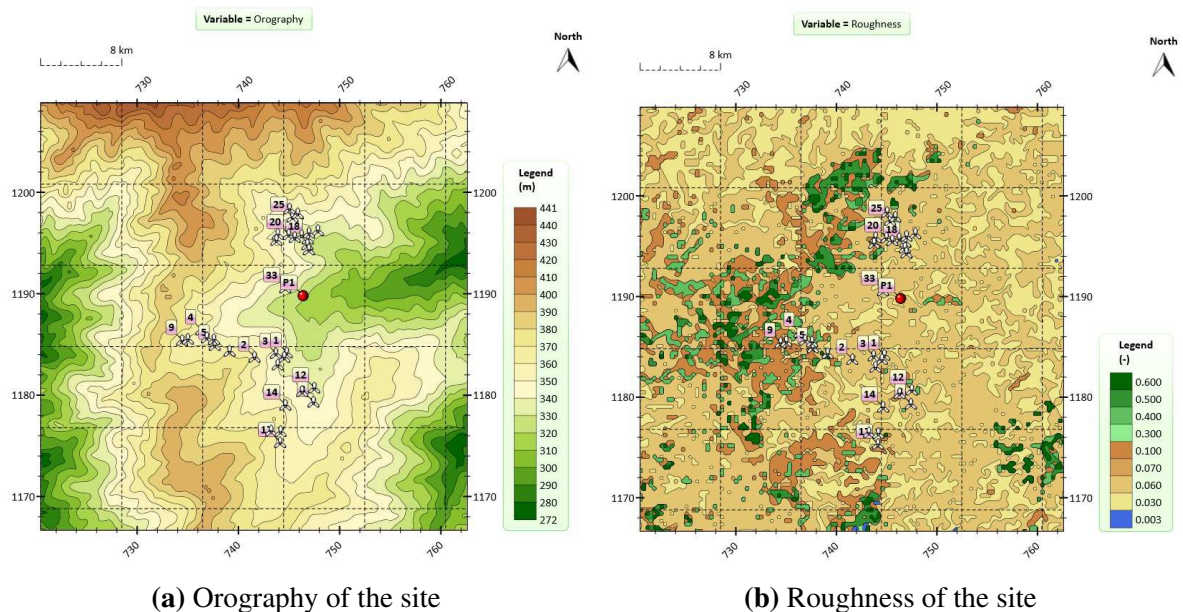


Fig. 5.11. Flowchart for simulating wind farm using Meteodyn simulation software tool.

Also, the terrain data (in-terms of orography and roughness) of the site is shown in Fig. 5.12.

Table 5.10. Description of wind farm (site-II) for simulation using Meteodyn.

Projection :	UTM - 72°E - 78°E - Northern Hemisphere - WGS84	
Site centre:	X Coordinates (m):	741541
	Y Coordinates (m):	1187738
	Latitude (decimal °):	10.736736
	Longitude (decimal °):	77.208577
Radius of results display (m):	21065	
Orography	SRTM3correctedByMeteodyn_3arcsec_N20_E70.tif	
Roughness	1_ESA_10arcsec_India.tif	
Mapping	South-West point (m; m):	(731866; 1174638)
	North-East point (m; m):	(751216; 1200838)
Mast	UTM- (746393, 1189810, 410)	85 m

**Fig. 5.12.** Terrain data in-terms of orography and roughness at site-II

5.3.2.1 Description of Wind Farm Layout at Site- II

The wind farm consists of 33 wind turbines that are located at different areas of the site are listed in Table 6.5. This table provides information of wind turbine positions in-terms of its UTM coordinates (Easting and Northing) and height above mean seal level. Similarly, the information of wind turbines used and their properties are listed in Table 5.2. The power curve and thrust curve for the wind turbines used for the study are shown in Fig. 5.6. The wind-rose diagram and histogram showing the distribution of wind speed are shown in Fig. 5.13. Table 5.11 provides information on wind speed distribution for 12 directional sectors. It is observed from the table that about 44.1 % of

the wind is flowing from 270 sector (West direction).

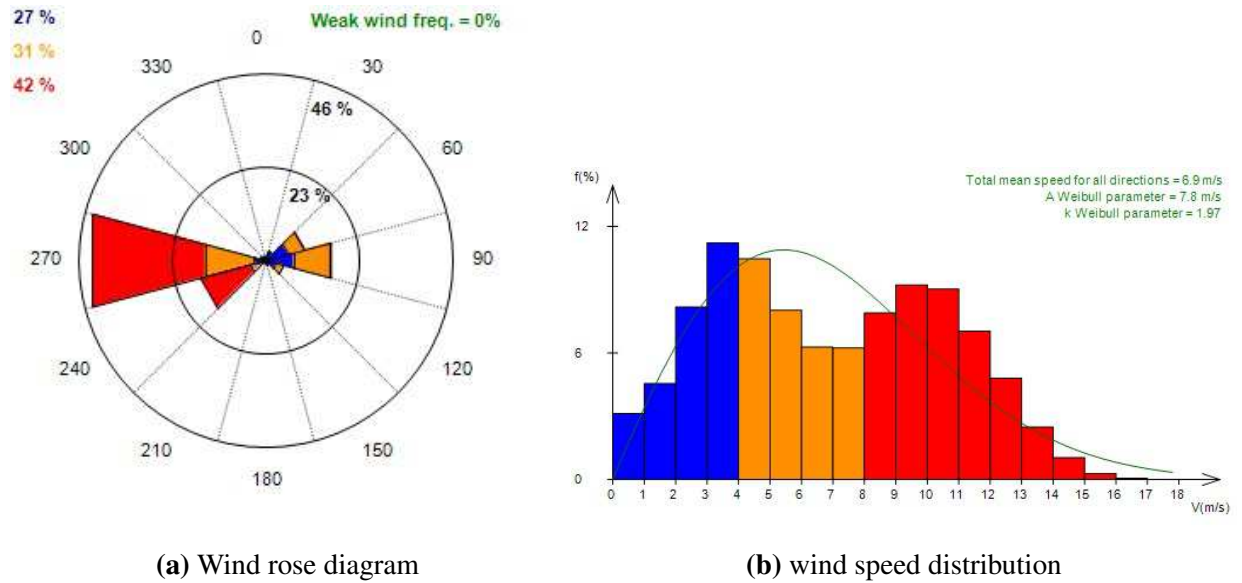


Fig. 5.13. Wind rose and histogram of wind speed distribution at site-II.

Table 5.11. Wind speed distribution for 12 directional sectors at site-II

Directional sectors (deg)	0	30	60	90	120	150	180	210	240	270	300	330
Mean wind speed (m/s)	2.4	3	3.8	4.3	3.7	2.6	2.2	2.3	9.3	8.8	2.8	2.3
% of distribution	1.1	2.4	10	16.6	4.5	1.2	0.6	0.6	16.6	44.1	1.5	0.7

5.3.2.2 Simulation of Model Wind Farm using Meteodyn (Site-II)

The digital model represents the computational domain where the RANS equations have been numerically solved. In total, 12 simulations have been performed in order to have a 3D wind field for every 30 degree sector. The horizontal and vertical resolution setting used by Meteodyn are 50 m and 4 m. With these settings, the number of cells, convergence rate and simulation time at the end of the simulation are presented in Table 5.12. From the table, it is observed that the maximum number of cells used for simulation are 18.93 million cells, but the average number of cells used for simulation are 15.63 million cells.

Table 5.12. CFD directional calculations properties (site-II).

Sectors	Number of cells (in millions)	Convergence rate (%)	Simulation time
30	17.47	99.7	02:13:00
60	18.93	100	01:49:48
90	10.5	100	00:43:48
120	17.47	100	01:11:48
150	18.93	99.9	02:13:48
180	10.5	100	00:52:48
210	17.47	100	01:21:48
240	18.93	100	01:15:48
270	10.5	100	00:36:48
300	17.47	100	01:54:48
330	18.93	100	01:59:48
360	10.5	100	01:14:48

5.3.2.3 Simulation Results Obtained using Meteodyn Software (Site-II)

This section describes the results obtained after integration of the real climatology of the site. Table 5.13 gives detailed characteristics of the site including mean wind speed, Weibull parameters (scale, c and shape, k) and wind power density for the site. It is observed from the table that the minimum mean wind speed of 6.71 m/s occurs at turbine ID-21 and maximum mean wind speed of 6.97 m/s at turbine ID-14. Further, the wind power density is recorded to be minimum for turbine ID-21 with 351 W/m² and maximum of 397.4 W/m² recorded for wind turbine ID-14. The wind speed and wind power density map for the site-II are shown in Figs. 5.14 and 5.15, respectively.

The annual energy production (AEP) with and without wake, wake losses and capacity factor are presented in Table 5.14. From the table, it is observed that the minimum AEP without wake is estimated as 5296 MWh/year for turbine ID-21 and maximum of 5627 MWh/year is estimated for turbine ID-14. The maximum wake loss is estimated to be 5.8 % for turbine ID-19. Similarly, the minimum and maximum AEP with wake is estimated as 5031 MWh/year for turbine ID-19 and 5619 MWh/year for turbine ID-14, respectively. The minimum and maximum capacity factor is estimated as 38.29 % and 42.76 % for turbine ID-19 and turbine ID-14, respectively.

The wind-farm production characteristics using Meteodyn software for the entire Model wind farm are listed in Table 5.15. The gross AEP (without wake) is estimated as

Table 5.13. Variation of average wind speed, Weibull parameters and wind power density at site-II using Meteodyn

Turbine ID	Average speed (m/s)	Weibull parameters		WPD (W/m ²)
		<i>c</i> (m/s)	<i>k</i>	
1	6.83	7.69	1.98	369.3
2	6.85	7.72	1.97	375.3
3	6.87	7.74	1.97	376.9
4	6.71	7.55	1.96	358.8
5	6.86	7.72	1.95	382.1
6	6.72	7.57	1.95	361.3
7	6.80	7.65	1.96	371.0
8	6.84	7.70	1.95	374.3
9	6.75	7.60	1.95	369.3
10	6.73	7.58	1.95	365.4
11	6.88	7.75	1.95	385.8
12	6.84	7.70	1.95	375.4
13	6.93	7.79	1.94	389.1
14	6.97	7.84	1.93	397.4
15	6.74	7.59	1.98	355.4
16	6.76	7.61	1.97	359.9
17	6.83	7.69	1.96	373.1
18	6.79	7.64	1.99	361.7
19	6.74	7.60	2.00	355.3
20	6.71	7.56	2.00	351.3
21	6.71	7.55	1.99	351.0
22	6.81	7.67	2.00	364.3
23	6.75	7.60	1.99	356.6
24	6.75	7.61	2.00	357.0
25	6.86	7.72	1.97	377.3
26	6.93	7.80	1.93	391.3
27	6.89	7.75	1.94	384.1
28	6.83	7.69	2.00	367.5
29	6.88	7.75	1.97	380.8
30	6.76	7.62	1.99	360.5
31	6.78	7.63	1.99	362.4
32	6.92	7.79	1.96	389.1
33	6.96	7.83	1.95	393.6

179.281 GWh/year. Therefore, the capacity factor estimated without considering the wake effect is estimated as 41.34 %. The total wake losses are estimated as 2.547 GWh/year. Thus, the net AEP estimated for the site after wake losses, is found to be 176.734 GWh/year (i.e., 1.42 % losses). Finally, the capacity factor of site-II with wake effect is estimated as 40.75 %.

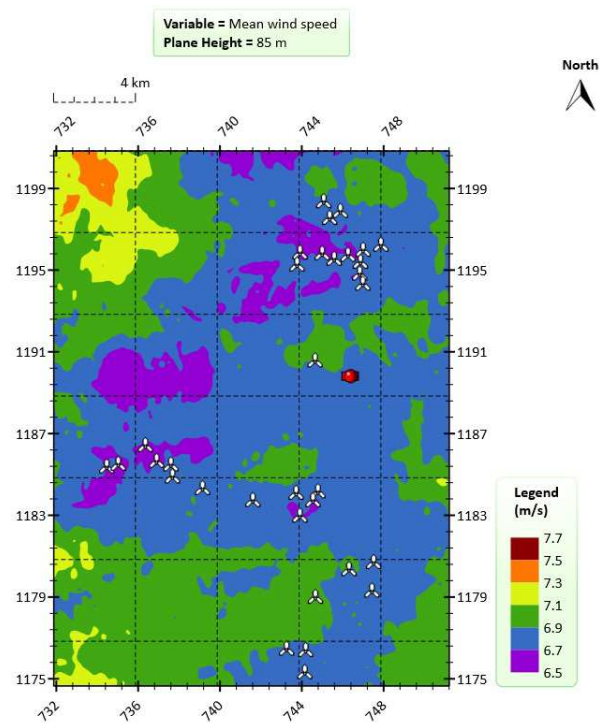


Fig. 5.14. Simulated average wind speed at hub height at site-II as obtained by using Meteodyn.

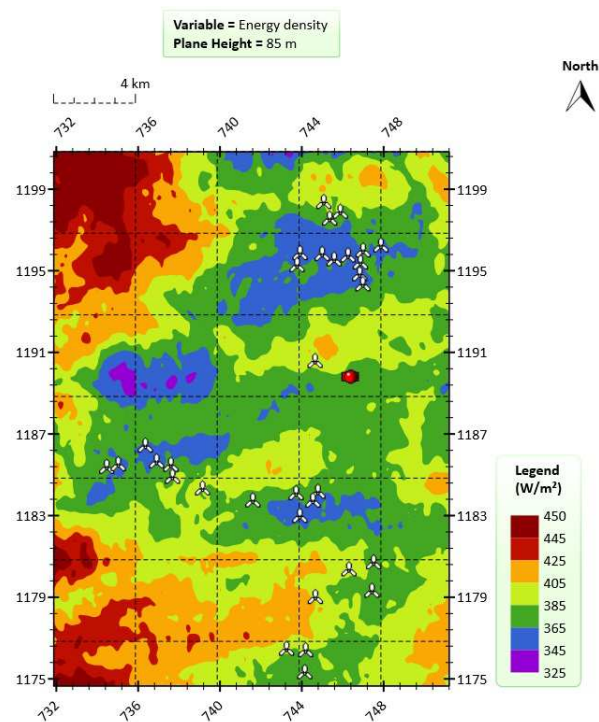


Fig. 5.15. Simulated wind power density at hub height at site-II as obtained by using Meteodyn.

Table 5.14. Comparison of AEP and capacity factor with and without wake effect at site-II generated by Meteodyn

Turbine ID	Without wake losses		Wake losses %	With wake losses	
	AEP (MWh/year)	Capacity factor (%)		AEP (MWh/year)	Capacity factor (%)
1	5443	41.42	2.7	5295	40.30
2	5461	41.56	0.6	5431	41.33
3	5488	41.77	1.4	5410	41.17
4	5296	40.30	0.4	5275	40.14
5	5482	41.72	0.5	5454	41.51
6	5315	40.45	1.5	5237	39.86
7	5408	41.16	2.7	5260	40.03
8	5479	41.70	0.6	5448	41.46
9	5347	40.69	0.8	5304	40.37
10	5324	40.52	4.7	5076	38.63
11	5498	41.84	0.3	5484	41.74
12	5472	41.64	1.2	5404	41.13
13	5575	42.43	0.3	5556	42.28
14	5627	42.82	0.1	5619	42.76
15	5327	40.54	0.7	5287	40.24
16	5354	40.75	0.2	5342	40.65
17	5453	41.50	0	5452	41.49
18	5394	41.05	2.4	5265	40.07
19	5342	40.65	5.8	5031	38.29
20	5301	40.34	4.3	5074	38.61
21	5296	40.30	0.6	5264	40.06
22	5419	41.24	2.7	5272	40.12
23	5347	40.69	2.5	5212	39.67
24	5346	40.68	0.4	5324	40.52
25	5493	41.80	0.4	5473	41.65
26	5580	42.47	0.4	5555	42.28
27	5533	42.11	3.3	5353	40.74
28	5445	41.44	3.4	5257	40.01
29	5517	41.99	1.5	5435	41.36
30	5365	40.83	0.4	5342	40.65
31	5382	40.96	0.1	5377	40.92
32	5563	42.34	0.1	5558	42.30
33	5612	42.71	0	5610	42.69

Table 5.15. The wind-farm production characteristics using Meteodyn for site-II

No. of turbines	Capacity (MW)	Gross AEP (GWh/y)	Capacity factor (%)	Wake losses (GWh/y)	AEP with wake losses (GWh/y)	Capacity factor (%)
33	49.5	179.281	41.34	1.42	176.734	40.75

5.4 WindFarmer Simulation Software Tool

In the previous sections, the WindSim and Meteodyn softwares which are used for complex terrain for WRA are described. In this section, the Windfarmer software uses flat terrain for WRA is discussed. WindFarmer (Version 5.3.38) has been developed by GL Garrad Hassan to facilitate the design of wind farms, maximizing the power produced by the wind farm whilst minimizing environmental impact [163]. WindFarmer is a wind farm design software which allows to perform wind energy calculations by considering wind climatological and orographic conditions of a site. This software is developed to carry out wind energy simulations in order to investigate the interactions of wind turbines with the purpose of reaching the most optimum wind farm layout [164]. Thus, it is aimed to achieve maximum energy production by taking into the design constraints such as maximum ground slope, maximum allowable turbulence intensity, minimum turbine spacing etc. One of the important concern while optimizing wind farm layout is the relative position of wind turbines because incident wind speeds get affected by the presence of other turbines if they are too close to each other, i.e., wake effect.

5.4.1 Steps Involved in Simulation using WindFarmer

Following are the steps involved in simulation process using WindFarmer software.

1. Initially, enter the actual wind turbine positions in the wind-farm in terms of UTM coordinates from the Google earth.
2. Enter the climatology data, which includes wind speed and direction, also the position of met mast location in the wind farm from Google earth.
3. Enter the power curve and thrust coefficient curve details of the wind turbines used.
4. Download the site map on-line using Google earth, world imagery and SRTM data source, which contains the geographical information describing roughness, terrain and dimensions of the site location.

5. Create boundary of the site. Then using turbine importer, wind turbines are placed inside the boundary along with met mast.
6. Use “association method” for extrapolation at hub height, if met mast height and hub height are different.
7. Before optimization of wind turbines in the wind-farm, Park model is used for wind wake effect calculation.
8. For energy calculation and estimation of capacity factor, WindFarmer software uses “simple flow model” for calculation, which enables to calculate the actual energy yield and capacity factor of individual turbine.
9. The wind energy map and wind speed map for the entire boundary are obtained.
10. For optimization of wind farm layout, the modified Park wake model along with distance between two turbines, minimum slope of the turbine, along with number of iterations along with has to be specified.
11. Finally, the optimized wind farm layout with new wind turbine locations (UTM), along with optimized energy yield and capacity factor of the site are obtained.

Alternatively, the flowchart describing the steps to be followed is also shown in Fig. 5.16.

5.4.2 Simulation of Site II: Model Wind Farm using WindFarmer

The description of the site is already provided in Section 5.2.2. The terrain map and actual layout of wind turbines in the wind farm are shown in Fig. 5.17.

The wind resource for the entire wind farm is simulated using the time series wind data which is measured at a height of 85 m for two years (1 October 2010 to 30 September 2012). The wind speed map and wind power density map of the site are shown in Fig. 5.18.

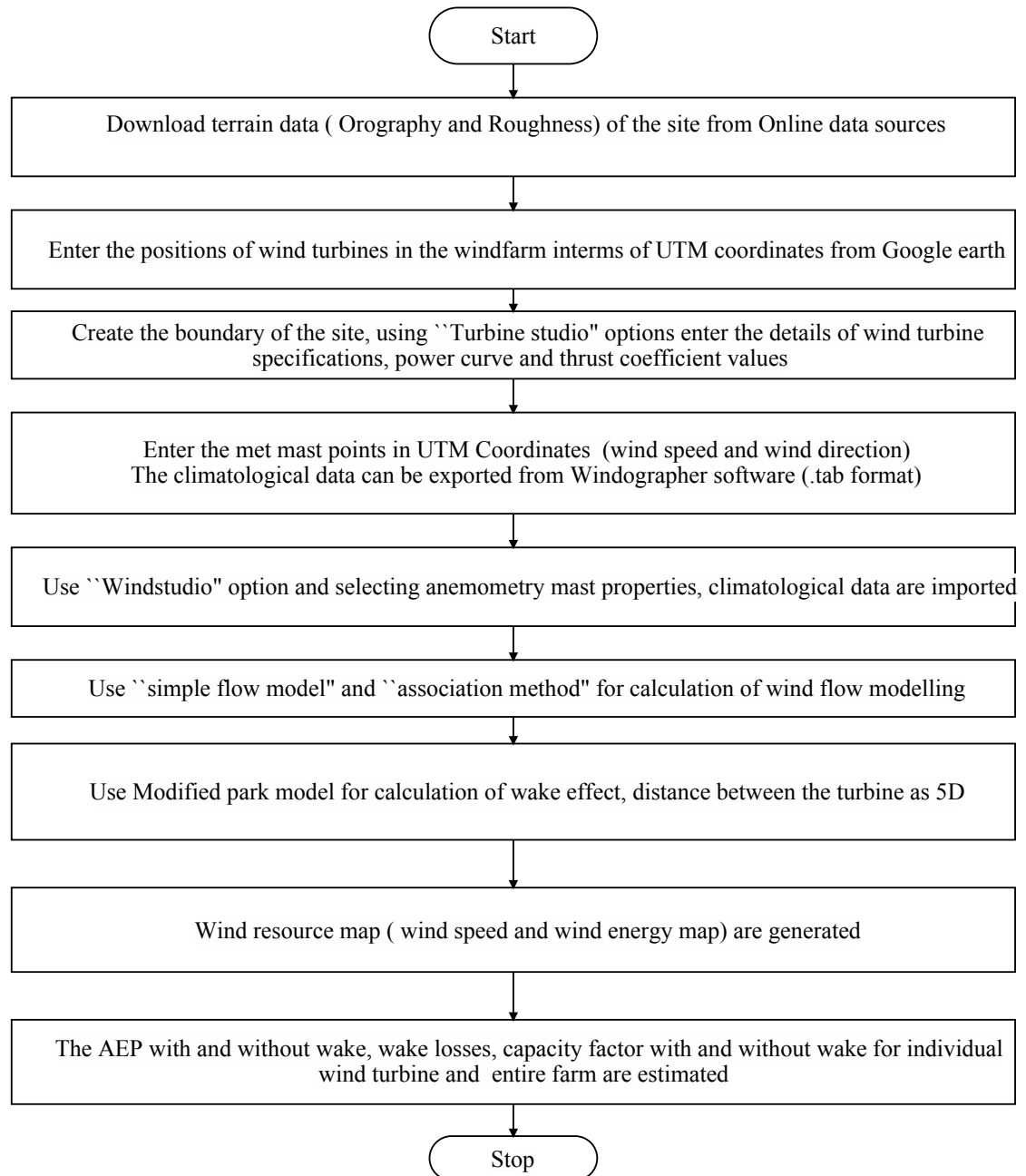


Fig. 5.16. Flowchart for simulating wind farm using WindFarmer software.

The mean wind speed, net energy yield (AEP) and capacity factor of the site before optimization are presented in Table 5.16. From the table, it is observed that maximum wind speed is estimated as 7.14 m/s for turbines (11 and 26) and minimum wind speed is estimated as 6.76 m/s for turbine ID-19. The maximum and minimum AEP without wake losses are 5812 MWh/year (turbine ID-9) and 5529 MWh/year (turbine ID-31), respectively and the corresponding capacity factors are 44.23 % and 42.08 %. Similarly,

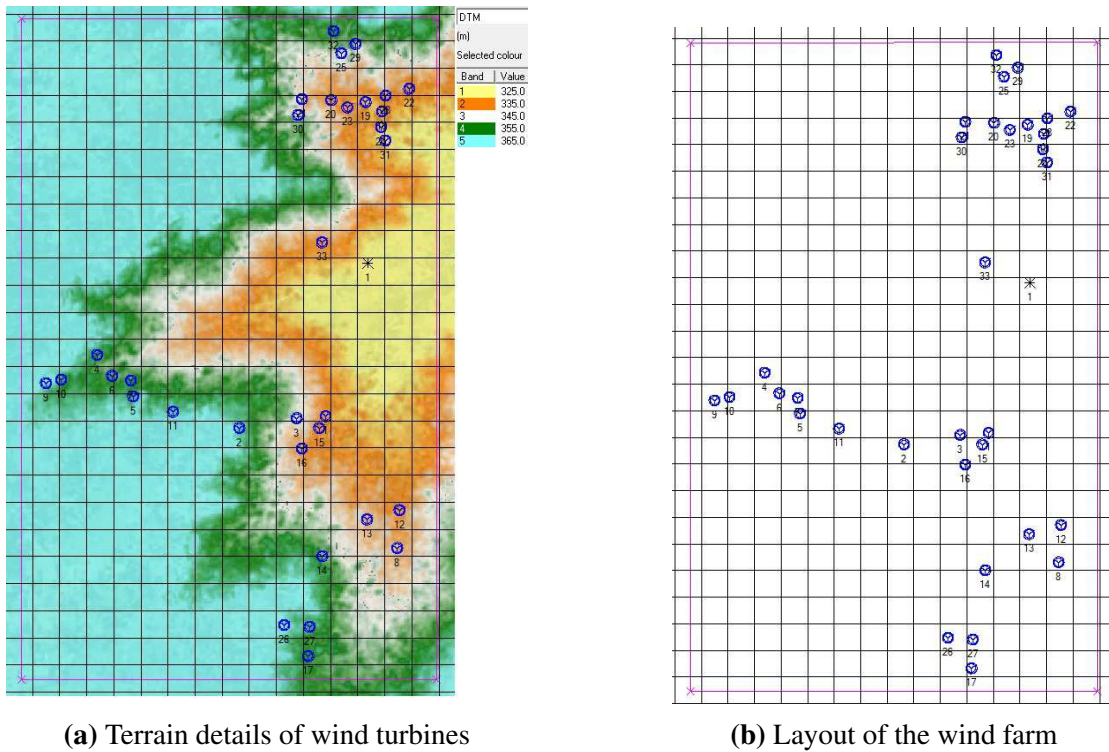


Fig. 5.17. Terrain and wind farm layout of site-II.

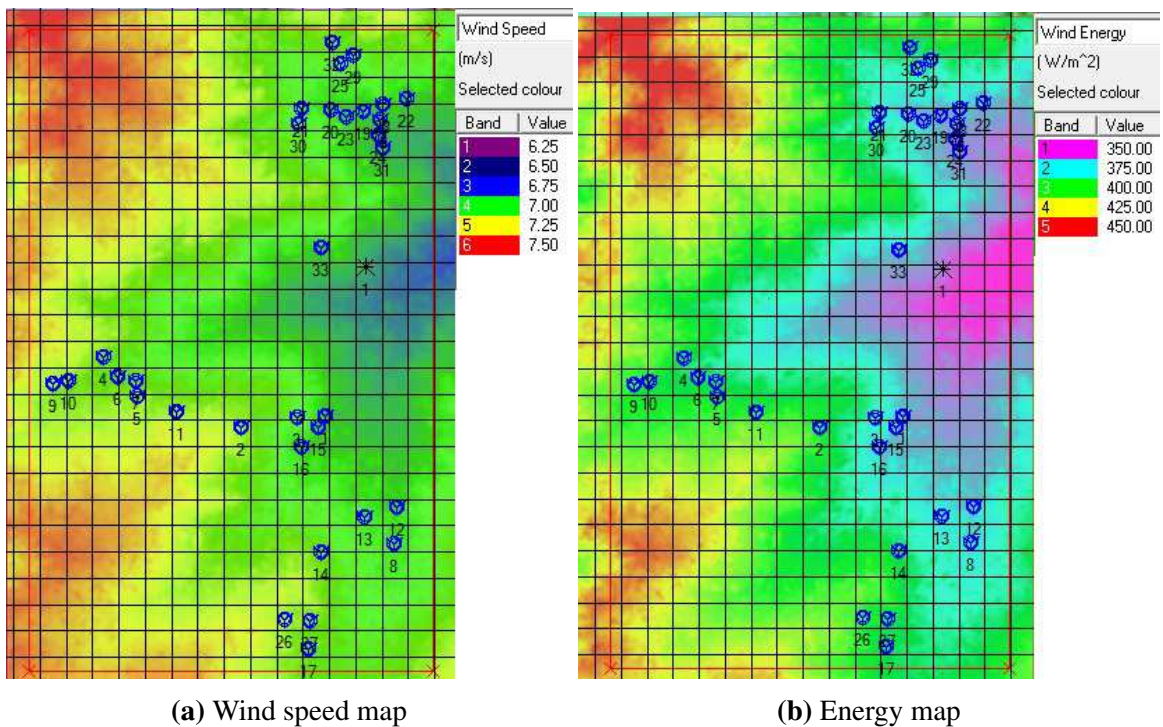


Fig. 5.18. Wind speed and wind power density map at site II.

the maximum and minimum AEP with wake losses are 5774 MWh/year (turbine ID-26) and 5262 MWh/year (turbine ID-19), respectively and the corresponding capacity

factors are 43.94 % and 40.05 %. The maximum wake losses is estimated as 5.36 % for turbine ID-19.

Table 5.16. Comparison of AEP and capacity factor with and without wake effect at site-II generated by WindFarmer simulation tool.

Turbine ID	Average wind speed (m/s)	Without wake		Wake Losses (%)	With wake losses	
		AEP (MWh/year)	capacity factor (%)		AEP (MWh/year)	capacity factor (%)
1	6.88	5577	42.44	2.65	5429	41.32
2	7.13	5792	44.08	0.66	5754	43.79
3	6.99	5670	43.15	1.46	5587	42.52
4	7.10	5750	43.76	0.50	5721	43.54
5	7.11	5767	43.89	0.68	5728	43.59
6	7.03	5727	43.58	1.66	5632	42.86
7	6.99	5733	43.63	3.17	5551	42.25
8	6.99	5627	42.82	0.59	5594	42.57
9	7.12	5812	44.23	0.98	5755	43.80
10	6.97	5780	43.99	4.67	5510	41.93
11	7.14	5782	44.00	0.31	5764	43.87
12	6.94	5596	42.59	1.22	5528	42.07
13	6.98	5623	42.79	0.46	5597	42.60
14	7.08	5710	43.46	0.18	5700	43.38
15	6.94	5584	42.50	0.66	5547	42.21
16	6.99	5617	42.75	0.23	5604	42.65
17	7.13	5756	43.81	0.02	5755	43.80
18	6.86	5561	42.32	2.57	5418	41.23
19	6.76	5560	42.31	5.36	5262	40.05
20	6.84	5592	42.56	3.49	5397	41.07
21	7.00	5647	42.98	0.55	5616	42.74
22	6.87	5587	42.52	2.92	5424	41.28
23	6.85	5577	42.44	2.78	5422	41.26
24	6.91	5542	42.18	0.56	5511	41.94
25	7.02	5670	43.15	0.49	5642	42.94
26	7.14	5805	44.18	0.53	5774	43.94
27	7.04	5767	43.89	2.79	5606	42.66
28	6.87	5612	42.71	3.30	5427	41.30
29	7.00	5687	43.28	1.81	5584	42.50
30	7.02	5667	43.13	0.51	5638	42.91
31	6.92	5529	42.08	0.16	5520	42.01
32	7.10	5734	43.64	0.12	5727	43.58
33	6.98	5599	42.61	0.05	5596	42.59

The wind-farm production characteristics using WindFarmer software for the entire site-II are listed in Table 5.17. The AEP (without wake) is estimated as 184.320 GWh/year. Therefore, the capacity factor estimated without considering the wake effect is estimated as 42.50 %. The total wake losses are estimated as 2.12 GWh/year. Thus, the net AEP estimated for the site after wake losses, is found to be 182.2 GWh/year (i.e., 1.15 % losses). The capacity factor of site-II with wake effect is estimated as 42.01 %.

Table 5.17. The wind-farm production characteristics using WindFarmer at site-II.

No. of turbines	Capacity (MW)	Gross AEP (GWh/y)	Capacity factor (%)	Wake losses (GWh/y)	AEP with wake losses (GWh/y)	Capacity factor (%)
33	49.5	187.039	43.13	2.72	184.320	42.50

5.5 Comparison of Softwares for Simulation of Wind Farm

The results of simulation of model wind farm using three softwares are compared. Table 5.18 gives detailed information regarding the softwares. The data requirement of the software is the same, which includes time series measured climate data, turbine power and thrust coefficient curve, locations of wind turbines and met mast location of the site. From the table, it is observed that WindSim and Meteodyn are used for complex terrain and these give the same information for a site. The solver used by WindSim is GCV solver and Meteodyn is MIGAL solver. The convergence rate is faster in Meteodyn compared to WindSim, the Meteodyn is efficient. Meteodyn software give characteristics of the site, namely the wind power density and wind resource maps in-terms of wind power density. Also, it is observed that Meteodyn does not have optimization module for maximizing energy capture. WindSim software doesn't generate wind power density maps. The wake model used by Windsim and Meteodyn are same. Thus, the calculation process of AEP and capacity factor are the same.

Table 5.18. Comparison of simulation softwares used for WRA

S.No	Characteristics / Features	Software(s)		
		Windsim	Meteodyn	WindFarmer
1	Modeling	Complex Terrain	Complex Terrain	Simple Terrain
		Non-linear flow model	Non-linear flow model	linear
		CFD ,RANS	CFD, RANS	simple flow model
2	Solver for CFD	GCV solver	MIGAL solver	-
3	Wake Model	Jensen (Park) model	Park model	Modified Park model and Eddy viscosity
4	Convergence rate	More iterations (500)	less iterations (25)	-
5	Response	Medium fast	fast	fast
6	Simulation time	More	More	less
7	Memory space	large memory	medium	less
8	WPD Maps	No	Yes	Yes
9	AEP	Yes	Yes	Yes
10	Wake losses	Yes	Yes	Yes
11	Capacity factor	Yes	Yes	Yes
12	Optimization of wind farm	Yes	No	Yes

5.6 Conclusion

In this chapter, industry standard software simulation tools are used to identify scope for re-powering existing wind farms by generating estimates of additional power generation capacity that can be installed in the existing wind farm by installing higher capacity turbines at higher heights and also by optional positioning of new turbines. Three softwares namely, WindSim, Meteodyn and Windfarmer are used to estimate the wind resource potential for the existing wind farm. In this chapter, the effect on terrain of site is considered on wind resource assessment study. The wind resource characteristics of the site are predicted at different locations of the site, where turbines can be installed. Further, the wind resource maps for the site are developed which provide insight to the developers to install turbines at the potential positions in wind farm to capture maximum

energy production. The characteristics of wind resource determined from the met mast location can be used to predict to other locations at the site where measurements are not available. This lead to improved accuracy of estimation of wind power potential at the site. The following conclusions are drawn:

WindSim software:

1. The annual energy production of the site-II without and with wake effect are estimated as 182.083 GWh/y and 179.8 GWh/y, respectively.
2. The capacity factor of the site-II without and with wake effect are estimated as 41.99 % and 41.47 %, respectively.

Meteodyn software:

1. The annual energy production without wake at the site-II is estimated as 179.281 GWh/y and with wake effect is 176.734 GWh/y.
2. The capacity factor of site-II, without and with wake are estimated as 41.34 % and 40.75 %, respectively.

Windfarmer software:

1. The annual energy production without wake at site-II is estimated as 187.039 GWh/y and with wake effect is 184.320 GWh/y.
2. The capacity factor of the site-II, without and with wake are estimated as 43.13 % and 42.50 %, respectively.

Chapter 6

Effectiveness of Positioning of Wind Turbine in a Wind Farm

6.1 Introduction

In the previous chapter, use of industry scale software simulation tools for obtaining aggregated wind power generation potential at a wind farm, was demonstrated. At design stage, the estimates help choosing a proper site for wind farm development. Next, it is important to identify positions of turbines on the wind farm site, such that the wind energy losses due to wake effects caused by other wind turbine in the vicinity are minimized. These are important factors in design of wind farm layout. An inadequately designed wind farm layout would lead to lower wind power capture as well as increased maintenance cost in a wind farm. The objectives of a wind farm design are to maximize the power production and to reduce the total cost associated with the wind farm operation and maintenance.

When a wind turbine extracts power from the wind, it generates a “wake” or turbulence that affect the wind speed and thus, reduces the power extracted by the turbine. Wind wake (also known as wind shade or mutual shelter effect) is a long trail of turbulent wake exiting the turbine with low wind speed. In large wind farms, wake effects lead to considerable power loss and thus must be minimized in order to maximize the output

power. In order to reduce the wake effects, the turbines have to be positioned appropriately. Thus, wind farm layout design is critically important in wind farm development.

Authors [88–91] have proposed a method to estimate power generation by individual turbine in a wind farm and also aggregated power generation at wind farm level. The authors have assumed the wind farm land to be divided into 100 regular square shaped cells (each cell of 200 m x 200 m) land area. Further, they have assumed that wind turbine is located at the centre of square cell, so that the effective distance between the two adjacent turbine is greater than 5 times the diameter of the turbine. In their work, the diameter of the turbine is thus assumed to be 40 m. In this chapter, work reported by Masetti *et al.* [88], Grady *et al.* [89], Marimidis *et al.* [91] and Emmami *et al.* [90], has been extended to determine position of turbines on estimated aggregated wind power generation at a wind farm level. In addition to the above investigations, the use of WindFarmer software simulation tool in developing optimum layout of wind farm is demonstrated. Using WindFarmer software simulation tool, optimum wind farm design layout is obtained for existing model wind farm and the simulation results are compared with actual position of wind turbines at the model wind farm.

6.2 Wind Wake Models

The average output power per turbine decreases due to wake effect caused by turbines in the wind farm. In addition, when the turbine extracts power from the wind, a wake occurs in downstream of the turbine. If another nearby turbine operates within this wake, the power output for this downstream turbine is reduced compared to the turbine operating in the free wind. Therefore, modeling of wake effects plays an important role.

Wind turbine wakes models can be divided into two main categories, namely, analytical wake models and computational wake models. An analytical wake model characterizes the velocity in a wake by a set of analytical expressions whereas in computational wake models, fluid flow equations, whether simplified or not, must be solved to obtain the wake velocity field.

Analytical Wake Models:

Analytical wake models are the simplest models, introduced by Lanchester [165]. These models are based on a control volume approach. Frandsen *et al.* [166] developed a generalization of the Lanchester [165] approximations and captured a family of previously developed wake models as well as advancing them to account for multiple interacting wakes. The model developed by Frandsen [166] is limited in that, it handles only regular array geometries, i.e., the wind turbines should be in straight rows with equidistant spacing between turbines in each row and equidistant spacing between rows.

One of the most widely used wake model was developed by Jensen [87, 167]. The author treated the wake behind the wind turbine as a turbulent wake which ignores the contribution of vortex shedding that is significant only in the near wake region. The wake model is, thus, derived by conserving momentum downstream of the wind turbine. The velocity in the wake is given as a function of downstream distance from the turbine hub and it is assumed that the wake expands linearly downstream.

Computational Wake Models:

Crespo *et al.* [168] carried out an extensive survey of different methods for modeling wind turbine wakes and reported that the computational wake model to be the best model. Crasto *et al.* [169] used CFD technique to model a single wake of a wind turbine using RANS equation.

Use of computational wake models has been rare due to high computation time and costs involved in obtaining results. In this chapter, Jensen model which is an analytical wake model adopted for modeling wind turbine wakes in the wind farm is used. Jensen wake model [87] is based on global momentum conservation in the wake downstream of the wind turbine. In this model, the wind farm is assumed to be a flat region and all wind turbines of same capacity are considered.

The schematic of wake model used in this study is shown in Fig. 6.1. Assuming that the turbine the wake has a radius r_o . As the wave propagates as shown in figure, the radius of the wake increases proportionally to the downstream distance, x . With the help of Betz theory and applying the continuity equation, the following expressions can

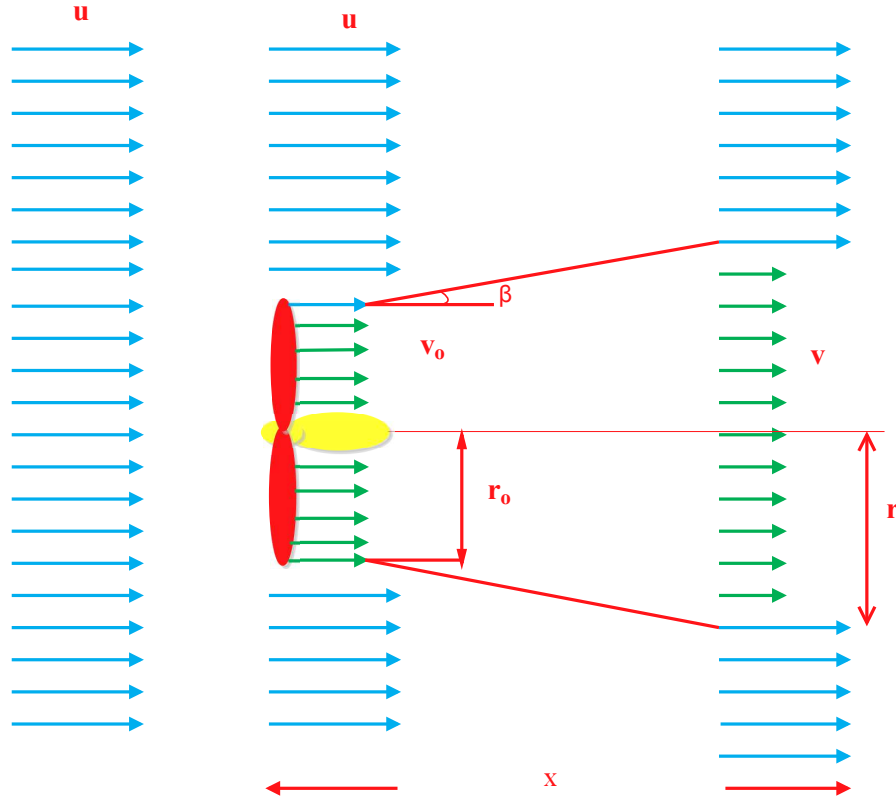


Fig. 6.1. Schematic of Jensen wake model [87]

be obtained [87]

$$\pi r_o^2 v_o + \pi(r^2 - r_o^2)u = \pi r^2 v \quad (6.1)$$

Assuming $v_o = \frac{1}{3}u$ and $r = \beta x + r_o$, then, the velocity of wake, v , at a distance, ' x ' simplifies to [87]

$$v = u \left[1 - 2e_1 \left(\frac{r_o}{r_o + \beta x} \right)^2 \right] \quad (6.2)$$

taking the axial induction factor, $e_1 = \frac{1}{3}$, where u is the mean wind speed, β is the entrainment constant and r is the downstream rotor radius. Also the power produced is given by the relation,

$$P = \frac{1}{2} \eta \rho A u^3 \quad (6.3)$$

Assuming $\eta = 40\%$, $\rho = 1.225 \text{ kg/m}^3$ and $A = \pi \times 20^2 \text{ sq.m}$, the power (kW) is calculated as

$$P = 0.3u^3 \quad (6.4)$$

where, η is the rotor efficiency, ρ is the air density and A is the rotor area. The downstream rotor radius r and the turbine coefficient C_T are evaluated as follows:

$$r = r_o \sqrt{\frac{1 - e_1}{1 - 2e_1}} \quad (6.5)$$

$$C_T = 4e_1(1 - e_1) \quad (6.6)$$

The entrainment constant (β) is given empirically as follows:

$$\beta = \frac{0.5}{\ln\left(\frac{h_b}{z_o}\right)} \quad (6.7)$$

where h_b is the hub height of the wind turbine and z_o is the surface roughness of the site.

Now, the aggregated wake loss at wind farm level is estimated as sum of wake losses due to individual turbines in the wind farm. The effect of wake loss is seen as resulting in reduction in wind speed. Down stream reduction in efficiency at wind farm level and increase in annual operational and maintenance cost of wind farm [87]:

$$1 - \left(\frac{v}{u}\right)^2 = \sum_{i=1}^N \left(1 - \frac{u_i}{u}\right)^2 \quad (6.8)$$

Mosetti *et al.* [88] had an assumption for the total cost of the wind turbines which indicates that the non-dimensionalized cost per year of a single turbine is one with a maximum reduction in cost of 1/3 for each additional wind turbine, when a large number of turbines are installed. The total cost/year of a wind farm is formulated as follows [88]:

$$\text{Cost} = N \left(\frac{2}{3} + \frac{1}{3} e^{(-0.000174N^2)} \right) \quad (6.9)$$

Where the cost is the total costs of wind turbines and the N is number of wind turbines have been installed in a wind park. The total efficiency (η_T) of the wind farm can be calculated as follows;

$$\eta_T = \frac{P_T}{0.3Nv^3} \quad (6.10)$$

The power curve presented in Mosetti *et al.* [88] study for the turbine under consideration yields the following expression for power:

$$P_T = \sum_{i=1}^N 0.3u_i^3 \quad (6.11)$$

The objective function to find the optimal result in-terms of minimum cost per unit of energy produced, is as follows

$$\text{Objective function} = \frac{\text{Cost}}{P_T} \quad (6.12)$$

6.3 Application of Genetic Algorithm to Optimize Positioning of Wind Turbines

In this chapter, genetic algorithm is proposed for positioning of wind turbines in a wind farm. The genetic algorithm is described in Sub-section A.1.

The parameters considered for simulation are:

1. Number of variables is taken as twice the number of turbines.
2. Population size used is the total number of solutions in a set.
3. Constraints considered is the size of the wind farm.
4. Optimization criteria considered is the maximum number of generations and tolerance.

The wind turbine data assumed for optimization of wind turbines in the wind farm is listed in Table 6.1.

Table 6.1. Wind turbine data assumed for simulation for position of turbines

S.No.	Parameters	Symbols	Values
1	Hub height	h_b	60 m
2	Rotor radius	r_0	20 m
3	Thrust coefficient	C_T	0.88
4	Ground roughness	z_o	0.3 m
5	Wind velocity	u_0	12 m/s
6	Axial induction factor	e_1	0.33
7	Entrainment constant	β	0.094

The flow chart describing the genetic algorithm used for this study is shown in Fig. 6.2:

6.3.1 Survey of Reported Results for Optimal Positioning of Wind Turbines

Various approach used for placement of wind turbines in a wind farm are discussed in Sub-section 2.3 of Chapter 2. The approach are briefly described in this section with their results for comparison.

Mosetti *et al.* [88] attempted to optimize the positioning of wind turbines in a wind farm by employing genetic algorithm. They used Jensen's analytical wake model for modeling the wakes of the wind turbines. To implement the calculation, they used a grid and set the distance between two adjacent nodes to be five times the wind turbine rotor diameters.

Grady *et al.* [89] attempted the same problem as Mosetti *et al.* [88]. Authors have used Jensen's analytical wake model and a genetic algorithm for optimization. Grady *et al.* showed that Mosetti *et al.* results are not optimum wind farm layout. They suggested

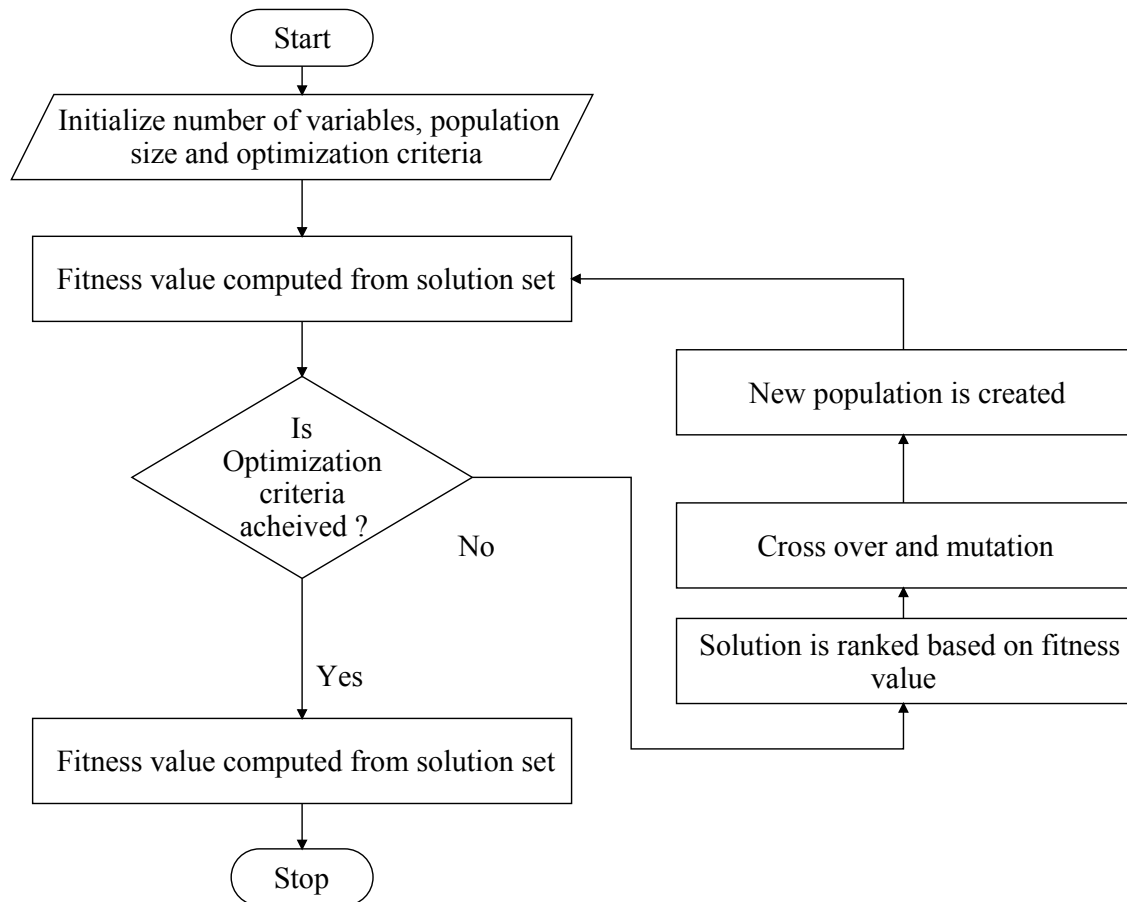


Fig. 6.2. Flow chart describing genetic algorithm for placement of wind turbines

that the probable cause is that the solution was not allowed to evolve for sufficient generations (i.e., it was not converged to the optimum point).

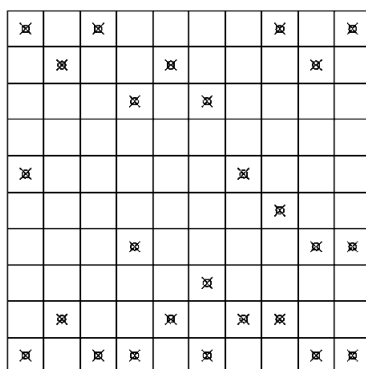
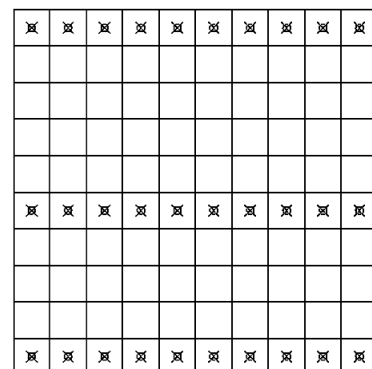
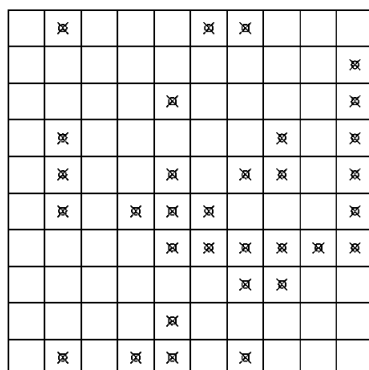
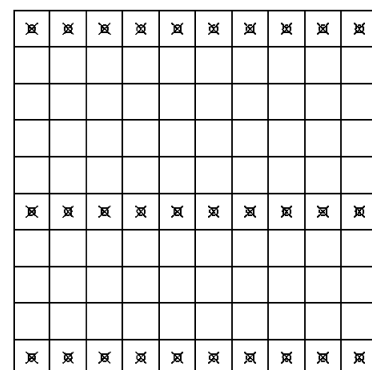
Marmidis *et al.* [91] also developed the same problem as Mosetti *et al.* [88] and Grady *et al.* [89]. The difference being that Marmidis *et al.* have analyzed only the simplest case in which wind comes from a fixed direction at a constant speed. Marmidis *et al.* used a Monte Carlo method for optimizing wind farm layout instead of a genetic algorithm.

Emami *et al.* [90] used objective function using genetic algorithm approach for the positioning of wind turbines in wind farm. The presented objective function, with its adjustable coefficients, provides more control on the cost, power and efficiency of wind farm in comparison with earlier objective functions. However, from the studies reported, the efficiency of the wind farm is less.

Table 6.2. Comparison of results obtained by researchers using GA and fixed position of wind turbines at centre of cell

	Mosetti <i>et al.</i> [88]	Grady <i>et al.</i> [89]	Marmidis <i>et al.</i> [91]	Emami <i>et al.</i> [90]		
				10	20	30
No. of turbines	26	30	32	10	20	30
Total Power (kW/year)	12352	14310	16395	5184	10164	14310
Fitness value	0.00162	0.001544	0.001411	0.1633	0.1514	0.12217
Efficiency	91.645	92.015	Not reported	100	98	92

From Table 6.2, it is observed that, the efficiency obtained by all the approaches is low. For comparison, Grady *et al.* and Emami *et al.* approaches used same number of turbines as 30. Where Grady's approach shows higher efficiency of 92.015 % when compared to Emami approach (92 %). The best optimal layout obtained by different approaches are shown in Figs. 6.3 and 6.4.

(a) Mosetti *et al.* [88] for 26 turbines(b) Grady *et al.* [89] for 30 turbines**Fig. 6.3.** Reported wind farm layout of 26 & 30 turbines(a) Marmidis *et al.* [91] for 32 turbines(b) Emami *et al.* [90] for 30 turbines**Fig. 6.4.** Reported wind farm layout of 32 & 30 turbines

6.4 Genetic Algorithm Based Proposed Approach of Positioning of Wind Turbines

In this section, genetic algorithm is used to find the optimal positioning of wind turbines in a wind farm. For the analysis the constant wind speed of 12 m/s in a uniform direction is considered as reported by other researchers [88–91]. so that the wake created depends only on the downstream distance. In this work, the new approach has been proposed which does not restrict the positioning of the turbines in centre of cell but it can be placed anywhere within the cell provided they are minimum five times the rotor diameter, distance apart and deliver better output. The case study considers 600 individuals to evolve over 3000 generations.

of position of

Table 6.3. Comparison of results obtained by the proposed approach using GA with variation of wind turbines.

No. of turbines	10	20	26	30	32
Total power (kW/year)	5184	10365	13476	15537	16571
Fitness value	0.00182	0.00160	0.00148	0.00142	0.00139
Efficiency (%)	100	99.99	99.98	99.90	99.89

It is observed from Table 6.3 that, the results in terms of power and efficiency are better than that of the earlier approaches reported in Table 6.2. Results are computed for different number of turbines such as, 10, 20, 26, 30 and 32. It is observed that, their corresponding power in-terms of kW/year are 5184, 10365, 13476, 15537 and 16571, respectively. The corresponding efficiencies are 100 %, 99.99 %, 99.98 %, 99.90 % and 99.89 %, respectively.

It is noted that, for the placement of 20 turbines, the power and efficiency are increased by 1.97 % and 2.03 %, respectively. Similarly for 26 and 30 turbines, power and efficiency is increased by 9.09 % and 8.57 %, respectively.

Table 6.3 also indicates that in each of the cases, the turbine configuration produces larger power output giving better efficiency. The fitness values obtained are also lesser than the values reported earlier. Thus, it can be concluded that with the new approach using genetic algorithm for placing the wind turbines in a wind farm can be used for placing wind turbines in a wind farm more optimally.

The new optimal layout of different wind turbines such as, 10, 20, 26, 30 and 32 are shown in Figs. 6.5, 6.6, 6.7, 6.8 and 6.9, respectively.

Table 6.4 shows the improvement in efficiency compared to the existing method (refer Table 6.2).

Table 6.4. Comparison of increase in efficiency with reported results.

No. of turbines	20	26	30
Increase in efficiency (%)	2.03	9.09	8.57

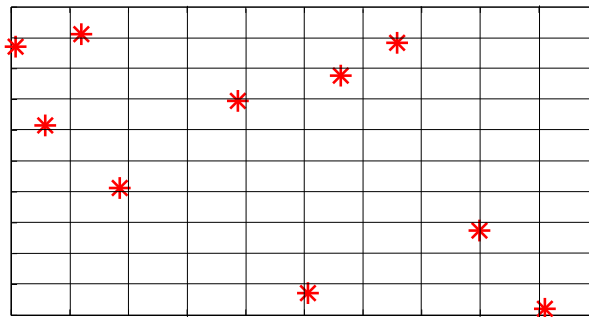


Fig. 6.5. Proposed wind farm layout of wind turbines consisting of 10 turbines.

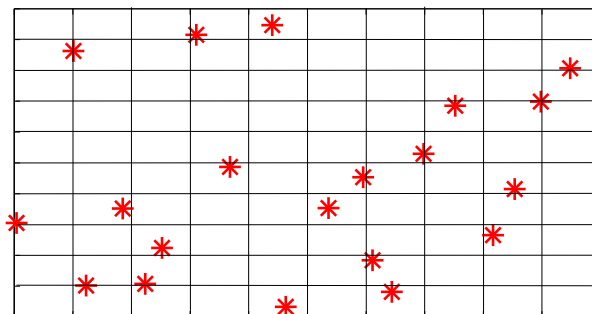


Fig. 6.6. Proposed wind farm layout of wind turbines consisting of 20 turbines.

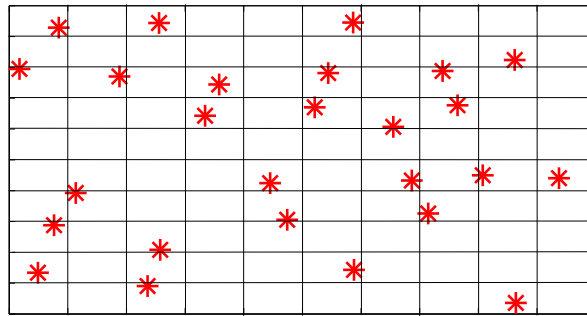


Fig. 6.7. Proposed wind farm layout of wind turbines consisting of 26 turbines.

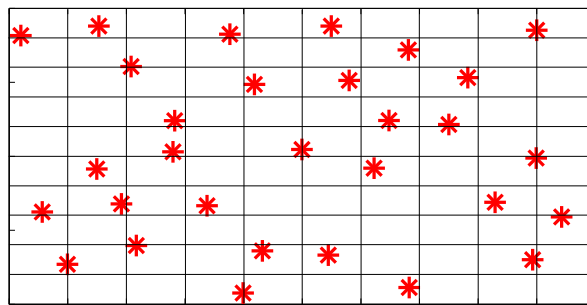


Fig. 6.8. Proposed wind farm layout of wind turbines consisting of 30 turbines.

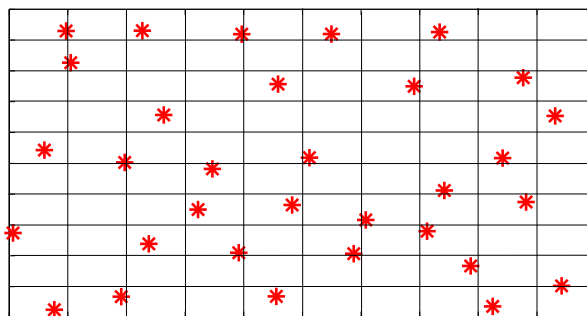


Fig. 6.9. Proposed wind farm layout of wind turbines consisting of 32 turbines.

The particle swarm optimization (PSO) can also be used to determine optimum position of turbine in wind farm. The results obtained using PSO show that the power generation efficiency of individual turbine corresponding to optimum position is lesser than that obtained by GA. These results are provided in Appendix C.

6.5 Optimization of Positioning of Wind Turbines using WindFarmer Software Simulation Tool

The WindFarmer software can be used for optimizing layout of wind farm corresponding to annual energy production and capacity factor of the site. The process of wind farm designing is an iterative process where-in the position of turbines are changed iteratively, after calculating the annual energy production and capacity factor [164]. WindFarmer uses a “simple flow model” that combines customizable vertical shear models and a simple horizontal model that is based on the terrain height. The “simple flow model” is used to compute the change in wind speed between the height above ground level at which the wind speed is measured at the hub height. This can be performed by two wind shear models, namely, log law and power law. WindFarmer also uses “association method” to improve the accuracy of estimation of frequency distribution of wind speed at hub heights. First energy calculations are done by simulation of the wind farm using the software; this takes into account wake effect caused by turbines. Then optimum position of wind turbines in a wind farm corresponding to maximize the net energy yield and capacity factor at a site is determined. The flowchart describing the steps in simulation are shown in Fig. 6.10.

6.5.1 Optimizing Layout of Model Wind Farm

The description of the model wind farm site is as presented in Sub-section 5.2.2. The terrain map and actual layout of wind turbines in the wind-farm are shown in Fig. 5.17. The wind turbine positions in-terms of UTM Coordinates, nearest turbine before optimization is reproduced as shown in Table 6.5. The simulation is carried out in model wind farm and new positions of wind turbines in the wind farm are listed in Table 6.6. It is observed from the table that, there is significant change in the position of turbine from the original locations (refer Table 6.5).

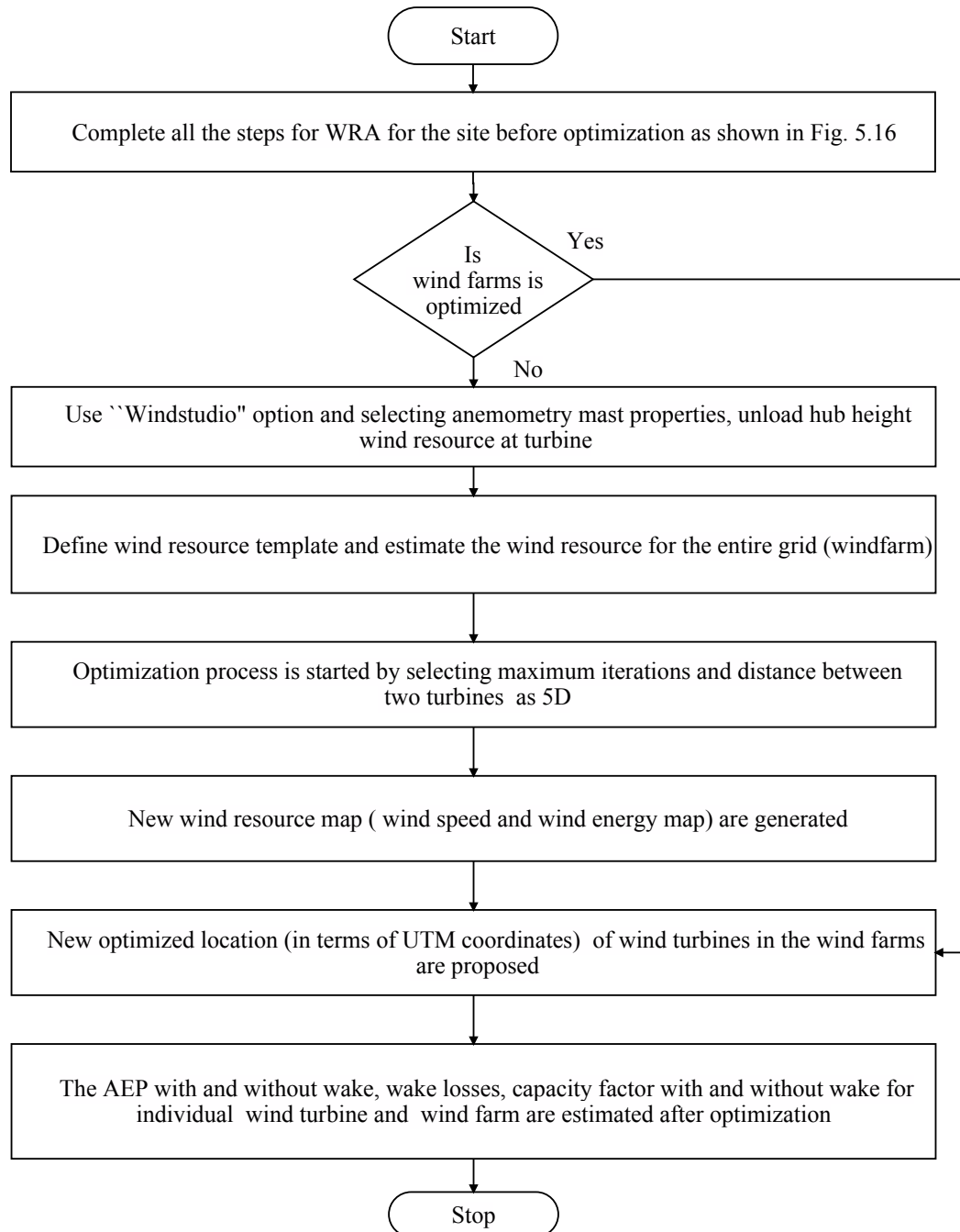


Fig. 6.10. Flowchart for optimization of locations of wind turbine using WindFarmer software.

The effect of optimum layout of wind farm can be seen from Table 6.7, in which average wind speed, net energy yields and capacity factor of the turbine are shown corresponding to each position. From the table, it is observed that the maximum wind speed estimated corresponding to optimization is 7.51 m/s for turbine ID-6 and minimum wind speed is estimated as 7.26 m/s for turbine ID-22. Similarly, the maximum energy yield

Table 6.5. Location of wind turbine positions specified in terms of UTM coordinates at site-II, before optimization.

Turbine ID	Eastings (m)	Northings (m)	Height (m)	Nearest turbine ID	Distance to nearest turbine (m)
1	744820	1184171	333	15	499.2
2	741636	1183743	361	3	2145.7
3	743752	1184099	345	15	899.5
4	736383	1186434	356	6	948.9
5	737708	1184902	358	7	590.9
6	736932	1185660	353	7	720.8
7	737632	1185488	353	5	590.9
8	747458	1179314	340	12	1397.5
9	734493	1185390	364	10	580.7
10	735059	1185520	360	9	580.7
11	739179	1184331	360	5	1577.9
12	747541	1180709	335	13	1251.2
13	746338	1180365	339	12	1251.2
14	744693	1179009	350	13	2131.8
15	744575	1183736	334	1	499.2
16	743936	1182983	338	15	987.6
17	744176	1175324	357	27	1082.9
18	746895	1195407	331	24	577.0
19	746290	1195750	331	18	695.5
20	745026	1195822	335	23	645.3
21	743944	1195863	342	30	605.9
22	747898	1196242	334	28	905.8
23	745613	1195554	333	20	645.3
24	746861	1194831	329	31	518.4
25	745392	1197556	345	29	623.0
26	743285	1176472	363	27	936.3
27	744219	1176406	358	26	936.3
28	747026	1195997	338	18	604.4
29	745914	1197896	347	25	623.0
30	743798	1195275	345	21	605.9
31	747015	1194336	327	24	518.4
32	745103	1198371	354	25	864.7
33	744680	1190579	336	31	4423.5

and capacity factor are estimated as 6148 MWh/year and 46.75 % for the same turbine, i.e., turbine ID-6. The minimum energy yield and capacity factor are estimated as 5797 MWh/year and 44.09 % for the turbine ID-31. The optimization power curve for different iterations is shown in Fig. 6.11. It is observed from the figure that, the net yield (MWh/year) remains constant after 70 iterations indicating that the wind turbine positions are optimized. The optimum layout is shown in Fig. 6.12.

From Table 6.8, it is observed that, there is an increase of net energy yield (AEP) with wake losses from 184.32 GWh/year to 198.15 GWh/year, (i.e., about 7.50 % increase

Table 6.6. Position of wind turbine in-terms of UTM coordinates after optimization.

Turbine ID	Eastings (m)	Northings (m)	Height (m)	Nearest turbine ID	Distance to nearest turbine (m)
1	735398	1178897	398	12	607.5
2	734355	1195367	406	4	488.7
3	733648	1174653	396	11	766.5
4	734630	1194963	403	2	488.7
5	733984	1177306	397	31	502.9
6	733862	1198821	418	30	719.3
7	734882	1198768	411	30	594.3
8	734082	1180132	395	27	1163.6
9	737279	1196585	403	13	441.0
10	735463	1180189	394	14	440.4
11	733731	1175415	394	17	439.5
12	734849	1178637	400	27	579.3
13	737649	1196345	402	9	441.0
14	735290	1180594	398	10	440.4
15	734118	1177842	396	5	552.5
16	735339	1196588	406	25	652.2
17	733710	1175854	391	11	439.5
18	736372	1197029	407	32	508.8
19	736652	1196239	401	9	716.1
20	735193	1197758	404	33	432.7
21	734736	1198095	408	30	418.1
22	736040	1193918	394	29	718.5
23	735246	1195776	404	16	817.3
24	734950	1194570	409	4	506.8
25	735059	1197177	409	20	596.3
26	735153	1193797	394	24	799.2
27	734797	1179214	400	12	579.3
28	734142	1194314	398	4	812.0
29	735833	1193230	392	22	718.5
30	734431	1198381	412	21	418.1
31	734067	1176810	394	5	502.9
32	736289	1197531	406	18	508.8
33	735597	1197603	407	20	432.7

in AEP) and also the capacity factor of the site increases from 42.5 % to 45.70 %, (i.e., about 7.52 % increase in capacity factor) after optimization.

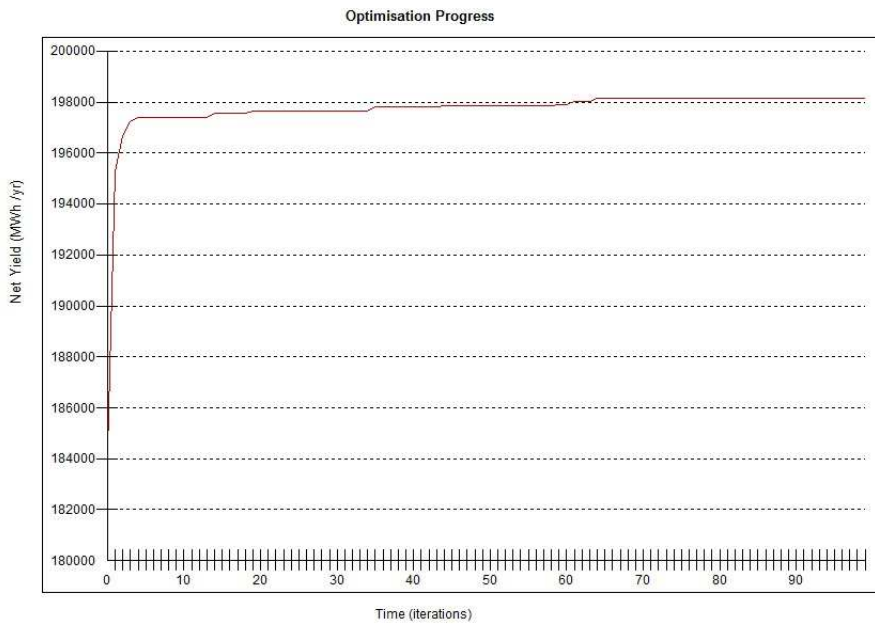


Fig. 6.11. The optimization curve for wind turbine positioning at model wind farm

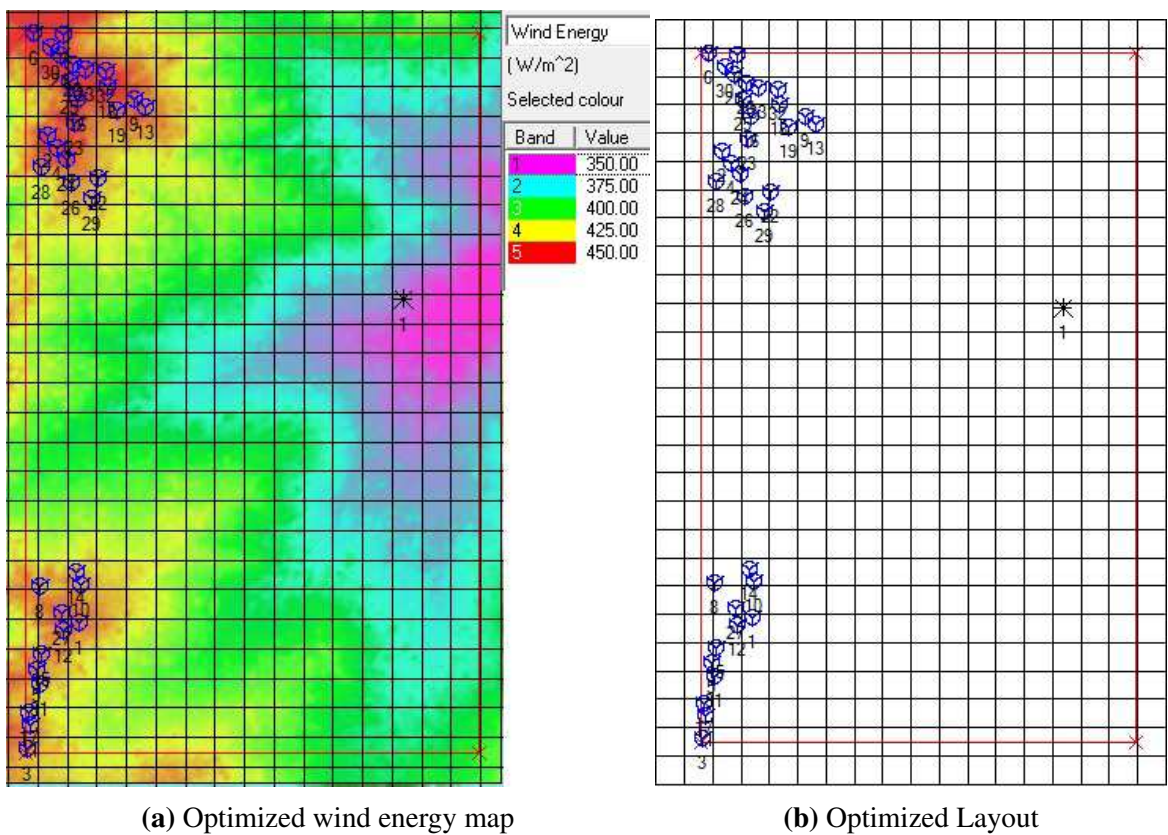


Fig. 6.12. Wind speed and wind energy map at site-II

Table 6.7. Average wind speed, AEP without and with wake, wake losses, capacity factor after optimization using WindFarmer

Turbine ID	Average wind speed (m/s)	Without wake		Wake Losses (%)	With wake losses	
		AEP (MWh/year)	capacity factor (%)		AEP (MWh/year)	capacity factor (%)
1	7.34	6052	46.06	1.70	5949	45.27
2	7.44	6106	46.47	0.39	6082	46.29
3	7.4	6039	45.96	0.02	6038	45.95
4	7.43	6089	46.34	0.31	6070	46.19
5	7.4	6047	46.02	0.10	6041	45.97
6	7.51	6187	47.09	0.63	6148	46.79
7	7.37	6143	46.75	3.11	5952	45.30
8	7.37	6036	45.94	0.46	6008	45.72
9	7.34	6089	46.34	2.45	5940	45.21
10	7.33	6023	45.84	1.28	5946	45.25
11	7.39	6028	45.88	0.05	6025	45.85
12	7.38	6065	46.16	0.66	6025	45.85
13	7.31	6078	46.26	3.26	5880	44.75
14	7.39	6053	46.07	0.56	6019	45.81
15	7.39	6040	45.97	0.17	6030	45.89
16	7.43	6110	46.50	0.69	6068	46.18
17	7.36	6007	45.72	0.05	6004	45.69
18	7.38	6115	46.54	2.22	5979	45.50
19	7.32	6076	46.24	2.37	5932	45.14
20	7.41	6097	46.40	0.74	6052	46.06
21	7.46	6123	46.60	0.39	6099	46.42
22	7.26	6028	45.88	3.20	5835	44.41
23	7.41	6096	46.39	0.97	6037	45.94
24	7.42	6132	46.67	1.66	6030	45.89
25	7.43	6131	46.66	1.06	6066	46.16
26	7.35	6030	45.89	0.70	5988	45.57
27	7.41	6069	46.19	0.23	6055	46.08
28	7.37	6055	46.08	0.73	6011	45.75
29	7.37	6012	45.75	0.07	6008	45.72
30	7.46	6147	46.78	0.65	6107	46.48
31	7.38	6028	45.88	0.07	6024	45.84
32	7.27	6112	46.51	5.15	5797	44.12
33	7.32	6117	46.55	3.48	5904	44.93

Table 6.8. Comparison of AEP and capacity factor (before and after) optimization at site-II using WindFarmer

Before optimization		After optimization		% Improvement in	
AEP (GWh/y)	Capacity factor (%)	AEP (GWh/y)	Capacity factor (%)	AEP	Capacity factor
184.32	42.5	198.15	45.70	7.50	7.52

6.6 Conclusion

In this chapter, genetic algorithm is used for obtaining optimum position of wind turbine in a wind farm. Unlike in the conventional approach wherein the wind turbines are placed at center of the cell, in this work, the approach of placing the turbines anywhere in the grid at a minimum distance of $5D$ from each other, is demonstrated. Such an approach not only reduces the overall wake effect in the farm and increased power generation. From the results obtained, it can be concluded that, the proposed approach improves speed and accuracy of optimization compared to conventional approach. It is concluded that optimum layout of model wind farm, obtained using WindFarmer, corresponds to increase in annual energy production and overall capacity factor by 7.50 % and 7.52 %, respectively. thus there is scope for re-powering wind farm. The following results are obtained using WindFarmer at model wind farm

1. The AEP and capacity factor of the site-II before optimization with wake losses are estimated as 184.32 GWh/year and 42.50 %, respectively.
2. The AEP and capacity factor of the site-II after optimization with wake losses are estimated as 198.15 GWh/year and 45.70 %, respectively.
3. The AEP is increased by by 13.83 GWh/year.

Chapter 7

Prediction of Power Generation in Wind farm

7.1 Introduction

With increasing penetration of wind power generation into power grid, the reliability of wind power generation and commitment ahead of schedule has become important developmental issues in wind power generation. There are sophisticated simulation tools which can be used to predict wind power generation, on the basis of wind climatological data at the wind farm site.

In this Chapter, a new approach (Feed forward neural network combined with GA) for prediction of wind power generation, when historical time series data on wind speed at the site is available. The approach uses genetic algorithm for optimizing the feed forward neural network, which is then used for predicting power generated in short term, ahead of schedule by few hours. The approach is thus useful for “now casting” of wind power generation. The results obtained using newly developed approach are compared with those obtained using back propagation algorithm. It is shown that the new developed approach leads to improved accuracy.

7.2 Prediction of Wind Power Generation

In this section, different approaches used by researchers for prediction of wind power generation using artificial neural network and genetic algorithm are described. Wind power generation is intermittent. When wind energy conversion systems have been connected to electric grid, the generated power must be utilized. Hence, prediction of wind power generation plays vital role. In the past decades, wide variety of algorithms have been applied. The accuracy further may be improved by applying hybrid algorithms.

7.2.1 Artificial Neural Networks

Artificial neural networks (ANN) or simply neural networks refer to a group of algorithms that typically operate on a large number of simple interconnected components or neurons [170]. ANN has been applied to various problems in different scientific disciplines, including applied mathematics, chemistry, physics, engineering, economics and finance. ANN has been widely used in solving problems related to prediction, classification, control and identification [131, 171]. The detailed information on ANN is provided in Appendix D.

7.2.1.1 Feed Forward Neural Network

The most simple type of artificial neural network is Feed Forward Neural Network (FFNN). In this network, information moves in only one direction, the forward direction. From the input nodes data flows through the hidden nodes and to the output nodes. There are two types of neural network: they are (i) single layer and (ii) multi-layer feed forward network.

(i). Single Layer Feed Forward Neural Network:

In this type of network, there are two layers, namely the input and the output layer. The input layer neurons receive the input signals and the output layer neurons generates the output signals. The synaptic links carrying the weights connect every input neuron to the output neuron. Such a network is said to be feed forward network. Despite the two

layers, the network is termed as single layer since it is the output layer, alone which performs computation. The input layer merely transmits the signals to the output layer. Hence, the name single layer feed forward network.

(ii). Multilayer Feed Forward Neural Network:

This network consists of multiple layers such as, input layer, hidden layer and output layer. Besides an input and an output layer, the network also consists of one or more intermediary layers called hidden layers. The computational units of the hidden layer are known as hidden neurons. The hidden layer helps in performing intermediary computations before directing the input to the output layer.

The input layer neurons are linked to the hidden layer neurons and the weights on these links are referred to as input-hidden layer weights. Again, the hidden layer neurons are linked to the output layer neurons and the corresponding weights are referred to as hidden-output layer weights. A multilayer feed forward network with l input neurons, m_1 neurons in the first hidden layer, m_2 neurons in the second hidden layer and n output neurons in the output layer is written as l - m_1 - m_2 - n . Fig. 7.1 illustrates a multilayer feed forward network with a configuration l - m - n .

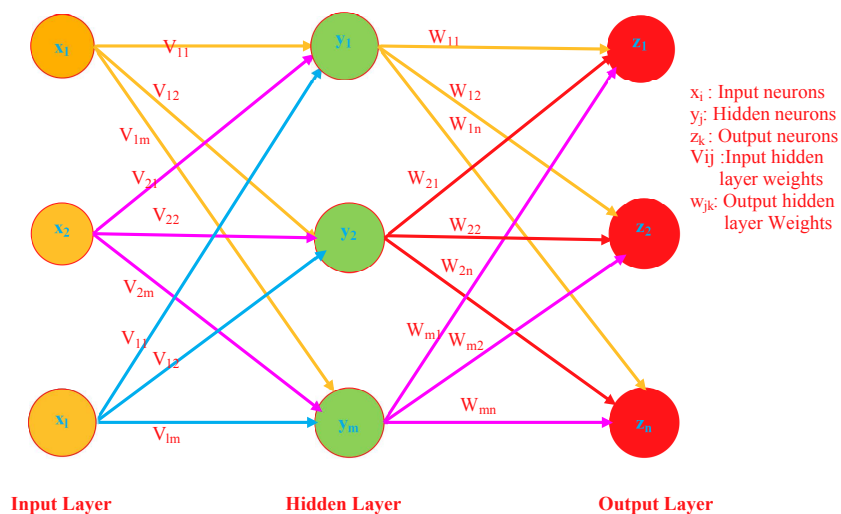


Fig. 7.1. General schematic architecture of multi layer feed forward neural network

7.2.2 Learning Algorithms in Artificial Neural Network

ANN resembles the human brain in learning through training and data storage. Based on learning strategy, three main categories of ANN are supervised learning, unsupervised learning and reinforced learning. The supervised type of learning since it is frequently used in the majority of ANN applications. The different types of learning algorithms are shown in Fig. 7.2.

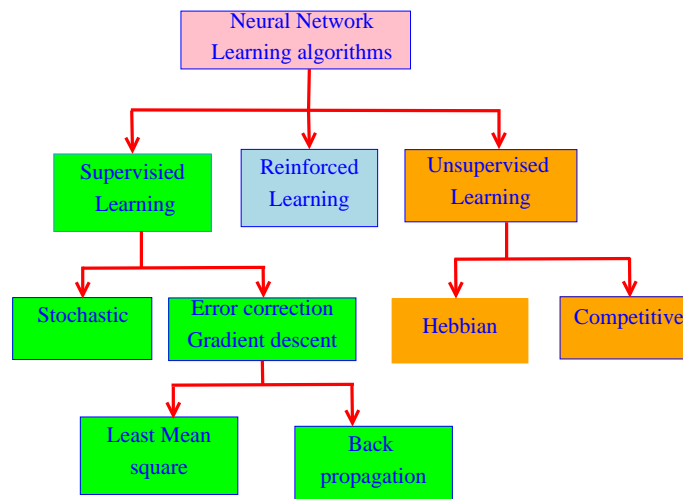


Fig. 7.2. Different learning algorithms of ANN

1. Supervised Learning:

In this type of learning, every input pattern that is used to train the network is associated with an output pattern, which is the target or the desired pattern. The comparison is made between the network's computed output and the correct expected output, to determine the error. The error can then be used to change network parameters, which result in an improvement in performance.

2. Unsupervised Learning:

In this learning method, the target output is not presented to the network. The network learns of its own by discovering and adapting to structural features in the input patterns.

3. Reinforced Learning:

In this method, the network does not present the expected answer but only indicates if the computed output is correct or in correct. The information provided

helps the network in its learning process. A reward is given for a correct answer computed and a penalty for a wrong answer. Reinforced learning is not popular form of learning.

Supervised and unsupervised learning methods are most popular learning algorithms. In this chapter, supervised learning, with back propagation technique is used in the neural network for generating predicted value of wind power generated at an instant in near future.

7.2.2.1 Back Propagation Algorithm

Back propagation algorithm is a learning algorithm, which learns the weights of the FFNN. The goal, as in any algorithm is to minimize the error. Given a training set comprising a set of input vectors X_n , where $n = 1, \dots, N$, together with a corresponding set of target vectors t_n , the error is given by (7.1):

$$E(w) = \frac{1}{2} \sum_{n=1}^N y(X_n, w) - t_n^2. \quad (7.1)$$

This error is a function of the network weights w . The objective is to find the weights of the network when the error is minimum. The minimum of a error function occurs when the gradient of that function is zero. At each step the weight vector is moved in the direction of the greatest rate of decrease of the error function. So this approach is known as gradient descent or steepest descent. The flow diagram of back propagation is shown in Fig. 7.3.

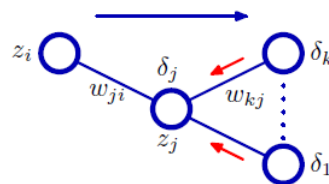


Fig. 7.3. Flow diagram of Back propagation of error [172]

The error at the output neuron is given by

$$\delta_k = y_k - t_k \quad (7.2)$$

Error at the hidden layer with the activation σ_h is given by

$$\delta_j = \sigma_h'(a_j) \sum_k w_{kj} \delta_k \quad (7.3)$$

$$w_{ji}(\tau + 1) = w_{ji}(\tau) - \eta_L \nabla E_n(w_{ji}(\tau)) \quad (7.4)$$

$$\frac{\partial E_n}{\partial w_{ji}} = \delta_j z_i \quad (7.5)$$

where η_L in (7.4) is known as the learning rate. Equation (7.4) gives the weights of the $(\tau + 1)^{th}$ epoch in relation with the τ^{th} epoch, w_{ji} represents the weights between i^{th} and j^{th} layer, w_{kj} is the weights between the layer j and the output layer k . z_i in (7.5) is the output at the i^{th} layer after applying the activation function (σ_h), δ_k is the error at the output layer, δ_j is the error at the hidden layer, ∇ is the gradient, y_k is the predicted output and t_k is the target output.

Performance Index - Mean Squared Error:

The network should be able to generalize and once trained it must be validated by testing its performance. The mean square error (MSE) has been used as the performance function.

The MSE is calculated by using (7.6). MSE is used as it gives a quadratic function in error. BPA, which uses steepest descent method converges for quadratic functions. Also derivative calculations are easy for the case of MSE, rather than RMSE [173]. MSE is scale-dependent and is widely used performance index in application of prediction problem.

$$MSE = \frac{1}{n} \sum_{i=1}^n (f_i - y_i)^2 \quad (7.6)$$

where f_i is the prediction value and y_i is the actual data value, n is the total number of data sets. The predictions are more accurate when MSE is close to zero.

7.3 Data from Model Wind Farm for Prediction of Wind Power Generation

The wind speed and wind power generation data are obtained from a Model wind farm, Periyapatti, TamilNadu, India. The data is measured for wind turbine having the rated capacity of 1500 kW, installed at a height of 85 m AGL, recorded at 10 minutes interval. The data measured over 11 months from 1 April 2014 to 28 February 2015 is used for training, validation and testing. Thus, the total data points are 48096. The monthly variation of wind speed data at the site for a period of 11 months is shown in Fig. 7.4. The data are normalized to a range between 0 and 1 using (7.7).

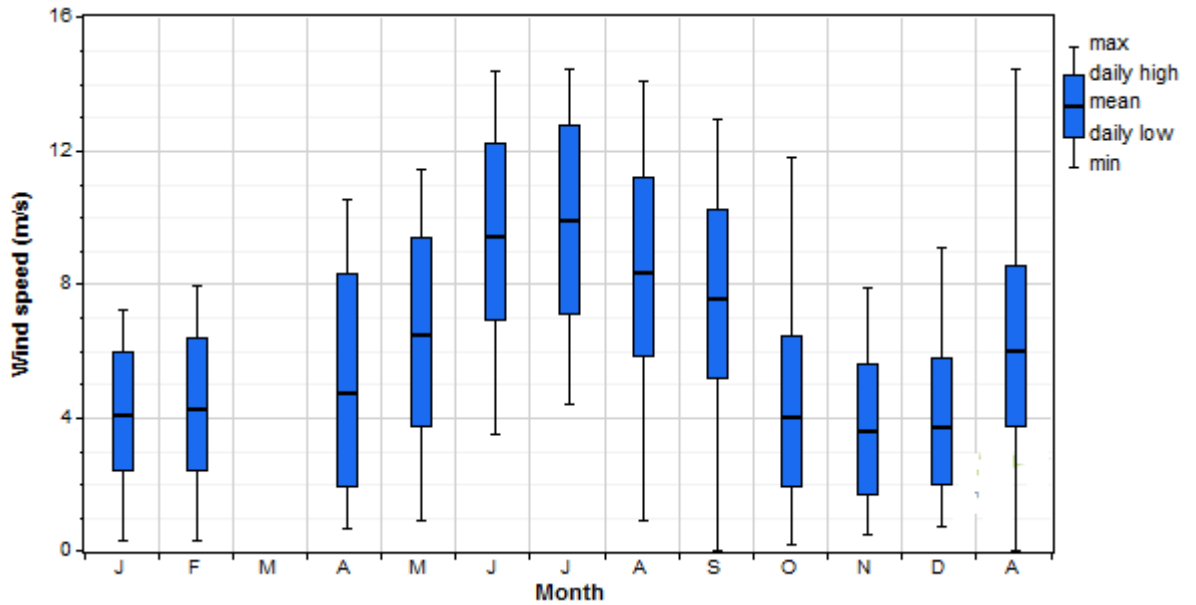


Fig. 7.4. Monthly variation of average wind speed at site-II

$$x_{norm} = \frac{(x - x_{min})}{(x_{max} - x_{min})} \quad (7.7)$$

where x_{norm} is the normalized data and x_{min} , x_{max} are minimum and maximum values in the data to be normalized. Normalization is used so as to standardized range of input data. A standard range makes the training speedy and more accurate [174]. For simulation, the data are divided into three sets: training set, validation set and testing set. The

predictions with reasonable accuracy can be obtained if minimum 70 % of input data is used for training, 15 % for validation and remaining 15 % for testing [175].

Architecture of Feed Forward Neural Network:

In multilayer feed forward neural network, there are three layers, namely, input layer, hidden layer and output layer. In this study, wind speed data is considered as input neuron in the input layer. The number of neurons in the hidden layer has significant influence in ANN architecture. Though these layer do not directly interact with the external environment, they have a tremendous influence on the final output. Using less number of neurons in the hidden layers will result in under fitting. Also using more number of neurons in the hidden layers may result in over fitting. Therefore choice of number of neurons in the hidden layer is of critical importance. As such there is no theoretical limit on the number of hidden layers but typically they are just one or two. In the present work, a single hidden layer has been chosen. Further, the number of neurons in the hidden layer is varied from 4 to 10 to get optimal solution. The wind power generated is taken as output neuron in the output layer. A bias variable, value of which is 1, is added to the input and hidden layer. This is done to cover all linear functions possible and not just the ones passing through the origin. Suppose there are n inputs and m neurons in the hidden layer. The inputs for each of the m neurons will be sum of the product of weights and the inputs including the bias variable. The weights will be different for each neuron. They are chosen randomly and then updated by the learning algorithm. These weights act as an input for the activation function at each neuron. Activation function accounts for the non-linearity of the neural networks. The activation function used in this study is sigmoid function (7.8) at the hidden layer and hyperbolic tangent sigmoid function (7.9) at the output layer.

$$\sigma_h(a) = \frac{1}{1 + \exp(-a)} \quad (7.8)$$

$$\sigma_h(a) = \frac{2}{1 + \exp(-2a)} - 1 \quad (7.9)$$

The ANN network architecture with feed forward neural network is shown in Fig. 7.5.

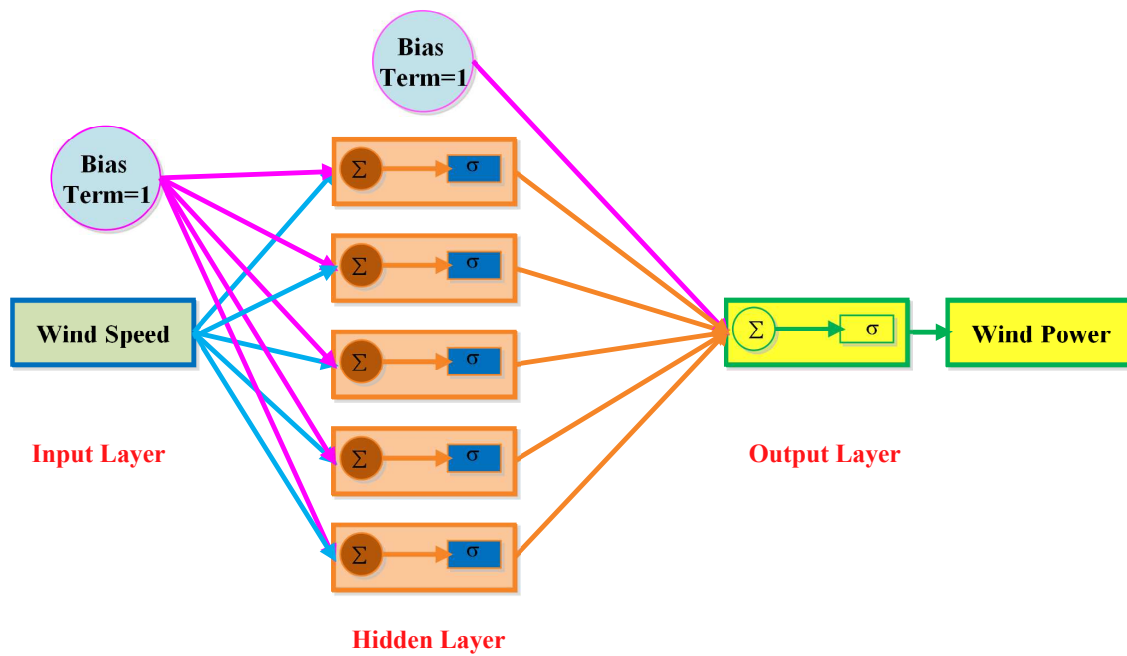


Fig. 7.5. Proposed neural network architecture for prediction of wind power generation

Training Set:

It is the data set, which is used to train the neural network and fix the weights. The larger the training set the more comprehensive learning will occur. In this study, two training data sets are used. One with 80 % of the total data set over 11 months as the training data, i.e. 38477 data points. The other has 90 % of the data points, i.e., 43286 data points. The error calculated during training is called training error.

Validation Set:

This set defines the performance of a network. The lower the validation error, the better the model is. For the 80 % training data set, 10 % of the data is used as the validation set, i.e., 4809 data points. For the 90 % of the data set, 5 % of data is used as validation set, i.e., 2405 data points.

Testing Set:

This data set is used to test the performance of the model. For the 80 % training data set, 10 % of the data is used for the testing set, i.e., 4810 data points. For the 90 % of the data set, 5 % is used for testing, i.e., 2405 data points. The error computed on the testing set is called testing error. Fig. 7.6 describes the methodology adopted for BPA and Fig. 7.7 describes the methodology adopted for FFNN-GA used for the study.

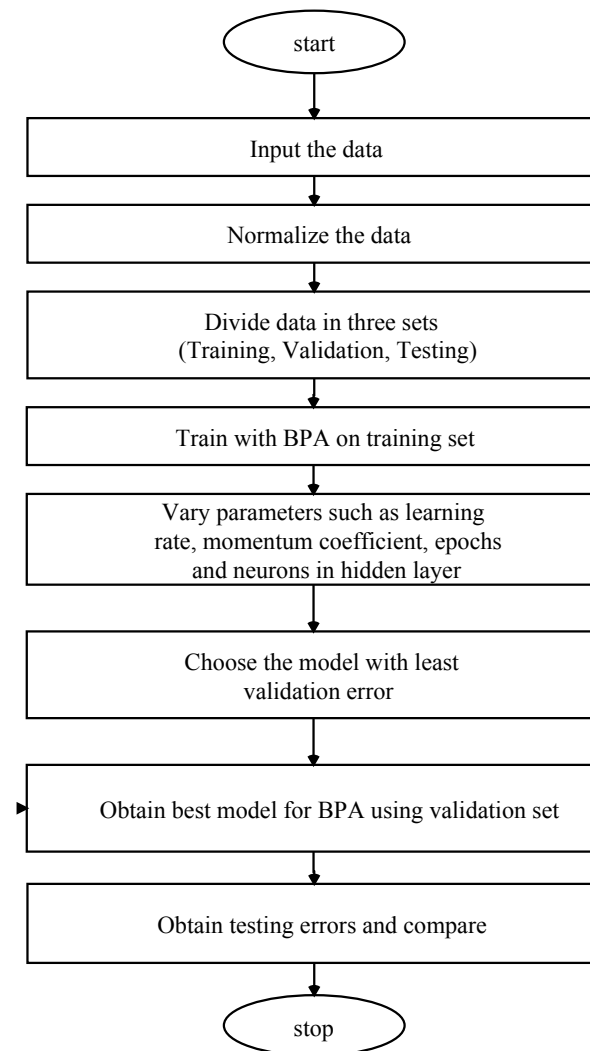


Fig. 7.6. Flowchart describing BPA algorithm used for predictions of wind power generation

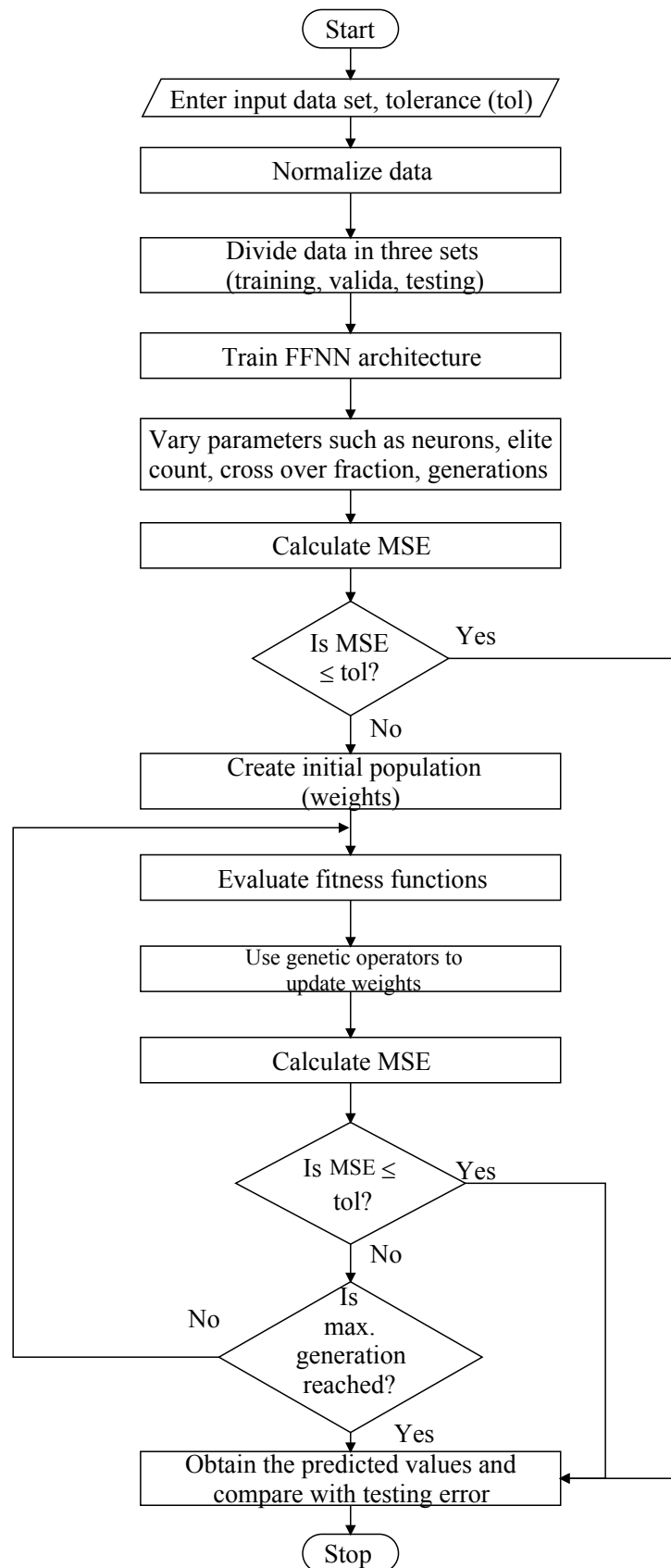


Fig. 7.7. Flowchart describing FFNN-GA algorithm used for predictions of wind power generation

The training algorithm is implemented through the following steps:

After normalizing the data, BPA and GA are used to train the data sets

1. The input wind speed and output wind energy data are normalized.
2. Parameters are varied in BPA are number of hidden neurons (4 to 10), learning rate (0.1, 0.5 & 0.9) and momentum coefficient (0.1, 0.5 & 0.9)
3. Parameters varied in GA are number of hidden neurons (4 to 10), elite count (0.10, 0.15 & 0.20), cross over fraction (0.7, 0.8 & 0.9)
4. The two algorithms namely, BPA and GA are used to train the network independently with their parameters
5. The training error and the validation error are computed for two algorithms
6. The model with the least validation error is selected, and its parameters are fixed.
7. The testing errors in terms of mean square error for the best models of BPA and GA are computed and compared
8. Best model for the prediction of wind power is selected on the basis of least error.

7.3.1 Results and Discussion of Prediction of Wind Power Generation

The two different algorithms of ANN, namely BPA and FFNN-GA are used for prediction of wind power generation. In BPA, the learning rate, momentum coefficient, number of neurons in the hidden layer and epochs are varied. For the 80 % training data, the best result among the 315 different combinations (shown in Appendix D) was found to be 5 neurons with 1500 epochs, learning rate as 0.5 and momentum coefficient as 0.1. This was chosen on the basis of least validation error of 0.00188 as shown in Table 7.1 and the corresponding testing error is 0.00223. For the 90 % training data, the best value of validation error is 0.00242 and the corresponding testing error is 0.00175. The testing error has decreased, by 15 %, whereas the validation error has

increased by 25 %, for an increase in the training data set. The minimum value of validation error for both the training data set is obtained with 5 neurons. The best learning rate is obtained as 0.9 and the momentum coefficient is changed as 0.5, as shown in Table 7.1.

Table 7.1. Best results for BPA with variation of training data sets

Training Data	Neurons	Epochs	Learning Rate	Momentum Coefficient	Training Error	Validation Error	Testing Error
80%	5	1500	0.5	0.1	0.01298	0.00188	0.00223
90%	5	500	0.9	0.5	0.01220	0.00242	0.00175

In GA, the parameters such as elite count and crossover fraction, along with the number of generations and the number of neurons in the hidden layer are varied. For the 80 % of training set, the minimum validation error is obtained as 0.00127, and the corresponding testing error is 0.00166 as listed in Table 7.2. The best architecture obtained while using GA is 4 neurons in the hidden layer, 300 generations, the crossover fraction is 0.9 and elite count of 20 %. For the 90 % set, the minimum validation error is 0.00185 and corresponding testing error is 0.00132. The number of neurons in the hidden layer is 4 and generation is 400. The crossover fraction is same as for the 80 %, but the elite count has decreased to 15 %. There is an increase of 38 % in validation error, and a decrease in testing error by 23.5 %, as the training data is increased from 80 % to 90 % is shown in Table 7.2 . It can be inferred from the discussions that the genetic algorithm has

Table 7.2. Best results for GA with variation of training data sets

Training Data	Neurons	Generations	Elite Count	Crossover Fraction	Training Error	Validation Error	Testing Error
80 %	4	300	0.20	0.9	0.01336	0.00127	0.00166
90 %	4	400	0.15	0.9	0.01203	0.00185	0.00132

outperformed BPA in both the training data sets. Also a notable observation is that the validation error has increased when increasing the training data for both the algorithm but the testing error has decreased.

The best prediction result obtained using GA for 10 % and 5 % of testing data are shown in Figs. 7.8 and 7.9, respectively.

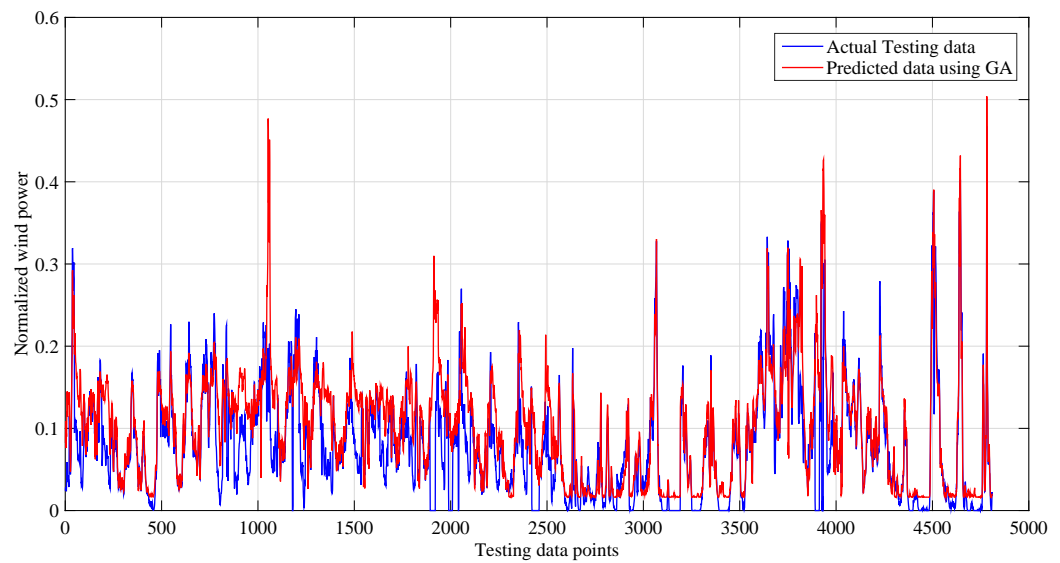


Fig. 7.8. Comparison of actual and predicted data using GA for 10 % testing data

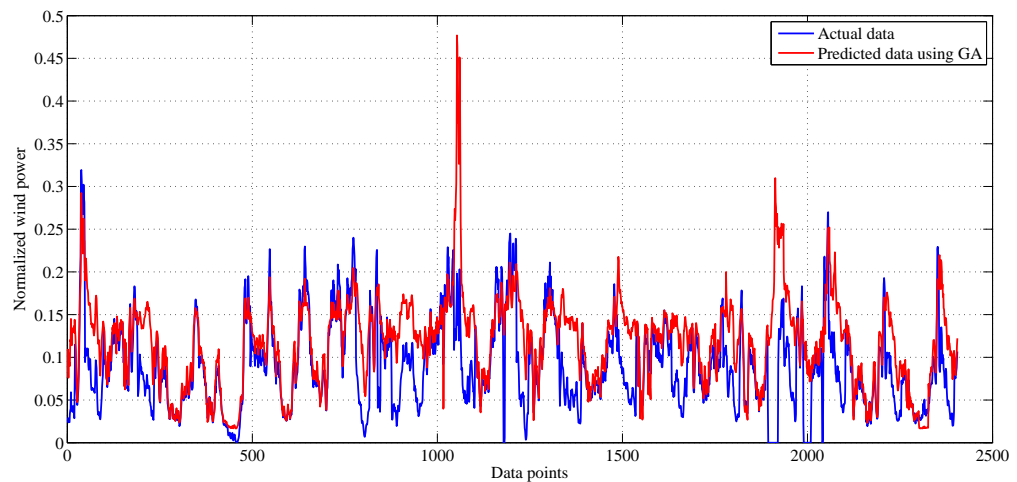


Fig. 7.9. Comparison of actual data and predicted data using GA for 5 % testing data

7.4 Conclusion

In this chapter, application of artificial neural network for predicting wind power generation over short intervals of few hours to few days is demonstrated by using two algorithms, namely, BPA and FFNN-GA. It is found that the predictions over this time scales can be generated with reasonable accuracy if minimum 70 % of input data is used for training, 15% for validation and remaining 15 % for testing. The results clearly

shows that the predicted wind power generation is in close agreement with actual wind power generation when time scale for prediction is minimum. The results are obtained for two time scales, 5 % of input data set and 10 % of input data set. The error of prediction depends on time scale of prediction. From the results, it is concluded that the error of prediction is minimum when genetic algorithm is employed in FFNN than that of back propagation algorithm as learning algorithm in artificial neural network. Thus, genetic algorithm is recommended over back propagation algorithm for application of prediction of wind power generation.

Chapter 8

Summary and Future Scope of Work

In this chapter, the major conclusions from the chapters are presented. Future scope for research is also presented.

8.1 Summary

The thesis relates on investigating modern heuristic techniques for wind resource assessment and computer simulation models for wind farms. The work carried out involves use of heuristic techniques for predicting cumulative installed wind power generation capacity in future, for assessment of available wind resource at a given site, for estimation of performance of existing wind farms, for optimizing position of wind turbine and predicting wind power generation in a wind farm are presented.

In the work, an improvised method for prediction of wind power generation capacity in future is developed. Accordingly, various options for realizing projected growth in wind power capacity are considered. Specifically, first the rate of growth of wind power generation capacity in future is predicted in the context of India and China, the two leading nations as far as wind power generation capacity addition is concerned. On the basis of growth in wind power generation capacity over the past years, the growth in future over longer term till 2050 is predicted. It is predicted that addition of wind power generation capacity in India will continue to increase. As the availability of wind resource is highly

site specific and the wind farms have been setup in almost all prospective sites, the option of increasing wind power generation capacity at the existing wind farm through re-powering is investigated. The industry scale commercial softwares are used for determining wind resource at any other point or on the site of the wind farm when data measured at one point is available. The software tools used also take into account details of terrain in terms of orography and roughness at the site. The options considered are: (i) installing wind turbine generators of higher capacity by way of new installations at greater hub heights in the existing wind farms, (ii) optimizing layout of wind farm in view of likely new capacity addition at the site of existing wind farms. Using Wind-Farmer software, optimal positioning of wind turbines in wind farm are carried out in the case of existing wind farm in India. The highlights of the thesis are as follows:

1. The logistic function method is used for predicting cumulative installed wind power generation capacity upto any year in future is demonstrated in the context of India and China. Next, genetic algorithm has been used to obtain refined values of regression coefficients required in logistic function method. It is shown that error in prediction is reduced by 67.9 % in the case of India and 59.38 % in the case of China. The results are obtained on the basis of assumptions that exploitable wind power generation capacity in India is 49130 MW and for China is 235000 MW. The results obtained using the proposed method shows that the installed wind power generation capacity will reach 99 % of 49130 MW by year 2032 in India and 232650 MW in China by the year 2024. Recent estimates of re-assessed potential of wind power generation may be used to obtain updated predictions.
2. Use of measured wind climate data for determining wind speed distribution characteristics at a site is demonstrated. The analytical expressions for conventional methods, Weibull distribution and Rayleigh distribution function for characterizing wind resource at two sites is obtained on the basis of actual measured wind climate data at two different sites. The site-I typifies experimental wind climate data measurement site and site-II typifies modern grid connected wind power plant in India. The specifications of Weibull probability density function at a site requires

values of shape parameter (k) and scale parameter (c). The error of estimation by using analytic expression is determined with respect to actual empirically observed wind speed distribution at the corresponding site. Further, five statistical methods are used to determine the values of k and c . All the methods have been used to obtain the values of k and c for the two sites. In each case, wind power potential corresponding to pairs of values of k and c is determined for the site and is compared with empirically observed wind power potential at the site. Thus the error of estimation is determined. A new method for obtaining refined values of k and c using genetic algorithm is developed. With use of refined values of k and c , the error in estimation is reduced by 12.24 %.

3. Next, use of industry scale commercial software namely WindSim, Meteodyn and WindFarmer are used to simulate the effect of terrain, on power generated wind farm is demonstrated. The results are obtained for existing wind farm in the state of Tamilnadu. The annual energy production and capacity factor by using these softwares for the site are determined. The capacity factor for the actual site is estimated as 38.3 %. From the results obtained it is found that capacity factor estimated by WindSim, Meteodyn and WindFarmer are 41.47 %, 40.75 % and 42.50 %, respectively. The results obtained it is found that WindSim and Meteodyn are in close agreement with the estimated data as these are simulation tools for complex terrain. The value of wind power density determined at the site is 371.572 W/m^2 is in close agreement using Meteodyn software as 367.5 W/m^2 . Among the software tools used it is found that the Meteodyn software predicts with highest accuracy followed by WindSim and WindFarmer.
4. A genetic algorithm-based technique is developed for searching optimum positions of wind turbines. Use of WindFarmer software for determining locations of wind turbines in a wind farm is demonstrated. It is found that the location of existing wind turbines in the existing wind farm are significantly differ from those recommended by WindFarmer, and therefore do not correspond to maximum possible power generation, thus there is scope for relocation of turbines in the existing wind farm in future. The wind farm simulation tool internally searches locations of wind turbines for maximum possible power generation. The actual capacity

factor determined by using the WindFarmer software for the existing wind farm is 42.5 %. The results of wind farm simulation model suggest that there is scope for relocating existing wind turbines to a new positions corresponding to maximum power production. Thus wind farm capacity factor can be increased to 45.70 %, leads to increase of annual energy production of 13.83 GWh/y and 7.52 % increase in capacity factor at the site.

5. Application of artificial neural network for predicting wind power generation over short intervals of few hours to few days is demonstrated by using two algorithms, namely, BPA and FFNN-GA. The results clearly shows that the predicted wind power generation is in close agreement with actual wind power generation when time scale for prediction is minimum. The results are obtained for two time scales, one equivalent to 10 % of total input data and second, equivalent to 5 % of total input data. The error of prediction depends on time scale of prediction. The accuracy of prediction depends on volume of data input as well as time scale of prediction. The results are obtained by varying the time scales of prediction when input data is available. It is found that predicted wind power generation closely matches with actual wind power generation when time scale of prediction is as short as possible. The results of analysis suggest that the FFNN-GA should be preferred for updating weights in ANN over BPA for application of prediction of wind power generation.

8.2 Future Scope of Work

The work presented in the thesis, may be extended as follow:

1. The genetic algorithm based logistic function method, as described in chapter-3, is tested in the cases of India and China, with reasonable accuracy. The method uses discrete data on recorded cumulative wind power generation capacity during the past years, for generating analytical representation of continuous curve. Although results obtained are reasonably accurate, further work for improving accuracy may be recommended.

2. There is scope for using newer artificial intelligence techniques for obtaining refined values of shape parameter, k , and scale parameter, c , required for determining Weibull probability distribution function for a given site. The results presented in the thesis can be compared with new results thus obtained.
3. In the present work, computer simulation tools, namely, WindSim, Meteodyn and WindFarmer have been used to estimate annual energy production and capacity of one of the existing wind farms. The work can be extended to other existing wind farm sites, to established usefulness of these software tools.
4. It is demonstrated that WindFarmer software can be used for to obtain additional optimum positions of wind turbines in existing wind farm. The difference in actual positions of existing wind turbines and recommended optimum positions of wind turbines, clearly suggest possible options of re-powering existing wind farm. This may be of interest to wind power developer. Similar results can be obtained for additional wind farm sites.
5. The techniques developed for assessment wind power potential can be applied to new prospective wind farm sites, including off-shore sites, using detailed time series data on wind speed, direction, air, temperature, humidity and air pressure at other wind farm sites.

Appendix A

Introduction to Genetic Algorithm

A.1 Evolutionary Algorithms - Genetic Algorithm

A variety of evolutionary algorithms (EA) have been developed. Authors have reported that the most popular of them are genetic algorithm (GA), evolutionary programming, differential evolution, evolution strategies, genetic programming, population-based incremental learning, particle swarm optimization and ant colony optimization [130–134]. The basic concept of all the above listed evolutionary algorithms is to simulate the evolution of individual structures via, processes of selection, reproduction and mutation.

Genetic algorithm is the most popular type of evolutionary algorithms [135]. This type of evolutionary algorithm is often used in optimization problems since genetic algorithm can find a good near-optimal feasible solutions in a reduced computational time [135]. Genetic algorithm is a kind of direct random search algorithm modeled after mechanics of biological evolution. The first step in GA is the random selection of initial search points from the total search space. Each and every point in the search space corresponds to one set of values for the parameters of the problem. Each parameter is coded with a string of bits. The individual bit is called “gene”. The total string of such genes of all parameters written in a sequence is called a “chromosome”. So there exists a chromosome for each point in the search space.

The set of search points selected and used for processing is called a “population”, i.e., population is a set of chromosomes. The number of chromosomes in a population is called “population size” and the total number of genes in a string is called “string length”. The population is processed and evaluated through various operators of GA to generate a new population and this process is carried out till global optimum point is reached.

A.1.1 Phases of GA

Genetic algorithm consists of a string representation of points in the search space, a set of genetic operators for generating new search points, a fitness function to evaluate the search points and a stochastic assignment to control the genetic operations. The basic genetic algorithm cycle is shown in Fig. A.1. It typically consists of three phases.

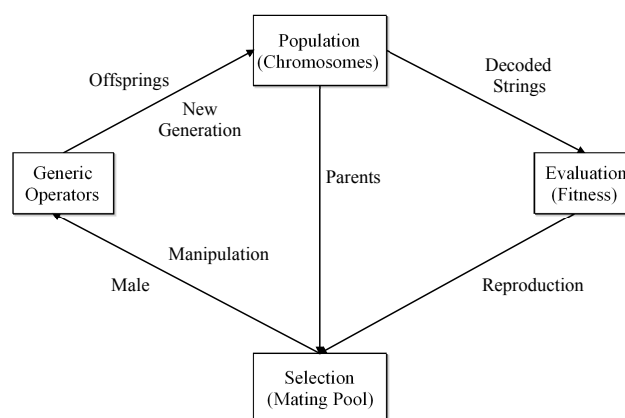


Fig. A.1. Basic schematic of genetic algorithm cycle

1. Initialization :

Initialization is the generation of initial population of chromosomes, i.e., initial search points. The population size and string length need to be judiciously selected before this job is performed. The size of the population, i.e., number of chromosomes in a population, is a direct indication of effective representation of whole search space in one population.

The population size affects both the ultimate performance and efficiency of GA. If it is too small, the chance that the members of a population cover the entire search

space is low. This results in difficulty in obtaining the global optimum solution and leads to a local optimum solution.

Large population size is preferable to avoid this premature convergence and to reach a global optimum point. But a too large population size decreases the rate of convergence and in the worst case may lead to divergence. So based on the size of search space the population size needs to be selected by trial and error.

After the selection of string length and population size, the initial population is generated as a set of strings of bits either 0 or 1. Random number generation techniques are used to accomplish this task. These strings of bits contain the information related to the parameters of the optimization problem in encoded format. Any of the encoding techniques can be used but binary encoding is convenient and mostly used.

2. Evaluation:

In the evaluation phase, suitability of each of the solutions from the initial set as the solution of the optimization problem is determined. For this function called “fitness function” is defined. This is used as a deterministic tool to evaluate the fitness of each chromosome. The optimization problem may be seeking minimum or maximum value of objective function.

In the case of maximization type of objective function, the fitness function can be a function of variables that bear direct proportionality relationship with the objective function. For minimization type of objective function problems, fitness function can be function of variables that bear inverse proportionality relationship with the objective function or can be reciprocal of a function of variables with direct proportionality relationship with the objective function. In either case, fitness function is so selected that the most fit solution is the nearest to the global optimum point.

3. Genetic Operation:

In this phase, the objective is the generation of new population from the existing

population with the examination of fitness values of chromosomes and application of genetic operators. These genetic operators are reproduction, crossover and mutation.

This phase is carried out repetitively or iteratively until optimum solution is obtained. The GA utilizes the notion of survival of the fittest by transferring the highly fit chromosomes to the next generation of strings and combining different strings to explore new search points.

Appendix B

Wind Resource Assessment at Model Wind Farm

B.1 Site-II: Model Wind Farm

The Model wind farm represents grid integrated wind farm in India situated at Periyapatti, TamilNadu (hereafter named as “Site-II”) (Lat. $10^{\circ}45'18.5''N$, Long. $77^{\circ}15'11.0''E$), altitude 327 m mean sea level. The site is located approximately 22 km from Udu-malpet, Coimbatore, TamilNadu. The main source of wind is expected through Palghat pass.

This section provides the detailed analysis of different distribution methods for Wind Resource assessment.

B.1.1 Standard Deviation Method-based Analysis

In this section, the Weibull parameters are determined by using standard deviation method as explained in section 4.3.2, and various parameters thus calculated are listed in Table B.1.

Table B.1. Month-wise variation of Weibull parameters and their associated statistical parameters using SD method at site-II

Month	V_{mW} (m/s)	k	c (m/s)	V_{mp} (m/s)	V_{maxE} (m/s)	WPD_C (W/m ²)	WPD_V (W/m ²)	WPD_E (%)	RMSE	R^2
Oct-10	7.543	2.449	8.506	6.865	10.855	421.128	405.519	4.923	0.020	0.369
Nov-10	3.344	1.718	3.751	2.258	5.878	51.808	50.090	2.224	0.019	0.722
Dec-10	4.240	2.136	4.788	3.563	6.523	83.738	81.297	-1.839	0.017	0.803
Jan-11	4.290	2.594	4.831	4.004	6.022	74.339	72.039	2.153	0.010	0.937
Feb-11	4.300	2.512	4.846	3.959	6.118	76.545	73.860	0.890	0.006	0.972
Mar-11	4.709	2.210	5.317	4.048	7.118	111.292	106.527	0.518	0.005	0.967
Apr-11	5.000	1.793	5.621	3.565	8.539	164.597	157.338	2.030	0.009	0.832
May-11	8.947	4.123	9.853	9.211	10.845	535.642	511.276	1.338	0.011	0.890
Jun-11	10.315	5.462	11.178	10.771	11.835	760.249	731.692	-0.123	0.008	0.945
Jul-11	10.904	6.802	11.675	11.405	12.126	863.305	831.822	-0.058	0.008	0.953
Aug-11	10.209	5.472	11.062	10.661	11.710	736.765	709.686	0.251	0.005	0.979
Sep-11	9.919	5.788	10.713	10.367	11.276	667.910	642.440	-0.004	0.006	0.975
Oct-11	4.683	1.944	5.281	3.642	7.601	123.731	119.034	0.415	0.007	0.929
Nov-11	3.459	1.866	3.896	2.581	5.757	52.091	50.424	-4.125	0.017	0.837
Dec-11	3.722	2.418	4.198	3.366	5.387	51.072	49.523	0.127	0.015	0.893
Jan-12	4.052	3.583	4.497	4.105	5.090	52.477	50.955	-0.124	0.011	0.963
Feb-12	4.567	2.827	5.127	4.393	6.195	84.802	81.739	0.519	0.006	0.976
Mar-12	4.871	1.965	5.494	3.825	7.854	137.618	131.448	0.091	0.006	0.953
Apr-12	5.284	2.035	5.964	4.278	8.349	169.630	161.602	1.562	0.009	0.881
May-12	9.931	4.310	10.909	10.261	11.918	721.994	689.541	0.832	0.006	0.955
Jun-12	10.831	6.534	11.621	11.329	12.106	851.236	817.811	-0.105	0.009	0.938
Jul-12	10.673	5.991	11.506	11.160	12.073	826.820	795.330	-0.004	0.006	0.973
Aug-12	10.166	5.445	11.018	10.615	11.669	728.179	701.203	0.069	0.007	0.954
Sep-12	9.632	5.234	10.463	10.048	11.131	624.990	600.471	0.313	0.006	0.968
Whole data	6.913	2.013	7.802	5.546	10.991	384.041	369.593	2.795	0.011	0.650

It is observed from Table B.1 that, V_{mW} varies from minimum of 3.344 m/s in November 2010 to maximum of 10.904 m/s in July 2011. Similarly, k varies from minimum of 1.718 occurring on November 2010 to maximum of 6.802 occurring on July 2011. Also, c varies from minimum of 3.751 m/s occurring on November 2010 to maximum of 11.675 m/s occurring on July 2011. The values of k and c over a period of two years are estimated as 2.013 and 7.802 m/s, respectively, as listed in Table B.1.

It is observed from the table, that the V_{mp} varies from minimum of 2.258 m/s to maximum of 11.405 m/s and V_{maxE} varies from 5.090 m/s in January 2012 to maximum of 12.126 m/s in July 2011. The values of V_{mW} , V_{mp} and V_{maxE} for the complete data are 6.913 m/s, 5.546 m/s and 10.991 m/s, respectively.

From the table, it is observed that WPD_{WC} corresponding to ρ_C varies from a minimum of 51.072 W/m² in the month of December 2011 to a maximum of 863.305 W/m² in the month of July 2011 and WPD_{WH} corresponding to ρ_H varies from 49.523 W/m² to a maximum of 831.822 W/m².

The percentage change in the variation of wind power density for the complete data is calculated using the actual value (359.544 W/m²) to that of the wind power density estimated using Weibull parameters (369.593 W/m²) is found to be 2.795 %. Also, from the table, the RMSE and R^2 for the whole data is found to be 0.0107 and 0.650, respectively.

B.1.2 Energy Pattern Factor Method-based Analysis

In this section, the Weibull parameters are determined by using standard deviation method as explained in section 4.3.3, and various parameters thus calculated are listed in Table B.2.

Table B.2. Month-wise variation of Weibull parameters and their associated statistical parameters using EPF method at site-II

Month	V_{mW} (m/s)	k	c (m/s)	V_{mp} (m/s)	V_{maxE} (m/s)	WPD_C (W/m ²)	WPD_V (W/m ²)	WPD_E (%)	RMSE	R^2
Oct-10	7.543	2.583	8.494	7.028	10.605	405.187	390.169	0.951	0.019	0.388
Nov-10	3.344	1.754	3.756	2.321	5.795	50.531	48.854	-0.296	0.019	0.717
Dec-10	4.240	2.106	4.787	3.526	6.574	84.862	82.388	-0.521	0.017	0.800
Jan-11	4.290	2.631	4.829	4.026	5.987	73.635	71.356	1.185	0.010	0.939
Feb-11	4.300	2.520	4.845	3.965	6.109	76.371	73.692	0.660	0.006	0.972
Mar-11	4.709	2.231	5.317	4.073	7.083	110.369	105.643	-0.316	0.005	0.966
Apr-11	5.000	1.831	5.627	3.656	8.421	160.614	153.531	-0.439	0.010	0.814
May-11	8.947	3.541	9.937	9.048	11.277	567.862	542.030	7.434	0.015	0.801
Jun-11	10.315	3.878	11.400	10.556	12.691	839.096	807.578	10.235	0.012	0.852
Jul-11	10.904	4.119	12.010	11.226	13.222	970.211	934.829	12.318	0.017	0.769
Aug-11	10.209	3.902	11.279	10.455	12.541	811.643	781.813	10.440	0.014	0.824
Sep-11	9.919	3.954	10.950	10.172	12.144	740.678	712.432	10.890	0.014	0.838
Oct-11	4.683	1.962	5.283	3.674	7.558	122.517	117.866	-0.570	0.007	0.926
Nov-11	3.459	1.803	3.890	2.485	5.884	54.120	52.387	-0.392	0.018	0.823
Dec-11	3.722	2.415	4.198	3.364	5.390	51.124	49.574	0.231	0.015	0.892
Jan-12	4.052	3.218	4.522	4.029	5.255	55.134	53.535	4.932	0.013	0.949
Feb-12	4.567	2.765	5.131	4.362	6.248	85.978	82.872	1.913	0.007	0.972
Mar-12	4.871	1.978	5.495	3.848	7.824	136.703	130.574	-0.574	0.006	0.951
Apr-12	5.284	2.080	5.965	4.352	8.248	166.111	158.250	-0.545	0.009	0.868
May-12	9.931	3.590	11.022	10.064	12.470	772.100	737.395	7.830	0.009	0.889
Jun-12	10.831	4.078	11.936	11.141	13.164	954.018	916.557	11.957	0.016	0.800
Jul-12	10.673	3.993	11.776	10.956	13.037	919.671	884.645	11.226	0.015	0.815
Aug-12	10.166	3.885	11.234	10.406	12.501	802.606	772.874	10.298	0.013	0.837
Sep-12	9.632	3.849	10.650	9.849	11.874	685.252	658.369	9.986	0.014	0.829
Whole data	6.913	2.083	7.805	5.701	10.783	371.572	357.593	-0.543	0.011	0.615

It is observed from Table B.2 that, V_{mW} varies from minimum of 3.344 m/s in November 2010 to maximum of 10.904 m/s in July 2011. Similarly, k varies from minimum of 1.754 occurring on November 2010 to maximum of 4.119 occurring on July 2011. Also, c varies from minimum of 3.756 m/s occurring in November 2010 to maximum

of 12.010 m/s occurring in July 2011. The values of k and c over a period of two years are estimated as 2.083 and 7.805 m/s, respectively, as listed in Table B.2.

It is observed from the table, that the V_{mp} varies from minimum of 2.321 m/s to maximum of 11.226 m/s and V_{maxE} varies from 5.255 m/s in January 2012 to maximum of 13.222 m/s in July 2011. The values of V_{mW} , V_{mp} and V_{maxE} for the complete data are 6.913 m/s, 5.701 m/s and 10.783 m/s, respectively.

From the table, it is observed that WPD_{WC} corresponding to ρ_C varies from a minimum of 50.531 W/m² in the month of November 2010 to a maximum of 970.211 W/m² in the month of July 2011 and WPD_{WH} corresponding to ρ_H varies from 48.854 W/m² to a maximum of 934.829 W/m².

The percentage change in the variation of wind power density for the complete data is calculated using the actual value (359.544 W/m²) to that of the wind power density estimated using Weibull parameters (357.593 W/m²) is found to be -0.543 %. Also, from the table, the RMSE and R^2 for the whole data is found to be 0.0112 and 0.615, respectively.

B.1.3 Maximum Likelihood Method-based Analysis

In this section, the Weibull parameters are determined by using maximum likelihood method as explained in section 4.3.4. The Weibull parameters and its associated parameters determined using MLE method are listed in Table B.3. It is observed from Table B.3 that, V_{mW} varies from minimum of 3.326 m/s in November 2010 to maximum of 10.880 m/s in July 2011. Similarly, k varies from minimum of 1.614 occurring on November 2010 to maximum of 6.402 occurring on July 2011. Also, c varies from minimum of 3.713 m/s occurring on November 2010 to maximum of 11.686 m/s occurring on July 2011. The values of k and c over a period of two years are estimated as 1.948 and 7.768 m/s, respectively, as listed in Table B.3.

It is observed from the table, that the V_{mp} varies from minimum of 2.040 m/s to maximum of 11.380 m/s and V_{maxE} varies from 5.110 m/s in January 2012 to maximum of

Table B.3. Month-wise variation of Weibull parameters and their associated statistical parameters using MLE method at site-II

Month	V_{mW} (m/s)	k	c (m/s)	V_{mp} (m/s)	V_{maxE} (m/s)	WPD_C (W/m ²)	WPD_V (W/m ²)	WPD_E (%)	RMSE	R^2
Oct-10	7.440	2.320	8.398	6.585	10.980	421.546	405.921	5.027	0.020	0.324
Nov-10	3.326	1.614	3.713	2.040	6.118	55.257	53.424	9.030	0.019	0.730
Dec-10	4.233	2.093	4.779	3.504	6.583	84.869	82.395	-0.513	0.017	0.800
Jan-11	4.261	2.543	4.800	3.944	6.031	73.833	71.548	1.457	0.010	0.929
Feb-11	4.282	2.468	4.827	3.911	6.140	76.577	73.891	0.932	0.007	0.969
Mar-11	4.694	2.161	5.301	3.977	7.177	112.443	107.628	1.557	0.005	0.966
Apr-11	4.988	1.729	5.596	3.396	8.729	170.577	163.054	5.737	0.008	0.856
May-11	8.937	4.407	9.805	9.249	10.674	522.581	498.809	-1.133	0.009	0.918
Jun-11	10.299	5.227	11.188	10.743	11.904	764.214	735.509	0.398	0.007	0.949
Jul-11	10.880	6.402	11.686	11.380	12.193	865.708	834.137	0.220	0.007	0.958
Aug-11	10.199	5.492	11.049	10.652	11.691	734.089	707.109	-0.113	0.005	0.980
Sep-11	9.902	5.585	10.717	10.345	11.320	669.420	643.892	0.222	0.005	0.977
Oct-11	4.674	1.896	5.267	3.546	7.701	126.259	121.466	2.467	0.007	0.937
Nov-11	3.446	1.809	3.876	2.484	5.850	53.318	51.612	-1.867	0.018	0.824
Dec-11	3.695	2.322	4.170	3.272	5.449	51.570	50.007	1.105	0.016	0.876
Jan-12	4.041	3.500	4.491	4.079	5.110	52.580	51.055	0.072	0.011	0.965
Feb-12	4.546	2.777	5.107	4.348	6.208	84.559	81.504	0.231	0.007	0.974
Mar-12	4.863	1.923	5.482	3.742	7.943	140.060	133.781	1.868	0.005	0.958
Apr-12	5.278	2.002	5.956	4.215	8.419	171.872	163.738	2.904	0.008	0.890
May-12	9.931	4.531	10.879	10.296	11.793	711.261	679.291	-0.667	0.006	0.956
Jun-12	10.813	6.171	11.637	11.309	12.179	855.153	821.574	0.355	0.008	0.949
Jul-12	10.657	5.779	11.511	11.139	12.118	828.624	797.065	0.215	0.006	0.973
Aug-12	10.156	5.355	11.018	10.601	11.691	728.868	701.867	0.164	0.007	0.955
Sep-12	9.623	5.281	10.448	10.041	11.103	621.962	597.562	-0.173	0.006	0.970
whole data	6.888	1.948	7.768	5.366	11.165	392.767	377.991	5.131	0.010	0.674

11.686 m/s in July 2011. The values of V_{mW} , V_{mp} and V_{maxE} for the complete data are 6.888 m/s, 5.366 m/s and 11.165 m/s, respectively.

From the table, it is observed that WPD_{WC} corresponding to ρ_C varies from a minimum of 51.570 W/m² in the month of December 2011 to a maximum of 865.708 W/m² in the month of July 2011 and WPD_{WH} corresponding to ρ_H varies from 50.007 W/m² to a maximum of 834.137 W/m².

The percentage change in the variation of wind power density for the complete data is calculated using the actual value (359.544 W/m²) to that of the wind power density estimated using Weibull parameters (377.991 W/m²) is found to be 5.131 %. Also, from the table, the RMSE and R^2 for the whole data is found to be 0.0103 and 0.674, respectively.

B.1.4 Rayleigh Distribution Method-based Analysis

In this section, Rayleigh distribution method as explained in section 4.4 is used for the analysis. Similar to that of Weibull distribution methods, various parameters are determined using Rayleigh distribution method are listed in Table B.4.

Table B.4. Month-wise variation scale parameter and its associated statistical parameters using Rayleigh distribution method at site-II

Month	V_{mR} (m/s)	c_R (m/s)	V_{mpR} (m/s)	V_{maxR} (m/s)	WPD_R (W/m ²)	WPD_{VR} (W/m ²)	WPD_E (%)	RMSE	R^2
Oct-10	7.543	8.512	6.019	12.038	502.378	483.758	25.166	0.021	0.264
Nov-10	3.344	3.774	2.668	5.337	43.776	42.324	-13.624	0.021	0.661
Dec-10	4.240	4.785	3.383	6.766	89.223	86.622	4.591	0.018	0.787
Jan-11	4.290	4.841	3.423	6.847	92.436	89.575	27.020	0.017	0.799
Feb-11	4.300	4.852	3.431	6.862	93.051	89.787	22.645	0.013	0.890
Mar-11	4.709	5.313	3.757	7.514	122.196	116.964	10.367	0.006	0.953
Apr-11	5.000	5.642	3.989	7.979	146.304	139.852	-9.309	0.012	0.708
May-11	8.947	10.095	7.138	14.277	838.110	799.985	58.562	0.027	0.333
Jun-11	10.315	11.639	8.230	16.460	1284.509	1236.261	68.751	0.026	0.335
Jul-11	10.904	12.304	8.701	17.401	1517.548	1462.205	75.681	0.032	0.245
Aug-11	10.209	11.520	8.146	16.291	1245.335	1199.566	69.452	0.029	0.291
Sep-11	9.919	11.192	7.914	15.828	1142.034	1098.483	70.979	0.029	0.305
Oct-11	4.683	5.285	3.737	7.474	120.235	115.671	-2.422	0.008	0.917
Nov-11	3.459	3.903	2.760	5.520	48.445	46.894	-10.836	0.016	0.862
Dec-11	3.722	4.200	2.970	5.939	60.345	58.515	18.308	0.021	0.793
Jan-12	4.052	4.572	3.233	6.465	77.842	75.585	48.151	0.033	0.657
Feb-12	4.567	5.153	3.644	7.288	111.476	107.449	32.137	0.018	0.797
Mar-12	4.871	5.496	3.886	7.772	135.223	129.161	-1.651	0.006	0.948
Apr-12	5.284	5.962	4.216	8.431	172.635	164.465	3.361	0.008	0.891
May-12	9.931	11.206	7.924	15.847	1146.225	1094.703	60.080	0.022	0.378
Jun-12	10.831	12.221	8.642	17.284	1487.065	1428.673	74.512	0.030	0.251
Jul-12	10.673	12.043	8.516	17.032	1423.034	1368.837	72.103	0.029	0.284
Aug-12	10.166	11.471	8.111	16.222	1229.511	1183.964	68.965	0.028	0.308
Sep-12	9.632	10.869	7.686	15.371	1046.004	1004.969	67.888	0.029	0.300
Whole data	6.913	7.801	5.516	11.032	386.682	372.135	3.502	0.011	0.656

It is observed from the table, c_R varies from minimum of 3.774 m/s occurring in November 2010 to maximum of 12.304 m/s occurring in July 2011. The value of c_R for the complete data is estimated as 7.801 m/s as listed in Table B.4.

It is observed that the V_{mR} varies from minimum of 3.344 m/s in November 2010 to maximum of 10.904 m/s in July 2011. The V_{mpR} varies from minimum of 2.668 m/s in November 2010 to maximum of 8.704 m/s in July 2011 and V_{maxER} varies from 5.337 m/s in November 2010 to 17.401 m/s in July 2011. The values of V_{mR} , V_{mpR} and V_{maxER} , for the complete data are 6.913 m/s, 5.516 m/s and 11.032 m/s, respectively.

From the table, it is observed that the values of wind power density (WPD_{RC}) corresponding to ρ_C varies from a minimum of 43.776 W/m^2 in the month of November 2010 to a maximum of 1517.548 W/m^2 in the month of July 2011 and WPD_{RH} corresponding to ρ_H varies from 42.324 W/m^2 to a maximum of 1462.205 W/m^2 .

The percentage change in WPD_{RC} (386.682 W/m^2) to WPD_{RH} (372.135 W/m^2) is -3.76% , for the whole data. Also the percentage change variation of wind power density calculated using the actual value (359.544 W/m^2) to that of the wind power density estimated using Rayleigh parameters (372.135 W/m^2) is found to be 3.502% , for the complete data. Also, from the table the RMSE and R^2 for the complete data is found to be 0.0106 and 0.656 , respectively.

B.1.5 Comparison of Weibull Distribution Method to Rayleigh Distribution Method

In this section, the results of the comparative study of Weibull distribution methods and Rayleigh distribution method are presented. From Table B.5, it is observed that for the complete data the graphical method found to be the best method for site-II in terms of accuracy in fitting the PDF as indicated by RMSE and R^2 values.

B.1.6 Variation of Wind Power Density with Height

Using the value of WPD at 85 m height AGL, the WPD at different heights, viz., 100 m , 120 m and 150 m AGL, are estimated using the power law equation (4.46) and (4.48), respectively. The procedure is detailed in the form of flowchart shown in Fig. 4.3. The wind data recorded at two different heights (70 m and 85 m) are available, α is calculated using 4.47. The extrapolated values of WPD at different heights are listed in Table B.6.

The WPDs estimated for heights 100 m and 150 m AGL are found to be 389.64 W/m^2 and 476.18 W/m^2 , respectively.

Table B.5. Best values of RMSE and R^2 from different distribution methods for site-II

Month Year	RMSE	R^2	Method
Oct-10	0.0194	0.388	EPF
Nov-10	0.0183	0.737	GP
Dec-10	0.0170	0.803	SD
Jan-11	0.0095	0.939	EPF
Feb-11	0.0064	0.972	EPF
Mar-11	0.0055	0.967	SD
Apr-11	0.0074	0.888	GP
May-11	0.0095	0.918	MLE
Jun-11	0.0073	0.949	MLE
Jul-11	0.0075	0.958	MLE
Aug-11	0.0048	0.980	MLE
Sep-11	0.0054	0.977	MLE
Oct-11	0.0065	0.940	GP
Nov-11	0.0173	0.837	SD
Dec-11	0.0152	0.893	SD
Jan-12	0.0107	0.965	MLE
Feb-12	0.0063	0.976	SD
Mar-12	0.0053	0.960	GP
Apr-12	0.0074	0.914	GP
May-12	0.0059	0.956	MLE
Jun-12	0.0079	0.949	MLE
Jul-12	0.0056	0.973	SD
Aug-12	0.0071	0.955	MLE
Sep-12	0.0061	0.970	MLE
Whole data	0.0098	0.703	GP

Table B.6. Variation of wind power density with height (AGL) at site-II

Month Year	WPD _{m70} (W/m ²)	WPD _{m85} (W/m ²)	α	WPD ₁₀₀ (W/m ²)	WPD ₁₂₀ (W/m ²)	WPD ₁₅₀ (W/m ²)
Oct-10	355.959	386.493	0.155	416.908	453.886	503.637
Nov-10	43.154	49.000	0.199	53.984	60.182	68.744
Dec-10	71.355	82.820	0.287	95.273	111.486	135.129
Jan-11	58.624	70.520	0.336	83.066	99.815	124.977
Feb-11	62.430	73.209	0.296	84.568	99.422	121.198
Mar-11	93.042	105.978	0.256	120.043	138.055	163.819
Apr-11	139.902	154.208	0.192	169.302	188.000	213.719
May-11	466.032	504.524	0.137	539.256	581.075	636.695
Jun-11	677.117	732.594	0.154	789.599	858.847	951.918
Jul-11	775.798	832.306	0.132	887.432	953.633	1041.413
Aug-11	661.447	707.908	0.126	752.683	806.294	877.131
Sep-11	599.270	642.467	0.126	683.276	732.149	796.749
Oct-11	111.664	118.541	0.113	125.271	133.277	143.776
Nov-11	46.453	52.593	0.191	57.725	64.080	72.818
Dec-11	42.822	49.460	0.233	55.419	62.961	73.604
Jan-12	44.520	51.019	0.214	56.621	63.641	73.429
Feb-12	70.512	81.316	0.243	91.536	104.537	122.989
Mar-12	119.153	131.328	0.203	144.982	161.995	185.559
Apr-12	145.869	159.117	0.172	173.074	190.193	213.466
May-12	633.815	683.849	0.134	729.980	785.445	859.097
Jun-12	759.196	818.667	0.139	876.251	945.686	1038.200
Jul-12	739.658	795.359	0.131	847.679	910.480	993.710
Aug-12	653.862	700.717	0.128	745.979	800.245	872.062
Sep-12	558.652	598.596	0.127	636.865	682.716	743.350
whole data	332.249	359.544	0.165	389.643	426.419	476.185

Appendix C

Optimizing Position of Wind Turbine using PSO

C.1 Simulation of Wind Farm using Particle Swarm Optimization

Particle swarm optimization technique can be used to find the optimal position of wind turbines in a wind farm for increased power generation efficiency. The simulation is carried out using MATLAB.

The data used for simulation is as given in Table 6.1. The results are computed for different number of turbines and are shown in Table C.1. The tabulated data indicates optimum position of turbine corresponds to larger power output than recorded at the wind farm. Table C.2 shows the improvement in efficiency compared to the existing

Table C.1. Comparison of results obtained by the proposed approach using PSO with variation of wind turbines.

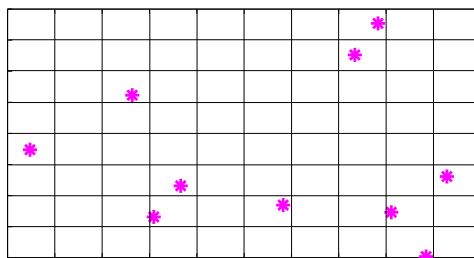
	Results using PSO				
No. of turbines	10	20	26	30	32
Total Power (kW/year)	5184	10365	13471	15019	16552
Fitness value	0.00182	0.00160	0.00148	0.00142	0.00139
Efficiency %	100	99.94	99.71	99.67	99.72

method shown in Table 6.2 to that of using the present approach of placements of wind turbines using PSO.

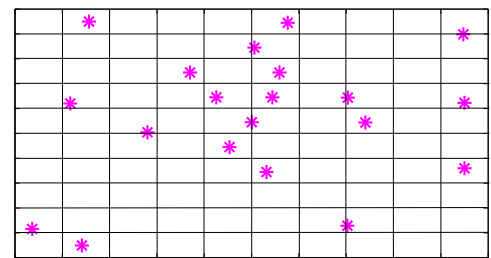
Table C.2. Increase in efficiency using PSO

No. of turbines	20	26	30
Increase in efficiency (in %)	1.94	8.089	7.68

The optimal layout using PSO for different wind turbines are shown in Figs. C.1, C.2, C.3.

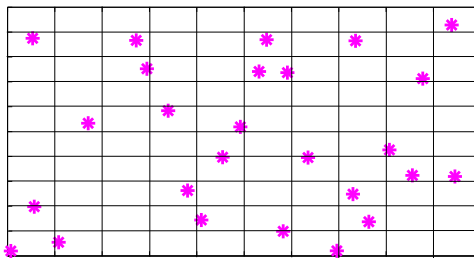


(a) layout of 10 turbines

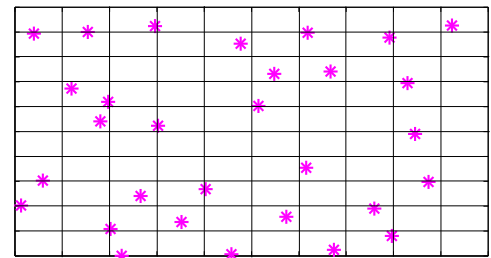


(b) layout of 20 turbines

Fig. C.1. Proposed wind farm layout of wind turbines consisting of 10 & 20 turbines using PSO



(a) layout of 26 turbines



(b) layout of 30 turbines

Fig. C.2. Proposed wind farm layout of wind turbines consisting of 26 & 30 turbines using PSO

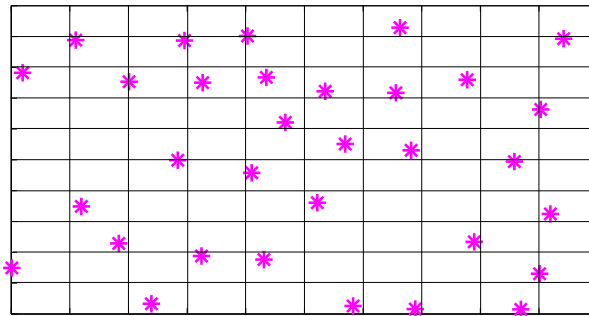


Fig. C.3. Proposed wind farm layout of wind turbines consisting of 32 turbines using PSO

Appendix D

Architecture of Artificial Neural Network using BPA and GA

D.1 Artificial Neural Network

Artificial neural networks (ANN) or simply neural networks refer to a group of algorithms that typically operate on a large number of simple interconnected components or neurons [170]. ANN is an information-processing paradigm that is inspired by the biological nervous systems, such as the brain and nervous system for processing information. It is composed of a large number of highly interconnected processing elements (neurons) working in unison to solve specific problems. ANN has been applied to various problems in different scientific disciplines, including applied mathematics, chemistry, physics, engineering, economics and finance. ANN has been widely used in solving problems related to prediction, classification, control and identification [131, 171]. The detailed information on ANN is provided in AppendixD.

An ANN consists of a set of highly interconnected processing units, called nodes or units. Each unit is designed to mimic its biological counterpart, the neuron. Each node accepts a weighted set of inputs and responds with an output. ANN resembles the biological neuron in acquiring knowledge by learning from examples and storing this information in inter-neuron connection strengths called “weights”.

Structure of Artificial Neural Network:

The ANN consists of unit or neuron which in-turn consists of summer and activation function, to mimic its biological counter part-the neuron. As shown in Fig. D.1, the

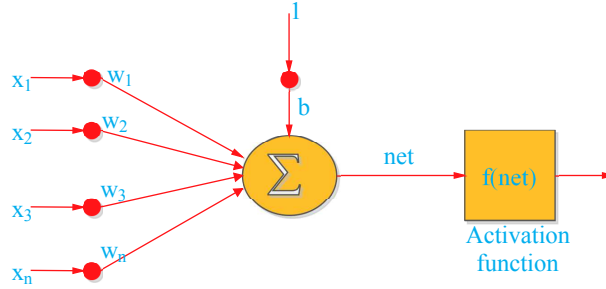


Fig. D.1. Basic structure of a artificial neuron

basic structure of a artificial neuron consists of inputs, x_1, x_2, \dots, x_n to the neuron with corresponding weights w_1, w_2, \dots, w_n which model the synaptic neural connections in biological nets and act in such a way as to increase or decrease the input signals to the neuron. A threshold term 'b' is added to the inputs. Generally, inputs, weights, thresholds and neuron output could be either real value or binary or bipolar value. All inputs are multiplied by their corresponding weights and added together to form the net input to the neuron called net. The mathematical expression for net can be written as:

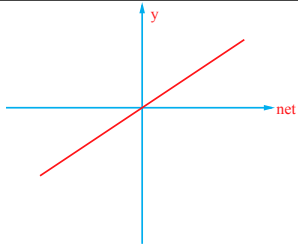
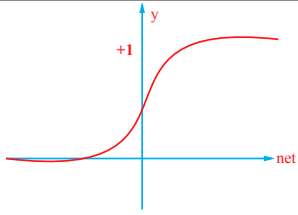
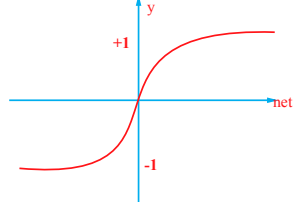
$$net = \sum_{i=1}^N w_i x_i + b = w_1 x_1 + w_2 x_2 + \dots w_n x_n + b \quad (D.1)$$

The neuron behaves as an activation or mapping function $f(net)$ to produce an output y which can be expressed as:

$$y = f(net) = f\left(\sum_{i=1}^N w_i x_i + b\right) \quad (D.2)$$

where f is called the neuron activation function or the neuron transfer function. Some examples of the neuron activation functions are shown in Table D.1.

Table D.1. Types of activation function in ANN

S.No.	Activation Function	Mathematical expressions	Function
1	Linear	$y = f(net) = f\left(\sum_{i=1}^N w_i x_i + b\right)$	
2	Sigmoid	$y = \frac{1}{1 + \exp\left(\frac{-net}{T}\right)}$	
3	Tansigmoid	$y = \tanh(net) = \frac{1 - \exp(-net)}{1 + \exp(-net)}$	

D.2 Details of Parametric Variation of Back Propagation Algorithm in Deciding the ANN Architecture

The important parameters that affect the performance of BPA in the artificial neural network are, number of neurons in the hidden layer, learning rate and momentum coefficient. These parameters are varied with variation of epochs. The parameters varied in the architecture are number of neurons in hidden layer from 4 to 10, learning rate (0.1, 0.5 & 0.9) and momentum coefficient (0.1, 0.5 & 0.9). Total there are 315 combinations. Out of these combinations, one combination will be selected as the parameters in the artificial neural network. This is selected on the basis of least validation error. The training error is denoted as Train_E , Validation error is denoted as Val_E and Testing error is denoted as Test_E .

In this study, two training data sets are used. One with 80 % of the total data set over 11 months as the training data, i.e. 38477 data points. The other has 90 % of the data points, i.e., 43286 data points. The different combinations of 80 % of the total data set

are listed in Tables D.2 and D.3. Similarly, for 90 % of input data as training data, the best combination is listed in Tables D.4 and D.5.

D.3 Details of Parametric Variation of Genetic Algorithm in Deciding the ANN Architecture

The important parameters that affect the performance of genetic algorithm as learning algorithm in the artificial neural network are, number of neurons in the hidden layer, elite count and cross over fraction. These parameters are varied with variation of generations. The parameters varied in the architecture are number of neurons in hidden layer from 4 to 10, elite count (0.10, 0.15 & 0.20), cross over fraction (0.7, 0.8 & 0.9). The results obtained for different combinations consisting of 80 % of the total data are listed in Tables D.6 and D.7 and 90 % of the total data are listed in Tables D.8 and D.9.

Table D.2. Variation of parameters of BPA for 80 % of input data for Training

learning rate =0.1 and momentum coefficient=0.1																					
Neurons	4			5			6			7			8			9			10		
	Train _E	Val _E	Test _E	Train _E	Val _E	Test _E	Train _E	Val _E	Test _E	Train _E	Val _E	Test _E	Train _E	Val _E	Test _E	Train _E	Val _E	Test _E	Train _E	Val _E	Test _E
500	0.0130	0.0026	0.0031	0.0130	0.0026	0.0032	0.0127	0.0021	0.0025	0.0128	0.0024	0.0028	0.0126	0.0021	0.0024	0.0125	0.0023	0.0027	0.0126	0.0024	0.0028
1000	0.0126	0.0024	0.0027	0.0130	0.0026	0.0031	0.0126	0.0023	0.0026	0.0126	0.0023	0.0028	0.0126	0.0021	0.0024	0.0130	0.0026	0.0031	0.0127	0.0024	0.0028
1500	0.0126	0.0023	0.0027	0.0128	0.0027	0.0032	0.0126	0.0023	0.0026	0.0127	0.0022	0.0025	0.0126	0.0024	0.0028	0.0126	0.0022	0.0027	0.0126	0.0024	0.0028
2000	0.0132	0.0026	0.0030	0.0129	0.0023	0.0027	0.0126	0.0021	0.0024	0.0126	0.0025	0.0029	0.0126	0.0023	0.0027	0.0126	0.0023	0.0026	0.0125	0.0023	0.0026
2500	0.0127	0.0026	0.0031	0.0127	0.0023	0.0027	0.0127	0.0023	0.0027	0.0126	0.0023	0.0028	0.0126	0.0023	0.0026	0.0125	0.0023	0.0027	0.0126	0.0023	0.0027
learning rate=0.5 and momentum coefficient=0.1																					
500	0.0129	0.0024	0.0027	0.0129	0.0023	0.0028	0.0128	0.0024	0.0028	0.0130	0.0019	0.0022	0.0126	0.0024	0.0028	0.0132	0.0027	0.0031	0.0126	0.0023	0.0027
1000	0.0127	0.0024	0.0028	0.0131	0.0020	0.0023	0.0126	0.0023	0.0028	0.0128	0.0023	0.0027	0.0126	0.0023	0.0027	0.0126	0.0023	0.0028	0.0126	0.0020	0.0023
1500	0.0127	0.0026	0.0030	0.01298	0.00188	0.00223	0.0127	0.0022	0.0025	0.0127	0.0026	0.0030	0.0126	0.0023	0.0027	0.0127	0.0023	0.0027	0.0126	0.0023	0.0027
2000	0.0127	0.0024	0.0028	0.0127	0.0023	0.0027	0.0126	0.0025	0.0029	0.0127	0.0026	0.0031	0.0126	0.0024	0.0028	0.0126	0.0022	0.0026	0.0126	0.0024	0.0027
2500	0.0127	0.0023	0.0026	0.0127	0.0023	0.0028	0.0126	0.0023	0.0028	0.0126	0.0022	0.0026	0.0126	0.0021	0.0024	0.0126	0.0021	0.0025	0.0127	0.0026	0.0030
learning rate=0.9 and momentum coefficient=0.1																					
500	0.0128	0.0027	0.0032	0.0131	0.0027	0.0032	0.0127	0.0023	0.0025	0.0128	0.0024	0.0029	0.0127	0.0023	0.0027	0.0126	0.0024	0.0028	0.0127	0.0022	0.0026
1000	0.0127	0.0024	0.0028	0.0131	0.0023	0.0028	0.0128	0.0023	0.0026	0.0127	0.0025	0.0030	0.0126	0.0021	0.0024	0.0126	0.0022	0.0026	0.0126	0.0023	0.0026
1500	0.0126	0.0024	0.0028	0.0129	0.0027	0.0032	0.0126	0.0021	0.0024	0.0126	0.0022	0.0026	0.0127	0.0025	0.0029	0.0127	0.0020	0.0024	0.0127	0.0024	0.0027
2000	0.0128	0.0025	0.0029	0.0128	0.0027	0.0032	0.0126	0.0021	0.0024	0.0126	0.0023	0.0028	0.0126	0.0023	0.0027	0.0125	0.0022	0.0027	0.0126	0.0021	0.0024
2500	0.0126	0.0025	0.0030	0.0128	0.0028	0.0033	0.0126	0.0022	0.0026	0.0126	0.0025	0.0029	0.0126	0.0021	0.0025	0.0125	0.0022	0.0027	0.0126	0.0023	0.0026
learning rate=0.1 and momentum coefficient=0.5																					
500	0.0127	0.0026	0.0030	0.0130	0.0025	0.0031	0.0127	0.0023	0.0027	0.0129	0.0025	0.0029	0.0127	0.0026	0.0030	0.0126	0.0023	0.0027	0.0127	0.0023	0.0027
1000	0.0126	0.0025	0.0029	0.0128	0.0027	0.0032	0.0127	0.0024	0.0028	0.0126	0.0023	0.0027	0.0126	0.0024	0.0027	0.0126	0.0025	0.0029	0.0126	0.0023	0.0026
1500	0.0127	0.0026	0.0031	0.0128	0.0028	0.0034	0.0126	0.0022	0.0026	0.0126	0.0023	0.0028	0.0125	0.0023	0.0027	0.0125	0.0022	0.0026	0.0125	0.0023	0.0026
2000	0.0126	0.0026	0.0030	0.0127	0.0027	0.0032	0.0126	0.0024	0.0027	0.0126	0.0024	0.0028	0.0126	0.0023	0.0027	0.0125	0.0023	0.0027	0.0125	0.0023	0.0027
2500	0.0126	0.0025	0.0029	0.0127	0.0026	0.0031	0.0126	0.0023	0.0026	0.0125	0.0023	0.0027	0.0125	0.0023	0.0027	0.0125	0.0022	0.0026	0.0125	0.0023	0.0027
learning rate=0.5 and momentum coefficient=0.5																					
500	0.0128	0.0026	0.0030	0.0131	0.0022	0.0027	0.0127	0.0024	0.0027	0.0126	0.0024	0.0028	0.0126	0.0023	0.0027	0.0125	0.0022	0.0026	0.0127	0.0026	0.0029
1000	0.0127	0.0026	0.0030	0.0127	0.0026	0.0031	0.0127	0.0023	0.0026	0.0126	0.0024	0.0028	0.0126	0.0024	0.0028	0.0125	0.0022	0.0026	0.0125	0.0023	0.0027
1500	0.0126	0.0025	0.0029	0.0127	0.0026	0.0031	0.0126	0.0022	0.0026	0.0125	0.0024	0.0028	0.0125	0.0023	0.0027	0.0125	0.0023	0.0027	0.0125	0.0023	0.0026
2000	0.0126	0.0025	0.0029	0.0126	0.0024	0.0028	0.0125	0.0022	0.0025	0.0125	0.0023	0.0027	0.0125	0.0023	0.0027	0.0125	0.0022	0.0026	0.0125	0.0023	0.0026
2500	0.0126	0.0026	0.0031	0.0126	0.0025	0.0030	0.0125	0.0022	0.0026	0.0125	0.0023	0.0028	0.0125	0.0023	0.0027	0.0127	0.0023	0.0027	0.0125	0.0023	0.0027
learning rate=0.9 and momentum coefficient=0.5																					
500	0.0129	0.0026	0.0029	0.0130	0.0021	0.0025	0.0127	0.0024	0.0027	0.0129	0.0024	0.0027	0.0126	0.0024	0.0027	0.0126	0.0023	0.0027	0.0129	0.0025	0.0028
1000	0.0127	0.0026	0.0030	0.0128	0.0029	0.0035	0.0126	0.0022	0.0026	0.0126	0.0025	0.0029	0.0126	0.0023	0.0027	0.0126	0.0023	0.0027	0.0127	0.0023	0.0027
1500	0.0126	0.0025	0.0029	0.0127	0.0027	0.0032	0.0126	0.0022	0.0026	0.0125	0.0024	0.0028	0.0126	0.0023	0.0027	0.0125	0.0023	0.0027	0.0125	0.0023	0.0026
2000	0.0126	0.0025	0.0029	0.0127	0.0026	0.0031	0.0126	0.0022	0.0026	0.0125	0.0024	0.0028	0.0126	0.0023	0.0027	0.0125	0.0022	0.0027	0.0125	0.0023	0.0026
2500	0.0126	0.0025	0.0030	0.0127	0.0025	0.0030	0.0126	0.0022	0.0026	0.0125	0.0024	0.0028	0.0125	0.0023	0.0027	0.0125	0.0023	0.0027	0.0125	0.0023	0.0027

Table D.3. Variation of parameters of BPA for 80 % of input data for Training (contd.)

learning rate=0.1 and momentum coefficient=0.9																					
Neurons	4			5			6			7			8			9			10		
	Train _E	Val _E	Test _E	Train _E	Val _E	Test _E	Train _E	Val _E	Test _E	Train _E	Val _E	Test _E	Train _E	Val _E	Test _E	Train _E	Val _E	Test _E	Train _E	Val _E	Test _E
500	0.0128	0.0026	0.0030	0.0131	0.0021	0.0025	0.0127	0.0025	0.0029	0.0126	0.0024	0.0029	0.0126	0.0023	0.0027	0.0125	0.0022	0.0026	0.0126	0.0023	0.0027
1000	0.0127	0.0025	0.0029	0.0127	0.0026	0.0031	0.0126	0.0022	0.0026	0.0126	0.0024	0.0029	0.0126	0.0023	0.0027	0.0125	0.0022	0.0026	0.0125	0.0023	0.0027
1500	0.0126	0.0025	0.0030	0.0127	0.0026	0.0031	0.0126	0.0023	0.0026	0.0125	0.0023	0.0027	0.0125	0.0023	0.0027	0.0125	0.0022	0.0026	0.0125	0.0023	0.0026
2000	0.0126	0.0026	0.0030	0.0127	0.0026	0.0030	0.0125	0.0022	0.0025	0.0125	0.0024	0.0028	0.0125	0.0023	0.0027	0.0125	0.0022	0.0027	0.0125	0.0023	0.0027
2500	0.0126	0.0025	0.0030	0.0126	0.0025	0.0030	0.0126	0.0022	0.0026	0.0126	0.0024	0.0029	0.0125	0.0023	0.0027	0.0125	0.0022	0.0026	0.0125	0.0023	0.0027
learning rate=0.5 and momentum coefficient=0.9																					
500	0.0127	0.0025	0.0029	0.0129	0.0028	0.0034	0.0126	0.0023	0.0026	0.0126	0.0024	0.0028	0.0128	0.0023	0.0027	0.0126	0.0023	0.0027	0.0125	0.0023	0.0027
1000	0.0126	0.0026	0.0031	0.0129	0.0028	0.0034	0.2036	0.0050	0.0091	0.0126	0.0024	0.0028	0.0126	0.0024	0.0028	0.0126	0.0023	0.0027	0.0125	0.0023	0.0027
1500	0.0127	0.0026	0.0031	0.0127	0.0027	0.0031	0.0126	0.0022	0.0026	0.0125	0.0024	0.0028	0.0126	0.0023	0.0027	0.0125	0.0022	0.0026	0.0125	0.0023	0.0026
2000	0.0126	0.0025	0.0029	0.0126	0.0024	0.0029	0.0125	0.0022	0.0026	0.0125	0.0023	0.0027	0.0125	0.0023	0.0027	0.0125	0.0022	0.0026	0.0125	0.0023	0.0027
2500	0.0126	0.0025	0.0029	0.0125	0.0023	0.0027	0.0126	0.0022	0.0026	0.0125	0.0023	0.0028	0.0126	0.0023	0.0027	0.0125	0.0022	0.0026	0.0125	0.0023	0.0026
learning rate=0.9 and momentum coefficient=0.9																					
500	0.0127	0.0025	0.0029	0.0131	0.0020	0.0023	0.0126	0.0023	0.0026	0.0130	0.0023	0.0028	0.0127	0.0023	0.0026	0.0126	0.0023	0.0027	0.0127	0.0024	0.0028
1000	0.0126	0.0026	0.0031	0.0128	0.0027	0.0032	0.0126	0.0022	0.0026	0.0126	0.0024	0.0028	0.0128	0.0024	0.0027	0.0125	0.0022	0.0026	0.0125	0.0023	0.0027
1500	0.0126	0.0025	0.0030	0.0127	0.0027	0.0032	0.0125	0.0022	0.0026	0.0126	0.0025	0.0029	0.0126	0.0023	0.0027	0.0125	0.0022	0.0026	0.0125	0.0023	0.0027
2000	0.0125	0.0024	0.0028	0.0126	0.0024	0.0029	0.0126	0.0022	0.0026	0.0125	0.0023	0.0026	0.0126	0.0023	0.0027	0.0125	0.0022	0.0026	0.0125	0.0023	0.0026
2500	0.0126	0.0025	0.0029	0.0127	0.0027	0.0031	0.0125	0.0022	0.0025	0.0125	0.0022	0.0026	0.0125	0.0023	0.0027	0.0125	0.0022	0.0026	0.0126	0.0023	0.0027

Table D.4. Variation of parameters of BPA for 90 % of input data for Training

learning rate=0.1 and momentum coefficient=0.1																					
Neurons	4			5			6			7			8			9			10		
	Train _E	Val _E	Test _E	Train _E	Val _E	Test _E	Train _E	Val _E	Test _E	Train _E	Val _E	Test _E	Train _E	Val _E	Test _E	Train _E	Val _E	Test _E	Train _E	Val _E	Test _E
500	0.0116	0.0032	0.0022	0.0118	0.0028	0.0015	0.0115	0.0029	0.0020	0.0121	0.0032	0.0017	0.0115	0.0027	0.0017	0.0119	0.0026	0.0018	0.0119	0.0035	0.0023
1000	0.0116	0.0033	0.0023	0.0117	0.0035	0.0017	0.0116	0.0029	0.0021	0.0115	0.0033	0.0017	0.0115	0.0031	0.0019	0.0117	0.0031	0.0022	0.0114	0.0026	0.0016
1500	0.0115	0.0034	0.0021	0.0118	0.0037	0.0017	0.0115	0.0030	0.0020	0.0117	0.0033	0.0016	0.0116	0.0030	0.0018	0.0115	0.0029	0.0017	0.0114	0.0030	0.0017
2000	0.0116	0.0032	0.0022	0.0117	0.0036	0.0017	0.0115	0.0029	0.0020	0.0114	0.0030	0.0016	0.0115	0.0030	0.0019	0.0114	0.0030	0.0017	0.0116	0.0029	0.0018
2500	0.0115	0.0032	0.0020	0.0116	0.0035	0.0017	0.0115	0.0030	0.0019	0.0114	0.0032	0.0016	0.0114	0.0030	0.0018	0.0114	0.0030	0.0017	0.0114	0.0030	0.0017
learning rate=0.5 and momentum coefficient=0.1																					
500	0.0117	0.0028	0.0021	0.0119	0.0033	0.0016	0.0115	0.0028	0.0019	0.0118	0.0030	0.0019	0.0114	0.0028	0.0017	0.0114	0.0028	0.0016	0.0115	0.0027	0.0017
1000	0.0116	0.0031	0.0022	0.0119	0.0031	0.0016	0.0115	0.0029	0.0019	0.0115	0.0030	0.0016	0.0115	0.0031	0.0018	0.0115	0.0032	0.0018	0.0116	0.0029	0.0018
1500	0.0116	0.0032	0.0021	0.0118	0.0037	0.0019	0.0114	0.0028	0.0018	0.0117	0.0031	0.0017	0.0114	0.0030	0.0018	0.0114	0.0031	0.0018	0.0115	0.0027	0.0016
2000	0.0115	0.0034	0.0021	0.0118	0.0041	0.0019	0.0114	0.0028	0.0018	0.0114	0.0030	0.0016	0.0114	0.0030	0.0018	0.0114	0.0029	0.0016	0.0114	0.0029	0.0017
2500	0.0115	0.0033	0.0021	0.0116	0.0032	0.0016	0.0114	0.0028	0.0018	0.0115	0.0033	0.0017	0.0114	0.0030	0.0018	0.0114	0.0028	0.0017	0.0116	0.0030	0.0017
learning rate=0.9 and momentum coefficient=0.1																					
500	0.0119	0.0033	0.0025	0.0121	0.0028	0.0016	0.0114	0.0029	0.0018	0.0117	0.0031	0.0018	0.0116	0.0032	0.0021	0.0122	0.0035	0.0026	0.0116	0.0029	0.0018
1000	0.0117	0.0031	0.0022	0.0118	0.0035	0.0017	0.0114	0.0027	0.0017	0.0114	0.0030	0.0016	0.0115	0.0028	0.0017	0.0115	0.0030	0.0018	0.0116	0.0031	0.0018
1500	0.0115	0.0029	0.0019	0.0117	0.0037	0.0018	0.0114	0.0027	0.0017	0.0115	0.0034	0.0018	0.0114	0.0030	0.0018	0.0114	0.0030	0.0017	0.0114	0.0030	0.0017
2000	0.0115	0.0033	0.0021	0.0118	0.0033	0.0017	0.0114	0.0028	0.0018	0.0114	0.0032	0.0016	0.0114	0.0030	0.0018	0.0114	0.0030	0.0017	0.0114	0.0030	0.0017
2500	0.0115	0.0031	0.0020	0.0116	0.0034	0.0017	0.0114	0.0029	0.0018	0.0114	0.0032	0.0016	0.0114	0.0030	0.0018	0.0114	0.0031	0.0017	0.0114	0.0030	0.0017
learning rate=0.1 and momentum coefficient=0.5																					
500	0.0116	0.0036	0.0020	0.0118	0.0033	0.0016	0.0116	0.0030	0.0021	0.0117	0.0029	0.0017	0.0115	0.0030	0.0019	0.0114	0.0031	0.0017	0.0114	0.0030	0.0017
1000	0.0115	0.0033	0.0020	0.0117	0.0039	0.0019	0.0116	0.0030	0.0020	0.0114	0.0033	0.0016	0.0116	0.0030	0.0018	0.0114	0.0031	0.0018	0.0114	0.0030	0.0017
1500	0.0115	0.0033	0.0020	0.0115	0.0034	0.0017	0.0114	0.0028	0.0018	0.0114	0.0033	0.0016	0.0114	0.0030	0.0018	0.0114	0.0031	0.0017	0.0114	0.0030	0.0017
2000	0.0114	0.0032	0.0018	0.0115	0.0035	0.0017	0.0114	0.0028	0.0018	0.0114	0.0031	0.0016	0.0114	0.0029	0.0018	0.0115	0.0030	0.0017	0.0114	0.0030	0.0018
2500	0.0115	0.0034	0.0020	0.0116	0.0036	0.0018	0.0114	0.0029	0.0018	0.0114	0.0031	0.0016	0.0114	0.0030	0.0018	0.0114	0.0030	0.0017	0.0114	0.0030	0.0017
learning rate=0.5 and momentum coefficient=0.5																					
500	0.0116	0.0033	0.0022	0.0119	0.0029	0.0016	0.0115	0.0030	0.0020	0.0116	0.0033	0.0017	0.0115	0.0033	0.0019	0.0116	0.0031	0.0018	0.0115	0.0030	0.0017
1000	0.0115	0.0031	0.0020	0.0118	0.0036	0.0017	0.0114	0.0029	0.0018	0.0114	0.0031	0.0016	0.0115	0.0030	0.0019	0.0114	0.0030	0.0017	0.0114	0.0030	0.0017
1500	0.0115	0.0032	0.0021	0.0116	0.0036	0.0018	0.0114	0.0029	0.0018	0.0114	0.0033	0.0017	0.0114	0.0030	0.0018	0.0114	0.0030	0.0017	0.0114	0.0030	0.0017
2000	0.0115	0.0032	0.0019	0.0116	0.0035	0.0017	0.0114	0.0028	0.0018	0.0114	0.0032	0.0016	0.0115	0.0030	0.0018	0.0114	0.0030	0.0017	0.0114	0.0030	0.0017
2500	0.0115	0.0032	0.0020	0.0115	0.0033	0.0017	0.0114	0.0028	0.0018	0.0114	0.0031	0.0016	0.0114	0.0030	0.0018	0.0114	0.0031	0.0017	0.0114	0.0030	0.0017
learning rate=0.9 and momentum coefficient=0.5																					
500	0.0115	0.0033	0.0021	0.0122	0.0024	0.0017	0.0115	0.0031	0.0021	0.0115	0.0033	0.0016	0.0115	0.0032	0.0020	0.0122	0.0035	0.0026	0.0118	0.0036	0.0023
1000	0.0116	0.0034	0.0021	0.0117	0.0037	0.0017	0.0114	0.0029	0.0018	0.0115	0.0033	0.0017	0.0114	0.0030	0.0018	0.0115	0.0030	0.0018	0.0114	0.0030	0.0017
1500	0.0115	0.0032	0.0020	0.0117	0.0037	0.0017	0.0114	0.0029	0.0018	0.0114	0.0031	0.0016	0.0115	0.0030	0.0020	0.0114	0.0030	0.0017	0.0114	0.0030	0.0017
2000	0.0115	0.0032	0.0020	0.0116	0.0037	0.0018	0.0114	0.0029	0.0018	0.0114	0.0031	0.0016	0.0114	0.0030	0.0018	0.0114	0.0030	0.0017	0.0114	0.0030	0.0017
2500	0.0115	0.0034	0.0020	0.0115	0.0034	0.0017	0.0114	0.0029	0.0018	0.0114	0.0032	0.0017	0.0114	0.0030	0.0018	0.0114	0.0031	0.0017	0.0114	0.0030	0.0017

Table D.5. Variation of parameters of BPA for 90 % of input data for Training (contd.)

learning rate=0.1 and momentum coefficient=0.9																					
Neurons	4			5			6			7			8			9			10		
	Train _E	Val _E	Test _E	Train _E	Val _E	Test _E	Train _E	Val _E	Test _E	Train _E	Val _E	Test _E	Train _E	Val _E	Test _E	Train _E	Val _E	Test _E	Train _E	Val _E	Test _E
500	0.0115	0.0034	0.0020	0.0117	0.0035	0.0017	0.0115	0.0030	0.0019	0.0115	0.0033	0.0017	0.0115	0.0030	0.0018	0.0114	0.0030	0.0016	0.0115	0.0031	0.0018
1000	0.0116	0.0034	0.0021	0.0116	0.0036	0.0017	0.0115	0.0030	0.0019	0.0114	0.0033	0.0017	0.0114	0.0030	0.0018	0.0114	0.0030	0.0017	0.0115	0.0030	0.0017
1500	0.0115	0.0034	0.0020	0.0116	0.0036	0.0018	0.0114	0.0028	0.0018	0.0114	0.0033	0.0017	0.0114	0.0030	0.0018	0.0114	0.0030	0.0017	0.0114	0.0030	0.0017
2000	0.0115	0.0033	0.0020	0.0114	0.0030	0.0017	0.0114	0.0028	0.0018	0.0114	0.0033	0.0017	0.0114	0.0030	0.0018	0.0113	0.0029	0.0016	0.0114	0.0030	0.0017
2500	0.0115	0.0033	0.0019	0.0115	0.0034	0.0017	0.0114	0.0029	0.0018	0.0113	0.0030	0.0016	0.0114	0.0030	0.0018	0.0113	0.0030	0.0017	0.0114	0.0030	0.0017
learning rate=0.5 and momentum coefficient=0.9																					
500	0.0115	0.0032	0.0020	0.0118	0.0039	0.0018	0.0119	0.0042	0.0025	0.0116	0.0034	0.0017	0.0115	0.0030	0.0017	0.0116	0.0031	0.0018	0.0115	0.0033	0.0019
1000	0.0115	0.0031	0.0021	0.0115	0.0034	0.0017	0.0115	0.0030	0.0019	0.0114	0.0033	0.0017	0.0114	0.0030	0.0018	0.0114	0.0030	0.0017	0.0114	0.0030	0.0017
1500	0.0115	0.0034	0.0020	0.0115	0.0034	0.0017	0.0114	0.0028	0.0018	0.0114	0.0031	0.0016	0.0114	0.0030	0.0018	0.0114	0.0030	0.0017	0.0114	0.0030	0.0017
2000	0.0115	0.0033	0.0020	0.0114	0.0032	0.0017	0.0114	0.0028	0.0018	0.0114	0.0033	0.0017	0.0114	0.0030	0.0018	0.0114	0.0030	0.0017	0.0115	0.0032	0.0019
2500	0.0115	0.0033	0.0019	0.0115	0.0035	0.0018	0.0114	0.0028	0.0018	0.0114	0.0031	0.0016	0.0115	0.0030	0.0019	0.0114	0.0031	0.0017	0.0114	0.0030	0.0017
learning rate=0.9 and momentum coefficient=0.9																					
500	0.0115	0.0030	0.0020	0.0117	0.0032	0.0016	0.0115	0.0030	0.0020	0.0115	0.0032	0.0017	0.0115	0.0030	0.0019	0.0115	0.0034	0.0018	0.0114	0.0030	0.0017
1000	0.0115	0.0034	0.0020	0.0116	0.0031	0.0016	0.0115	0.0029	0.0019	0.0114	0.0032	0.0017	0.0114	0.0030	0.0018	0.0114	0.0029	0.0017	0.0114	0.0030	0.0017
1500	0.0116	0.0034	0.0021	0.0116	0.0035	0.0018	0.0114	0.0028	0.0018	0.0114	0.0033	0.0017	0.0114	0.0030	0.0018	0.0114	0.0030	0.0016	0.0114	0.0030	0.0017
2000	0.0114	0.0033	0.0019	0.0115	0.0033	0.0017	0.0114	0.0028	0.0018	0.0113	0.0030	0.0016	0.0114	0.0030	0.0018	0.0114	0.0030	0.0017	0.0114	0.0030	0.0017
2500	0.0114	0.0032	0.0018	0.0115	0.0032	0.0017	0.0114	0.0028	0.0018	0.0113	0.0030	0.0016	0.0114	0.0030	0.0018	0.0113	0.0029	0.0017	0.0114	0.0030	0.0017

Table D.6. Variation of parameters of GA for 80 % of input data for Training

Elite count=0.1, cross over fraction=0.7																					
Neurons	4			5			6			7			8			9			10		
	Train _E	Val _E	Test _E	Train _E	Val _E	Test _E	Train _E	Val _E	Test _E	Train _E	Val _E	Test _E	Train _E	Val _E	Test _E	Train _E	Val _E	Test _E	Train _E	Val _E	Test _E
100	0.0125	0.0024	0.0029	0.0129	0.0034	0.0041	0.0131	0.0027	0.0033	0.0126	0.0023	0.0027	0.0137	0.0028	0.0033	0.0174	0.0053	0.0071	0.0144	0.0036	0.0044
200	0.0127	0.0023	0.0028	0.0125	0.0020	0.0023	0.0127	0.0021	0.0024	0.0134	0.0028	0.0033	0.0126	0.0019	0.0022	0.0128	0.0025	0.0029	0.0132	0.0024	0.0028
300	0.0125	0.0021	0.0024	0.0127	0.0022	0.0025	0.0126	0.0024	0.0028	0.0125	0.0026	0.0031	0.0126	0.0022	0.0025	0.0127	0.0021	0.0024	0.0126	0.0024	0.0028
400	0.0125	0.0021	0.0024	0.0126	0.0026	0.0030	0.0127	0.0021	0.0024	0.0126	0.0022	0.0025	0.0127	0.0022	0.0026	0.0125	0.0022	0.0026	0.0125	0.0023	0.0027
500	0.0127	0.0027	0.0033	0.0126	0.0020	0.0023	0.0132	0.0034	0.0039	0.0129	0.0028	0.0032	0.0125	0.0024	0.0028	0.0128	0.0024	0.0028	0.0125	0.0021	0.0025
Elite count=0.15, cross over fraction=0.7																					
100	0.0126	0.0020	0.0023	0.0135	0.0047	0.0058	0.0126	0.0021	0.0024	0.0129	0.0029	0.0036	0.0132	0.0021	0.0025	0.0126	0.0019	0.0022	0.0127	0.0020	0.0023
200	0.0126	0.0022	0.0026	0.0127	0.0025	0.0029	0.0126	0.0020	0.0023	0.0127	0.0023	0.0028	0.0127	0.0018	0.0021	0.0127	0.0026	0.0032	0.0126	0.0023	0.0026
300	0.0126	0.0022	0.0026	0.0126	0.0021	0.0025	0.0125	0.0026	0.0031	0.0136	0.0034	0.0039	0.0128	0.0021	0.0025	0.0125	0.0023	0.0027	0.0126	0.0021	0.0024
400	0.0135	0.0018	0.0023	0.0125	0.0022	0.0026	0.0127	0.0022	0.0026	0.0130	0.0016	0.0020	0.0125	0.0023	0.0027	0.0125	0.0027	0.0032	0.0133	0.0022	0.0027
500	0.0126	0.0022	0.0025	0.0126	0.0023	0.0027	0.0135	0.0036	0.0045	0.0125	0.0022	0.0025	0.0127	0.0023	0.0027	0.0127	0.0025	0.0030	0.0139	0.0040	0.0048
Elite count=0.20, cross over fraction=0.7																					
500	0.0127	0.0021	0.0025	0.0126	0.0022	0.0026	0.0126	0.0025	0.0030	0.0140	0.0018	0.0021	0.0137	0.0032	0.0039	0.0132	0.0030	0.0035	0.0126	0.0019	0.0021
1000	0.0126	0.0020	0.0023	0.0127	0.0023	0.0027	0.0127	0.0024	0.0029	0.0131	0.0024	0.0028	0.0127	0.0025	0.0029	0.0128	0.0031	0.0037	0.0127	0.0021	0.0025
1500	0.0141	0.0033	0.0039	0.0126	0.0022	0.0026	0.0127	0.0028	0.0034	0.0125	0.0021	0.0024	0.0127	0.0022	0.0025	0.0126	0.0023	0.0027	0.0126	0.0019	0.0023
2000	0.0127	0.0022	0.0026	0.0129	0.0023	0.0027	0.0127	0.0022	0.0026	0.0127	0.0020	0.0023	0.0142	0.0027	0.0032	0.0134	0.0037	0.0044	0.0126	0.0022	0.0025
2500	0.0126	0.0028	0.0033	0.0128	0.0030	0.0035	0.0126	0.0022	0.0026	0.0131	0.0024	0.0028	0.0127	0.0021	0.0024	0.0126	0.0021	0.0024	0.0126	0.0024	0.0028
Elite count=0.10, cross over fraction=0.8																					
500	0.0128	0.0023	0.0027	0.0126	0.0027	0.0032	0.0131	0.0027	0.0032	0.0125	0.0022	0.0026	0.0135	0.0044	0.0054	0.0131	0.0029	0.0035	0.0127	0.0020	0.0023
1000	0.0125	0.0021	0.0024	0.0129	0.0019	0.0022	0.0128	0.0026	0.0030	0.0125	0.0022	0.0026	0.0126	0.0021	0.0024	0.0132	0.0022	0.0026	0.0126	0.0023	0.0026
1500	0.0126	0.0022	0.0025	0.0132	0.0025	0.0029	0.0130	0.0023	0.0028	0.0132	0.0024	0.0029	0.0127	0.0029	0.0034	0.0125	0.0021	0.0025	0.0126	0.0021	0.0024
2000	0.0134	0.0022	0.0023	0.0132	0.0023	0.0028	0.0127	0.0022	0.0025	0.0125	0.0024	0.0028	0.0127	0.0024	0.0028	0.0127	0.0019	0.0021	0.0133	0.0022	0.0027
2500	0.0127	0.0020	0.0023	0.0128	0.0021	0.0025	0.0126	0.0021	0.0025	0.0140	0.0026	0.0035	0.0127	0.0024	0.0028	0.0134	0.0029	0.0035	0.0139	0.0040	0.0048
Elite count=0.15, cross over fraction=0.8																					
500	0.0127	0.0024	0.0028	0.0127	0.0022	0.0025	0.0125	0.0023	0.0026	0.0126	0.0026	0.0030	0.0126	0.0021	0.0024	0.0133	0.0024	0.0029	0.0131	0.0036	0.0045
1000	0.0128	0.0023	0.0027	0.0127	0.0018	0.0020	0.0126	0.0021	0.0025	0.0126	0.0020	0.0024	0.0130	0.0028	0.0033	0.0126	0.0022	0.0026	0.0136	0.0018	0.0021
1500	0.0127	0.0021	0.0025	0.0127	0.0025	0.0029	0.0128	0.0026	0.0031	0.0131	0.0030	0.0036	0.0129	0.0025	0.0029	0.0125	0.0027	0.0033	0.0144	0.0041	0.0052
2000	0.0127	0.0031	0.0038	0.0128	0.0022	0.0026	0.0128	0.0026	0.0031	0.0129	0.0029	0.0033	0.0129	0.0028	0.0034	0.0125	0.0021	0.0025	0.0127	0.0022	0.0025
2500	0.0129	0.0025	0.0030	0.0128	0.0026	0.0031	0.0133	0.0040	0.0047	0.0142	0.0024	0.0028	0.0127	0.0023	0.0027	0.0126	0.0023	0.0027	0.0126	0.0022	0.0026
Elite count=0.20, cross over fraction=0.8																					
500	0.0137	0.0025	0.0029	0.0126	0.0017	0.0020	0.0136	0.0033	0.0040	0.0126	0.0026	0.0031	0.0128	0.0020	0.0023	0.0126	0.0023	0.0027	0.0130	0.0029	0.0035
1000	0.0126	0.0025	0.0029	0.0131	0.0036	0.0043	0.0126	0.0027	0.0032	0.0125	0.0023	0.0028	0.0126	0.0020	0.0023	0.0133	0.0022	0.0027	0.0133	0.0030	0.0035
1500	0.0129	0.0018	0.0021	0.0127	0.0021	0.0025	0.0125	0.0023	0.0027	0.0131	0.0021	0.0025	0.0126	0.0024	0.0028	0.0153	0.0031	0.0041	0.0138	0.0025	0.0031
2000	0.0125	0.0022	0.0026	0.0142	0.0040	0.0046	0.0126	0.0027	0.0032	0.0128	0.0027	0.0032	0.0125	0.0022	0.0026	0.0125	0.0023	0.0027	0.0142	0.0035	0.0040
2500	0.0129	0.0019	0.0022	0.0126	0.0027	0.0031	0.0130	0.0025	0.0029	0.0127	0.0021	0.0024	0.0129	0.0022	0.0026	0.0127	0.0022	0.0025	0.0133	0.0030	0.0035

Table D.7. Variation of parameters of GA for 80 % of input data for Training (contd..)

Elite count=0.10, cross over fraction=0.9																					
Neurons	4			5			6			7			8			9			10		
	Train _E	Val _E	Test _E	Train _E	Val _E	Test _E	Train _E	Val _E	Test _E	Train _E	Val _E	Test _E	Train _E	Val _E	Test _E	Train _E	Val _E	Test _E	Train _E	Val _E	Test _E
500	0.0131	0.0024	0.0028	0.0128	0.0018	0.0021	0.0131	0.0023	0.0026	0.0127	0.0021	0.0025	0.0131	0.0019	0.0023	0.0125	0.0021	0.0025	0.0134	0.0029	0.0035
1000	0.0130	0.0025	0.0029	0.0127	0.0023	0.0028	0.0129	0.0020	0.0024	0.0126	0.0022	0.0026	0.0126	0.0023	0.0027	0.0133	0.0028	0.0034	0.0126	0.0020	0.0024
1500	0.0127	0.0021	0.0025	0.0128	0.0020	0.0023	0.0125	0.0025	0.0029	0.0125	0.0021	0.0024	0.0125	0.0022	0.0025	0.0126	0.0021	0.0025	0.0126	0.0023	0.0027
2000	0.0130	0.0024	0.0029	0.0128	0.0022	0.0025	0.0126	0.0022	0.0026	0.0130	0.0026	0.0031	0.0131	0.0027	0.0033	0.0129	0.0018	0.0021	0.0126	0.0026	0.0031
2500	0.0131	0.0026	0.0031	0.0126	0.0021	0.0025	0.0127	0.0021	0.0025	0.0125	0.0023	0.0027	0.0132	0.0022	0.0025	0.0127	0.0021	0.0024	0.0130	0.0025	0.0029
Elite count=0.15, cross over fraction=0.9																					
500	0.0133	0.0020	0.0024	0.0125	0.0020	0.0023	0.0128	0.0020	0.0023	0.0138	0.0041	0.0049	0.0131	0.0031	0.0038	0.0128	0.0020	0.0024	0.0134	0.0026	0.0031
1000	0.0128	0.0021	0.0025	0.0127	0.0021	0.0025	0.0127	0.0023	0.0027	0.0126	0.0024	0.0028	0.0130	0.0019	0.0022	0.0127	0.0022	0.0025	0.0127	0.0021	0.0025
1500	0.0130	0.0023	0.0027	0.0125	0.0020	0.0024	0.0125	0.0021	0.0024	0.0127	0.0024	0.0028	0.0127	0.0022	0.0026	0.0128	0.0023	0.0027	0.0127	0.0022	0.0025
2000	0.0128	0.0032	0.0038	0.0128	0.0026	0.0031	0.0130	0.0022	0.0026	0.0126	0.0025	0.0029	0.0145	0.0028	0.0034	0.0128	0.0021	0.0025	0.0133	0.0019	0.0022
2500	0.0134	0.0022	0.0026	0.0126	0.0024	0.0028	0.0127	0.0021	0.0025	0.0125	0.0021	0.0024	0.0132	0.0025	0.0030	0.0127	0.0023	0.0027	0.0131	0.0019	0.0022
Elite count=0.20, cross over fraction=0.9																					
500	0.0126	0.0022	0.0025	0.0126	0.0021	0.0024	0.0128	0.0026	0.0030	0.0131	0.0019	0.0022	0.0134	0.0026	0.0030	0.0130	0.0022	0.0026	0.0128	0.0022	0.0024
1000	0.0131	0.0023	0.0027	0.0131	0.0029	0.0034	0.0126	0.0021	0.0024	0.0126	0.0019	0.0021	0.0130	0.0027	0.0033	0.0127	0.0025	0.0030	0.0125	0.0022	0.0026
1500	0.01336	0.00127	0.00166	0.0131	0.0032	0.0039	0.0128	0.0029	0.0035	0.0125	0.0022	0.0026	0.0127	0.0024	0.0028	0.0129	0.0019	0.0022	0.0127	0.0021	0.0024
2000	0.0129	0.0020	0.0023	0.0125	0.0022	0.0025	0.0129	0.0030	0.0036	0.0129	0.0025	0.0029	0.0129	0.0016	0.0019	0.0127	0.0024	0.0028	0.0126	0.0020	0.0023
2500	0.0128	0.0025	0.0029	0.0126	0.0024	0.0028	0.0129	0.0026	0.0031	0.0127	0.0020	0.0024	0.0132	0.0017	0.0020	0.0125	0.0022	0.0025	0.0125	0.0022	0.0026

Table D.8. Variation of parameters of GA for 90 % of input data for Training

Elite count=0.10, cross over fraction=0.7																					
Neurons	4			5			6			7			8			9			10		
	Train _E	Val _E	Test _E	Train _E	Val _E	Test _E	Train _E	Val _E	Test _E	Train _E	Val _E	Test _E	Train _E	Val _E	Test _E	Train _E	Val _E	Test _E	Train _E	Val _E	Test _E
100	0.0114	0.0032	0.0017	0.0116	0.0021	0.0015	0.0114	0.0029	0.0016	0.0120	0.0033	0.0022	0.0118	0.0023	0.0018	0.0123	0.0031	0.0017	0.0117	0.0039	0.0019
200	0.0116	0.0027	0.0018	0.0123	0.0038	0.0024	0.0114	0.0032	0.0017	0.0114	0.0027	0.0017	0.0115	0.0026	0.0017	0.0119	0.0038	0.0023	0.0128	0.0041	0.0019
300	0.0116	0.0030	0.0016	0.0115	0.0029	0.0015	0.0114	0.0024	0.0014	0.0117	0.0032	0.0021	0.0115	0.0028	0.0017	0.0117	0.0034	0.0023	0.0117	0.0037	0.0022
400	0.0115	0.0036	0.0018	0.0113	0.0027	0.0016	0.0115	0.0026	0.0015	0.0114	0.0029	0.0017	0.0114	0.0028	0.0016	0.0118	0.0030	0.0021	0.0116	0.0038	0.0019
500	0.0114	0.0034	0.0017	0.0117	0.0031	0.0019	0.0114	0.0024	0.0015	0.0131	0.0049	0.0027	0.0115	0.0028	0.0017	0.0117	0.0032	0.0020	0.0123	0.0026	0.0021
Elite count=0.15, cross over fraction=0.7																					
100	0.0116	0.0031	0.0020	0.0116	0.0025	0.0016	0.0122	0.0054	0.0027	0.0122	0.0030	0.0023	0.0118	0.0028	0.0018	0.0121	0.0047	0.0023	0.0116	0.0040	0.0022
200	0.0117	0.0030	0.0019	0.0117	0.0033	0.0019	0.0117	0.0039	0.0022	0.0123	0.0059	0.0029	0.0115	0.0034	0.0017	0.0119	0.0040	0.0024	0.0114	0.0034	0.0017
300	0.0116	0.0025	0.0018	0.0123	0.0042	0.0021	0.0115	0.0029	0.0018	0.0114	0.0033	0.0018	0.0115	0.0027	0.0016	0.0114	0.0032	0.0017	0.0117	0.0040	0.0021
400	0.0114	0.0025	0.0015	0.0115	0.0028	0.0016	0.0116	0.0030	0.0020	0.0124	0.0040	0.0024	0.0121	0.0037	0.0018	0.0114	0.0031	0.0017	0.0131	0.0042	0.0026
500	0.0117	0.0020	0.0015	0.0121	0.0034	0.0019	0.0114	0.0026	0.0015	0.0125	0.0037	0.0025	0.0131	0.0053	0.0030	0.0117	0.0036	0.0021	0.0119	0.0039	0.0025
Elite count=0.20, cross over fraction=0.7																					
100	0.0124	0.0055	0.0032	0.0119	0.0036	0.0023	0.0119	0.0050	0.0023	0.0117	0.0025	0.0017	0.0117	0.0028	0.0019	0.0114	0.0031	0.0018	0.0122	0.0027	0.0022
200	0.0117	0.0029	0.0021	0.0125	0.0036	0.0026	0.0120	0.0038	0.0020	0.0115	0.0030	0.0016	0.0115	0.0029	0.0018	0.0114	0.0026	0.0017	0.0114	0.0028	0.0015
300	0.0114	0.0029	0.0016	0.0114	0.0032	0.0017	0.0114	0.0034	0.0018	0.0142	0.0034	0.0029	0.0115	0.0035	0.0018	0.0114	0.0025	0.0016	0.0115	0.0026	0.0016
400	0.0117	0.0030	0.0020	0.0114	0.0028	0.0017	0.0114	0.0032	0.0017	0.0155	0.0041	0.0031	0.0118	0.0031	0.0015	0.0114	0.0024	0.0016	0.0115	0.0030	0.0017
500	0.0116	0.0026	0.0015	0.0121	0.0037	0.0017	0.0117	0.0030	0.0021	0.0115	0.0035	0.0018	0.0118	0.0031	0.0015	0.0127	0.0044	0.0029	0.0114	0.0030	0.0016
Elite count=0.10, cross over fraction=0.8																					
100	0.0126	0.0032	0.0020	0.0115	0.0029	0.0017	0.0114	0.0028	0.0016	0.0114	0.0028	0.0016	0.0124	0.0035	0.0027	0.0117	0.0035	0.0024	0.0114	0.0028	0.0016
200	0.0114	0.0032	0.0016	0.0113	0.0031	0.0016	0.0114	0.0029	0.0018	0.0117	0.0029	0.0020	0.0115	0.0028	0.0017	0.0114	0.0032	0.0018	0.0113	0.0029	0.0017
300	0.0113	0.0028	0.0016	0.0114	0.0032	0.0018	0.0126	0.0040	0.0025	0.0115	0.0031	0.0018	0.0115	0.0030	0.0016	0.0117	0.0028	0.0018	0.0118	0.0029	0.0018
400	0.0114	0.0027	0.0016	0.0119	0.0038	0.0021	0.0116	0.0043	0.0022	0.0114	0.0029	0.0019	0.0117	0.0041	0.0023	0.0125	0.0050	0.0033	0.0114	0.0030	0.0017
500	0.0113	0.0029	0.0016	0.0114	0.0027	0.0016	0.0116	0.0022	0.0014	0.0115	0.0030	0.0016	0.0114	0.0031	0.0017	0.0114	0.0026	0.0014	0.0114	0.0036	0.0017
Elite count=0.15, cross over fraction=0.8																					
100	0.0116	0.0027	0.0018	0.0114	0.0031	0.0018	0.0115	0.0036	0.0020	0.0119	0.0048	0.0025	0.0117	0.0025	0.0017	0.0114	0.0026	0.0015	0.0124	0.0036	0.0023
200	0.0114	0.0027	0.0016	0.0119	0.0036	0.0022	0.0113	0.0028	0.0016	0.0115	0.0030	0.0017	0.0115	0.0030	0.0019	0.0115	0.0036	0.0017	0.0115	0.0025	0.0016
300	0.0116	0.0035	0.0020	0.0114	0.0028	0.0018	0.0140	0.0046	0.0024	0.0119	0.0027	0.0024	0.0117	0.0025	0.0017	0.0113	0.0028	0.0016	0.0113	0.0027	0.0015
400	0.0114	0.0033	0.0016	0.0121	0.0035	0.0026	0.0114	0.0032	0.0017	0.0116	0.0030	0.0017	0.0115	0.0027	0.0015	0.0114	0.0031	0.0017	0.0119	0.0040	0.0018
500	0.0115	0.0023	0.0017	0.0114	0.0030	0.0017	0.0115	0.0024	0.0015	0.0121	0.0045	0.0026	0.0119	0.0027	0.0018	0.0114	0.0036	0.0019	0.0113	0.0029	0.0016
Elite count=0.20, cross over fraction=0.8																					
100	0.0122	0.0032	0.0017	0.0115	0.0027	0.0016	0.0116	0.0025	0.0017	0.0114	0.0027	0.0017	0.0120	0.0048	0.0026	0.0116	0.0028	0.0016	0.0117	0.0036	0.0024
200	0.0118	0.0036	0.0020	0.0123	0.0040	0.0022	0.0113	0.0027	0.0016	0.0114	0.0027	0.0017	0.0114	0.0033	0.0018	0.0114	0.0031	0.0017	0.0118	0.0036	0.0018
300	0.0120	0.0040	0.0026	0.0114	0.0029	0.0015	0.0121	0.0035	0.0018	0.0117	0.0027	0.0018	0.0116	0.0035	0.0022	0.0114	0.0028	0.0017	0.0115	0.0027	0.0017
400	0.0114	0.0031	0.0017	0.0115	0.0039	0.0018	0.0114	0.0025	0.0015	0.0119	0.0042	0.0023	0.0116	0.0031	0.0019	0.0116	0.0028	0.0015	0.0114	0.0029	0.0016
500	0.0114	0.0029	0.0017	0.0120	0.0036	0.0022	0.0118	0.0036	0.0018	0.0121	0.0032	0.0025	0.0118	0.0029	0.0020	0.0114	0.0035	0.0019	0.0121	0.0028	0.0023

Table D.9. Variation of parameters of GA for 90 % of input data for Training (contd..)

Elite count=0.10, cross over fraction=0.9																					
Neurons	4			5			6			7			8			9			10		
	Train _E	Val _E	Test _E	Train _E	Val _E	Test _E	Train _E	Val _E	Test _E	Train _E	Val _E	Test _E	Train _E	Val _E	Test _E	Train _E	Val _E	Test _E	Train _E	Val _E	Test _E
100	0.0118	0.0033	0.0022	0.0113	0.0028	0.0016	0.0115	0.0035	0.0019	0.0120	0.0033	0.0023	0.0115	0.0034	0.0019	0.0117	0.0034	0.0021	0.0115	0.0027	0.0015
200	0.0114	0.0031	0.0016	0.0117	0.0030	0.0019	0.0115	0.0026	0.0016	0.0116	0.0033	0.0021	0.0119	0.0026	0.0018	0.0118	0.0036	0.0022	0.0118	0.0029	0.0018
300	0.0127	0.0037	0.0030	0.0114	0.0032	0.0018	0.0115	0.0029	0.0016	0.0113	0.0029	0.0016	0.0118	0.0035	0.0018	0.0114	0.0028	0.0016	0.0123	0.0057	0.0028
400	0.0114	0.0043	0.0021	0.0118	0.0031	0.0020	0.0115	0.0030	0.0019	0.0115	0.0032	0.0018	0.0114	0.0035	0.0018	0.0119	0.0026	0.0015	0.0116	0.0039	0.0023
500	0.0114	0.0025	0.0015	0.0115	0.0035	0.0021	0.0115	0.0035	0.0019	0.0117	0.0031	0.0016	0.0115	0.0025	0.0017	0.0120	0.0023	0.0017	0.0115	0.0029	0.0017
Elite count=0.15, cross over fraction=0.9																					
100	0.0114	0.0029	0.0017	0.0119	0.0036	0.0023	0.0116	0.0039	0.0021	0.0117	0.0030	0.0019	0.0113	0.0029	0.0016	0.0119	0.0037	0.0020	0.0119	0.0031	0.0020
200	0.0113	0.0030	0.0016	0.0125	0.0036	0.0026	0.0115	0.0033	0.0018	0.0114	0.0030	0.0017	0.0116	0.0027	0.0017	0.0115	0.0031	0.0017	0.0119	0.0033	0.0019
300	0.0119	0.0025	0.0022	0.0114	0.0032	0.0017	0.0114	0.0032	0.0017	0.0114	0.0032	0.0017	0.0115	0.0032	0.0018	0.0114	0.0027	0.0016	0.0114	0.0027	0.0015
400	0.01203	0.00185	0.00132	0.0114	0.0028	0.0017	0.0114	0.0026	0.0015	0.0114	0.0029	0.0016	0.0115	0.0033	0.0020	0.0114	0.0029	0.0017	0.0121	0.0025	0.0018
500	0.0114	0.0027	0.0017	0.0121	0.0037	0.0017	0.0121	0.0027	0.0019	0.0115	0.0033	0.0019	0.0114	0.0027	0.0016	0.0117	0.0030	0.0021	0.0114	0.0032	0.0018
Elite count=0.20, cross over fraction=0.9																					
100	0.0122	0.0042	0.0028	0.0115	0.0025	0.0017	0.0134	0.0053	0.0023	0.0114	0.0023	0.0015	0.0117	0.0023	0.0020	0.0125	0.0047	0.0027	0.0114	0.0025	0.0015
200	0.0118	0.0023	0.0017	0.0118	0.0040	0.0021	0.0119	0.0033	0.0017	0.0118	0.0047	0.0027	0.0114	0.0029	0.0016	0.0115	0.0024	0.0016	0.0115	0.0032	0.0017
300	0.0120	0.0028	0.0023	0.0118	0.0033	0.0020	0.0115	0.0029	0.0018	0.0117	0.0031	0.0017	0.0120	0.0030	0.0020	0.0117	0.0026	0.0018	0.0117	0.0025	0.0015
400	0.0117	0.0031	0.0016	0.0116	0.0031	0.0017	0.0114	0.0031	0.0018	0.0136	0.0039	0.0030	0.0122	0.0026	0.0018	0.0116	0.0028	0.0017	0.0114	0.0024	0.0015
500	0.0117	0.0033	0.0020	0.0132	0.0037	0.0032	0.0114	0.0028	0.0016	0.0120	0.0047	0.0024	0.0132	0.0031	0.0017	0.0114	0.0030	0.0016	0.0126	0.0037	0.0018

Bibliography

- [1] A. Estanqueiro, “A dynamic wind generation model for power systems studies,” *IEEE Transactions on Power Systems*, vol. 22, no. 3, pp. 920–928, 2007.
- [2] J. F. Manwell, *Wind Energy Explained Theory, Design and Application*. John Wiley & sons, 2002.
- [3] S. N. Bhadra, D. Kastha, and S. Banerjee, *Wind Electrical Systems*. Oxford University Press, 2005.
- [4] International Electrotechnical Commission, *International Standard IEC 61400-1*, Third edition ed., 2005-08.
- [5] N. Ullah and T. Thiringer, “Variable speed wind turbines for power system stability enhancement,” *IEEE Transactions on Energy Conversion*, vol. 22, pp. 52–60, March 2007.
- [6] M. Bahramipanah, S. Afsharnia, and Z. Shahoei, “A survey on the effect of different kinds of wind turbines on power system stability,” in *1st International Nuclear Renewable Energy Conference (INREC)*, pp. 1–6, March 2010.
- [7] “Global Wind Energy Council.” <http://www.gwec.net/>.
- [8] “Central Electricity Authority.” <http://www.cea.nic.in/>.
- [9] “Indian Wind Turbine Manufacturers Association.” <http://www.indianwindpower.com/>.
- [10] “Ministry of New and Renewable Energy.” <http://www.mnre.gov.in/>.
- [11] “National Institute of Wind Energy.” <http://niwe.res.in/>.

- [12] Y. Coughlan, P. Smith, A. Mullana, and M. O. Malley, "Wind turbine modeling for power system stability analysis- A system operator perspective," *IEEE Transactions on Power Systems*, vol. 22, no. 3, pp. 929–936, 2007.
- [13] S. Panda and N.P.Padhy, "Investigating the impact of wind speed on active and reactive power penetration to the distribution network," *International Journal of Electrical Systems Science and Engineering*, vol. 2, no. 10, pp. 171–177, 2008.
- [14] N. T. Linh, "Power quality investigation of grid connected wind turbines," in *4th IEEE Conference on Industrial Electronics and Applications (ICIEA)*, pp. 2218–2222, May 2009.
- [15] R. Melicio, V. Mendes, and J. Catalao, "Transient analysis of variable-speed wind turbines at wind speed disturbances and a pitch control malfunction," *Applied Energy*, vol. 88, no. 4, pp. 1322 – 1330, 2011.
- [16] M. Mabel and E.Fernandez, "Growth and Future trends of Wind Energy in India," *Renewable and Sustainable Energy Reviews*, vol. 12, no. 6, pp. 1745–1757, 2008.
- [17] I. Purohit and P. Purohit, "Wind Energy in India: Status and Future Prospects," *Journal of Renewable and Sustainable Energy*, vol. 1, pp. 42701–42719, 2009.
- [18] V.Vanitha and N.Devarajan, "Effect of wind speed changes on grid power quality at various levels of wind electric penetration -A laboratory investigation," *International Journal of Recent Trends in Engineering (IJRTE)*, vol. 1, pp. 8–13, May 2009.
- [19] K.Ulgen and A.Hepbasli, "Determination of Weibull parameters for wind energy analysis of Izmir, Turkey," *International Journal of Energy Research*, vol. 26, no. 6, pp. 495–506, 2002.
- [20] I.Youm, J.Sarr, M.Sall, A.Ndiaye, and M.M.Kane, "Analysis of wind data and wind energy potential along the northern coast of Senegal," *Rev. Energ. Ren.*, vol. 8, pp. 95–108, 2005.
- [21] E. Akpinar, "A Statistical Investigation of Wind energy Potential," *Energy Sources, Part A*, vol. 28, no. 9, pp. 807–820, 2006.

- [22] F.C.Odo, S.U.Offiah, and P.E.Ugwuoke, "Weibull distribution-based model for prediction of wind potential in Enugu, Nigeria," *Advances in Applied Science Research*, vol. 3, no. 2, pp. 1202–1208, 2010.
- [23] S. Ganesan and S. Ahmed, "Assessment of wind energy potential using topographical and meteorological data of a site in Central India (Bhopal)," *International Journal of Sustainable Energy*, vol. 27, no. 3, pp. 131–142, 2008.
- [24] I. Y.F.Lun and J. C.Lam, "A study of Weibull parameters using long-term wind observations," *Renewable Energy*, vol. 20, no. 2, pp. 145–153, 2000.
- [25] J. Liu and Y. Jiang, "A statistical analysis of wind power density based on the weibull models for fujian province in China," in *IEEE, World Non-Grid-Connected Wind Power and Energy Conference, WNWEC*, (Nanjing, China), pp. 1–4, Sept 2009.
- [26] D.A.Fadare, "A Statistical Analysis of Wind energy potential in Ibadan, Nigeria, based on Weibull Distribution Function," *The Pacific Journal of Science and Technology*, vol. 9, no. 1, pp. 110–119, 2008.
- [27] S. G. Jamdade and P. G. Jamdade, "Analysis of Wind Speed data for four locations in Ireland based on Weibull Distribution's Linear Regression Model," *International Journal of Renewable Energy Research*, vol. 2, no. 3, pp. 451–455, 2012.
- [28] A.N.Celik, "Assessing the suitability of wind speed probability distribution functions based on wind power density," *Renewable Energy*, vol. 28, no. 10, pp. 1563–1574, 2003.
- [29] D.Weisser, "A wind energy analysis of Grenada: An estimation using the Weibull density function," *Renewable Energy*, vol. 28, no. 11, pp. 1803–1812, 2003.
- [30] M. Rumbayan and K. Nagasaka, "Assessment of Wind energy potential in Indonesia using Weibull Distribution Function," *International Journal of Electrical and Power Engineering*, vol. 5, no. 6, pp. 229–235, 2011.

- [31] M.Dahbi, A.Benatiallah, and M.Sellam, "The Analysis of Wind Power Potential in Sahara site of Algeria-an estimation using the 'Weibull' density function," *Energy Procedia*, vol. 36, pp. 179–188, 2013.
- [32] B.G.Kumaraswamy, B.K.Keshavan, and S. H.Jangamshetti, "A Statistical Analysis of wind speed data in West central part of Karnataka based on Weibull distribution function," in *IEEE, Electrical Power and Energy Conference (EPEC)*, (Montreal, QC), pp. 1–4, Oct 2009.
- [33] B.G.Kumaraswamy, B.K.Keshavan, and Y.T.Ravikiran, "Analysis of seasonal wind and wind power density distribution in Aimangala wind farm at chitradurga Karnataka using two parameter Weibull distribution function," in *IEEE, Power and Energy Society General Meeting*, (San Diego, CA), pp. 1–4, July 2011.
- [34] A. N. Celik, "A statistical analysis of wind power density based on the Weibull and Rayleigh models at the southern region of Turkey," *Renewable Energy*, vol. 29, no. 4, pp. 593–604, 2003.
- [35] M. Gokcek, A. Bayulken, and S. Bekdemir, "Investigation of wind characteristics and wind energy potential in Kirklareli, Turkey," *Renewable Energy*, vol. 32, no. 10, pp. 1739–1752, 2007.
- [36] A. Ucar and F. Balo, "A seasonal analysis of wind turbine characteristics and wind power potential in Manisa, Turkey," *International Journal of Green Energy*, vol. 5, no. 6, pp. 466–479, 2008.
- [37] A. Ucar and F. Balo, "Investigation of wind energy potential in Kartalkaya-Bolu, Turkey," *International Journal of Green Energy*, vol. 6, no. 4, pp. 401–412, 2009.
- [38] M.Bilgili and B.Sahin, "Statistical Analysis of Wind energy density in the Western Region of Turkey," *Energy Sources, Part A: Recovery, Utilization, and Environmental Effects*, vol. 32, no. 13, pp. 1224–1235, 2010.
- [39] J. O. Okeniyi, I. F. Moses, and E. T. Okeniyi, "Wind characteristics and energy potential assessment in Akure, South west Nigeria: Econometrics and Policy Implications," *International Journal of Ambient Energy*, pp. 1–19, 2013.

- [40] S. A. Akdag and A. Dinler, "A new method to estimate Weibull parameters for wind energy applications," *Energy Conversion and Management*, vol. 50, no. 7, pp. 1761–1766, 2009.
- [41] U. Yildirim, F. Kaya, and A. Gungor, "Comparision of Moment and Energy Trend Factor Methods on Calculating Wind Energy Potential," in *International Research/Expert Conference*, (Dubai, UAE), pp. 331–334, Sept 2012.
- [42] Y. Zhou and S. J. Smith, "Spatial and temporal patterns of global onshore wind speed distribution," *Environmental Research Letters*, vol. 8, no. 3, pp. 1–8, 2013.
- [43] D. K. Kaoga, N. Djongyang, S. Y. Doka, and D. Raidandi, "Assessment of wind energy potential for small scale water pumping systems in the north region of Cameroon," *International Journal of Basic and Applied Sciences*, vol. 3, no. 1, pp. 38–46, 2014.
- [44] T.R.Ayodele, A.A.Jimoh, J.L.Munda, and J.T.Agee, "A Statistical Analysis of Wind Distribution and Wind power potential in the Coastal Region of South Africa," *International Journal of Green Energy*, vol. 10, no. 8, pp. 814–834, 2013.
- [45] N.Emami and A.Behbahaninia, "The Statistical Evaluation of Wind speed and power density in the Firouzkouh region in Iran," *Energy Resources Part A: Recovery, Utilization, and Environmental Effects*, vol. 34, no. 12, pp. 1076–1083, 2012.
- [46] Z. O. Olaofe and K. A. Folly, "Statistical Analysis of wind Resources at Darling for Energy production," *International Journal of Renewable Energy Research*, vol. 2, no. 2, pp. 250–261, 2012.
- [47] A. S. Ahmed, "Investigation of wind characteristics and wind energy potential at Ras Ghareb, Egypt," *Renewable and Sustainable Energy Reviews*, vol. 15, no. 6, pp. 2750 – 2755, 2011.

- [48] T. L. Tiang and D. Ishak, "Technical review of wind energy potential as small-scale power generation sources in Penang Island, Malaysia," *Renewable and Sustainable Energy Reviews*, vol. 16, no. 5, pp. 3034–3042, 2012.
- [49] E. K. Akpınar and S. Akpınar, "An Analysis of wind energy potential of Elazığ, Turkey," *International Journal of Green Energy*, vol. 1, no. 2, pp. 193–207, 2004.
- [50] K. M. Bataineh and D. Dalalah, "Assessment of wind energy potential for selected areas in Jordan," *Renewable Energy*, vol. 59, pp. 75–81, 2013.
- [51] Z. Azami, R. A. Mahir, A. R. Zainal, and S. Kamaruzzaman, "Fitting of statistical distributions to wind speed data in Malaysia," *European Journal of Scientific Research*, vol. 26, pp. 6–12, Jan 2009.
- [52] J. V. Seguro and T. W. Lambert, "Modern Estimation of the parameters of the Weibull wind speed distribution for wind energy analysis," *Journal of Wind Engineering and Industrial Aerodynamics*, vol. 85, no. 5, pp. 75–84, 2000.
- [53] S. F. Khahro, K. Tabbassum, A. M. Soomro, L. Dong, and X. Liao, "Evaluation of wind power production prospective and Weibull parameter estimation methods for Babaurband, Sindh Pakistan," *Energy Conversion and Management*, vol. 78, pp. 956–967, 2014.
- [54] A. K. Azad, M. G. Rasul, and T. Yusaf, "Statistical Diagnosis of the Best Weibull Methods for Wind Power Assessment for Agricultural Applications," *Energies*, vol. 7, pp. 3056–3085, 2014.
- [55] D. Indhumathy, C. Sessaiah, and K. Sukkiramathi, "Estimation of Weibull Parameters for Wind speed calculation at Kanyakumari in India," *International Journal of Innovative Research in Science Engineering and Technology*, vol. 3, no. 1, pp. 8340–8345, 2014.
- [56] D. K. Kaoga, D. Raidandi, N. Djongyang, and S. Y. Doka, "Comparison of Five numerical methods for estimating Weibull parameters for wind energy applications in the district of Kousseri, Cameroon," *Asian Journal of Natural and Applied Sciences*, vol. 3, no. 1, pp. 72–87, 2014.

- [57] T. P. Chang, "Performance comparison of six numerical methods in estimating Weibull parameters for wind energy application," *Applied Energy*, vol. 88, no. 1, pp. 272–282, 2011.
- [58] P. A. C. Rocha, R. C. de Sousa, C. F. de Andrade, and M. E. V. da Silva, "Comparison of seven numerical methods for determining weibull parameters for wind energy generation in the northeast region of Brazil," *Applied Energy*, vol. 89, no. 1, pp. 395–400, 2012.
- [59] A. Genc, M. Erisoglu, A. Pekgor, G. Oturanc, A. Hepbasli, and K. Ulgen, "Estimation of Wind power potential using Weibull Distribution," *Energy Sources*, vol. 27, no. 9, pp. 809–822, 2005.
- [60] H.S.Bagiorgas, G.Mihalakakou, and D.Matthopoulos, "A Statistical Analysis of Wind Speed Distributions in the area of Western Greece," *International Journal of Green Energy*, vol. 5, no. 1-2, pp. 120–137, 2008.
- [61] A. M. M. I. Mukut, M. Q. Islam, and M. M. Alam, "Analysis of Wind Characteristics in Coastal Areas of Bangladesh," *Journal of Mechanical Engineering*, vol. 39, no. 1, pp. 45–49, 2008.
- [62] F.C.Odo and G.U.Akubue, "Comparative Assessment of Three Models for Estimating Weibull Parameters for Wind Energy Applications in a Nigerian Location," *International Journal of Energy Science*, vol. 2, no. 1, pp. 22–25, 2012.
- [63] S. A.Ahmed, "Comparative study of four methods for estimating Weibull parameters for Halabja, Iraq," *International Journal of Physical Sciences*, vol. 8, no. 5, pp. 186–192, 2013.
- [64] S. Mathew, *Wind Energy: Fundamentals, Resource Analysis and Economics*. Springer-Verlag Berlin Heidelberg, 2006.
- [65] I. T. Togrul and M. I. Kizi, "Determination of Wind energy potential and Wind speed data in Bishkek, Kyrgyzstan," *International Journal of Green Energy*, vol. 5, no. 3, pp. 157–173, 2008.

- [66] E. K. Akpınar and S. Akpınar, "An assessment on seasonal analysis of wind energy characteristics and wind turbine characteristics," *Energy Conversion and Management*, vol. 46, no. 11-12, pp. 1848–1867, 2005.
- [67] A. Balouktsis, D. Chassapis, and T. D.Karapantsios, "A Nomogram Method for Estimating the energy produced by Wind Turbine Generators," *Solar Energy*, vol. 72, no. 3, pp. 251–259, 2002.
- [68] B.Dursun and B.Alboyachi, "An evaluation of Wind energy Characteristics for Four different locations in Balikesir," *Energy Sources, Part A*, vol. 33, no. 11, pp. 1086–1103, 2011.
- [69] E. Akpınar, "An assessment of wind turbine characteristics and wind energy characteristics for electricity production," *Energy Sources- A*, vol. 28, pp. 941–953, 2006.
- [70] M. S. Adaramola, M. Agelin-Chaab, and S. S. Paul, "Assessment of wind power generation along the coast of Ghana," *Energy Conversion and Management*, vol. 74, pp. 61–69, 2014.
- [71] S. O. Oyedepo, M. S. Adaramola, and S. S. Paul, "Analysis of wind speed data and wind Energy potential in three selected loactions in south-east Nigeria," *International Journal of Energy and Enviromental Engineering*, vol. 3, no. 7, pp. 1–13, 2012.
- [72] O. S. Ohunakin, O. M. Oyewola, and M. S. Adaramola, "Economic analysis of wind energy conversion systems using levelized cost of electricity and present value cost methods in Nigeria," *International Journal of Energy and Enviromental Engineering*, vol. 4, no. 2, pp. 1–8, 2013.
- [73] Y.Himri, S.Rehman, B.Draoui, and S.Himri, "Wind power potential assessment for three locations in Algeria," *Renewable and Sustainable Energy Reviews*, vol. 12, no. 9, pp. 2495–2504, 2008.
- [74] R.M.R.Kainkwa, "Wind speed pattern and the available wind power at Basotu, Tanzania," *Renewable Energy*, vol. 21, no. 2, pp. 289–295, 2000.

- [75] M.L.Ray, A.L.Rogers, and J.G.McGowan, "Analysis of wind shear models and trends in different terrains," in *Conference Proceedings, American Wind Energy Association Windpower*, (Pittsburgh, PA, USA), pp. 1–14, June 2006.
- [76] K. Tar, "Some Statistical Characteristics of monthly average wind speed at various Heights," *Renewable and Sustainable Energy Reviews*, vol. 12, no. 6, pp. 1712–1724, 2008.
- [77] S. Rehman and N. M.Al-Abbadi, "Wind shear coefficient, turbulence intensity and wind power potential assessment for Dhulom, Saudi Arabia," *Renewable Energy*, vol. 33, no. 12, pp. 2653–2660, 2008.
- [78] M.Elamouria and F. Amara, "Wind Energy potential in Tunisia," *Renewable Energy*, vol. 33, no. 4, pp. 758–768, 2008.
- [79] J.Leroy, "Wind field simulations at Askervein hill," tech. rep., Vector AS, 1999.
- [80] T.Wallbank, "WindSim validation study, CFD Validation in complex terrain," tech. rep., 2008.
- [81] D. Weir and A. Gravdahl, "WindSim: Micrositing with Numerical Simulations: A Simple Approach," tech. rep., NZ Wind Energy Conference and Exhibition, Wellington, 2011.
- [82] A.R.Gravdahl, "The sensitivity on numerical field modeling," tech. rep., WindSim AS, Wind Power Exhibition, Los Angeles, 2007.
- [83] A.R.Gravdahl, "Power prediction and siting -when the terrain gets rough," tech. rep., WindSim AS, Wind Power Exhibition, Los Angeles, 2007.
- [84] A. Gravdahl, G.Crasto, F.Castellani, and E. Piccioni, "Wake modeling with the actuator disc concept," *Energy Procedia*, vol. 24, pp. 385–392, 2012.
- [85] N.Simisiroglou, "Wind resource assessment comparison on a complex terrain employing Windpro and WindSim," Master's thesis, Gotland University, June 2012.

- [86] D.Fallo, "Wind energy resource evaluation in a site of central Italy by CFD simulations," Master's thesis, Universita degli Studi di Cagliari, Italy, 2008.
- [87] N.O.Jensen, "A note of wind generator interaction," *Roskilde: Riso National Laboratory*, 1993.
- [88] G. Mosetti, C. Poloni, and B. Diviacco, "Optimization of wind turbine positioning in large wind farms by means of a genetic algorithm," *Journal Wind Eng Ind Aerodyn*, vol. 51, no. 1, pp. 105–116, 1994.
- [89] S.A.Grady, M.Y.Hussaini, and M.M.Abdullah, "Placement of wind turbines using genetic algorithms," *Journal of Renewable Energy*, vol. 30, no. 2, pp. 259–270, 2005.
- [90] E. Alireza and N. Pirooz, "New approach on optimisation in placement of wind turbines within wind farm by genetic algorithms," *Journal of Renewable Energy*, vol. 35, no. 7, pp. 1559–1564, 2010.
- [91] M. Grigorios, L. Stavros, and P. Eleftheria, "Optimal placement of wind turbines in a wind park using Monte Carlo simulation," *Journal of Renewable Energy*, vol. 33, no. 7, pp. 1455–1460, 2008.
- [92] J. S. Gonzaleiz, A. G. G. Rodriguez, J. C. Mora, J. R. Santos, and M. B. Payan, "Optimization of wind farm turbines layout using an evolutive algorithm," *Renewable Energy*, vol. 35, no. 8, pp. 1671 – 1681, 2010.
- [93] C. M. Ituarte-Villarreal and J. F. Espiritu, "Optimization of wind turbine placement using a viral based optimization algorithm," *Procedia Computer Science*, vol. 6, pp. 469 – 474, 2011.
- [94] P.-Y. Yin and T.-Y. Wang, "A GRASP-VNS algorithm for optimal wind-turbine placement in wind farms," *Renewable Energy*, vol. 48, pp. 489 – 498, 2012.
- [95] S. Pookpant and W. Ongsakul, "Optimal placement of wind turbines within wind farm using binary particle swarm optimization with time-varying acceleration coefficients," *Renewable Energy*, vol. 55, no. 0, pp. 266 – 276, 2013.

- [96] M. Lei, L. Shiyan, and J. Chuanwen, "A review on the forecasting of wind speed and generated power," *Renewable and Sustainable Energy Reviews*, vol. 13, no. 4, pp. 915–920, 2009.
- [97] Y.-K. Wu and J.-S. Hong, "A literature review of wind forecasting technology in the world," in *IEEE, Power Tech*, pp. 504–509, July 2007.
- [98] S. Aggarwal and M. Gupta, "Wind Power Forecasting: A Review of Statistical Models," *International Journal of Energy Science (IJES)*, vol. 3, no. 1, pp. 1–10, 2013.
- [99] W.-Y. Chang, "A Literature Review of Wind Forecasting Methods," *Journal of Power and Energy Engineering*, vol. 2, pp. 161–168, 2014.
- [100] J.-S. Hong, "Evaluation of the high-resolution model forecasts over the Taiwan area during gimex," *Weather and Forecasting*, vol. 18, pp. 836–846, Oct 2003.
- [101] S. Al-Yahyai, Y. Charabi, and A. Gastli, "Review of the use of Numerical Weather Prediction (nwp) Models for wind energy assessment," *Renewable and Sustainable Energy Reviews*, vol. 14, no. 9, pp. 3192 – 3198, 2010.
- [102] M. Milligan, M. Schwartz, and Y. Wan, "Statistical wind power forecasting models: Results for U.S. Wind farms," in *in Proc. Wind Power*, (Austin, TX), pp. 1–14, National Renewable Energy Laboratory, 2003.
- [103] J. Torres, A. Garcaia, M. D. Blas, and A. D. Francisco, "Forecast of hourly average wind speed with ARMA models in Navarre (Spain)," *Solar Energy*, vol. 79, no. 1, pp. 65 – 77, 2005.
- [104] C. Wang, Z. Lu, and Y. Qiao, "Modeling of wind pattern and its application in wind speed forecasting," in *International Conference on Sustainable Power Generation and Supply (SUPERGEN)*, pp. 1–6, April 2009.
- [105] M. Miranda and R. Dunn, "One-hour-ahead wind speed prediction using a Bayesian methodology," in *IEEE, Power Engineering Society General Meeting*, pp. 6–12, 2006.

- [106] E. Erdem and J. Shi, "ARMA based approaches for forecasting the tuple of wind speed and direction," *Applied Energy*, vol. 88, no. 4, pp. 1405 – 1414, 2011.
- [107] R.G.Kavasseri and K.Seetharaman, "Day-ahead wind speed forecasting using f-ARIMA models," *Renewable Energy*, vol. 34, no. 5, pp. 1388–1393, 2009.
- [108] I.J.Ramirez-Rosado, L.A.Fernandez-Jimenez, C.Monteiro, J.Sousa, and R. Bessa, "Comparison of two new short-term wind-powerforecasting systems," *Renewable Energy*, vol. 34, no. 7, pp. 1848–1854, 2009.
- [109] A. More and M. Deo, "Forecasting wind with neural networks," *Marine Structures*, vol. 16, no. 1, pp. 35 – 49, 2003.
- [110] K. Rohrig and B. Lange, "Application of wind power prediction tools for power system operations," in *IEEE, Power Engineering Society General Meeting*, pp. 5 –12, 2006.
- [111] P. Fonte and J.C.Quadrado, "Ann approach to weces power forecast," in *10th IEEE Conference on Emerging Technologies and Factory Automation*, vol. 1, pp. 1069–1072, Sep 2005.
- [112] S. Li, D.C.Wunsch, E. OHair, and M.G.Giesselmann, "Using neural networks to estimate wind turbine power generation," *IEEE Transactions onEnergy Conversion*, vol. 16, pp. 276–282, Sep 2001.
- [113] E.Fernandez and M. Mabel, "Assessment of Wind energy of potential sites in India: An ANN based approach," in *Proceedings of the international congress on renewable energy*, (Pune,India), pp. 170 – 178, Jan 2005.
- [114] X.Wang, G.Sideratos, N.Hatziargyriou, and L.H.Tsoukalas, "Wind speed forecasting for power system operational planning," in *International Conference on Probabilistic Methods Applied to Power Systems*, (Montreal,QC), pp. 470–474, Sept 2004.
- [115] M. C. Mabel and E. Fernandez, "Analysis of wind power generation and prediction using ANN: A case study," *Renewable Energy*, vol. 33, no. 5, pp. 986 – 992, 2008.

- [116] I.G.Damousis and P. Dokopoulos, "A fuzzy expert system for the forecasting of wind speed and power generation in wind farms," in *22nd IEEE Power Engineering Society International Conference on Power Industry Computer Applications, 2001. PICA 2001. Innovative Computing for Power - Electric Energy Meets the Market*, pp. 63–69, 2001.
- [117] S.A.P.Kani and G. Riahy, "A new ANN-based methodology for very short-term wind speed prediction using markov chain approach," in *IEEE Canada, Electric Power Conference (EPEC)*, pp. 1–6, Oct 2008.
- [118] M.Negnevitsky, P.Johnson, and S.Santoso, "Short term wind power forecasting using hybrid intelligent systems," in *IEEE, Power Engineering Society General Meeting*, pp. 1–4, June 2007.
- [119] H. Liu, H.-Q. Tian, C. Chen, and Y. fei Li, "A hybrid statistical method to predict wind speed and wind power," *Renewable Energy*, vol. 35, no. 8, pp. 1857 – 1861, 2010.
- [120] J. Catalao, H. Pousinho, and V. Mendes, "Short-term wind power forecasting in Portugal by neural networks and wavelet transform," *Renewable Energy*, vol. 36, no. 4, pp. 1245 –1251, 2011.
- [121] C.W.Potter and W.Negnevitsky, "Very short-term wind forecasting for tasmanian power generation," *IEEE Transactions on Power Systems*, vol. 21, no. 2, pp. 965–972, 2006.
- [122] G.Sideratos and N.D.Hatziargyriou, "An advanced statistical method for wind power forecasting," *IEEE Transactions on Power Systems*, vol. 22, no. 1, pp. 258–265, 2007.
- [123] R.Jursa and K.Rohrig, "Short-term wind power forecasting using evolutionary algorithms for the automated specification of artificial intelligence models," *International Journal of Forecasting*, vol. 24, no. 4, pp. 694–709, 2008.

- [124] J. Shi, J. Guo, and S. Zheng, "Evaluation of hybrid forecasting approaches for wind speed and power generation time series," *Renewable and Sustainable Energy Reviews*, vol. 16, no. 5, pp. 3471 – 3480, 2012.
- [125] J. Shi, Z. Ding, W.-J. Lee, Y. Yang, Y. Liu, and M. Zhang, "Hybrid forecasting model for very-short term wind power forecasting based on grey relational analysis and wind speed distribution features," *IEEE Transactions on Smart Grid*, vol. 5, pp. 521–526, Jan 2014.
- [126] B. Agarwal, *Basic Statistics*. New Age International Publishers, 2006.
- [127] "The Wind Power." <http://www.thewindpower.net/>.
- [128] P. Rohatgi, R. Kalpana, and R. Bowonder, *Technical Forecasting*. Tata McGraw Hill Publishing Company Limited, 1982.
- [129] N. Meade and T. Islam, "Forecasting with growth curves: An empirical comparison," *International Journal of Forecasting*, vol. 11, no. 2, pp. 199 – 215, 1995.
- [130] M. Mitchell, *An Introduction to Genetic Algorithms*. Cambridge, MA : MIT Press/Addison-Wesley, 1996.
- [131] A. P. Engelbrecht, *Computational intelligence: An introduction*. John Willey and Sons, Ltd, 2007.
- [132] S. Rajasekaran and G. Pai, *Neural Networks, Fuzzy Logic and Genetic Algorithms: Synthesis and Applications*. Prentice Hall of India, 2003.
- [133] Z. Michalewicz, *Genetic algorithms + data structures = Evolving programs*. Springer-Verlag, 1996.
- [134] K. Chong and S. H. Zak, *An Introduction to Optimization*. John Wiley and Sons, 2 ed., 2004.
- [135] D. E. Goldberg, *Genetic algorithm in search, optimization and machine learning*. Addison Wesley, 1989.

- [136] T. Chai and R. R. Draxler, "Root mean square error (rmse) or mean absolute error (mae)? – Arguments against avoiding RMSE in the literature," *Geosci. Model Dev.*, vol. 7, pp. 1247–1250, 2014.
- [137] V. Nelson, *Wind Energy: Renewable Energy and the Environment*. CRC Press, Taylor and Francis group, 2009.
- [138] M. C. Brower, *Wind Resource Assessment: A practical guide to developing a wind project*. Wiley: A John Wiley and Sons, 2012.
- [139] I. AWS Scientific, "Wind Resource Assessment Hand book," tech. rep., National Renewable Energy Laboratory, 1997.
- [140] V. Warudkar and S. Ahmed, "Wind Resource Assessment: A Review," *International Journal of Mining, Metallurgy and Mechanical Engineering*, vol. 1, no. 3, pp. 204–207, 2013.
- [141] A. Keyhani, M. Ghasemi-Varnamkhashti, M. Khanali, and R. Abbaszadeh, "An assessment of wind energy potential as a power generation source in the capital of iran, Tehran," *Energy*, vol. 35, pp. 188–201, 2010.
- [142] A. Picard, R. S. Davis, M. Glaser, and K. Fujii, "Revised formula for the density of moist air (cipm-2007)," *Metrologia*, vol. 45, pp. 149–155, 2008.
- [143] R. Shelquist, "Equations Air Density and Density Altitude," 2009.
- [144] N. M. Al-Abadi and S. Rehman, "Wind speed and Wind power Characteristics for Gassim, Saudi arabia," *International Journal of Green Energy*, vol. 6, no. 2, pp. 201–217, 2009.
- [145] B. Weibull, Stockholm, and Sweden, "A Statistical Distribution function of Wide Applicability," *Journal of Applied Mechanics Transactions of ASME*, no. 18, pp. 292–297, 1951.
- [146] T. J. Chang, Y. T. Wu, H. Y. Hsu, C.-R. Chu, and C.-M. Liao, "Assessment of wind characteristics and wind turbine characteristics in Taiwan," *Renewable Energy*, vol. 28, no. 6, pp. 851–871, 2003.

- [147] J. Earnest, *Wind Power Technology*. PHI Learning Pvt. Ltd., 2014.
- [148] J.A.Carta, P.Ramarez, and S.Velazquez, “A review of wind speed probability distributions used in wind energy analysis case studies in the Canary Islands,” *Renewable and Sustainable Energy Reviews*, vol. 13, no. 5, pp. 933–955, 2009.
- [149] M. Jamil, S. Parsa, and M. Majidi, “Wind power statistics and an evaluation of wind energy density,” *Renewable Energy*, vol. 6, no. 5-6, pp. 623 – 628, 1995.
- [150] A. Mostafaeipour, A. Sedaghat, A. Dehghan-Niri, and V. Kalantar, “Wind energy feasibility study for city of Shahrabak in Iran,” *Renewable and Sustainable Energy Reviews*, vol. 15, no. 6, pp. 2545 – 2556, 2011.
- [151] A. N. Celik, “Review of Turkey’s current energy status: A case study for wind energy potential of Canakkale province,” *Renewable and Sustainable Energy Reviews*, vol. 15, no. 6, pp. 2743 – 2749, 2011.
- [152] M.L.Kubik, P.J.Coker, and C.Hunt, “Using meteorological wind data to estimate turbine generation output: A sensitivity analysis,” *World Renewable Energy Congress*, pp. 4074–4081, 2011.
- [153] A. Shata and R. Hanitsch, “Evaluation of wind energy potential and electricity generation on the coast of Mediterranean Sea in Egypt,” *Renewable Energy*, vol. 31, no. 8, pp. 1183–1202, 2006.
- [154] A. Shata and R. Hanitsch, “The potential of electricity generation on the east coast of Red Sea in Egypt,” *Renewable Energy*, vol. 31, no. 10, pp. 1597–1615, 2006.
- [155] N.Boccard, “Capacity factor of wind power realized values vs. estimates,” *Energy Policy*, vol. 37, pp. 2679–2688, 2009.
- [156] “windographer Software for data analysis.” <https://www.windographer.com>.
- [157] “ReGen Powertech.” <http://www.regenpowertech.com/>.
- [158] “Suzlon.” <http://www.suzlon.com/>.

- [159] M. Strack and V. Riedel, "State of the art in application of flow models for micro-siting," in *In: Proceedings of DEWEK*, Wilhelmshaven, Germany, 2004.
- [160] "WindSim Software." <http://www.windsim.com/>.
- [161] C. Meissner, *WINDSIM Getting Started- WINDSIM 7*. WindSim AS, Fjordgaten 15, N-3125 Tonsberg, Norway +47 33 38 18 00, 8 ed., January 2015.
- [162] "Metodyn WT Software." <http://meteodyn.com/en/>.
- [163] "WindFarmer Software." <https://www.dnvgl.com/services/windfarmer-3766>.
- [164] *DNV-GL - WINDFARMER Theory Manual*, version 5.3 ed., April 2014.
- [165] F.W. Lanchester, "A contribution to the theory of propulsion and the screw propeller," *Transactions of the Institution of Naval Architects*, pp. 98–116, 1915.
- [166] Frandsen, Sten, Barthelmie, Rebecca, Pryor, Sara, Rathmann, Ole, Larsen, Søren, Højstrup, Jørgen, Thøgersen, and Morten, "Analytical modelling of wind speed deficit in large offshore wind farms," *Wind Energy*, vol. 9, no. 1-2, pp. 39–53, 2006.
- [167] I. Katic, J. Højstrup, and N. Jensen, "A simple model for cluster efficiency," in *Proceedings of the European Wind Energy Conference and Exhibition*, (Rome-Italy), pp. 407–410, Oct 1986.
- [168] A. Crespo, J. Hernandez, and S. Frandsen, "Survey of Modelling Methods for Wind Turbine Wakes and Wind farms," *Wind Energy*, vol. 2, no. 1, pp. 1–24, 1999.
- [169] G. Crasto and A. R. Gravdahl, "Cfd wake modeling using a porous disc," in *European Wind Energy Conference and Exhibition*, (Brussels-Belgium), pp. 1–9, 31 March-3 April 2008.
- [170] D. Kriesel, *A Brief Introduction to Neural Networks*. 2007.
- [171] C. M. Bishop, *Neural Networks for Pattern Recognition*. Clarendon Press Oxford, 1995.

-
- [172] C. M. Bishop, *Pattern Recognition and Machine Learning*. Springer, 2006.
- [173] R. J. Hyndman and A. B. Koehler, “Another look at measures of forecast accuracy,” *International Journal of Forecasting*, vol. 22, no. 4, pp. 679–688, 2006.
- [174] J. Sola and J. Sevilla, “Importance of input data normalization for the application of neural networks to complex industrial problems,” *IEEE Transactions on Nuclear Science*, vol. 44, pp. 1464–1468, Jun 1997.
- [175] B. Tarawneh, “Pipe pile setup: Database and prediction model using artificial neural network,” *Soils and Foundations*, vol. 53, no. 4, pp. 607 – 615, 2013.

Publications Based on Present Work

Journal:

1. M.K. Deshmukh and C. Balakrishna Moorthy, “Application of Genetic Algorithm to Neural Network Model for Estimation of Wind Potential”, Journal of Engineering, Science and Management Education, Vol.2, page 42-48, Oct 2010.
2. M.K. Deshmukh and C. Balakrishna Moorthy, “A New Approach for Prediction of Growth of Onshore Wind power potential”, International Journal of Electrical and Electronics and Electronics Engineering Research (IJEEER), Vol.3, No.1, page 107-122, Mar 2013.
3. C. Balakrishna Moorthy, M.K. Deshmukh and Darshana Mukherejee, “New Approach for Placing Wind Turbines in a Wind Farm Using Genetic Algorithm”, Journal of Wind Engineering, Multi science and Co publications, Vol.38, No.6, page 633–642, 2014.
4. C. Balakrishna Moorthy and M.K. Deshmukh, “A new approach to optimise placement of wind turbines using particle swarm optimisation ”, International Journal of Sustainable Energy, Taylor and Francis publications, Vol.34, No.6, page 396-405, 2015.
5. C.Balakrishna Moorthy, Ankur Agarwal and M.K.Deshmukh,“Artificial Intelligence Techniques for Wind Power Prediction: A Case Study” - (Accepted for publication - Indian Journal of Science and Technology)
6. C. Balakrishna Moorthy and M.K. Deshmukh, “Estimation of wind power potential in a region of Goa, India using Weibull distribution function” – (under Review - International Journal of Energy and clean Environment)
7. C. Balakrishna Moorthy, M.K. Deshmukh and A. Hemanth Kumar, “Assessment of wind energy potential using Weibull and Rayleigh distribution in a region of Goa, India”- (under Review- Journal of Renewable and sustainable Energy reviews)

Conference:

1. M.K.Deshmukh and C.Balakrishna Moorthy “A New Approach for Estimation of Output of Wind Energy Conversion Systems” at International Conference on Emerging Trends on Engineering Technologies, at Noorul Islam University, Tamil-Nadu, on 25-26, March 2010, pp 321-326.
2. C.Balakrishna Moorthy, Ankur Agarwal and M.K.Deshmukh, “Artificial Intelligence Techniques for Wind Power Prediction: A Case Study” International Conference on Soft Computing in Applied Sciences & Engineering (ICSCASE-2015), at Noorul Islam University, TamilNadu, on 23-24 July 2015, pp 136-142.

Training attended:

1. Seventh National training Course on “Fundamentals of Wind Energy” organized and conducted by Centre for wind Energy Technology [CWET] during 28 & 29 May 2009 at Chennai.
2. Two days workshop on “Wind Energy: 20 by 2020 - challenges and opportunities ahead in India” at New Delhi from 11th and 12th February, 2010.
3. National training Course on “Wind Resource Assessment and wind turbine technology” organized and conducted by Centre for wind Energy Technology [CWET] during 1-12 August 2013 at Chennai.
4. National training Course on “WINDSIM software for Wind Resource assessment”, at Chennai, 19 September 2014.

Brief Biography of the Candidate

C.Balakrishna Moorthy completed his Bachelor of Engineering degree in the Electrical and Electronics Engineering discipline, from 'The Indian Engineering College', Vadakankulam, Tamil Nadu, India, in 2001. He obtained his Master of Engineering degree in the Power Systems Engineering from Annamalai University, Tamilnadu, India, in 2002. He has been carrying out research in the area of Wind Energy since 2008 at BITS, Pilani, K.K. Birla Goa campus, India. He is also working as a Lecturer, Department of EEE and E&I at BITS, Pilani, K.K.Birla Goa campus, Goa, India, since November 2006.

Prior to this, he worked as a Lecturer at 'The Indian Engineering College' for one and half years, from January 2003 to May 2004, Further, he worked in "Sun College of Engineering and Technology", Nagercoil, India, from June 2004 to October 2006. His major research interests are Renewable Energy, Wind Energy, Wind Resource Assessment, Power Quality and Grid Integration. He has published papers in various international journals.

Brief Biography of the Supervisor

Dr. M. K. Deshmukh is Professor and Head of Department of EEE and E&I. He has extensive research and consultancy experience in the areas of Renewable Electric Power Generation, Energy Conservation Management and Planning, and published more than 35 research papers in reputed journals. He has obtained his M.Tech. degree in Energy Studies in the year 1986 at Indian Institute of Technology, Delhi and obtained his Ph.D. degree on Energy Conservation Management at the same Institute in the year 1993. Currently he is working in the areas of smart grids, wind power generation, solar photovoltaic power generation, on campus and in the region. His teaching interests include Renewable Energy, Wind Electrical Systems, PV Devices, Environmental Management, in addition to discipline specific courses such as Electrical Machines, Communication Systems, Satellite Communication, Measurement Systems, Power Electronics, Control Systems, Power Systems, Medical Instrumentation and Brain Computer Interface. He is Faculty Advisor for extension activities of the Department, involving undergraduate and postgraduate students of the Department, alumni of the Department, Experts from Industry, Govt. and Non - governmental agencies in the state. He has been Faculty Advisor for the Students' Chapter of EWB - Engineers Without Borders since April, 2011.

Prior to his present assignment, he has joined as Assistant Professor at BITS, Pilani, Rajasthan and later at BITS, Pilani Goa-Campus, where he also served as Faculty In - charge (Faculty Affairs), Faculty In - Charge (Admin). He has worked at Centre of Energy Studies and Research, Indore, as research scientist for a period of ten years. He has been instrumental in developing collaboration between Institute and other agencies including Industry, Govt. and Non - Govt. agencies, during initial phase of Institute in Goa. Currently, his assignments include implementation of Institute's MoU with National Institute of Wind Energy, Chennai, India and WindSim, Norway, where he has undergone advanced training on simulation & modeling of wind energy systems. He is professional member of IEEE and Life Member of ISTE , IPTA, SEST and EWB.